INFORMATION TO USERS

This manuscript has been reproduced from the microfilm master. UMI films the text directly from the original or copy submitted. Thus, some thesis and dissertation copies are in typewriter face, while others may be from any type of computer printer.

The quality of this reproduction is dependent upon the quality of the copy submitted. Broken or indistinct print, colored or poor quality illustrations and photographs, print bleedthrough, substandard margins, and improper alignment can adversely affect reproduction.

In the unlikely event that the author did not send UMI a complete manuscript and there are missing pages, these will be noted. Also, if unauthorized copyright material had to be removed, a note will indicate the deletion.

Oversize materials (e.g., maps, drawings, charts) are reproduced by sectioning the original, beginning at the upper left-hand corner and continuing from left to right in equal sections with small overlaps. Each original is also photographed in one exposure and is included in reduced form at the back of the book.

Photographs included in the original manuscript have been reproduced xerographically in this copy. Higher quality 6" x 9" black and white photographic prints are available for any photographs or illustrations appearing in this copy for an additional charge. Contact UMI directly to order.

UMI

A Bell & Howell Information Company
300 North Zeeb Road, Ann Arbor MI 48106-1346 USA
313/761-4700 800/521-0600

Université d'Ottawa · University of Ottawa

Visualization of Flow Past a Model of the CF-18 Aircraft in a Water Tunnel

by

Warren R. Dunn

A thesis presented to the
School of Graduate Studies and Research
in partial fulfillment of the
requirement for the degree of

MASTER of APPLIED SCIENCE
in
MECHANICAL ENGINEERING

Ottawa-Carleton Institute for Mechanical and Aerospace Engineering
Department of Mechanical Engineering
University of Ottawa
Ottawa, Ontario, Canada
December 1997

Abstract

Incompressible flow past a 1:48 scale model of the CF-18 fighter aircraft was studied in a water tunnel at the University of Ottawa. The tests were conducted at the relatively low Reynolds number of 3450, based on the free stream velocity and the wing's mean aerodynamic chord. Flow visualization records were obtained for flow around different stores, the Leading Edge Extension (LEX) vortex, and the forebody vortex, at various angles of attack. The flows were visualized using water-based dye, a non-Newtonian shear-thickening dye, and hydrogen bubbles.

The stores were mostly studied in the low angle of attack range between α = -1° and α = 5°. At these angles, their effect on the flow was local. Decreasing the spacing between stores caused the flow to slow down considerably because of the interaction of the separated flow on the wing with the boundary layers of the individual stores.

The LEX vortex became stronger as the angle of attack was increased, and the location of its breakdown moved upstream. The breakdown location showed good correlation with results of other model and full-scale studies. The forebody vortex was weaker than the LEX vortex, and was consistently drawn towards the LEX until the two vortices began interacting. The initial interaction location depended on the aircraft's angle of attack.

The variation of the LEX vortex bursting location with angle of attack is only weakly sensitive to Reynolds number and, therefore, the water tunnel tests can provide a good simulation of full-scale flow characteristics. On the other hand, flow characteristics near surfaces change substantially with increasing Reynolds number, so that the water tunnel results in such regions must be viewed with reservation, when considering their relevance to the high Reynolds number flow around the aircraft. Another effect that the present results cannot simulate, even approximately, is the effect of compressibility.

Acknowledgments

I would like to thank Professor S. Tavoularis for the opportunity to assist in the construction of the water tunnel and perform studies using that facility. His guidance, persistence and advice, concerning this project and others, and his timely editing of this thesis are greatly appreciated. I would also like to thank Dr. B.H.K. Lee of the NRC for his guidance in defining this topic of study, and for reviewing the drafts of this thesis. Much of the information concerning the CF-18 came from his archives.

I am grateful to Lt. Hassan Naqvi of the DND for his interest in this project, for the unclassified dimensions of the CF-18, and the list of store configurations used in this study.

I am also grateful to the Mechanical Engineering machine shop staff at the University of Ottawa in the design and construction of the model positioning system and other utilities used in conjunction with the water tunnel. Design of the model positioning system would have been incomplete without the valuable contribution of Mr. M. Makasare.

I would also like to thank the Electronics laboratory and the machine shop in the Department of Physics for their contributions towards accessories used in this study.

I am thankful for the friendship of Ben Kislich-Lemyre, Sadok Guellouz, Mohsen Ferchichi, Sebastien Marineau-Mes and many others, who gave me more time than I asked for. They made my time at the University of Ottawa both informative and enjoyable, as we discussed aerodynamics and topics completely unrelated.

I am especially thankful for the support of my family and friends, who helped me adapt to long-distance relationships, and supported me through the entire thesis. Finally, I would like to thank Joanne Brebion, who supported me from afar as she completed her own studies, then joined me in trying to create a living so far from everything we knew, and finally for agreeing to marry me.

Contents

List of Tables

List of Figures

List of Plates

Nomenclature

V_I	Engine inlet velocity
U_∞	Nominal centerline velocity
V_I/U_∞	Engine inlet ratio
α	Angle of incidence
x-	Direction parallel to the water tunnel's longitudinal axis
y-	Direction parallel to the water tunnel's transverse axis
z-	Direction parallel to the water tunnel's vertical axis
V_s	Stokes velocity
g	Gravitational acceleration
d_b	Diameter of gas bubbles
ρ_b	Density of gas bubbles
ρ_w	Density of water
ν_w	Kinematic viscosity of water
f	Laser focal length
d	Distance from laser head to the water tunnel's side wall
U_∞	Component of the free-stream velocity parallel to the x-axis

U_∞	Component of the freestream velocity parallel to the y-axis
$\Delta x, \Delta y, \Delta z$	Laser control volume dimensions
b	Breadth of the water tunnel
Re	Reynolds number
$\bar{c}$	Mean aerodynamic chord of the aircraft's wing
x_n	Distance along the aircraft or model as measured from the tip of the nose
ℓ	Total length of the aircraft or model

Chapter 1

Introduction

1.1 Background and Motivation

At moderate to high angles of attack, modern fighter aircraft fly under complex flow conditions, created largely by three-dimensional flow separation from their the wings, fuselage and control surfaces. Such conditions have a significant effect on the handling characteristics and the structural integrity of the aircraft.

The F-18 (Figure 1) is a highly maneuverable fighter aircraft, employed in the military service of many nations worldwide. In Canada, the aircraft is designated the CF-18. The excellent maneuverability of the aircraft is due in part to its slender forebody, delta wing configuration, and twin tails. To generate additional lift at high angles of attack, the aircraft is equipped with two

very low aspect ratio, highly swept Wing Leading Edge Root Extensions (LEX), attached to the fuselage just ahead of the main wings.

The sharp, highly swept, leading edge of the LEX generates a vortex, which flows downstream approximately parallel to the LEX, separating from the aircraft at high angles of attack. A typical LEX vortex trajectory is shown in Figure 2.

Large vortices are also generated by flow over the fuselage forebody, which has an oblate, elliptical cross-section that tapers into an ogive nose-cone of circular cross-section. In general, the flow splits at the nose and runs along the cylinder until it separates and forms two counter-rotating vortices (Ramirez, 1990). The forebody vortex location on one side of the aircraft is also shown in Figure 2.

While these vortical flows provide the benefit of increased lift, they may also have an adverse effect on control and maneuverability, because of their interactions with each other and with the aircraft. One example of this is buffeting of the vertical tails. The LEX vortex core stagnates, suddenly increasing in diameter as it bursts, upstream of or between the vertical tails. The resulting chaotic flow impacts on the vertical tails causing large and sometimes uncontrollable vibrations.

NASA initiated the High Alpha Technology Program (HATP), which used wind tunnel testing of scale models, CFD codes, as well as full scale flight testing of a highly instrumented F-18 (High Alpha Research Vehicle, or HARV) to study these vortex flows and their effects on the flow field surrounding the aircraft. Its

main objective was to develop a greater understanding of these phenomena that would assist the prediction and control of the vortex flows on present and future aircraft designs (Fisher et al. 1990a).

All of these studies, and many others not related to the HATP, have dealt with a clean F-18 wing (with no stores), and concentrated on the behaviour of the flow on the top side of the aircraft, where flow separations occurs.

In its combat role, the F-18 carries a multitude of stores and pylons on the underside of its wings and fuselage, such as fuel tanks, bombs, and missiles, of various shapes and sizes. The flow-fields generated by the stores interact with each other, which may result in very complex aerodynamic flow phenomena. Very few studies have been carried out on the flow beneath the wings.

The first step towards understanding the complex flows about the CF-18 is to identify their structures and locations relative to the aircraft. Although natural visualization of the LEX and forebody vortical flows on full scale aircraft is sometimes possible when they fly on days of appropriate temperature and humidity, controlled studies can only be performed in the laboratory (in wind tunnels or water tunnels), or on a highly instrumented, and thus expensive, aircraft such as NASA's HARV. Pressure and force measurements can then be made in the areas of interest, and flow visualization can be performed.

One of the major advantages of using a water tunnel over a wind tunnel for scale model studies is the convenience of flow visualization. In order to visualize the flow near the aircraft model in a wind tunnel, small particles are injected into the air upstream of the model, however, they tend to diffuse very quickly in

high energy regions, such as the vortices. In water tunnel studies, the lower velocity allows the visualization agents to follow the flow patterns accurately for a longer time and distance. A wide variety of methods exist for flow visualization in water. These include dirt particles suspended in the water, hydrogen or other gas bubbles, and many types of dye, including water-based and non-Newtonian, fluorescent and non-fluorescent, permitting clearer visualization of flow patterns, which makes their interpretations much easier.

The difference in Reynolds number between the full scale CF-18 in flight and a model of the aircraft in a water tunnel is too large to permit even a rough estimation of dynamic similarity using the model. There will certainly be differences between the laminar flows in the water tunnel and the corresponding turbulent flows in flight, especially in the viscous flow regions close to the model, where the stores are located. In addition, compressibility effects experienced by the full scale CF-18, operating at high subsonic speeds, will be absent in any water tunnel studies.

Despite these differences, it still seems worthwhile to conduct water tunnel studies of low Reynolds number flows around the forebody, LEX and stores of the CF-18. In particular, as few flow visualization studies have been performed on the stores, any information regarding their effect on the flow would be useful. The development of computational codes dealing with the CF-18 could also benefit from such results. It is customary to test the initial stages of development of high Reynolds number CFD codes using low Reynolds number flows, because of the reduced requirements in terms of grid size, computing time, and computer memory.

1.2 Objectives

The primary objective of the present study is to carry out a visualization study of the flow field around a model of the CF-18 fighter aircraft in a water tunnel facility. Of particular interest is the flow around the LEX and fuselage of the model at moderate to high angles of attack, and around the stores and pylons on the lower surface of the aircraft at low angles of attack.

Secondary objectives of this study, and prerequisites to the primary objective, are to document the flow characteristics of the unobstructed water tunnel, to develop and implement the methods of flow visualization best suited for use in this facility, and to design accessories to the water tunnel capable of positioning and traversing both the model and the visualization tools in a satisfactory manner.

1.3 Thesis Organization

This thesis is divided into six chapters for clarity of presentation. The first chapter contains an introduction to the flow phenomena of interest on the CF-18 fighter aircraft, and specifies the objectives of this study. Chapter 2 presents a review of the vast amount of relevant unclassified literature on the CF-18. The experimental facilities, accessories and techniques are described in Chapter 3, along with an error estimation for each component.

Flow quality measurements and flow visualization photographs are presented in Chapter 4. The flow visualization results are discussed in Chapter 5, and conclusions drawn from these results appear in Chapter 6.

Five appendices follow these chapters. Appendix A compiles the technical drawings created specifically for this study, including, first and foremost, the model positioning system. Appendix B compiles drawings and sketches relating to the water tunnel in general, while schematics for the electronic circuits designed for this study are presented in Appendix C. Appendix D lists some general procedures for mounting and dismounting the model and flow visualization components, and Appendix E contains a record of the Tecplot data files used to generate the aircraft frame, stores and the dye lines used in the analysis.

Chapter 2

Literature Review

As a fighter aircraft serving a worldwide domain, the F-18 has been studied in many facilities in many nations. Most studies overlap in their focus on the flows that have the greatest effects on the aircraft. As such, the LEX and forebody vortices, because of their strong effects on the maneuverability and structural integrity of the vertical tails, have been especially scrutinized, by means of force and pressure measurements along the length of the unburst and burst vortical regions, and by flow visualization of the vortex structures. The flow around the aircraft's stores has been studied with much less intensity, and only a couple of limited-scope flow visualization studies are available in the open literature.

2.1 Leading Edge Extension (LEX)

The leading edge extension is a high angle of attack lift augmentation device employed by the CF-18. According to Hebbar and Leedy (1992), stable vortical flow is induced above the main wings at high angles of attack by the LEX. While the main wings would normally stall at these angles, the lower pressures that are created on their upper surfaces by the LEX vortices increase lift, and delay massive flow separation (stall) to even higher angles of attack. Thus this very highly swept, very low aspect ratio wing has been credited with greatly increasing the aircraft's maximum lift coefficient. Due to the interaction of the vortical flow the LEX produces with the tail control surfaces, it has also been credited with enhancing maneuverability (Lee et al, 1990). These same vortices, however, are amenable to "bursting", which is the source of highly complex turbulent flow, and can lead to severe buffeting of the vertical tails.

The LEX vortex rolls up along the LEX leading edge, following a path roughly parallel to the leading edge along the fuselage (Fisher et al, 1990b). At a location along this path, which is highly dependent on angle of attack, the vortex bursts (Figure 3). Photographs of the LEX vortices (by, for example, Erickson, 1991, Fisher et al, 1990b, and Del Frate et al, 1990) show that they are very tightly wound. One of these photographs has been reproduced here in Figure 4. Del Frate et al (1990) describe the bursting phenomenon as "a stagnation of the core flow with a sudden expansion in core diameter," which is distinctly visible in the photographs shown in Figures 3 and 4.

The change in LEX vortex bursting location with angle of attack has been studied by many authors. For example, Wentz (1987) showed that the LEX vortex bursts just ahead of the vertical tails at an angle of attack of 25°. Data from Del Frate et al (1990) and Fisher et al (1990b) show that bursting occurs farther upstream as the angle of attack is increased. Hebbar et al (1992) studied a dynamic model using a variable pitch system, which showed that with a pitch-down motion, bursting occurs closer to the LEX apex than in the static case, while during a pitch-up motion, bursting occurs farther from the LEX apex. The effects became more pronounced as the pitch rate was increased. Magill et al (1996) added to this by studying simultaneous model motions in pitch and yaw.

Shah (1991) showed that significant changes in the LEX vortex structure and location could be produced by relatively small changes in LEX span and chord.

It was postulated by Ghaffari et al (1993) that the pressure gradient formed by the vertical tails themselves may cause the vortex to become unstable and burst, with the chaotic flow that results loading the vertical tails in an unsteady manner. Yet removing the aircraft's vertical tails, as in experiments performed by Wentz (1987), had negligible effect on the flow field, and the vortices burst at the same location as with the tails attached. However, after removal of the wings of the aircraft, the vortices were located farther inboard, and refrained from bursting up to angles of attack of 30°, indicating that the adverse pressure gradient produced on the wing is dominant in the vortex bursting process. Oil streak surface flow visualization on the LEX and upper wing surface by Lee et al (1994), Lee and Marineau-Mes (1996) and Brown et al (1990), show that indeed the LEX vortex is prominent on the wing's upper surface.

Erickson (1982) studied the effect of wing sweep and angle of sideslip (yaw) on the vortex trajectory, and found that the vortex follows the wing sweep angle in a linear fashion, becoming parallel to it at high angles of attack, and that an asymmetry of the vortex core with respect to the aircraft plane of symmetry can form even at small angles of sideslip. The asymmetry due to yaw causes the windward vortex to burst much closer to the LEX apex than it normally would, showing that bursting location is not only a function of angle of attack, but also of sideslip. It was further shown that downward leading edge flap deflections tended to stabilize the LEX vortices, while downward deflections of the trailing edge flaps tended to destabilize it.

Thompson (1990) was unable to determine any significant effect of flap settings on the LEX vortex. Neither did airbrake deployment position (see Figure 1) nor horizontal stabilizer deflection angles seem to have any effect on vortex bursting location. The variation of engine inlet flow rates, however, drastically altered the structures and locations of the LEX vortices. It has been noted by Thompson (1990) that a realistic flow field will only result by simulating flow through the model's engine inlets. It was reported that the F-18 inlet velocity ratios (V_I / U_∞, where V_I is the inlet velocity and U_∞ is the nominal free stream velocity), for typical air combat maneuvering periods at angles of attack higher than 15°, were greater than 3.0 for more than half the period, with a peak value of 5.5. These velocity ratios were tested with the model in that study. An increase in the engine inlet ratio moved the LEX vortex bursting location downstream, by as much as 20% of the aircraft length at high values. The bursting location was drawn closer to the aircraft. Martin and Thompson

(1991) observed complex flows for no engine inlet flow, and conventional patterns were seen until $V_j/U_\infty = 8.1$, when flow was drawn from the upper to the lower surface and entered the engines.

In addition to tail buffet load alleviation, other goals of these LEX vortex studies were to understand the flow in the vicinity of the LEX in order to increase controllability of the aircraft. Empirical testing of the aircraft led to the development of the LEX fence (Erickson, 1991), a small trapezoidal fin that sits perpendicular to the LEX, just ahead of its junction with the main wing (see Figure 1).

According to studies performed by Erickson (1991), the LEX vortex breakdown appears to be more gradual with the fence in place. The fence also reduces the turbulence level within the burst flow, while only minimally affecting the aircraft's aerodynamic and stability characteristics at subsonic and transonic speeds. According to Shah (1991), the LEX fence separates the LEX vortex into two co-rotating vortices, the interaction of which tends to move the vortex system outboard, away from the tails. As the energy of the vortex is spread over a larger region, the burst vortical flows which do impact on the vertical tails have less rotational kinetic energy than they do without the fence.

Bean et al (1993) showed that Tangential Leading-Edge Blowing (TLEB) along the LEX can reduce the effective angle of attack of the vortex, relocating it inboard, and reducing its strength from the leading edge.

CFD predictions of the flow around this complex aircraft have generally been difficult to produce. However, while computational models of the entire aircraft

still experienced difficulties, models of the aircraft body forward of the wings have recently been able to accurately predict LEX vortex paths and structures. Cummings et al (1992) have made such predictions, which agree well with in-flight data.

2.2 Forebody

The slender ogive cylinder shape of the CF-18's forebody causes two counter-rotating vortices to form. The forebody vortices are similar to the LEX vortices in structure, but they follow slightly different paths, passing symmetrically over the aircraft's canopy, with their stable cores remaining very close to the surface of the aircraft (Fisher et al, 1990b).

The F-18 High Alpha Research Vehicle (HARV) used by NASA in its High Alpha Technology Program (HATP) has been flown numerous times to provide flow visualization records of the forebody and LEX vortices. Separation and reattachment lines caused by the forebody vortices are shown by surface flow visualization, using dyes emitted by small holes in the aircraft forebody. Photographs of these lines can be found in reports by Fisher et al (1988), Fisher et al (1990a), Fisher et al (1990b), Fisher and Meyer (1988), Del Frate et al (1990) and Bjarke et al, 1992). One of these photographs has been reproduced in Figure 5. Results from numerical simulations by Thomas et al (1989) are included in this figure for comparison purposes. It can be seen that the computational results correlate well with the data from the HARV. The CFD results also correlate well with pressure measurements taken by the HARV

instruments, indicating that these studies can help verify evolving numerical codes.

It was detected in flight tests that a small yawing motion can produce a large corresponding asymmetry between the vortex trajectories with respect to the aircraft's plane of symmetry. Yet, even in the absence of sideslip, it has been reported that the forebody vortices can become asymmetric. Erickson (1991) reported asymmetric pressure distributions along the forebody at high angle of attack, indicating that one vortex had moved towards the forebody surface, the other slightly away. Fisher et al (1990b) observed wing rock at an angle of attack of 45°, attributable to alternating asymmetry in the forebody vortices.

Sufficiently far from the nose, the trajectories of the forebody and LEX vortices are close enough that they can influence each other. When the two vortices interact, the forebody vortex is pulled beneath the LEX vortex, and is then redirected outboard (Del Frate et al, 1990, Fisher et al, 1990b). This indicates that the forebody vortex is the weaker of the two. This agrees with data from Wentz (1987), which showed that the forebody vortex has lower circulation than the LEX vortex.

At an angle of attack of 30°, the point of interaction of these two vortices is just aft of the LEX-wing-leading-edge-flap junction (Del Frate et al, 1990, Fisher et al, 1990b), and it moves forward as the angle of attack is increased. If the LEX vortex is eliminated, by removing the LEX altogether (Wentz, 1987), the forebody vortices burst at angles of attack above 20°. However, the burst

forebody vortices remain close to the fuselage centerline even at high angles of attack, resulting in a weaker interaction with the tails.

Suarez and Malcolm (1994) studied methods of forebody vortex control. They found that jet blowing in the nose region affected the directional stability of the forebody vortices, increasing or decreasing asymmetry, depending on where the blowing took place. A single rotatable tip strake produced early separation of the forebody vortex, thus giving better directional control. Even better control was achieved by using a pair of rotatable tip strakes. Finally, a single vertical nose strake had a tendency to restore symmetry to the forebody vortices at high angles of attack.

2.3 Stores

Stores may be carried by the CF-18 in order to complete many types of missions. Coupled to the wings by pylons, these attachments can take the form of various combinations of missiles, bombs or fuel tanks.

Early fighters used to carry their stores in a cargo bay. Present day fighter aircraft, however, normally carry external stores. Such stores are much more versatile: they may be easily interchanged, require much smaller carriage spaces (Ozcan et al, 1995). However, external stores create additional drag, and the flow-field in the vicinity of the stores is extremely complex.

Ozcan et al (1995) studied an external bomb carriage used by the Turkish Air Force. Larger forces were measured on the aircraft when mounted with rocket launchers than with bombs. Surface flow visualization on a non-axisymmetric

carriage produced separation and reattachment lines. Streamlines were reconstructed from those lines, showing vortical patterns around the stores. CFD of the same carriage correctly produced the velocity field, and was verified using the flow visualization results. Additionally, CFD analysis predicts other flow features, such as large-scale vortices, attributed to inviscid separation from the sharp edges, and small scale-vortices, attributed to cross-flow separation of the boundary layer.

Studies of forces caused by stores have been performed by Marsden and Haines (1967), Stahara (1980), and Dollyhigh et al (1978), who measured the drag of elliptical stores on an F-16. Furthermore, Chen and Liu (1990) developed a computational method for predicting the flow around stores, the results of which compared well with force data, and Monta (1980) found that adding stores, such as Maverick missiles, MK-84 bombs and external wing fuel tanks, to an F-16 resulted in changes in the aircraft pitching moment.

Pressure measurements in a wind tunnel by Dowgwillo et al (1996), using pressure sensitive paint on an F-15 aircraft model were performed for various stores, such as LANTIRN pods, AIM-9 missiles and conventional bombs. Low pressure regions were observed in the areas of blunt store shoulders, sensor pods, the bulged landing gear door and the inboard store boat-tails. Regions of high pressure were observed around the forebody, engine inlets, outboard store boat-tails, and the store's nose. Most tests were performed with the central fuel tank mounted. Removal of this tank caused a significant change in the pressure field about the mid-stores, but little change in pressure around the outboard stores.

According to Tijdeman et al (1979), wing-tip missiles can be treated as endplates, increasing circulation and loads on the wing surface. According to Haines (1980), clustering stores together can increase drag by a factor of 1.75 to 1.9 from the drag on individual stores.

Pylons are used to carry stores for military aircraft, but different models of pylons are also used to carry the engine nacelles of commercial aircraft. The pylons on a low wing transport model was studied by Naik and Ingraldi (1993), with no nacelles attached. Three pylon shapes were studied, an airfoil design, a "compression" design (with a maximum thickness at the wing's trailing edge) and a hybrid, with the airfoil shape along the outboard side and the compression shape along the inboard side. With these shapes, and the pylon trailing edge extending aft of the wing trailing edge, the pressure distributions obtained were very close to those obtained for a clean wing. This implies a small loss of lift and minimum flow separation at the pylon-wing junction.

Results from a CFD study by Kaykayoglu and Yalcmel (1996) suggest that the store wake would deflect upward near the store trailing edge at positive angles of attack, and continue to rise downstream. At negative angles of attack, it is predicted that the wake would once again deflect slightly upward at the store trailing edge, but then it would follow a steep downward slope as it moves downstream. For positive angles of attack, the lateral size of the wake increases with increase in angle of attack. Additionally, the presence of the store generates its own vortical patterns, which interact with the wing-tip vortices.

Several other CFD methods have been developed for determining the interaction of stores with each other, the pylons and the entire aircraft (AGARD, 1995). There seem to be as many methods as there are studies. Most of these methods isolate the local flow around the store from the global flow around the aircraft, yet link these two systems together by combining adjoining nodes or imbedding one into the other. Very few of these codes have been validated by flow visualization data. The reader is directed to the AGARD Stores Conference Proceedings for further details (AGARD, 1995).

2.4 Justification of Water Tunnel Studies

Traditional studies of the vortical flow field around fighter aircraft have been performed in wind tunnel facilities (e.g.: Erickson et al, 1989) or in full scale flight tests (e.g.: Fisher et al, 1990b). Though tests of the F-18 have been performed in water tunnels (e.g.: Thompson, 1990), these facilities have typically been excluded from force and pressure measurement studies because of their inability to simulate compressibility effects, and their restriction to low Reynolds numbers. This prevents dynamic similarity of model studies and full-scale investigations, and makes correlations between the tests and the full-scale flows difficult.

Some phenomena, however, may be represented by water tunnel results, especially when considering the qualitative nature of flow visualization.

As the LEX vortices originate on the sharp leading edge of the LEX, where flow separation occurs regardless of whether the flow is laminar or turbulent,

the generation of the LEX vortices will be accurately represented in the water tunnel. According to Erickson (1982), water tunnel studies of these vortical flows are best suited to high angle-of-attack configurations, when the vortex is much larger than the wing boundary layer thickness, and the vortex is located far from the wing.

Erickson (1982), Lowson and Riley (1995), and Thompson (1990), among others, have shown that LEX vortex characteristics, such as bursting location, are essentially independent of Reynolds number at high angles of attack. LEX vortex breakdown locations are shown for the full-scale HARV, wind tunnel and water tunnel tests for high angles of attack in the graphs given by Del Frate et al (1990) and by Erickson (1980), reproduced here in Figure 6. Ramirez (1990) reported that no appreciable change in the vortex core location could be observed with a variation of the Reynolds number. Even force measurements in the water tunnel at high angles of attack, as measured by Suarez and Malcolm (1994), showed good correlation with wind tunnel and full-scale flight data, indicating near independence from Reynolds number.

The effect of Reynolds number change on flow interactions due to the stores has not been studied. Phenomena that occur close to the surface of the model are known to be sensitive to Reynolds number variation (Erickson, 1982). Other events, however, can be expected to be comparable in low-speed water-tunnel and high-speed wind-tunnel studies. In view of the limited knowledge available on the flow beneath the F-18 wing carrying stores, any information obtained in the low-Reynolds number regime could still be useful, for example, in the validation of emerging CFD codes.

2.5 Flow Visualization

Normally, the flow around the model is invisible, because its optical properties are no different from those of the surrounding fluid. Introducing particles into the flow, such as smoke, mists, bubbles or dyes, allows the visualization of the model's wake and other vortical patterns.

Unfortunately, the injection of particles into the flow introduces some disturbance of the flow by the injection device. This necessitates a very small injection tube, to avoid the formation of a large wake. Merzkirch (1987) reports that Pitot tubes and hypodermic needles are suitable for injecting dye into water, because of their very small outer diameters.

Dye is well suited to the visualization of low-speed water flows because it is neutrally buoyant, has good visibility and low diffusivity (Merzkirch, 1987). Dye injected into the flow traces out streaklines, which flow downstream over the model. The dye will be neutrally buoyant in water if it has a large water base, preferably taken from the water tunnel itself. Good visibility can be achieved by using a dark dye on a light-coloured, well-lit background. As the dye flows downstream, however, it tends to diffuse, which makes it more difficult to see. Apparently, adding milk to the dye mixture can increase its stability in shear flows (Merzkirch, 1987).

There are alternatives to the standard water-based or alcohol-based dyes. Hoyt and Sellin (1995, 1996) experimented with many different chemical combinations, such as aqueous polyethylene oxide (PEO) solutions, in an attempt to create a fluid with the same optical properties as water, and as many

of its physical properties as possible, but which would hold together in high shear flows. The result was a water-based non-Newtonian fluid which became thicker as shear increased, allowing it to follow mixing flows more visibly.

A fluorescent dye offers excellent visibility when illuminated by a laser at a wavelength to which it is sensitive. Dyes such as rhodamine and fluoresceine, which emit light only at specific wavelengths, different from that of the incident light, are used for this purpose. For optimal photography of the flows, a film that is highly sensitive at these wavelengths should be used (Merzkirch, 1987).

Extensive release of dyes into a closed circuit facility may contaminate the water, thus necessitating occasional replacement of the water.

A method for visualizing the flow without contamination is by generating hydrogen bubbles. As the bubbles are produced by the electrolysis of water, they are either absorbed back into the water, or rise to the surface and escape, farther downstream.

Applying a dc voltage between two submerged electrodes ionizes the water in their vicinities, with oxygen ions being attracted to the anode, and hydrogen ions being attracted to the cathode (Merzkirch, 1987).

As hydrogen is released at double the volume of oxygen, hydrogen is the desired tracer. The cathode is thus made into a very thin wire stretched across the length of the section to be visualized. Hydrogen bubbles form along the thin wire and are swept downstream by the flow. Because of their small size, they follow the flow well, with the only other force acting on them (other than low viscous drag) being buoyancy. Pulsing the voltage in the wire can produce

timelines in the flow. Covering sections of the wire, or creating kinks in it, will produce streaklines. A carbon rod can be used as the anode, and should be placed downstream to avoid disturbing the flow.

As the wire cathode is typically on the order of 0.05 mm or smaller, and the bubbles are of comparable sizes, the disturbance to the flow field is minimal.

2.6 Conclusion

The flow about the F-18 has been studied by many investigators in laboratories worldwide. A large number of studies have focused on the LEX and forebody vortices, simply because they have the strongest effect on the aircraft's performance. Thus a wealth of information exists for the study of the aircraft's upper surface. The flow near its lower surface, however, remains relatively unexplored. Visualization of the flow past a model of this aircraft would be performed best with dyes or hydrogen bubbles, as the flow in the areas of interest is expected to be laminar at the speeds used in the water tunnel.

Chapter 3

Facilities and Experimental Procedures

Flow visualization experiments were performed in the new water tunnel facility at the University of Ottawa using dyes and hydrogen bubbles on a 1:48 scale model of the CF-18 aircraft, with a clean wing, or carrying various stores, while immersed. A laser Doppler velocimeter was used to measure the flow velocity at various positions in the water tunnel.

3.1 Water Tunnel Facility

The water tunnel at the University of Ottawa (Figure 7) is a closed-circuit, recirculating facility capable of holding up to 16 m^3 of water. It has a test section approximately 4 m long, with a cross-section 0.50 m wide and 0.75 m high. It is enclosed on three sides by 9.5 mm thick glass walls, while the top surface is open

to the air, but may be covered by removable Plexiglas sections. All instruments and models are placed in the test section from the top.

The flow is produced by a Cascade 0.3 m (12") diameter axial flow pump, which is driven by a 5.6 kW (7.5 hp) GE motor, providing a maximum head of 2.13 m (7 ft) at 126 rad/s (1200 rpm). A Siemens Relcon Q2000 motor controller allows the flow rate to be varied in order to give test section velocities between 0.05 m/s and 0.30 m/s respectively, at a water height of 0.70 m.

Water is first pumped into a large settling chamber, where it passes through two perforated plates and one plastic screen of different solidities in order to even out the flow non-uniformity, and to dampen any vortices or other large scale motions. The flow is then accelerated through a three-sided contraction (the top surface remains free), which changes the passage area from 1.5 m by 2.4 m to 0.5 m by 0.75 m over a 1.5 m length. After passing through the test section, the water recovery tank redirects the flow through a large pipe below the tunnel back to the pump. A window is located at the back of the water recovery tank for viewing from the downstream end.

The facility uses several devices to reduce flow disturbances in the test section. Besides the screen and two perforated plates, a vertical perforated cylinder in the settling chamber allows the water coming from the pump to be dispersed along its entire depth. The cylinder was wrapped with another plastic screen of relatively high solidity to pressurize the fluid in the cylinder, and thus even out its exit velocity. A plunger is located inside the perforated cylinder, to absorb the vertical momentum from the inrushing water. The plunger was

submerged to prevent air from entering the water through the turbulent mixing that occurs in this area. In the test section, boundary layer removal slots were mounted flush with the glass along the walls and floor, at two downstream locations. Water is drawn from the boundary layer at these locations by a 124 W (1/6 hp) pump situated under the recovery tank. Once the flow enters the recovery tank, it is directed to the sides by two vanes, where it is drained to the pipes below without disturbing the main flow area. Once again, vertical perforated cylinders and plungers permit a smooth and airless flow out of the tank.

3.2 Water Tunnel Utilities

3.2.1 Water Treatment and Suction

The 124 W (1/6 hp) pump, mentioned above, serves as an independent suction device for the tunnel. This is advantageous in that it can also serve as a utility pump, which can be used at any time, whether the main pump is in operation or not. Water from the tunnel is filtered and chlorinated in this way, and a suction tube is run by this pump to remove any deposits on the tunnel floor. A diagram of this setup is shown in Figure 8. When running unattended, the small pump is controlled by a timer that allows it to draw water for filtering and chlorinating, on a 12 hour schedule, normally 6 hours on, followed by 6 hours off.

The same pump also produces the suction that was used to draw water from the aircraft model engine inlets. Because this pump does not use a controller, as

the main pump does, the valves that direct the flow to the filter, chlorinator and boundary layer devices have to be adjusted until the desired flow rate is obtained.

3.2.2 Traversing System

Steel rails are mounted on the frame of the water tunnel, allowing carriages to move along the length, width and depth of the test section, providing access to every location therein. Two cylindrical rails mounted above the test section permit smooth manual positioning of a carriage along its longitudinal (x-) axis (see Figure 9). A second carriage runs along rails normal to the first set, atop the x-axis carriage, from one side of the test section to the other, along its transverse (y-) axis. Instruments were attached to a vertical vernier mounted to the y-axis carriage for this study to provide access to a partial tunnel depth. Between these carriages, each equipped with its own scale, readable to 0.5 mm, instruments can be placed at any position inside the tunnel.

There is provision to add a second traversing system along the length of the tunnel on its side, and also a third one below the test section.

3.2.3 Model Positioning System

The model positioning system, based on an earlier design by Zwart (1995a), provides precise rotation in the pitch and yaw axes (Figure 10). It was designed to keep the center of rotation of the model, namely the wing leading edge-LEX junction, in the same place through changes in both axes. For this study, the center of rotation is located at half the full water height, or 0.35 m from the

bottom. Thus, the pitch-controlling C-strut is actually an arc that makes up part of the circumference of the circle centered on the model's center of rotation. The C-strut is mounted on a plate which can rotate the model in yaw relative to the fixed mounting brackets. The complete set of drawings for this system, including dimensions, is presented in Appendix A.

The model positioning system is mounted above the tunnel, thus avoiding the need for complicated mounts inside the test section. However, this leads to a conflict with the x-axis carriage and could present problems for experiments that require the carriage to be directly above the model. To resolve this, in the future, the entire system can be modified for mounting inside the tunnel, although a drop in the water level may then be necessary in order to maintain the model near the flow centerplane.

A pointer mounted on one of the C-strut supports indicates the pitch location, scribed to half degree increments on the C-strut, through its full range of 40 degrees. The ± 30° yaw position, scribed to one degree increments, is indicated by a pointer on the mount base.

3.3 Model

Because of their reputation for accuracy, plastic hobby models have often been used for flow visualization, force and pressure measurements in small scale studies of the CF-18 fighter aircraft. Thompson (1990) and Ramirez (1990), among others, have verified the accuracy of various hobby models.

Two identical 1:48 scale plastic hobby models by Revell (CF-18 Hornet D-Day version, model number 05629-0389) were used for this study, modified to allow

mounting onto the sting and for engine inlet flow. One was used for lower surface (store) flow studies, and the other was used for upper surface flow studies. The leading edge and trailing edge flaps were kept at 0°, and the horizontal stabilizers were attached to the model at 0°. The LEX fence was used in all configurations.

3.3.1 Model Sting

The sting was comprised of three pieces, namely a block of aluminum which connected two aluminum rods (Figure 11). One of these rods was attached to the C-strut of the model pitch mount, and was threaded so as to allow small corrections in the model position. The second rod was attached to a stainless steel plate at the rear of the model, axial to the model, and was threaded for small positioning corrections or changes in the roll angle. For added stability, the stainless steel plate was screwed into another stainless steel plate inside the model, through one of the engine outlets.

3.3.2 Errors in Model Positioning

The pitch of the aircraft is defined as the angle between the line connecting the tip of its nosecone to the centerline of its engine nozzles and the horizontal direction. It has been verified that the undisturbed flow direction was horizontal.

The pitch of the model was adjusted often during this study, so it was essential to determine the actual pitch angle. Scale marks were scribed onto the C-strut with an accuracy of ±0.1°, using a computer generated template. The

pitch pointer could be positioned up to 0.5° along the C-strut, so that the 0° pitch line would correspond to a scribed mark, as this line will vary from one mount to another, depending on how the mount is built. As this was done by eye, the estimated uncertainty in the positioning system pitch angle was ±0.2°.

The model sting was attached to the C-strut and the model with a set of nuts, turning the entire pitch assembly into a rigid body. Thus the sting did not contribute any errors to the pitch angle. However, measuring the exact 0° pitch angle was found to be a difficult process, and was only accurate to ±1°.

The yaw rotation feature of the positioning system was not used for this study. The 0° yaw angle was located by scribing a line, using a milling machine, between the center of rotation and the pointer, parallel to the positioning system's machined edge. The position of this mark is accurate to 0.007°. However, the pointer was positioned along the mark by eye, for which the estimated uncertainty is ±0.1°. The scale marks were again scribed onto the mount using a computer generated template, with an accuracy of ±0.1°. The positioning system was mounted to the tunnel using a dial guage, dowels and a level, to ensure that its axes were parallel to the tunnel axes. The overall uncertainty of the yaw angle due to the positioning system was ±0.2°.

The model was aligned in yaw with the positioning system by eye, and was accurate to approximately ±0.5°, while at 0° pitch angle. This uncertainty increased as angle of attack was increased, until, at 40°, the uncertainty was about ±1.5°, due to the method used.

3.3.3 Engine Flow

To allow simulation of the flow through the aircraft's engines, the original model engine inlets were cut open to their maximum size. Plastic tubing of 6 mm (1/4") interior diameter was inserted into each engine inlet and attached to a Y connector. This allowed the flow to exit the model through a single engine outlet, as the second outlet was being used by the sting (Figure 12). The plastic tube then ran from the model engine outlet to the 124 W (1/6 hp) pump for suction (see Section 3.2.1).

An engine inlet ratio of unity was used for this study, making the flow speed through the engines the same as the tunnel speed. Thus both the tunnel water speed and the engine inlet speed were 0.070 m/s, as measured in Section 4.1.2.

Ramirez (1990) gave the single engine inlet area of a full scale F-18 at high angles of attack to be 0.394 m^2 (610 in^2). Scaled to the model size, this gives an engine inlet area of:

$$0.394\ m^2 \times (1/48)^2 = 1.71 \times 10^{-4}\ m^2$$

Assuming that the area does not change significantly from high to low angles of attack, the desired volume flow rate can be calculated simply by multiplying the model engine inlet area by the engine inlet velocity and doubling the result (for two engines):

$$Q = 1.71 \times 10^{-4}\ m^2 \times 0.070\ m/s \times 2 = 2.39 \times 10^{-5}\ m^3/s.$$

The volume flow meter available on the water tunnel was scaled in gallons per minute (gpm), so it is useful to convert this result into 0.380 gpm.

The exact inlet flow velocity used was 0.4 gpm, resulting an inlet velocity ratio of $V_I / U_c = 1.05$ for all configurations in this study.

3.3.4 Store Configurations

The CF-18 aircraft is capable of carrying stores at nine stations underneath its wings and fuselage. These are labeled 1 through 9, beginning at the port wing-tip (Figure 13). On each wing, stores can be carried on the wing-tip and at two locations directly under the wing (an outboard and an inboard store). Additional stores can be carried on the fuselage beside the engines and one store can be carried along the aircraft centerline.

Nine different types of stores (including pylons) were tested while mounted on the aircraft model in eleven different configurations.

The pylons used in this study (Table 1) were scaled models of the SUU-63/A Wing Pylon and the SUU-62/A Centerline Pylon. The wing pylon alone was capable of carrying only one store; however, when a BRU-33/A Vertical Ejector Rack (VER) was attached to the pylon, two stores could be carried at one station.

The stores used in this study (Table 1) were scaled models of the 330 US Gallon External Fuel Tank (330 USG EFT), the Aim 7 Fuselage Missiles and Aim 9 Wing-tip Missiles, the MK82 and MK83 bombs and the GBU-12 bomb. The first configuration studied was the clean wing, that is, completely without stores, to be used as a reference configuration. The eleven configurations, including the clean wing, are shown in Figure 14, and are summarized in Table 2.

Note that photographs were only taken of stores placed at stations 5 through 9, because the camera was best suited for photography on that side of the aircraft. In view of results showing little mutual effect of stores on the same wing (see Chapter 5), it is unlikely that stores on one wing would measurably affect the flow around stores on the other wing.

3.4 Visualization and Measurement Instrumentation

3.4.1 Dyes

Many different dyes were tested for use in this study. Just a few grains of the powdered dyes Methyl Violet, Congo Red or Fluorescein Sodium Salt in a 1.5 x 10^{-3} m^3 volume of water produced a solution concentrated enough to be visible in the small flow visualization streak. Congo Red did not stay mixed and was therefore not used in this study. Methyl Violet produced a deep purple dye stream that could be seen best with the direct lighting of a normal phosphorescent light bulb. Fluorescein Sodium Salt was best seen when illuminated by the laser. All of these dyes were neutrally buoyant in the water tunnel.

A non-Newtonian fluid was produced according to the recipe provided by Hoyt and Sellin (1995, 1996). This fluid is reported to have properties comparable to those of water except for its shear-thickening property, whereby the fluid becomes more viscous and has less diffusion when exposed to high shear. It was thought that this fluid could be useful in highly chaotic areas

around the model. The formulation for each of the chemicals used in this fluid is given below.

To create a 2% solution of C16TASal. 5 mL of cetyltrimethyl-ammonium bromide was dissolved into about 400 mL of distilled water. resulting in a cloudy solution. Five mL of sodium salicylate was added to this solution. The final 500 mL solution was achieved by slowly adding more distilled water.

In a second container. a ½% PEO solution was created by adding 1.25 mL polyethylene oxide to 200 mL distilled water. Distilled water was added until a 250 mL solution was achieved. The PEO dissolved overnight. without stirring.

These two solutions were then combined in the following ratio: 1 part PEO to 2 parts C16TASal to 4 parts distilled water.

The dyes Methyl Violet. Congo Red and Fluorescein Sodium salt were tested for colouring this mixture. Once again. however. Congo Red did not remain mixed with the solution. Both Methyl Violet and Fluorescein Sodium Salt performed very well. colouring the non-Newtonian filament so that it could be easily followed through the flow field.

It was found that the non-Newtonian fluid dissolved quickly in a large. unmoving body of water. Thus there was no concern that the fluid might contaminate the water tunnel. even after a substantial amount had been used. Contamination by the large amount of dye being poured into the tunnel also seemed to be negligible. as the large volume of water in the tunnel was not noticeably coloured throughout the entire period of this study. It is likely that the same process used to chlorinate the water also bleached the dye.

3.4.2 Dye Injection System

The dye was stored in two 1 litre cylindrical canisters, which were pressurized using the 550 kPa air supply available in the laboratory. For ease of access and refill, the canisters were located underneath the tunnel, attached to the steel frame. The dye was forced through plastic tubes up the side of the tunnel, through the free water surface, and injected into the flow through two injection tubes, of 0.39 mm inner diameter, at the desired location.

As the regulator on the high pressure air supply could not show small pressure variations, the pressure was adjusted in small increments until the dye leaving the injection tube produced a thin streak. All the adjustments were made by eye. A streak that expanded when introduced into the flow was considered to be faster than the water in the tunnel, while a streak that thinned out was considered too slow. The photographs taken after the dye injection had been calibrated in this way show that this process is fairly repeatable, as all dye streaks had approximately the same size. It may be estimated that the dye was injected into the flow at a speed within ±10% of the flow speed.

The dye traces out streaklines in the water tunnel, namely lines which are the locus of all the points in the water that have passed through the injection tube locations. In the case of steady flow, streaklines are identical to streamlines, which are tangential to the water velocity at every point (Kline, 1972).

In order to ensure proper positioning of the dye streak, a stainless steel tube was used as a rigid mount for the injection tube (Figure 15). The stainless steel

tube also contained the plastic tubing carrying the dye, and was bent into an L-shape to avoid disturbing the flow about the model. The tubing system was placed upstream and to the side of the model. The 6.4 mm diameter base of the injection tube was mounted to the tip of the L with a set screw. As the injection tube base tapered down to the 0.71 mm outside diameter of the injection tube exit, only the smallest tube ever neared the vicinity of the model that was being studied.

Horizontal motion for one injection tube, in both streamwise and transverse directions, was provided by the x- and y-axis carriages, while vertical motion was provided by the vertical traverse (see Section 3.2.2) mounted to the carriages by a 1 m long angle aluminum arm. The second injection tube was mounted on a two-axis (vertical and transverse) positioning system, located just upstream of the model positioning system. Figure 16 shows the relative positions of these systems above the tunnel.

Positioning of the dye tubes was very accurate and repeatable. The location of the injection tube mounted to the two-axis positioning system was controlled by two cranks, each with a dial guage readable to 0.01 mm. As the carriages were only built with scales readable to 0.5 mm, dial guages, readable to 0.01 mm, were used to locate the position of the other injection tube. Because the injection tubes were attached to the positioning systems by set screws, realignment after the set screws were loosened introduced higher inaccuracies. For this reason, the set screws were kept tight throughout a given store configuration.

A solenoid valve could be used to control the flow of dye into the water tunnel. An electrical switch permitted manual opening and closing of the valve, so a continuous streak of dye could be injected. A switch and timer combination also allowed the dye streak to be turned off automatically, providing small streaks and preventing dye waste between camera setups. A link to the camera allowed an exposure to be taken once sufficient dye had emerged into the flow. The pulsing feature did not work as expected, as once the valve was closed, the pressure that had built up in the line took a long time to be relieved. Thus the dye streak would not end abruptly when the valve was closed. The circuit diagram for this system is available in Appendix C.

3.4.3 Hydrogen Bubbles

The hydrogen bubble wire setup (Figure 17) included a power source, to provide electrolysis of the water, an electronic pulsing circuit, based on the design by Budwig and Peattie (1989), and the wire itself. The circuit diagram is shown in Appendix C. Voltage to the wire could be pulsed either by a trigger switch, to produce a single line of bubbles, or from the square wave output of a function generator. The latter method was used almost exclusively, producing short timelines of hydrogen bubbles at a frequency set by the generator, normally 7 Hz. This made the lines easy to follow as they were swept downstream.

A continuous sheet of bubbles forms a visible three dimensional sheet in the flow, however, the distinct pulsed lines were found to be more useful, as they could be illuminated in high contrast to the background. These timelines were

then followed as they twist and turn in response to various flow patterns, such as the LEX and forebody vortices, or obstruction by the stores.

A 0.40 m long, vertically mounted, hydrogen bubble wire was used to obtain large-scale flow visualization, required to determine the general flow quality of the tunnel. This wire was mounted between two flat plastic supports, attached to a thin plastic rod, which was placed inside a stainless steel tube for added stiffness (Figure 18). The bubble wire was mounted in such a way that it was in contact with a stainless steel screw. Voltage was then applied to the system through a wire leading from the pulsing circuit to this screw. All electrically conducting surfaces other than the bubble wire were coated with silicon sealer, for safety purposes, and so that they would not produce stray bubbles.

A shorter hydrogen bubble wire was used to visualize specific areas around the model, and was created variable in length, from 10 to 100 mm (see Figure 19). The 0.04 mm diameter wire was supported by two conducting pins, pressed into thin plastic plates for easy removal if the wire broke or otherwise needed to be replaced. One pin was soldered to an electrical wire, which led to the pulsing circuit. The plastic plates insulated the mount from the live wire. The position of each plate was locked in place with set screws along a stainless steel T, thus fixing the length of the wire. As was the case for the dye injection system, an L-shaped stainless steel tube was used to support the hydrogen bubble wire, in the same manner. A plug was mounted snug in the end of this tube, allowing the wire system to be mounted in either the horizontal or vertical direction, and was held in place with a pin. As with the other hydrogen bubble system, all

electrically conducting surfaces, other than the wire itself, were coated with silicon sealer.

As the bubble wire was mounted on the same system as the dye injection tubes, using an identical mount, it was subject to the same positioning uncertainty.

Hydrogen bubbles tend to rise in water, because of their much lower density. However, it is assumed that the Reynolds number based on their rise velocity is small compared to 1, so that their motion can be determined from Stokes' Law:

$$V_s = \left(\frac{g d_b^2}{18 \nu_w}\right)\left(1 - \frac{\rho_b}{\rho_w}\right)$$

where the water kinematic viscosity is ν_w = 1.0 x 10^{-6} m^2/s, the gravitational acceleration (g) is 9.81 m/s^2 and the particle density for hydrogen bubbles, ρ_b, is negligible compared to the density of water, ρ_w. Studies summarized by Merzkirch (1987) have shown that, in general, the size of the bubbles, d_b, is of the order of the wire diameter. Thus a wire diameter of 0.04 mm gives a rise velocity (Stokes velocity) of V_s = 0.87 mm/s, giving a Reynolds number of 0.035, justifying the use of Stokes' theory. Assuming that no extra vertical momentum is added by the flow speed of 70 mm/s, this velocity dictates that the bubbles would rise by 4.1 mm across the entire 330 mm length of the model, and by much less over the length of a typical store. Therefore, under the present conditions, hydrogen bubbles do indeed mark the flow accurately.

A common annoyance after several minutes of producing hydrogen bubbles was the buildup of contaminants on the wire, causing fewer bubbles to emerge.

or even completely blocking sections of the wire. This was resolved either by removing the wire from the tunnel and re-immersing it, or by setting the frequency to a high pulsing rate (on the order of 1 to 10 kHz) for a few seconds, then resetting it. The latter technique produced so many bubbles that any contaminants were swept off the wire.

3.4.4 Laser

Standard Laser Doppler Velocimetry (LDV) was performed to determine the speed of the water in which the CF-18 model was studied. Velocity measurements in the water tunnel were necessary for several reasons. First, while good flow quality could be seen by watching the smooth dye streak or a sheet of hydrogen bubbles deformed only by buoyancy (such tests were also performed), it was necessary to ensure a relatively constant velocity in the areas of study. Also, the free stream fluid velocity must be known to compute the Reynolds number (see Section 4.2), and to estimate the engine inlet speed (see Section 3.3.3), which are functions of free stream speed.

An Optikon 5 W argon ion laser supplied a cyan beam (composed of green and blue light, at wavelengths of 488.0 nm and 514.5 nm, respectively) through a fiber optic cable to the Dantec LDV equipment (Figure 20). More information concerning the laser can be found in the Optikon laser manual, and information on the LDV equipment and software can be found in the Dantec manuals (1992).

The laser head could be fitted with one of three lenses, with focal lengths of 160 mm, 300 mm and 600 mm, respectively. The 600 mm lens was selected in order to gain access to the tunnel's entire cross-section without changing

attachments. Unfortunately, this meant that the control volume was rather large (see below), thus introducing the possibility of a velocity variation within the control volume itself, especially close to the walls.

As only average values were needed, and high precision in determining velocity profiles was not necessary, the laser head was attached to the tunnel's traversing system (see Section 3.2.2) using only a crude mount, made of square steel tubing and angle iron welded together in an L shape (see Figure 20). The laser head could be mounted on any of twenty-one evenly spaced holes on the vertically-mounted angle iron, giving the desired vertical location. Cross-stream and transverse motions were made using the tunnel's traversing system, however, only a millimeter scale was used for determining the carriage positions.

Uncertainty in the control volume location was caused by the use of clearance holes in the mount, which allowed slight variations in the head's vertical position, and caused difficulty in ensuring that the head was aligned perpendicular to the glass. If touched, the mount took several seconds to become still.

The focal length of the 600 mm lens is equal to its nominal value when operating in air. However, the lens was used at various distances from the tunnel wall, thus it was partly in air, and partly in water. Ignoring any distortions caused by the glass wall, and given the index of refraction of water as 1.33, the actual focal length of the lens (f), and therefore the location of the center of the control volume, could be calculated by:

$$f = 800 - 0.33\,d$$

where d was the distance from the laser head to the glass wall of the tunnel.

The position of the carriage could be read to within 0.5 mm. However, due to complications in converting the scale reading into the distance from the laser head to the glass, d could only be calculated to an uncertainty of ± 2 mm. Thus it was estimated that the control volume location in both the vertical and horizontal planes was accurate to ± 2 mm.

The laser was operated at 700 mW, giving adequate power for the beam to shine through the large volume of water. However, particle seeding was necessary in order for the laser Doppler software to calculate the tunnel speed. About 1 mL of silicon carbide (1.5 μm diameter) was mixed into about 10 L of water, which was then added to the tunnel at the rear. The particles were thus mixed into the flow by the pump impeller.

The Laser Doppler setup was controlled by the Dantec software called FlowWare (version 2.2). The settings in the Control and Acquire section were configured using suggestions by Zwart (1995b)

In the *Setup* section, the following settings were modified from the defaults.

Electronics

Dimension	2D
Burst Detector Mode	Trigger on U1/ext. inhibit
Photomultipliers	57x08

If the Burst Detector Mode is set to 800 Hz or to 1.25 kHz, the system will sample the flow at that rate, regardless of the presence of particles in the control

volume. Thus it is likely that very few particles will fit the criteria for a valid sample. When set to "Trigger on U1/ext. inhibit", the system will only take samples when particles pass through the control volume, and a much higher validation rate can be achieved.

Optics

	U_x	U_y
Wavelength (nm)	488.0	514.5
Gaussian Beam Diameter (nm)	1.3	1.3
Beam Collimater Exp.	1	1
Beam Expander Exp.	1.0	1.0
Beam Separation (mm)	26.87	26.87
Lens Focal Length (mm)	600	600

The program uses the above data to calculate the fringe spacing, which is 14.5 μm for 26 fringes in the U_x direction, and 15.3 μm for 26 fringes in the U_y direction. The measurement volume is also calculated by the program, and is accessed by pressing Control-V at this point in the setup:

	Δx (mm)	Δy (mm)	Δz (mm)
U_x	0.38	0.38	30.3
U_y	0.10	0.10	32.0

Bandwidths

	U_x	U_y
Bandwidth (MHz)	0.12	0.12

Gain	High	High
Frequency Shift (MHz)	40	40

The above settings permit a velocity range of -0.87 to 0.87 m/s. Unfortunately, the 600 mm lens allows only an 8 mm/s resolution when determining the measured velocity.

In the *Acquire* section, the following settings were modified from the software defaults.

Validation

Validate	Both [U_x and U_y]
Cutoff	-3 dB
Accepted Fringe Count	0 to 156

Error Display was used to check the signal and velocity. High Voltage was adjusted as necessary (from 1200 to 2000 V) to keep the photomultiplier current around 50 μA, as recommended in the Dantec manuals. This keeps a consistent amount of reflected light reaching the photomultipliers, avoiding bias because of light loss in a large volume of water.

LDV measurements were made to determine the range of tunnel speeds, and to provide a velocity map to determine flow quality. For these purposes, measurements were made at 15 different pump speeds, all at the test section centerline near the test section entrance. One measurement was taken at each pump speed, except at study operating speed of 9 Hz, which was measured 6 times. Thus the potential for spurious datapoints was high. Measurements to be used for flow quality were also taken, at thirty-five points at each of two cross-

sectional locations in the test section, one at the entrance, and one at the model location downstream. Each point was sampled only once.

3.4.5 Illumination and Photography

Illumination was produced using a Buhl Optical projector with a 150 W bulb, which provided very uniform light across the entire beam, and a custom-made 100 W spotlight.

A flat mirror reflected light from the horizontal projector vertically to another flat mirror immersed in the water downstream of the model (Figure 21). Both of these mirrors could be adjusted to illuminate the area of the model being studied, but, coming from the downstream location, tended to cast shadows toward the front of the model. The spotlight was used to illuminate the areas in shadow, wherever possible. Normally, the spotlight was placed so that it shone through the side wall of the tunnel, either upstream or downstream of the model. Occasionally, the spotlight was placed on top of the tunnel so that it could shine directly on the bottom of the model, but there was generally no room for this positioning (see the crowded workspace in Figure 16), and most areas of interest could normally be illuminated from the side.

When used as the flow visualization tool, the purple dye could be seen best when the background model was illuminated. Figure 21 illustrates a typical mirror setup at low angle of attack. For higher angles of attack, only the mirror location angle had to be adjusted.

The hydrogen bubbles were much more difficult to photograph, as the bubbles were lit with an angle of 135° between the light source and the camera for best visibility, and the background model was kept as dark as possible to increase contrast. Combined with the short exposures required to track a line of bubbles without streaking, most still photographs were very dark. The mirror location shown in Figure 21 was modified slightly in order to be better suited to viewing the hydrogen bubbles at low angles of attack. As the angle of attack was adjusted, the mirror had to be lowered or raised in the tunnel, and its angle had to be adjusted accordingly, to keep as little of the model lit as possible. This was a difficult and tedious task, and was best performed with the assistance of another person.

A Nikon FE2 35 mm camera was used for taking still pictures of the model. The camera had a variable shutter speed and f-stop, and could be fitted with various interchangeable lenses. Loblaws Photoshop 400 speed film was used for all exposures of the stores, and for dye visualization exposures of the LEX and forebody vortices. It produced good quality photos, comparable to those taken during test runs with Fuji ASA 400 film, and was not as expensive to process. The ASA 400 was chosen as the minimum film speed, after tests with ASA 100 and 200 speed films produced very dark pictures. Kodak Royal Gold ASA 1000 film was used to take good photographs of the LEX vortices at high speed, as visualized by the shear-thickening dye, however, the hydrogen bubbles were very dark. Kodak TMax P3200 black and white film was used to successfully capture images of the LEX vortices using hydrogen bubbles.

Photographs were taken from below the tunnel and from the side. When viewing from the side, the camera was mounted on a tripod so that the entire wing of the model was visible, when a Tamron 90 mm lens was used. The front of the lens was placed at about 380 mm from the tunnel wall, at the wing level. When viewing the wing's lower surface from below the tunnel (the wing's lower surface faced upwards, because the model was mounted upside-down, see Section 3.2.3), a mirror was mounted upstream of the model, directly above the camera, barely fully immersed so as to disturb the flow about the model as little as possible (see Figure 21). The mirror was aligned so that the camera could capture the entire wing in one frame. The lower fuselage was photographed in the same way. The Tamron 90 mm lens was coupled with a Vivitar 2x macro focusing teleconverter and Vivitar automatic extension tubes (12 mm and 36 mm), bringing the total focal length to 228 mm, to give the proper magnification. A Nikon DR-3 right angle viewing attachment was used for ease of focusing when the camera was tilted upward. The camera lens was placed in contact with the bottom wall of the tunnel. Photographs of the top surface of the model (i.e. the LEX and forebody), were taken by placing the camera directly below the area of interest, using either the Tamron 90 mm lens alone, or a 52 mm Nikon lens.

In order to avoid disturbing the camera on its tripod, the trigger was pressed using the "START" button on a custom-made circuit, shown in Appendix C, which incorporates a solenoid switch that depressed the camera's remote cable.

Video images of the flow were captured using a GE 8 mm Camcorder with an 8x telephoto zoom lens. The camcorder recorded images from the side and below

the tunnel when following the dye lines. Hydrogen bubbles flowing over the stores were best seen from above the tunnel. while those bubbles entrained in the forebody and LEX vortices were best seen from the side or below the tunnel.

3.5 Tecplot Flow Visualization Software

Tecplot is a software package that allows computer generation of XY plots. and 3D surfaces. among other features. Complex 3D surfaces must be generated by providing Cartesian coordinates for the points on the surface. and can thus be tedious to create. However. once the surfaces are created. they can be rotated in any direction. shaded to show lighting effects. or magnified to show small areas. Other data. such as velocity vectors or contours. can be added to the plots.

The water tunnel speed was plotted in contours using this program. as will be discussed in Section 4.1.2. The velocity contours were flooded with different shades of grey. to show the trend in the velocity.

The wing surface used in the analysis of the stores in Section 5.2 was created from measurements of the model surface. point-by-point. with a vernier caliper. As the forebody and tail sections were not required for these plots. and the measuring process was tedious. only the section of the wings was created. Although exact shape of the wings was not fully represented. it was deemed to be sufficient as a reference for locating the dye streaks.

The coordinates of points along the thirty one dye streaks photographed in this study over the clean wing were measured directly from the photographs.

and they were scaled to the model size using a reference easily visible in the photograph, and accurately measurable on the model.

The contours of the wing pylon, EFT, VER, and MK-82 bomb were also mapped using a vernier caliper. In the case of the stores with axi-symmetric cross-sections, one quarter of the model was created, and mirror images created the remainder of the computer surface. Each of these models was created separately, so it was necessary to import them into the same file that created the wing surface, and move them using position transformations to the appropriate location.

The dye lines photographed in Configuration 6a (see Table 2) were measured in the photograph and scaled to the model size, after which they were plotted alongside these surfaces.

The input files for the wing and store surfaces, as well as the dye lines, have been included in Appendix E.

Chapter 4

Experimental Results

This chapter presents velocity measurements taken in the water tunnel, and introduces the flow visualization results, which will be discussed in the following chapter.

4.1 Water Tunnel Flow Characteristics

4.1.1 Water Speed Versus Pump Rotational Speed

Velocity measurements in the water tunnel were taken with a Laser Doppler Velocimetry (LDV) system. The centerline velocity, 0.42 m from the test section entrance, was measured at pump rotational speeds varying from 5 Hz to 40 Hz, according to the setting of the motor controller. The water height in the test section was kept constant at 0.70 m throughout these tests. Figure 22 shows how the centerline water speed varied under these conditions. This plot could be

used as a rough guide for determining the water speed from the motor controller indication.

The water velocity variation is a slightly non-linear function of the pump speed. The plot shows that, at the maximum water height, water speeds from 0.05 m/s to 0.30 m/s are within the range of this facility; higher velocities in the test section could be safely achieved with a lower water height, if necessary.

Looking at a pump rotational speed of 9 Hz, which was used throughout the study, it can be seen that the resulting tunnel centerline speed was very repeatable, even after raising and lowering the pump speed several times.

The LDV output at zero water velocity (0 Hz) was measured in order to determine possible offsets of the LDV measurements, but none was found. Because the motor can not operate at speeds below 5 Hz, no measurements were taken in the range of 0 to 5 Hz. Furthermore, although the pump can be operated up to 60 Hz, it was not run at speeds higher than 40 Hz, because of noise in the pump enclosure, possibly due to vibration or cavitation.

4.1.2 Flow Quality at a Nominal Tunnel Speed

The flow speed in the water tunnel was chosen for flexibility in photographing the flow visualization media immersed in flows around the upper and lower surfaces of the CF-18 model. After studying the behaviour of the dye and hydrogen bubbles at several pump speeds, a value of 9 Hz on the motor controller was chosen.

Figure 23 shows contours of the streamwise velocity component, measured at two cross-sections, and normalized by the nominal centerline velocity, U_c = 0.070 m/s; the latter was determined by averaging all measured values within the cores of the two cross-sections, which corresponded to 75% of the tunnel area. Thus the nominal centerline velocity is actually slightly lower than the peak centerline velocity.

All three axes were normalized by the width of the tunnel, b = 550 mm, but measurements in the vertical direction were restricted up to about 90% of the water's height because of practical limitations. Most flow visualization was done in the range of $-0.25 < z/b < 0$, $0.6 < y/b < 0.8$, and $0.66 < x/b < 0.81$.

The flow speed was relatively close to the nominal centerline velocity in the cores of both sections. It dropped below the 95% U_c level in the wall regions, which extended by less than z/b = 0.1 from the walls, and y/b = 0.1 from the floor of the tunnel, except in the corner regions, where the effects extended farther from the walls. In the case of the x/b = 0 plane, near the test section entrance, the tunnel velocity was quite uniform (within ±2%) throughout the core. Farther downstream, at x/b = 0.75, wall effects extended farther, however, the speed variation in the entire core of this plane did not exceed 5 - 7%, which is comparable to the uncertainty of these measurements. Therefore, the tunnel flow can be considered to be adequately uniform for the present study.

At both measuring stations, the flow was slower above y/b = 1.0 than in the core region, and varied irregularly near the top of the measured region. This is attributable to the mainly stagnant, often recirculating flow observed on the free

surface (made visible by small amounts of floating dust and oil), which was caused by the Plexiglas covers located farther downstream.

Figure 24 shows velocity contours for the vertical component of the velocity, normalized by the nominal centerline velocity, at the same cross-sections as the results shown in Figure 23. The vertical velocity magnitude at these locations was less than 5% U_∞, which is comparable to the uncertainty of the present measurements.

Plates 1 and 2 show typical flow patterns in the unobstructed tunnel, using water-based-dye and hydrogen-bubble visualization, respectively. The distortion of the dye streakline (Plate 1) is negligible. The hydrogen bubble timelines (Plate 2) present very little distortion, mainly attributable to buoyancy and non-uniform bubble production due to irregular adherence of dirt to the wire.

4.1.3 Flow Distortion Due to Mirrors

The model of the CF-18 is shown at its fixed location in the test section in Plate 3a. There was concern that by submerging a mirror at a close downstream location, the flow around the model might be affected. To test this, a dye streak was injected into the flow under steady conditions in the unobstructed tunnel (see Plate 3b), at the same water height and speed as in the test conditions. A mirror was then submerged at the normal mirror location in the test section. The dye streak was deflected slightly downwards, but the effect could not be seen upstream of the model sting location (Plate 3c). The camera was kept at a fixed position while all three photographs in Plate 3 were taken.

4.1.4 Flow Distortion Due to Model Blockage

While the actual aircraft usually flies in what can be considered an infinite medium, the water tunnel walls enclose the scale model, and may affect the flow-field in its vicinity (Rae and Pope, 1984).

While studying circular cylinders in a wind tunnel at various Reynolds numbers, Modi and El-Sherbiny (1971) determined that cylinders with blockage ratios (cylinder area to tunnel cross-sectional area) of less than 10% had only very small variations in their flow-fields. While the CF-18 model is more complex than the cylinders, these results can provide a guide to the overall effect of tunnel blockage on the model's flow-field. The CF-18 model blocks about 0.9% of the water tunnel's cross-sectional area at $\alpha = 5°$, to a maximum of 5% at $\alpha = 39°$.

According to Erickson (1991), differences in tunnel properties during various studies, such as tunnel size and shape, sting size and area blockage by the model, had a negligible effect on the LEX bursting locations. In the absence of water tunnel wall correction factors, the wall correction factors for lift and streamline curvature presented by Rae and Pope (1984) for wind tunnels were calculated, and found to be very small.

4.2 Calculation of the Flow Reynolds number

The Reynolds number for flows over three-dimensional wings is usually defined as

$$Re = \frac{U_c \bar{c}}{\nu}$$

where U_c is the mean centerline velocity, $\bar{c}$ is the mean aerodynamic chord of the CF-18's wing, calculated by dividing the area of a single wing planform by the span of the wing, and ν is the kinematic viscosity of the fluid. For the present model and flow conditions, $U_c = 0.070$ m/s, $\bar{c} = 0.074$ m, and $\nu = 1.5 \times 10^{-6}$ m^2/s for water at 20° C. Therefore, the Reynolds number was 3450.

4.3 Flow Visualization About the Stores

Flow visualization about the stores of the CF-18 model was made mainly with the water-based methyl violet dye. Effort was made to place the injection tubes at locations that ensured dye streaks parallel to the undisturbed flow.

A complete list of all photographs that are available for this study is presented in Table 3. Each photograph is identified by two numbers, separated by a dash. The first number corresponds to the film roll and second number to the frame on that film. The table also includes information on the store configuration (see Table 2 and Figure 14), the model angle of attack, the camera view (side or bottom), and the exposure characteristics (f-stop and shutter speed). For all photographs taken from the side, the 90 mm lens was used, while all bottom views used a combination of lenses and extension rings with a total focal length of 228 mm (see Section 3.4.4). The last column in the table contains a graphical depiction of the approximate location of the dye injection tube(s), from the front view of the model.

Film rolls numbered 1 to 7 were used for the development of the photographic process, especially when photographing the hydrogen bubbles. Because most of these photographs captured the same features, using different f-stops or shutter speeds, many were underexposed, or out of focus, and they were not included in the table.

All dye streaks taken with the clean wing in film rolls 8 to 10 were combined onto a computer generated surface representation of the wing, custom-made using the Tecplot software package (see Section 3.5, and Appendix E), for better viewing and comparisons. The clean wing profiles are shown in Figures 25 to 27.

The angle of attack for Plates 4 through 11 is $\alpha = 5°$. Note the shadows of the dye lines are often visible against the stores or the wing's lower surface, projected by the light source from below the tunnel.

In the bottom view of the aircraft, a streakline can be observed in close proximity to an AIM 9 wing-tip missile (Plate 4). From the side, it can be seen that the streakline follows the wing-tip vortex trajectory from the wing bottom surface to the top surface (Plate 5).

The wing pylon at the outboard station (station 8) is seen to disrupt the flow of two streaklines only slightly, in the bottom view of the wing provided by Plate 6. The side view is not presented because the streakline did not visibly deviate from the wing contour from that viewing angle. Addition of the VER to that pylon created a bluff body disturbance to the flow (Plate 7).

The flow past the external fuel tank (EFT) at the inboard station (station 7) followed the profile of the tank, as shown in Plates 8 (bottom view) and 9 (side view). The streaklines around a single MK 82 bomb mounted on the VER/ pylon assembly at station 8 are shown in a bottom view in Plate 10, while Plate 11 displays the region of influence of the single bomb from the side.

An assembly of an EFT/ pylon pair and a two-MK 82 /VER/ pylon system were added to the computer generated surface of the wing using Tecplot in Figures 28 to 30, in order to better visualize the streaklines flowing past this configuration.

High angles of attack caused cross-flow and separation around the stores, as evidenced by flow around the two MK 83 bombs shown at $\alpha = 25°$ in Plate 12.

Plate 13 displays streaklines between an EFT, at station 7, and a GBU-12 bomb, at station 8, at $\alpha = 5°$. Finally, the cross-flow and separation observed at high angles of attack is shown around two GBU-12 bombs at $\alpha = 20°$ in Plate 14.

4.4 Vortex Flow Visualization

Table 4 lists the photographs available covering the top surface of the model, namely the LEX and forebody vortices. The table lists photograph number (as defined for Table 3), angle of attack, whether the camera was positioned to give a top or side view of the model, the lens used, and the exposure characteristics (as described for Table 3). The column "Method" describes which of the three methods was used in visualizing the flow feature: water-based dye ("water dye"), shear-thickening dye ("shear dye") or hydrogen bubbles ("bubbles"). The column

"Feature" describes which vortex can be seen in the photograph. All vortex visualization was performed with clean wings (Configuration 1).

Water-based dye was used to visualize the LEX vortex at various angles of attack, two of which are shown in Plates 15 ($\alpha = 5°$) and 16 ($\alpha = 20°$). The LEX vortex can also be seen using the hydrogen bubble method in Plate 17 ($\alpha = 25°$).

A comparison of flow visualization using the water-based dye and that using the shear-thickening dye can be made by comparing Plates 18 and 19, respectively, both of which were photographed at $\alpha = 35°$. Note the shadow of the dye line projected onto the LEX by the light source from below. The top view of the LEX vortex at $\alpha = 35°$, as visualized by the shear-thickening dye, is displayed in Plate 20, which shows the complex structure of the burst vortex.

A pair of forebody vortices can be seen in Plate 21 ($\alpha = 25°$), visualized using the water-based dye. They were located much closer to the model centerline than the LEX vortices were. One of these vortices can be seen interacting with the LEX vortex in Plate 22, at the same angle of attack.

Finally, one of the best photographs using hydrogen bubble visualization, showing the LEX vortex core at $\alpha = 20°$, is presented in Plate 23.

Chapter 5

Discussion of the Flow Visualization Results

This chapter presents a discussion of the flow patterns about the various CF-18 model configurations and their applicability to the actual aircraft. This is followed by a brief discussion on the usefulness of the flow visualization techniques to the understanding of the flow phenomena in this study.

5.1 Flow Visualization About the Stores

Flow about the CF-18 stores was visualized using the water-based methyl violet dye and hydrogen bubbles. The hydrogen bubble images were only captured on video.

5.1.1 Clean Wing (Configuration 1)

The clean wing configuration (without stores or pylons) was visualized to provide a reference to which the other store configurations could be compared. Dye streaks from the photographs were discretized and drawn together with the computer-generated aircraft surface using Tecplot (Figures 25 to 27).

Dye injected close to the surface of the wing followed the contour of the wing at $\alpha = 0°$. The streaklines were on vertical planes parallel to the wing's chord, except in the region close to the fuselage, where these lines moved towards the wing-tips and away from the body of the aircraft. Outboard of the wing-tip, the streaklines were drawn into the wing-tip vortex.

Streaklines originating at vertical positions $0.15\bar{c}$ and $0.30\bar{c}$ (where $\bar{c}$ is the mean chord length, equal to 0.074 m for the model, and 3.5 m for the actual aircraft) from the lower wing surface at $\alpha = 0°$ were essentially parallel to the free-stream flow direction, except when closer than $0.10\bar{c}$ to the fuselage. This indicates that, at $\alpha = 0°$, the influence of the wing on the flow is restricted to a region within the distances $0.10\bar{c}$ outboard of the fuselage and $0.15\bar{c}$ from the wing lower surface.

Close to the lower surface of the fuselage, all streaklines remained parallel to the free-stream flow direction. Along the fuselage centerline, streaklines indicated that no cross-flow from one side of the aircraft to the other was present.

5.1.2 Missiles (Configurations 2 and 4)

The addition of the AIM 9 wing-tip missile (configuration 2) had little effect on the flow around the wing's lower surface inboard of the wing-tip at α = 5°. Streaklines located just inboard of the missile's axis consistently remained parallel to that axis.

However, streaklines initially on the vertical plane containing the missile's axis were drawn around the wing-tip, towards the wing's upper surface, approximately midway along the missile's length. When located outboard of the wing-tip missile, but still within the influence of the wing-tip vortex, the streaklines were typically drawn into the vortex at a downstream position near that of the missile's tail fins (Plates 4 and 5).

Streaklines in the vicinity of the AIM 7 fuselage missiles (configuration 4) remained parallel to the free-stream flow direction at α = 5°. No noticeable deviation from the clean wing profile was observed for streaklines located inboard, outboard, or along the missile's axis.

5.1.3 Pylon and Vertical Ejector Rack (VER) (Configurations 3 and 5a)

The wing pylon (configuration 3) presented very little disturbance to the flow near the wing's lower surface (Plate 6). Streaklines located outboard of the pylon were deflected towards the wing-tips, with the deflection being the largest when the streakline started near the edge of the pylon farthest from the wing.

No studies were performed of the centerline pylon in the absence of stores.

The pylon's shape was such that any store mounted to it had a small incidence angle (about 4° to 5°) away from the wing. The local flow near a store correlated with the angle of attack of the particular store, rather than the overall angle of attack of the aircraft. For example, when the VER was mounted to the pylon (configuration 5a), a large flow separation region formed when the aircraft was at $\alpha = 0°$, while, when the aircraft was at an angle of attack of 5°, orienting the VER nearly parallel to the flow (Plate 7), the separation region was much smaller.

5.1.4 External Fuel Tanks (EFT) (Configurations 3 and 4)

Flow around an EFT mounted to the wing pylon at station 7 (configuration 3) followed closely the contour of the tank (Plate 8). At the tail end of the tank, the relatively small distance between two adjacent streaklines indicated that this streamlined store had a narrow wake. As they moved from the wing's leading edge towards its trailing edge, the streaklines were deflected away from the wing (Plate 9), indicating the formation of a separated flow region near the store.

The EFT mounted along the fuselage centerline (configuration 4) displayed similar flow features to those described above.

At 20° angle of attack, separated cross-flow moved outboard around the wing-mounted EFT, creating a swirling flow around the stores.

5.1.5 MK-82 Bombs on VER (Configurations 5b and 6a)

Flow around a single MK-82 bomb mounted to the VER and pylon at station 8 (configuration 5b) followed the bomb's contour until about midway along its length (Plate 10). Downstream of that location, streaklines on either side of the bomb remained relatively parallel to each other, instead of following the bomb's contour. This indicates that the wake of the tail-finned bomb was relatively wider than the wake of the more streamlined EFT. As they moved downstream, the streaklines were deflected away from the wing, much as they did in the case of the EFT, thus inferring some flow separation towards the tail of the bomb.

The effect of the MK-82 on the flow-field around the lower wing was quite local. A streakline located just 0.6 maximum bomb diameters from the MK-82 centerline, in a direction away from the wing, was deflected by the bomb's shoulder, but remained parallel to the free stream flow direction downstream of the shoulder (Plate 11) instead of following its contour. The streakline trajectories did not change significantly when the angle of attack was changed from 0° to 5°.

All dye streaks photographed around two MK-82 bombs mounted to the VER (configuration 6a) were reproduced digitally onto a single plot, and were displayed together with the wing and store surfaces using Tecplot.

Because the two bombs were spaced closely together, their wakes merged to form a single wake, as evidenced by streaklines on either side of the pair (Figure 28). Because of their inclination to the wing, the axes of the bombs were roughly parallel (within 1°) to the free stream flow direction while the aircraft was at an

angle of attack of 5°, and they were inclined by approximately -6° to the flow while the aircraft was at $\alpha = -1°$. Thus the wake of the bombs was smaller at $\alpha = 5°$ than at $\alpha = -1°$. From the side view, it could be seen that there was less flow separation from the wing at $\alpha = 5°$ than at $\alpha = -1°$.

The close spacing of the two bombs allowed their boundary layers to interact, creating a region of slow moving fluid between them, especially at $\alpha = -1°$, when the bombs were at approximately -6° incidence to the flow. Dye injected into the flow in these regions followed unsteady trajectories, which oscillated irregularly and slowly between paths parallel to the bombs' axes and paths that were deflected around the slow flow region (Figure 29). As the streaklines switched from the former trajectory to the latter, dye became caught in the wake, and took as long as 30 seconds to diffuse. At 20° angle of attack, the streaklines passed between the two bombs without showing any sign of a slow-flow region.

Streaklines located between the bomb rack and the EFT showed little or no interaction between the effects of the stores at different stations. Streaklines starting midway between the two stations were parallel to the wing's chord, while those starting closer to the EFT followed the contour of the tank, and those injected closer to the bomb generally remained parallel to the wing's chord (Figure 30).

5.1.6 MK-83 Bombs on VER (Configurations 6b and 7)

The flow around a single MK-83 bomb mounted to the VER (configuration 6b) was comparable to the flow around a single MK-82 mounted to the VER.

The bomb's region of influence was larger in all directions, but this can be attributed to its larger size.

The effect of mounting a second MK-83 to the VER (configuration 7) was similar to the effect of adding a second MK-82 to configuration 5b. The single wake generated by the two bombs was smaller for an angle of attack of 5° than for α = -1°. The streaklines located between the two bombs oscillated in the same manner as with the two MK-82 bombs. Furthermore, streaklines located between the bomb rack and the EFT indicated little or no interaction between effects generated by either store.

At 15° angle of attack, a streakline located 1.5 bomb diameters from the axis of one bomb, in a direction away from the wing, remained parallel to the bomb's axis, while a streakline in the same plane, but located at an even level with the bomb's shoulder, was caught in the separated cross-flow that swirled around the bombs. At α = 25° (Plate 12), streaklines located at both above positions were affected by the cross-flow.

5.1.7 EFT and GBU-12 Bomb (Configuration 8a)

The GBU-12 bomb, mounted at station 8, affected the flow around the wing's lower surface very little, at both -1° and 5° angle of attack. The bomb's tail fins caused the streaklines to be deflected slightly away from the bomb, but this effect persisted only over a short distance, as these streaklines were deflected back towards the bomb's axis immediately downstream of its tail fins.

Dye injected into the flow between the GBU-12 (station 8) and the EFT (station 7) at $\alpha = 5°$, remained undeflected when injected in the area of the bomb. Streaklines originating close to the EFT followed the contour of the tank (Plate 13), like those observed in configurations 3, 5b, 6a, 6b and 7.

5.1.8 Two GBU-12 Bombs (Configuration 8b)

At low angles of attack, the effects of two GBU-12 bombs, mounted to the inboard and outboard pylons (stations 7 and 8), were restricted to the vicinity of each bomb. The only noticeable effect was a slight deflection of the streaklines near the tail fins of either bomb.

As the flow disturbances caused by either bomb were similar and did not interact with each other, one may describe the two flows separately. Streaklines passing between the inboard GBU-12 and the fuselage, both close to the wing and at the level of the AIM 7 missile, closely matched those observed in that same region for the clean wing.

At 20° angle of attack, cross-flow towards the wing tips separated at the bombs and created vortices (Plate 14), similar to those observed for other stores at high α.

5.2 Upper Surface Vortex Flow Visualization

Flow on the upper half of the CF-18 model was dominated by the LEX and forebody vortices. The LEX vortices were visualized using water-based and shear-thickening dyes, as well as hydrogen bubbles. The forebody vortices and

the forebody/ LEX vortex interactions were visualized only with the water-based dye. Images of the vortices were captured with still photography and video.

5.2.1 LEX Vortices

The LEX vortices were generated at the apex of the LEX and were, in general, swept downstream parallel to the aircraft's centerline until they burst. At 5° angle of attack (Plate 15), the vortices were swept past the aircraft's tails into its wake without losing their structure. Increasing the angle of attack by a small amount strengthened the adverse pressure gradient on the wing enough to initiate bursting. The bursting location was outboard of the tails at $\alpha = 10°$, and remained in the vicinity of the tails until around $\alpha = 20°$ (Plate 16), where it was located just upstream of the tail leading edges. As the angle of attack was increased, the adverse pressure gradient on the wing also increased, and the LEX vortex burst farther upstream, near the wing leading edge flap (25°, Plate 17), until it burst beside the cockpit at $\alpha = 35°$ (Plates 18, 19 and 20) and $\alpha = 39°$.

These results show excellent agreement with the bursting locations found by Thompson (1990) and others, as shown by Figure 6. This figure has been reproduced as Figure 31, with points added that represent the results of this study. It can be seen that the relative locations of vortex bursting essentially coincide with those in the other studies in the angle of attack range above $\alpha = 20°$. However, there is a discrepancy between the low- and high-Reynolds number results at low angles of attack. This may be explained by the location of the LEX vortices at low angles of attack, immersed in the viscous flow region

close to the LEX at low-Reynolds number, where they would be less affected at higher Reynolds numbers.

At angles of attack greater than about 20°, the vortices were located along an axis inclined away from the aircraft surface. At angles of attack below 20°, the vortices lay close to the surface of the LEX, and their stability and other characteristics were probably affected by the viscous fluid in that region.

A simple 2D analysis shows that the downstream distance traveled by a point on a dye streak as it revolves around the vortex is inversely proportional to the strength of the vortex. Thus the wavelength of the dye streak, measured as the distance between points one revolution downstream of each other, should decrease as the vortex strength increases. This analysis is approximate because it is based on 2D aerodynamics. However, it can be seen that the wavelength of the dye streak decreased as the angle of attack was increased from $\alpha = 5°$ (Plate 15) to $\alpha = 10°$ (Plate 16). As these two pairs of vortices were located at approximately the same distance from the LEX, speeds nearby should be comparable, so one may conclude that the vortex would be stronger at $\alpha = 10°$. The wavelength, and thus the vortex strength, continued to decrease as the angle of attack was increased.

At the highest angles of attack studied ($\alpha = 35°$ and $\alpha = 39°$), the LEX vortices were slightly asymmetric. This could be due to sideslip, induced by a slight misalignment of the model at high angles of attack (see Section 3.3.2). This would be consistent with the asymmetry observed by Erickson (1982) at very small sideslip angles. An explanation for this may be the asymmetry of the

forebody vortices at small sideslip angles, which may, through strong interactions, cause the LEX vortices to become asymmetric as well.

Thompson (1990) observed that dye injected near the lower surface of the LEX, close to its apex, had a tendency to flow upstream until it reached the apex, at which point it would be drawn to the upper surface and enter the LEX vortex. This phenomenon was observed at all angles of attack in the present study.

5.2.2 Forebody Vortices and Their Interaction With the LEX Vortices

Photographs of the forebody vortex were taken at 15°, 25° (Plate 21) and 35°. The forebody vortices had very long wavelengths compared to most of the LEX vortices observed, indicating that they were weaker than the LEX vortices. The forebody vortex wound its way above and to the side of the cockpit, down the middle of the fuselage, until it interacted with the LEX vortex, where it became so disturbed that it could not be distinguished from the burst LEX vortex a short distance downstream of the initial interaction location. After observing the vortices for a long time, it was determined that they were symmetric most of the time, with occasional asymmetry observed for short periods of 10 to 15 seconds at a time.

At α = 15°, the forebody vortex was pulled beneath the LEX vortex around the mid-chord of the wing. The interaction location moved upstream at α = 25° (Plate 22) and α = 35°.

The forebody vortex was deflected away from the fuselage towards the LEX over a shorter downstream distance as the angle of attack was increased, indicating a stronger interaction between the two vortices. This is likely due to the increasing strength of the LEX vortex at higher angles of attack.

5.3 Applicability of the Present Results to Flows Around the Actual Aircraft

Although the Reynolds number used in this study is several orders of magnitude lower than those experienced in flight by the actual CF-18, visualization studies around the stores and vortices may still provide some useful information.

In the model study, all flows were laminar, while the same regions around the actual aircraft in flight would be turbulent. Because of the large difference in Reynolds number, the viscous regions in the model study, when scaled by the model dimensions, are expected to be thicker than those around the actual aircraft.

A rough estimate of Reynolds number effects can be based on the growth equations for constant-pressure laminar and turbulent boundary layers over a flat plate, which are, respectively,

Laminar $$\frac{\delta}{x} = \frac{5.48}{\sqrt{\mathrm{Re}_x}}$$

Turbulent $$\frac{\delta}{x} = \frac{0.382}{\mathrm{Re}_x^{1.5}}$$

where δ/x is the boundary layer thickness normalized by the distance along the wing chord from the leading edge (Fox and McDonald, 1992). For the present study, in which the flow was laminar, with a Reynolds number at the wing trailing edge of 3450, $\delta/x = 0.093$. The Reynolds number at the wing trailing edge in flight is approximately 10^6 (Del Frate et al, 1990), giving $\delta/x = 0.015$. With a boundary layer thickness, at the wing trailing edge, of 9.3% of the wing chord length for the water tunnel study as compared to 1.5% of the wing chord length for the aircraft in flight, some conditions, such as the slow-flow region between the two MK-82 bombs or the two MK-83 bombs, may not occur on the actual aircraft.

The stores are immersed in the separated flow region around lower wing of the model, as evidenced by the streaklines in Plates 9 and 13, which were deflected away from the wing as they flowed downstream. However, as can be seen in Plate 11, in which one streakline was barely affected even by the bomb, the stores are near the edge of the separated flow region. As the turbulent boundary layer around the actual aircraft in flight would delay flow separation along the wing, the stores may not be immersed in this viscous flow region at all. At higher angles of attack, where the separated region on the wing's lower surface was smaller than at lower angles of attack, the fact that the stores seem to have a small effect on the flow-field at the slow tunnel speeds suggests that at the higher in-flight speeds, they may have an even smaller effect.

In the case of the closely-spaced pair of bombs mounted on the VER (configurations 6a or 7), the boundary layers over the bombs and the VER were thick enough to interact with each other, causing the low speed zones between

the stores. The spacing of the bombs (4% of a mean chord length apart) may then not be appropriate for flows in this range of Reynolds number. However, the boundary layers on the actual aircraft in flight may be thin enough so that they do not interact, and the recirculation zone seen between the MK-82s in Figure 30, and between the MK-83s at low angles of attack, may be avoided.

The LEX and forebody vortices appear to correlate well with higher Reynolds number studies in terms of their trajectories, bursting, and interaction locations at angles of attack higher than 10°. The structures of the vortices, especially at lower angles of attack, however, may be different, due to structural differences between laminar and turbulent vortices. At very low angles of attack, the vortices sheared into the shape of a ribbon (see Plate 15), which is strictly a laminar flow phenomenon (Faler and Leibovich, 1977), and should not occur on the actual aircraft in flight, where these vortices are turbulent.

5.4 Comparison of Flow Visualization Methods

The water-based methyl violet dye was the method of choice when visualizing the flow about the stores under the CF-18 model. It was quick and easy to mix, required water only from the tunnel, and was easy to see. The flow of this dye out of the injection tube was also very simple to control. However, when the flow became more complicated, the dye streak became unstable, and was impossible to follow accurately. While visualizing the LEX vortices, for example, the streak would often spread out to form a thin ribbon, which became extremely difficult to see.

The shear-thickening, non-Newtonian methyl violet dye held to the vortical patterns of the LEX and forebody vortices much better at most angles of attack, as can be seen by comparing Plate 18 (water based dye) with Plates 19 and 20 (shear thickening dye). It was easier to see the structure of the vortex, because the dye streak remained a streak even at a distance far downstream. It was easily entrained in the vortex core, or could be injected on an outer radius of the vortex to show how the vortex grew. Additionally, the burst structure could be seen using this dye, which avoided the diffusion that the water-based dye experienced in this area.

Working with the shear thickening dye, however, was more difficult than with the water-based dye. Creating the component mixtures took hours of waiting for the chemicals to dissolve. If, at any point, the mixture was shaken (creating a high shear in the fluid), bubbles would form in the resulting viscous fluid, which would also take hours to clear. A higher pressure was necessary to push the dye through the injection tube, often creating high enough shear to clog the small tube. Attempts to clear the tube by increasing the pressure were not successful, and they might have made the situation worse. The solution was to lower the pressure, then raise it slowly again after a 30 to 60 second wait.

The hydrogen bubbles were successful in showing the three dimensional structure of the LEX vortex, as part of the bubble line was caught in the vortex core (Plate 23), and other parts of the line were caught at various radii from the core, showing various swirling trajectories within the vortex. Taking advantage of the timelines produced by pulsing the voltage across the wire, it is possible to determine relative speeds within the vortex. Qualitatively, it can be seen that

the vortex core moved fastest, actually combining the bubbles from sequential timelines, and that the outlying radius moved more slowly in the downstream direction. The flow completely outside the vortex was used as a reference velocity, as the bubble wire was sufficiently large to produce bubbles far enough from the model to be outside its area of influence.

The hydrogen bubbles were difficult to see and to record photographically with a fixed camera position, that is, with the camera lens perpendicular to the glass walls of the tunnel, which provided the lowest level of distortion due to refraction. A very high speed film was required to capture the fast-moving timelines, and a dark background was best suited for viewing them. It was thus difficult to obtain lighting conditions that lit the bubbles well. The best lighting was achieved when the light passed tangentially to the model's upper surface. In that case, the bubbles were lit, but most of the model was kept dark.

Chapter 6

Conclusions and Recommendations for Future Studies

The objectives of this study were to carry out visualization studies of the flow field around the stores. LEX and forebody of a CF-18 fighter aircraft model in the water tunnel. and to determine the suitability of the water tunnel facility and the visualization methods towards studies of this type. Towards that objective. the following conclusions can be drawn.

1. The tests were conducted at the relatively low Reynolds number of 3450. based on the free stream velocity and the wing's mean aerodynamic chord. Higher Reynolds numbers could be achieved in the facility by increasing the free stream velocity. but only by a factor of 3 at most. and at the expense of clarity of visualization images.

2. Most stores had a local effect on the flow-field around the CF-18 model in the low angle of attack range, from -1° to 5°. At α = 5°, when the stores were roughly parallel to the flow direction, separation would probably be delayed at the much higher Reynolds number flows around the actual aircraft. At α = 20°, vortical flows, arising from the interaction of the stores with separated cross-flow from the fuselage toward the wing-tips, could be seen.

3. The spacing of the stores has an effect on the flow around them. The flow between stores at two stations (Plate 13), which were approximately $0.2\bar{c}$ apart at their closest points, behaved as if the stores were isolated. However, when the two MK-82s were placed side-by-side on the VER, approximately $0.04\bar{c}$ apart at their closest, the flow between them became very slow. This effect will probably be less pronounced, if not entirely absent, on the actual aircraft, due to the thinner boundary layers produced at the higher Reynolds number.

4. The LEX vortex bursting location moved from a location near the tail fins at α= 20°, closer to the nose of the aircraft as the angle of attack was increased, in conformity with the well-documented behaviour in other water- and wind-tunnel studies, and in flight.

5. The LEX vortices increased in strength as the angle of attack was increased, as indicated by the decreasing wavelength of the dye streaks caught in the vortices.

6. The forebody vortices were much weaker than the LEX vortices at all angles of attack above $\alpha = 10°$. They followed paths close to the aircraft centerline until they began interacting with the LEX vortices. The beginning of this interaction region moved upstream, toward the nose of the aircraft, as the angle of attack was increased.

7. The forebody vortices were symmetric about the aircraft centerline most of the time. Occasionally, the vortices became asymmetric, but only for periods of 10 to 15 seconds at a time, after which they became symmetric once again.

8. The water-based methyl violet dye produced a highly visible streak that followed most flows, which for the model studies were laminar, without diffusing. However, it diffused quickly in the high shear regions of the burst LEX vortices. The violet colour was easily photographed against the model when visualizing flows around the stores, and in the LEX and forebody vortices.

9. The shear-thickening methyl violet dye was the method best suited to visualizing the high shear regions of the burst LEX vortices. However,

there were problems associated with injecting the dye into the flow. It is recommended that a larger injection tube be used when performing experiments with this dye.

10. The hydrogen bubble flow visualization method was successful in showing a cross section of the vortices, but the locations of LEX vortex bursting and LEX/ forebody vortex interaction were difficult to determine because of the chaotic behaviour of the bubbles in that area.

11. It is recommended that the clean wing configuration be studied in more detail, at various angles of attack, in order to determine the extent of flow separation from the lower surface. A detailed study of one store or a small number of stores mounted to the wing's lower surface at various angles of attack should also be performed, with the specific objective of determining the effect of the interaction between separated flow regions originating at the stores and at the wing. Hydrogen bubbles might be best suited to this purpose, as the entire wing could be photographed at once.

References

AGARD Fluid Dynamics Symposium, 1995, "Aerodynamics of Store Integration and Separation", AGARD-CP-570.

Bean, D.E., Greenwall, D.I., and Wood, N.J., 1993, "Vortex Control Technique for the Attenuation of Fin Buffet", J. Aircraft, 30, 847-853.

Bjarke, L.J., Del Frate, J.H., and Fisher, D.F., 1992, "Summary of the Forebody High-Angle-of-Attack Aerodynamics Research on the F-18 and the X-29A Aircraft", SAE-TP-921996.

Bore, C., 1995, "Aerodynamics of Store Integration and Separation", AGARD-CP-570.

Budwig, R., and Peattie, R., 1989, "Two New Circuits for Hydrogen Bubble Flow Visualization", J. Phys. E: Sci. Instrum., 22, 250-254.

Chen, P.C., and Liu, D.D., 1990, "Unsteady Supersonic Computations of Arbitrary Wing-Body Configurations Including External Stores", J. Aircraft, 27, 108-116.

Cummings, R.M., Rizk, Y.M., Schiff, L.B., and Chaderjian, N.M., 1992, "Navier-Stokes Predictions for the F-18 Wing and Fuselage at Large Incidence", J. Aircraft, 294, 565-574.

Dantec, 1992, LDV Software Manual, Dantec Inc.

Del Frate, J.A., Fisher, D.F., and Zuniga, F.A., 1990. "In-Flight Flow Visualization with Pressure Measurements at Low Speeds on the NASA F-18 High Alpha Research Vehicle", NASA-TM-101726.

Dollyhigh, S.M., Sangiorgio, G., and Monta, W.J., 1978. "Effects of Stores on Longitudinal Aerodynamic Characteristics of a Fighter at Supersonic Speeds", NASA-TP-1175.

Dowgwillo, R.M., Morris, M.J., Donovan, J.F., and Menne, M.E., 1996. "Pressure Sensitive Paint in Transonic Wind-Tunnel Testing of the F-15", J. Aircraft, 33, 109-116.

Erickson, G.E., 1982. "Water Tunnel Studies of Leading-Edge Vortices", J. Aircraft, 19, 442-448.

Erickson, G.E., 1991. "Wind Tunnel Investigation of Vortex Flows on F/A-18 Configuration at Subsonic Through Transonic Speeds", NASA-TP-3111.

Erickson, G.E., Hall, R.M., Banks, D.W., Del Frate, J.H., Schreiner, J.A., Hanley, R.J., and Pulley, C.T., 1989. "Experimental Investigation of the F/A-18 Vortex Flows at Subsonic Through Transonic Speeds", AIAA-89-2222.

Faler, J.H. and Leibovich, S., 1977. "Disrupted States of Vortex Flow and Vortex Breakdown", Phys. Fluids, 20, 1385-1400.

Fisher, D.F., Banks, D.W., and Richwine, D.M., 1990a. "F-18 High Alpha Research Vehicle Surface Pressures: Initial In-Flight Results and Correlation with Flow Visualization and Wind-Tunnel Data", NASA-TM-101724.

Fisher, D.F., Del Frate, J.H., and Richwine, D.M., 1990b, "In-Flight Visualization Characteristics of the NASA F-18 High Alpha Research Vehicle at High Angles of Attack", NASA-TM-4193.

Fisher, D.F., and Meyer, R.R., Jr., 1988, "Flow Visualization Techniques for Flight Research", NASA-TM-100455.

Fisher, D.F., Richwine, D.M., and Banks, D.W., 1988, "Surface Flow Visualization of Separated Flows on the Forebody of an F-18 Aircraft and Wind-Tunnel Model", NASA TM 100436, also AIAA-88-2112.

Fox, R.W., and McDonald, A.J., 1992, Introduction to Fluid Mechanics, Joahn Wiley & Sons, Inc., New York.

Ghaffari, F., Luckring, J.M., Thomas, J.L., Bates, B.L., and Biedrow, R.T., 1993, "Multiblock Navier-Stokes Solutions About the F/A-18 Wing-LEX-Fuselage Configuration", J. Aircraft, 30, 293-303.

Haines, A.B., 1980, "Prospects for Exploiting Favourable and Minimizing Adverse Aerodynamic Interference in External Store Installations", AGARD-CP-285, FDP Symposium.

Hebbar, S.K., and Leedy, D.H., 1992, "Wind Tunnel Investigation of a Fighter Model at High Angles of Attack", J. Aircraft, 29, 1091-1097.

Hebbar, S.K., Platzer, M.F., and Cavazos, O.V., 1992, "Pitch Rate/Sideslip Effects on Leading Edge Extension Vortices of an F/A-18 Aircraft Model", J. Aircraft, 29, 720-723.

Hoyt, J.W., and Sellin, R.H.J., 1995, "A Turbulent-Flow Dye Streak Technique", Exper. Fluids, 20, 38-41.

Hoyt, J.W., and Sellin, R.H.J., 1996, "Visualization of Flow Around Circular Cylinders at High Reynolds Numbers", Engineering Turbulence Modeling and Experiments, 3, 381-390, Rodi, W., Bergeles, G. (editors), Elsevier Science B.V..

Kaykayoglu, C.R., and Yalcmel, M., 1996, "Unsteady Subsonic Aerodynamics for Maneuvering Wing/Forebody/Pylon/Store Configuration and Store Separation Including Wake Effects", AGARD-CP-570.

Kline, S.J., 1972, "Flow Visualization", Illustrated Experiments in Fluid Mechanics, National Committee for Fluid Mechanics Films.

Lee, B.H.K., Brown, D., Tang, F.C., and Plosenski, M., 1993, "Flow Field in the Vicinity of an F/A-18 Vertical Fin at High Angles of Attack", J. Aircraft, 30, 69-74.

Lee, B.H.K., Brown, D., Zgela, M., and Poirel, D., 1990, "Wind Tunnel Investigation and Flight Tests of Tail Buffet on the CF-18 Aircraft", AGARD-CP-483, Sorrento, Italy.

Lee, B.H.K., and Marineau-Mes, S., 1996, "Mach Number and Angle of Attack Effects on the Flow Past a Fighter-Type Wing at High Incidence", AIAA-96-2510.

Lee, B.H.K., Valerio, N.R., and Tang, F.C., 1994, "Steady and Unsteady Pressure Distributions on an F/A-18 Wing at alpha=30 Deg", J. Aircraft, 31, 862-867.

Lowson, M.V., and Riley, A.J., 1995, "Vortex Breakdown Control by Delta Wing Geometry", J. Aircraft, 32, 832-838.

Kislich-Lemyre, B., 1997, Private Communication, University of Ottawa.

Magill, J.C., Darden, L.A., and Konerath, N.M., 1996, "Flow Visualization During Multiple-Axis Motions using a Wind-Driven Manipulator", J. Aircraft, 33, 163-170.

Marsden, P., and Haines, A.B., 1967, "Aerodynamic Loads on External Stores: A Review of Experimental Data and Method of Prediction", ARC R&M 3503.

Martin, C.A., and Thompson, D.H., 1991, "Scale Model Measurements of Fin Buffet due to Vortex Bursting on F/A-18", AGARD-CP-497.

Merzkirch, W., 1987, Flow Visualization, Second Edition, Academic Press, Inc., Orlando, USA.

Modi, V.J., and El-Sherbiny, S., 1971, "Effect of Wall Confinement on Aerodynamics of Stationary Circular Cylinders", Wind Effects on Buildings and Structures, Proceedings, 365-375, Tokyo.

Monta, W.J., 1980, "Effect of Conventional and Square Stores on the Longitudinal Aerodynamic Characteristics of a Fighter Aircraft Model at Supersonic Speeds", NASA-TM-81791.

Naik, D.A., and Ingraldi, A.M., 1993, "Experimental Study of Pylon Cross Sections for a Subsonic Transport Airplane", J. Aircraft, 30, 676-681.

Optikon, Laser Manual, Optikon Corporation.

Ozcan, O., Unal, M.F., Aslan, A.R., Bozkurt, Y., and Aydin, N.H., 1995. "Aerodynamic Characteristics of External Store Configurations at Low Speeds". J. Aircraft, 32, 161-170.

Rae, W.H. Jr., and Pope, A., 1984. Low-Speed Wind Tunnel Testing, 376-394. John Wiley & Sons, New York.

Ramirez, E.J., 1991. "A Water Tunnel Flow Visualization of the Vortex Flow Structures on the F/A-18 Aircraft", NASA Ames Research Center.

Shah, G.H., 1991. "Wind Tunnel Investigation of Aerodynamic and Tail Buffet Characteristics of Leading-Edge Extension Modifications to the F/A-18". AIAA-91-2889-CP.

Stahara, S.S., 1980, "Study of Transonic Flow Fields About Aircraft: Application to External Stores", AGARD-CP-285, FDP Symposium.

Suarez, C.J., and Malcolm, G.N., 1994. "Water Tunnel force and Moment Measurements on an F/A-18", AIAA-94-1802, 12th Applied Aerodynamics Conference.

Thomas, J.L., Walters, R.W., Reu, T., Ghaffari, F., Weston, R.P., and Luckring, J.M., 1989. "A Patched-Grid Algorithm for Complex Configurations Directed Towards the F/A-18 Aircraft", AIAA-89-0121.

Thompson, D.H., 1990. "Water Tunnel Flow Visualization of Vortex Breakdown over the F/A-18", Aeronautical Research Labs., Flight Mechanics Rept. 179, Australia.

Tijdeman, H., van Nunen, J.W.G., Kraan, A.N., Persoon, A.J., Poestkoke, R., Roos, R., Schippers, P., Siebert, C.M., 1979, "Transonic Wind-Tunnel Tests on an Oscillating Wing with External Stores: Part I-IV, the Wing with Tip Store", Air Force Flight Dynamics Lab., AFFDL TR-78-194, Wright-Patterson AFB, USA.

Wentz, W.H., Jr., 1987, "Vortex-Fin Interaction on a Fighter Aircraft", AIAA-87-2474, AIAA 5th Applied Aerodynamics Conference, Monterey, USA.

Zwart, P., 1995a, "Design of a Water Tunnel Positioning System", Internal Report, Department of Mechanical Engineering, University of Ottawa.

Zwart, P., 1995b, "Grid Turbulence in Compressible Flow", Master's Thesis, Department of Mechanical Engineering, University of Ottawa.

Tables

Table 1: Characteristic shapes of the stores used on the CF-18.

Store	Front View	Side View
Centerline Pylon		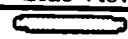
Wing Pylon		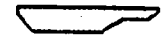
Vertical Ejector Rack (VER)		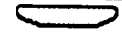
AIM 9 Missile		
AIM 7 Missile		
330 USG External Fuel Tank		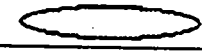
MK 82 Bomb		
MK 83 Bomb		
GBU 12-Bomb		

Table 2: Summary of store configurations presented in Figure 14. The numbers in this table indicate the store stations, also defined in this figure.

Config.	1	2	3	4	5a	5b	6a	6b	7	8a	8b
CL Pylon				5	5	5	5	5	5	5	5
Wing Pylon			2,3 7,8	2,3 7,8	2,3 7,8	2,3 7,8	2,3 7,8	2,3 7,8	2,3 7,8	2,3 7,8	2,3 7,8
VER					2,8	2,8	2,8	2,8	2,8	2	2
AIM 9		1,9	1,9	1,9	1,9	1,9	1,9	1,9	1,9	1,9	1,9
AIM 7				4,6	4,6	4,6	4,6	4,6	4,6	4,6	4,6
EFT			7	5,7	3,5 7	3,5 7	3,5 7	3,5 7	3,5 7	3,5 7	3,5
1 MK 82						8					
2 MK 82							8				
1 MK 83								8			
2 MK 83									8		
GBU-12										8	7,8

Table 3: Frames corresponding to visualization of the flow about the stores.

Photo No.	Config.	α	View	Lens (mm)	Exposure Characteristics	Tube Location
08-02	1	5°	bottom	228	f 2.5, 1/30 s	
08-03	1	5°	bottom	228	f 2.5, 1/30 s	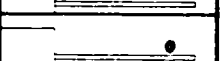
08-04	1	5°	bottom	228	f 2.5, 1/30 s	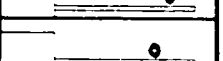
08-05	1	5°	bottom	228	f 2.5, 1/30 s	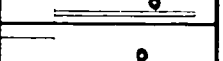
08-06	1	5°	bottom	228	f 2.5, 1/30 s	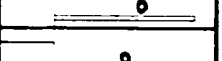
08-07	1	5°	bottom	228	f 2.5, 1/30 s	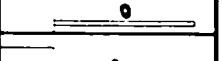
08-08	1	5°	bottom	228	f 2.5, 1/30 s	
08-09	1	5°	bottom	228	f 2.5, 1/30 s	
08-10	1	5°	bottom	228	f 2.5, 1/30 s	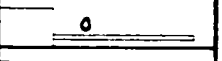
08-11	1	5°	side	90	f 2.5, 1/125 s	
08-12	1	5°	side	90	f 5.6, 1/30 s	
08-13	1	5°	side	90	f 5.6, 1/30 s	
08-14	1	5°	side	90	f 5.6, 1/30 s	
08-15	1	5°	side	90	f 5.6, 1/30 s	
08-16	1	5°	side	90	f 5.6, 1/30 s	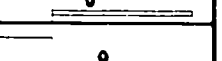
08-17	1	5°	side	90	f 5.6, 1/30 s	
08-18	1	5°	side	90	f 5.6, 1/30 s	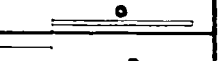
08-19	1	5°	side	90	f 5.6, 1/30 s	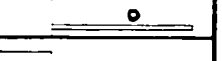
08-20	1	5°	side	90	f 5.6, 1/30 s	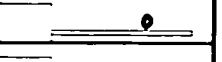
08-21	1	5°	side	90	f 5.6, 1/30 s	
08-22	1	5°	side	90	f 5.6, 1/30 s	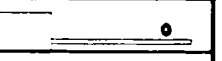
08-23	1	5°	side	90	f 5.6, 1/30 s	
08-24	1	5°	side	90	f 5.6, 1/30 s	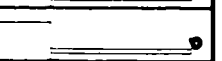

Table 3: Frames corresponding to visualization of the flow about the stores.

Photo No.	Config.	α	View	Lens (mm)	Exposure Characteristics	Tube Location
08-25	1	5°	side	90	f 5.6, 1/30 s	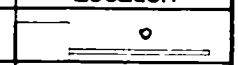
09-01	1	5°	side	90	f 5.6, 1/30 s	
09-02	1	5°	side	90	f 5.6, 1/30 s	
09-03	1	5°	side	90	f 5.6, 1/30 s	
09-04	1	5°	side	90	f 5.6, 1/30 s	
09-05	1	5°	side	90	f 5.6, 1/30 s	
09-06	1	5°	side	90	f 5.6, 1/30 s	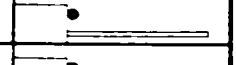
09-07	1	5°	bottom	228	f 2.5, 1/30 s	
09-08	1	5°	bottom	228	f 2.5, 1/30 s	
09-09	1	5°	bottom	228	f 2.5, 1/30 s	
09-10	1	5°	bottom	228	f 2.5, 1/30 s	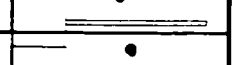
09-11	1	5°	bottom	228	f 2.5, 1/30 s	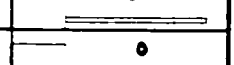
09-12	1	5°	bottom	228	f 2.5, 1/30 s	
09-13	1	5°	bottom	228	f 2.5, 1/30 s	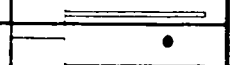
09-14	1	5°	bottom	228	f 2.5, 1/30 s	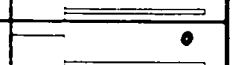
09-15	1	5°	bottom	228	f 2.5, 1/30 s	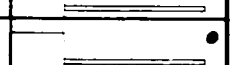
09-16	1	5°	bottom	228	f 2.5, 1/30 s	
09-17	1	5°	bottom	228	f 2.5, 1/30 s	
09-18	1	5°	bottom	228	f 2.5, 1/30 s	
09-19	1	5°	bottom	228	f 2.5, 1/30 s	
09-20	1	5°	bottom	228	f 2.5, 1/30 s	
09-21	1	5°	bottom	228	f 2.5, 1/30 s	
09-22	1	5°	bottom	228	f 2.5, 1/30 s	
09-23	1	5°	bottom	228	f 2.5, 1/30 s	

Table 3: Frames corresponding to visualization of the flow about the stores.

Photo No.	Config.	α	View	Lens (mm)	Exposure Characteristics	Tube Location
09-24	1	5°	bottom	228	f 2.5, 1/30 s	
09-25	1	5°	bottom	228	f 2.5, 1/30 s	
10-01	1	5°	bottom	228	f 2.5, 1/30 s	
10-02	1	5°	bottom	228	f 2.5, 1/30 s	
10-03	1	5°	side	90	f 5.6, 1/30 s	
10-04	1	5°	side	90	f 5.6, 1/30 s	
10-05	1	5°	side	90	f 5.6, 1/30 s	
10-06	1	5°	side	90	f 5.6, 1/30 s	
10-07	1	5°	side	90	f 5.6, 1/30 s	
10-08	1	5°	side	90	f 5.6, 1/30 s	
10-09	1	5°	side	90	f 5.6, 1/30 s	
10-10	1	5°	side	90	f 5.6, 1/30 s	
10-11	1	5°	side	90	f 5.6, 1/30 s	
10-12	1	5°	side	90	f 5.6, 1/30 s	
10-13	1	5°	side	90	f 5.6, 1/30 s	
10-20	1	5°	bottom	228	f 2.5, 1/30 s	
10-21	1	5°	bottom	228	f 2.5, 1/30 s	
10-23	1	5°	bottom	228	f 2.5, 1/30 s	
10-24	1	5°	bottom	228	f 2.5, 1/30 s	
11-01	2	5°	bottom	228	f 2.5, 1/30 s	
11-02	2	5°	bottom	228	f 2.5, 1/30 s	
11-03	2	5°	bottom	228	f 2.5, 1/30 s	
11-04	2	5°	bottom	228	f 2.5, 1/30 s	
11-05	2	5°	bottom	228	f 2.5, 1/30 s	

Table 3: Frames corresponding to visualization of the flow about the stores.

Photo No.	Config.	α	View	Lens (mm)	Exposure Characteristics	Tube Location
11-06	2	5°	bottom	228	f 2.5, 1/30 s	
11-07	2	5°	bottom	228	f 2.5, 1/30 s	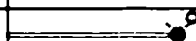
11-08	2	5°	side	90	f 2.5, 1/30 s	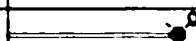
11-09	2	5°	side	90	f 2.5, 1/30 s	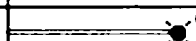
11-10	2	5°	side	90	f 2.5, 1/30 s	
11-11	2	5°	side	90	f 2.5, 1/30 s	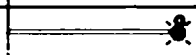
11-12	2	5°	side	90	f 2.5, 1/30 s	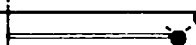
11-13	2	5°	side	90	f 2.5, 1/30 s	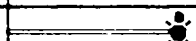
11-14	2	5°	side	90	f 2.5, 1/30 s	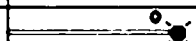
11-15	3	5°	bottom	228	f 2.5, 1/30 s	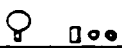
11-16	3	5°	bottom	228	f 2.5, 1/30 s	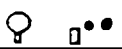
11-17	3	5°	bottom	228	f 2.5, 1/30 s	
11-18	3	5°	bottom	228	f 2.5, 1/30 s	
11-19	3	5°	bottom	228	f 2.5, 1/30 s	
11-20	3	5°	bottom	228	f 2.5, 1/30 s	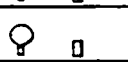
11-21	3	5°	side	228	f 2.5, 1/30 s	
11-22	3	5°	side	228	f 2.5, 1/30 s	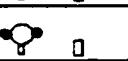
11-23	3	5°	side	228	f 2.5, 1/30 s	
11-24	3	5°	side	228	f 2.5, 1/30 s	
11-25	3	5°	side	228	f 2.5, 1/30 s	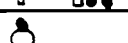
12-01	4	5°	bottom	228	f 2.5, 1/15 s	
12-02	4	5°	bottom	228	f 2.5, 1/15 s	
12-03	4	5°	bottom	228	f 2.5, 1/15 s	

Table 3: Frames corresponding to visualization of the flow about the stores.

Photo No.	Config.	α	View	Lens (mm)	Exposure Characteristics	Tube Location
12-04	4	5°	bottom	228	f 2.5, 1/15 s	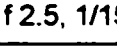
12-05	4	5°	bottom	228	f 2.5, 1/15 s	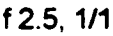
12-06	4	5°	bottom	228	f 2.5, 1/15 s	
12-07	4	5°	side	90	f 2.5, 1/15 s	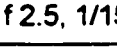
12-08	4	5°	side	90	f 2.5, 1/15 s	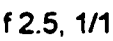
12-09	4	5°	side	90	f 2.5, 1/15 s	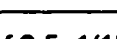
12-10	4	5°	side	90	f 2.5, 1/15 s	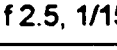
12-11	4	5°	bottom	228	f 2.5, 1/15 s	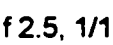
12-12	4	5°	bottom	228	f 2.5, 1/15 s	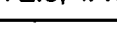
12-13	4	5°	bottom	228	f 2.5, 1/15 s	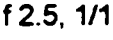
12-14	4	5°	bottom	228	f 2.5, 1/15 s	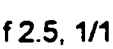
12-15	4	5°	bottom	228	f 2.5, 1/15 s	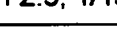
12-16	4	5°	bottom	228	f 2.5, 1/15 s	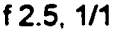
12-17	4	5°	side	90	f 5.6, 1/15 s	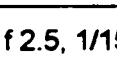
12-18	4	5°	side	90	f 5.6, 1/15 s	
12-19	4	5°	side	90	f 2.5, 1/30 s	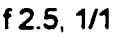
12-20	4	5°	side	90	f 2.5, 1/30 s	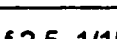
12-21	4	5°	side	90	f 2.5, 1/30 s	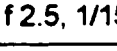
12-22	4	0°	side	90	f 2.5, 1/30 s	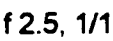
12-23	4	0°	bottom	228	f 2.5, 1/15 s	
12-24	4	0°	bottom	228	f 2.5, 1/15 s	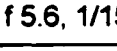

Table 3: Frames corresponding to visualization of the flow about the stores.

Photo No.	Config.	α	View	Lens (mm)	Exposure Characteristics	Tube Location
12-25	4	0°	side	90	f 2.5, 1/15 s	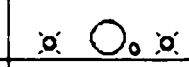
13-01	4	0°	bottom	228	f 2.5, 1/30 s	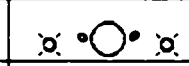
13-02	4	20°	bottom	228	f 2.5, 1/30 s	
13-03	5a	0°	bottom	228	f 2.5, 1/30 s	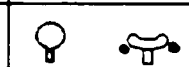
13-04	5a	0°	bottom	228	f 2.5, 1/30 s	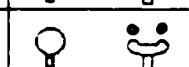
13-05	5a	0°	bottom	228	f 2.5, 1/30 s	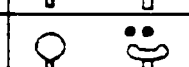
13-06	5a	0°	bottom	228	f 2.5, 1/30 s	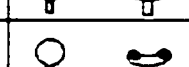
13-07	5a	0°	bottom	228	f 2.5, 1/30 s	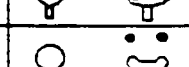
13-08	5a	0°	bottom	228	f 2.5, 1/30 s	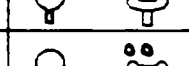
13-09	5a	0°	bottom	228	f 2.5, 1/30 s	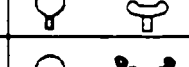
13-10	5a	5°	bottom	228	f 2.5, 1/30 s	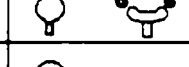
13-11	5a	5°	side	90	f 5.6, 1/30 s	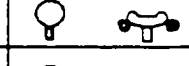
13-12	5a	5°	side	90	f 5.6, 1/30 s	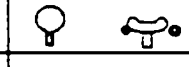
13-13	5a	5°	side	90	f 5.6, 1/30 s	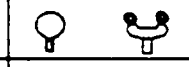
13-14	5a	5°	side	90	f 5.6, 1/30 s	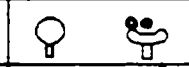
13-15	5a	0°	side	90	f 5.6, 1/30 s	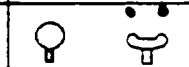
13-16	5a	0°	side	90	f 5.6, 1/30 s	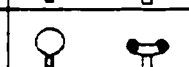
13-17	5a	0°	side	90	f 5.6, 1/30 s	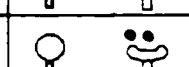
13-18	5b	5°	side	90	f 5.6, 1/30 s	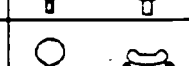
13-19	5b	5°	side	90	f 5.6, 1/30 s	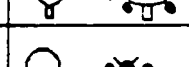

Table 3: Frames corresponding to visualization of the flow about the stores.

Photo No.	Config.	α	View	Lens (mm)	Exposure Characteristics	Tube Location
13-20	5b	5°	side	90	f 5.6, 1/30 s	
13-21	5b	5°	side	90	f 5.6, 1/30 s	
13-22	5b	5°	side	90	f 5.6, 1/30 s	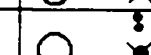
13-23	5b	5°	bottom	228	f 2.5, 1/30 s	
13-24	5b	5°	bottom	228	f 2.5, 1/30 s	
13-25	5b	5°	bottom	228	f 2.5, 1/30 s	
14-01	5b	0°	bottom	228	f 2.5, 1/30 s	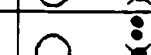
14-02	5b	0°	bottom	228	f 2.5, 1/30 s	
14-03	5b	0°	side	90	f 5.6, 1/30 s	
14-04	5b	0°	side	90	f 5.6, 1/30 s	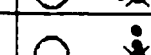
14-05	5b	0°	side	90	f 5.6, 1/30 s	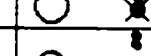
14-06	6a	5°	side	90	f 5.6, 1/30 s	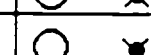
14-07	6a	5°	side	90	f 5.6, 1/30 s	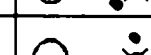
14-08	6a	5°	side	90	f 5.6, 1/30 s	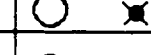
14-09	6a	5°	side	90	f 5.6, 1/30 s	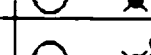
14-10	6a	5°	side	90	f 5.6, 1/30 s	
14-11	6a	5°	bottom	228	f 2.5, 1/30 s	
14-12	6a	5°	bottom	228	f 2.5, 1/30 s	
14-13	6a	5°	bottom	228	f 2.5, 1/30 s	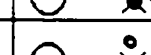
14-14	6a	5°	bottom	228	f 2.5, 1/30 s	
14-15	6a	-1°	bottom	228	f 2.5, 1/30 s	

Table 3: Frames corresponding to visualization of the flow about the stores.

Photo No.	Config.	α	View	Lens (mm)	Exposure Characteristics	Tube Location
14-16	6a	-1°	bottom	228	f 2.5, 1/30 s	
14-17	6a	-1°	bottom	228	f 2.5, 1/30 s	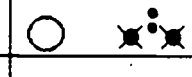
14-18	6a	-1°	bottom	228	f 2.5, 1/30 s	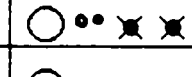
14-19	6a	-1°	side	90	f 5.6, 1/30 s	
14-20	6a	-1°	side	90	f 5.6, 1/30 s	
14-21	6a	-1°	side	90	f 5.6, 1/30 s	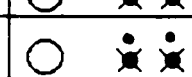
14-22	6a	-1°	side	90	f 5.6, 1/30 s	
14-24	6a	-1°	side	90	f 5.6, 1/30 s	
14-25	6a	20°	side	90	f 5.6, 1/30 s	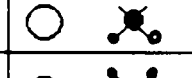
15-01	6b	5°	bottom	228	f 2.5, 1/30 s	
15-02	6b	5°	bottom	228	f 2.5, 1/30 s	
15-03	6b	5°	bottom	228	f 2.5, 1/30 s	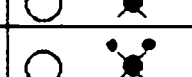
15-04	6b	-1°	bottom	228	f 2.5, 1/30 s	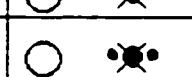
15-05	6b	-1°	bottom	228	f 2.5, 1/30 s	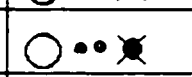
15-06	6b	-1°	bottom	228	f 2.5, 1/30 s	
15-07	6b	-1°	bottom	228	f 2.5, 1/30 s	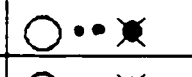
15-08	6b	5°	bottom	228	f 2.5, 1/30 s	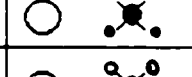
15-09	6b	5°	side	90	f 5.6, 1/30 s	
15-10	6b	5°	side	90	f 5.6, 1/30 s	
15-11	6b	5°	side	90	f 5.6, 1/30 s	

Table 3: Frames corresponding to visualization of the flow about the stores.

Photo No.	Config.	α	View	Lens (mm)	Exposure Characteristics	Tube Location
15-12	6b	5°	side	90	f 5.6, 1/30 s	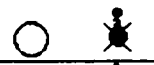
15-13	6b	5°	side	90	f 5.6, 1/30 s	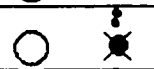
15-14	6b	-1°	side	90	f 5.6, 1/30 s	
15-15	6b	-1°	side	90	f 5.6, 1/30 s	
15-16	6b	-1°	side	90	f 5.6, 1/30 s	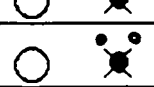
15-17	6b	-1°	side	90	f 5.6, 1/30 s	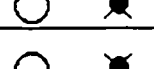
15-18	6b	-1°	side	90	f 5.6, 1/30 s	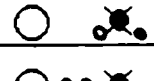
15-19	7	5°	side	90	f 5.6, 1/30 s	
15-20	7	5°	side	90	f 5.6, 1/30 s	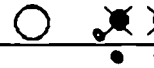
15-21	7	5°	side	90	f 5.6, 1/30 s	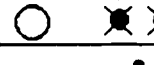
15-23	7	5°	side	90	f 5.6, 1/30 s	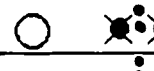
15-24	7	5°	side	90	f 5.6, 1/30 s	
15-25	7	5°	bottom	228	f 2.5, 1/30 s	
16-01	7	5°	bottom	228	f 2.5, 1/30 s	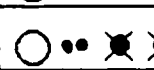
16-02	7	5°	bottom	228	f 2.5, 1/30 s	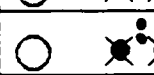
16-03	7	5°	bottom	228	f 2.5, 1/30 s	
16-04	7	-1°	bottom	228	f 2.5, 1/30 s	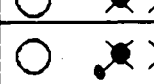
16-05	7	-1°	bottom	228	f 2.5, 1/30 s	
16-06	7	-1°	side	90	f 5.6, 1/30 s	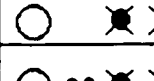
16-07	7	-1°	side	90	f 5.6, 1/30 s	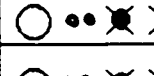

Table 3: Frames corresponding to visualization of the flow about the stores.

Photo No.	Config.	α	View	Lens (mm)	Exposure Characteristics	Tube Location
16-08	7	-1°	side	90	f 5.6, 1/30 s	
16-09	7	15°	side	90	f 5.6, 1/30 s	
16-10	7	15°	side	90	f 5.6, 1/30 s	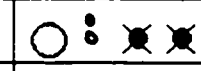
16-11	7	15°	side	90	f 5.6, 1/30 s	
16-12	7	15°	side	90	f 5.6, 1/30 s	
16-13	7	15°	bottom	228	f 2.5, 1/30 s	
16-14	7	15°	bottom	228	f 2.5, 1/30 s	
16-15	7	15°	bottom	228	f 2.5, 1/30 s	
16-16	7	15°	bottom	228	f 2.5, 1/30 s	
16-17	7	25°	bottom	228	f 2.5, 1/30 s	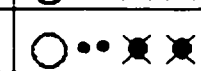
16-18	7	25°	bottom	228	f 2.5, 1/30 s	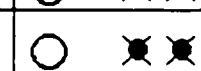
16-19	7	25°	bottom	228	f 2.5, 1/30 s	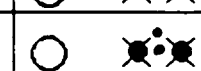
16-20	7	25°	side	90	f 5.6, 1/30 s	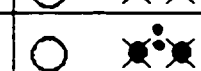
16-21	7	25°	side	90	f 5.6, 1/30 s	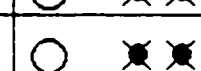
16-22	7	25°	side	90	f 5.6, 1/30 s	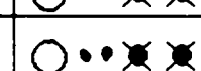
17-01	8a	0°	bottom	228	f 2.5, 1/30 s	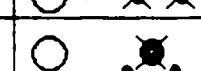
17-02	8a	5°	bottom	228	f 2.5, 1/30 s	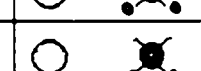
17-03	8a	5°	bottom	228	f 2.5, 1/30 s	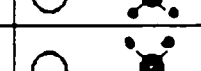
17-04	8a	5°	bottom	228	f 2.5, 1/30 s	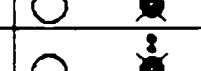
17-05	8a	5°	bottom	228	f 2.5, 1/30 s	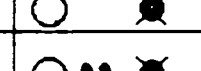

Table 3: Frames corresponding to visualization of the flow about the stores.

Photo No.	Config.	α	View	Lens (mm)	Exposure Characteristics	Tube Location
17-06	8a	5°	bottom	228	f 2.5, 1/30 s	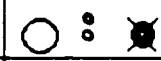
17-07	8a	5°	side	90	f 5.6, 1/30 s	
17-08	8a	5°	side	90	f 5.6, 1/30 s	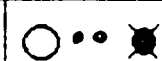
17-09	8a	5°	side	90	f 5.6, 1/30 s	
17-10	8a	5°	side	90	f 5.6, 1/30 s	
17-11	8a	5°	side	90	f 5.6, 1/30 s	
17-12	8a	-1°	side	90	f 5.6, 1/30 s	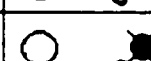
17-13	8a	-1°	side	90	f 5.6, 1/30 s	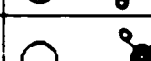
17-14	8a	-1°	side	90	f 5.6, 1/30 s	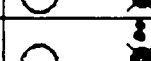
17-15	8a	-1°	side	90	f 5.6, 1/30 s	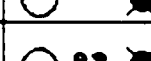
17-16	8a	-1°	side	90	f 5.6, 1/30 s	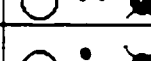
17-17	8a	-1°	bottom	228	f 2.5, 1/30 s	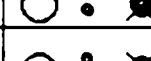
17-18	8a	-1°	bottom	228	f 2.5, 1/30 s	
17-19	8a	-1°	bottom	228	f 2.5, 1/30 s	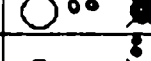
17-20	8a	-1°	bottom	228	f 2.5, 1/30 s	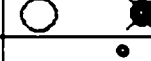
17-21	8a	-1°	bottom	228	f 2.5, 1/30 s	
17-22	8a	15°	bottom	228	f 2.5, 1/30 s	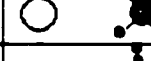
17-23	8a	15°	bottom	228	f 2.5, 1/30 s	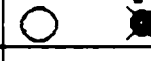
17-24	8a	15°	side	90	f 5.6, 1/30 s	
17-25	8a	15°	side	90	f 5.6, 1/30 s	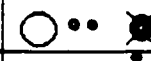

Table 3: Frames corresponding to visualization of the flow about the stores.

Photo No.	Config.	α	View	Lens (mm)	Exposure Characteristics	Tube Location
18-02	8b	5°	bottom	228	f 2.5, 1/30 s	
18-03	8b	5°	bottom	228	f 2.5, 1/30 s	
18-04	8b	5°	bottom	228	f 2.5, 1/30 s	
18-05	8b	5°	bottom	228	f 2.5, 1/30 s	
18-06	8b	5°	bottom	228	f 2.5, 1/30 s	
18-07	8b	5°	bottom	228	f 2.5, 1/30 s	
18-08	8b	5°	bottom	228	f 2.5, 1/30 s	
18-09	8b	5°	side	90	f 5.6, 1/30 s	
18-10	8b	5°	side	90	f 5.6, 1/30 s	
18-11	8b	5°	side	90	f 5.6, 1/30 s	
18-12	8b	5°	side	90	f 5.6, 1/30 s	
18-13	8b	5°	side	90	f 5.6, 1/30 s	
18-14	8b	5°	side	90	f 5.6, 1/30 s	
18-15	8b	5°	side	90	f 5.6, 1/30 s	
18-16	8b	-1°	side	90	f 5.6, 1/30 s	
18-17	8b	-1°	side	90	f 5.6, 1/30 s	
18-18	8b	-1°	bottom	228	f 2.5, 1/30 s	
18-19	8b	-1°	bottom	228	f 2.5, 1/30 s	
18-20	8b	15°	bottom	228	f 2.5, 1/30 s	
18-21	8b	15°	bottom	228	f 2.5, 1/30 s	

Table 3: Frames corresponding to visualization of the flow about the stores.

Photo No.	Config.	α	View	Lens (mm)	Exposure Characteristics	Tube Location
18-22	8b	15°	side	90	f 2.5, 1/30 s	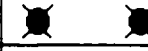
18-23	8b	15°	side	90	f 5.6, 1/30 s	
18-24	8b	15°	side	90	f 5.6, 1/30 s	

Table 4: Frames corresponding to flow visualization of the upper surface vortices.

Photo No.	α	View	Lens (mm)	Exposure Characteristics	Method	Feature
19-01	25°	top	52	f 1.4, 1/250 s	water dye	LEX vortex
19-02	25°	top	90	f 4, 1/125 s	water dye	LEX vortex
19-03	25°	side	52	f 4, 1/125 s	water dye	LEX vortex
19-04	25°	side	90	f 4, 1/90 s	water dye	LEX vortex
19-05	30°	side	52	f 4, 1/125 s	water dye	LEX vortex
19-06	35°	side	52	f 4, 1/125 s	water dye	LEX vortex
19-07	35°	side	90	f 4, 1/60 s	water dye	LEX vortex
19-08	39°	side	52	f 4, 1/90 s	water dye	LEX vortex
19-09	20°	side	52	f 4, 1/125 s	water dye	LEX vortex
19-10	15°	side	52	f 4, 1/125 s	water dye	LEX vortex
19-11	10°	side	52	f 4, 1/125 s	water dye	LEX vortex
19-12	5°	side	52	f 4, 1/125 s	water dye	LEX vortex
19-13	5°	top	52	f 4, 1/125 s	water dye	LEX vortex
19-14	10°	top	52	f 4, 1/125 s	water dye	LEX vortex
19-15	15°	top	52	f 4, 1/125 s	water dye	LEX vortex
19-16	20°	top	52	f 4, 1/125 s	water dye	LEX vortex
19-17	30°	top	52	f 4, 1/125 s	water dye	LEX vortex
19-18	30°	top	90	f 4, 1/125 s	water dye	LEX vortex
19-19	35°	top	52	f 4, 1/125 s	water dye	LEX vortex
19-20	35°	top	90	f 4, 1/125 s	water dye	LEX vortex
19-21	39°	top	52	f 4, 1/125 s	water dye	LEX vortex
19-22	39°	top	52	f 4, 1/125 s	water dye	LEX vortex
19-23	39°	top	90	f 4, 1/125 s	water dye	LEX vortex
19-24	25°	top	90	f 4, 1/125 s	water dye	LEX vortex
19-25	25°	top	90	f 4, 1/125 s	water dye	LEX vortex
20-01	25°	top	52	f 4, 1/125 s	water dye	Forebody vortices
20-02	25°	top	90	f 4, 1/125 s	water dye	Forebody vortices
20-03	25°	side	90	f 4, 1/125 s	water dye	Forebody vortices
20-04	25°	top	52	f 4, 1/125 s	water dye	Forebody/LEX interaction
20-05	25°	top	90	f 4, 1/125 s	water dye	Forebody/LEX interaction
20-06	25°	top	90	f 4, 1/125 s	water dye	Forebody/LEX interaction
20-07	35°	top	52	f 4, 1/125 s	water dye	Forebody/LEX interaction
20-08	35°	top	90	f 4, 1/125 s	water dye	Forebody/LEX interaction
20-09	35°	side	90	f 4, 1/125 s	water dye	Forebody/LEX interaction
20-10	35°	side	90	f 4, 1/125 s	water dye	Forebody/LEX interaction
20-11	35°	top	52	f 4, 1/125 s	water dye	Forebody/LEX interaction

Table 4: Frames corresponding to flow visualization of the upper surface vortices.

Photo No.	α	View	Lens (mm)	Exposure Characteristics	Method	Feature
20-12	35°	top	52	f 4, 1/125 s	water dye	Forebody vortices
20-13	35°	side	90	f 4, 1/125 s	water dye	Forebody vortices
20-14	35°	side	90	f 4, 1/125 s	water dye	Forebody vortices
20-15	15°	top	52	f 4, 1/125 s	water dye	Forebody vortices
20-16	15°	top	90	f 4, 1/125 s	water dye	Forebody vortices
20-17	15°	side	90	f 4, 1/125 s	water dye	Forebody vortices
20-18	15°	side	90	f 4, 1/125 s	water dye	Forebody vortices
20-19	15°	top	52	f 4, 1/125 s	water dye	Forebody/LEX interaction
20-20	15°	top	90	f 4, 1/125 s	water dye	Forebody/LEX interaction
20-21	15°	side	90	f 4, 1/125 s	water dye	Forebody/LEX interaction
20-22	15°	side	90	f 4, 1/125 s	water dye	Forebody/LEX interaction
21-01	30°	top	52	f 5.6, 1/125 s	shear dye	LEX vortex
21-02	30°	top	90	f 5.6, 1/125 s	shear dye	LEX vortex
21-03	30°	side	90	f 4, 1/250 s	shear dye	LEX vortex
21-04	25°	side	90	f 4, 1/250 s	shear dye	LEX vortex
21-05	25°	top	52	f 5.6, 1/125 s	shear dye	LEX vortex
21-06	25°	top	90	f 4, 1/125 s	shear dye	LEX vortex
21-07	20°	top	52	f 5.6, 1/125 s	shear dye	LEX vortex
21-08	20°	top	90	f 4, 1/125 s	shear dye	LEX vortex
21-09	20°	side	90	f 4, 1/250 s	shear dye	LEX vortex
21-10	35°	side	90	f 4, 1/250 s	shear dye	LEX vortex
21-11	35°	top	90	f 4, 1/125 s	shear dye	LEX vortex
21-12	35°	top	52	f 5.6, 1/125 s	shear dye	LEX vortex
21-13	30°	top	52	f 5.6, 1/250 s	bubbles	LEX vortex
21-14	30°	top	90	f 4, 1/250 s	bubbles	LEX vortex
21-15	30°	side	90	f 4, 1/250 s	bubbles	LEX vortex
21-16	35°	side	90	f 4, 1/250 s	bubbles	LEX vortex
21-17	35°	top	52	f 5.6, 1/250 s	bubbles	LEX vortex
21-18	35°	top	90	f 4, 1/250 s	bubbles	LEX vortex
21-19	35°	top	52	f 5.6, 1/60 s	bubbles	LEX vortex
21-20	25°	top	90	f 4, 1/60 s	bubbles	LEX vortex
21-21	25°	top	90	f 4, 1/125 s	bubbles	LEX vortex
21-22	25°	top	52	f 5.6, 1/125 s	bubbles	LEX vortex
21-23	25°	side	90	f 4, 1/125 s	bubbles	LEX vortex
21-24	25°	side	90	f 4, 1/60 s	bubbles	LEX vortex
22-01	20°	top	52	f 2.8, 1/250 s	bubbles	LEX vortex

Table 4: Frames corresponding to flow visualization of the upper surface vortices.

Photo No.	α	View	Lens (mm)	Exposure Characteristics	Method	Feature
22-02	20°	top	52	f 2.8, 1/500 s	bubbles	LEX vortex
22-03	20°	top	90	f 2.5, 1/250 s	bubbles	LEX vortex
22-04	20°	top	90	f 2.5, 1/125 s	bubbles	LEX vortex
22-05	20°	top	90	f 2.5, 1/250 s	bubbles	LEX vortex
22-06	20°	top	90	f 2.5, 1/250 s	bubbles	LEX vortex
22-07	20°	side	90	f 2.5, 1/250 s	bubbles	LEX vortex
22-08	25°	top	52	f 2.8, 1/250 s	bubbles	LEX vortex
22-09	25°	top	52	f 2.5, 1/500 s	bubbles	LEX vortex
22-10	25°	top	90	f 2.5, 1/250 s	bubbles	LEX vortex
22-11	25°	top	90	f 2.5, 1/500 s	bubbles	LEX vortex
22-12	25°	top	90	f 2.5, 1/250 s	bubbles	LEX vortex
22-13	25°	side	90	f 2.5, 1/250 s	bubbles	LEX vortex
22-14	25°	side	90	f 2.5, 1/250 s	bubbles	LEX vortex
22-15	30°	top	52	f 2.8, 1/125 s	bubbles	LEX vortex
22-16	30°	top	90	f 2.5, 1/125 s	bubbles	LEX vortex
22-17	30°	top	90	f 2.5, 1/250 s	bubbles	LEX vortex
22-18	30°	side	90	f 2.5, 1/250 s	bubbles	LEX vortex
22-19	30°	side	90	f 2.5, 1/125 s	bubbles	LEX vortex
22-20	35°	top	52	f 1.4, 1/500 s	bubbles	LEX vortex
22-21	35°	top	52	f 1.4, 1/250 s	bubbles	LEX vortex
22-22	35°	top	90	f 4, 1/125 s	bubbles	LEX vortex
22-23	35°	top	90	f 4, 1/125 s	bubbles	LEX vortex
22-24	35°	side	90	f 2.5, 1/125 s	bubbles	LEX vortex
22-25	35°	side	90	f 2.5, 1/125 s	bubbles	LEX vortex
22-26	35°	side	90	f 2.5, 1/250 s	bubbles	LEX vortex
22-27	39°	side	90	f 2.5, 1/250 s	bubbles	LEX vortex
22-28	39°	side	90	f 2.5, 1/250 s	bubbles	LEX vortex
22-29	39°	side	90	f 2.5, 1/250 s	bubbles	LEX vortex
22-30	39°	side	90	f 2.5, 1/250 s	bubbles	LEX vortex
22-31	39°	top	52	f 1.4, 1/1000 s	bubbles	LEX vortex
22-32	39°	top	52	f 2.8, 1/250 s	bubbles	LEX vortex
22-33	39°	top	90	f 2.5, 1/250 s	bubbles	LEX vortex
22-34	39°	top	90	f 2.5, 1/250 s	bubbles	LEX vortex
22-35	39°	top	90	f 4, 1/125 s	bubbles	LEX vortex
22-36	39°	top	52	f 2.8, 1/250 s	bubbles	LEX vortex
22-37	39°	side	90	f 2.5, 1/250 s	bubbles	LEX vortex

Figures

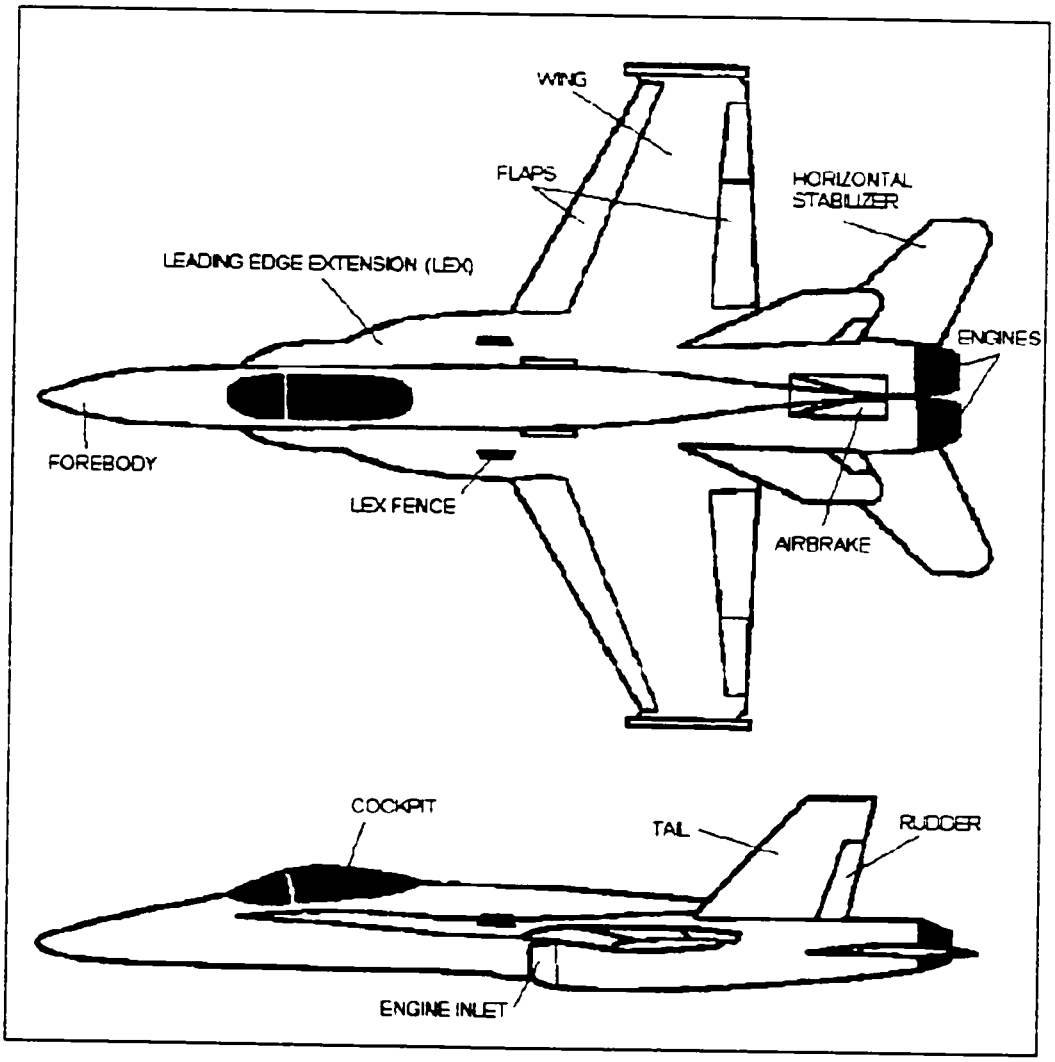

Figure 1: Top and side views of the CF-18 showing its major components.

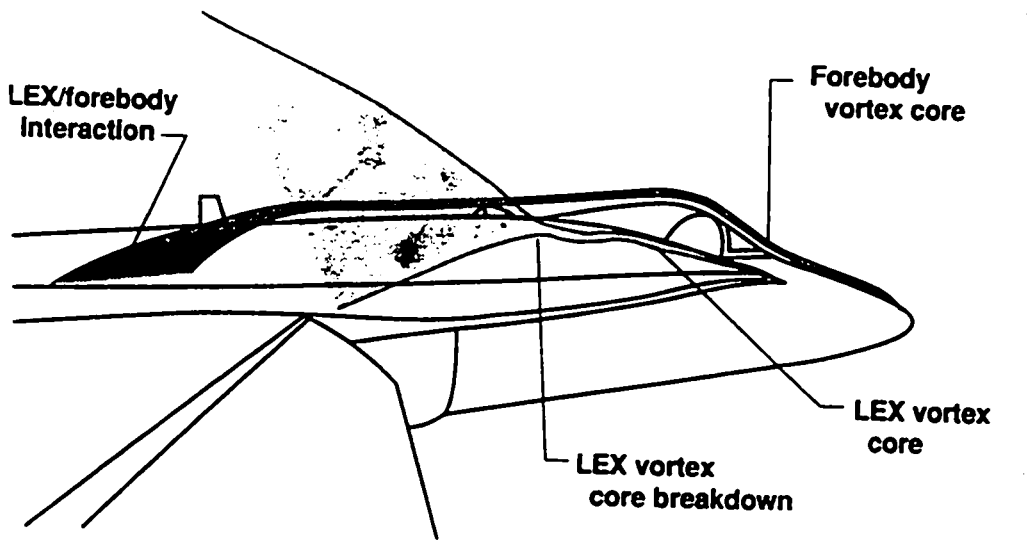

Figure 2: Sketch of the F-18 illustrating the LEX and forebody vortex locations (Del Frate et al, 1990).

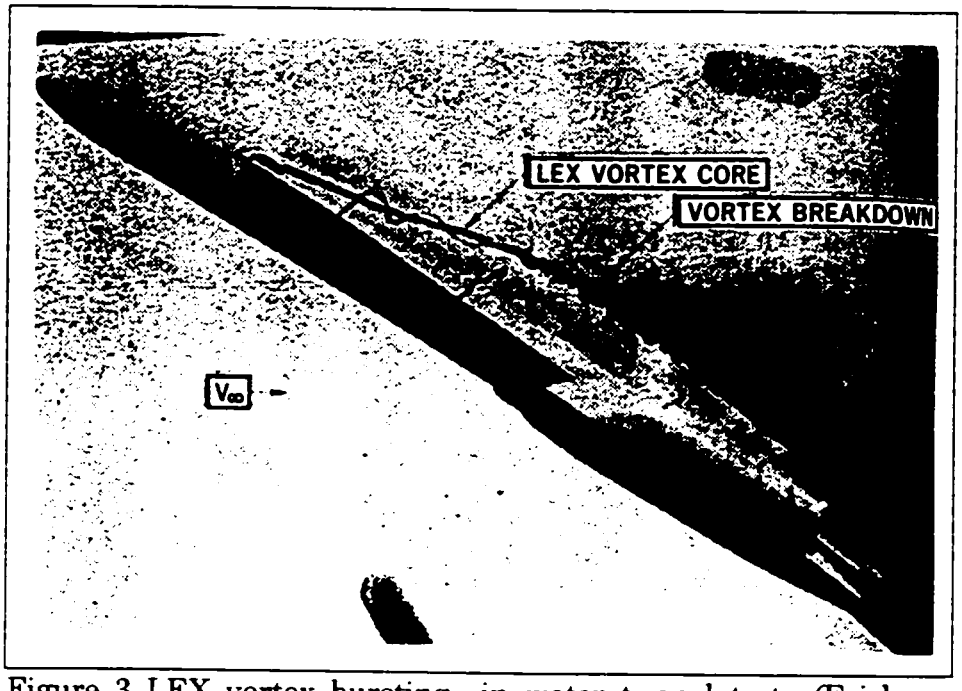

Figure 3 LEX vortex bursting in water tunnel tests (Erickson, 1982).

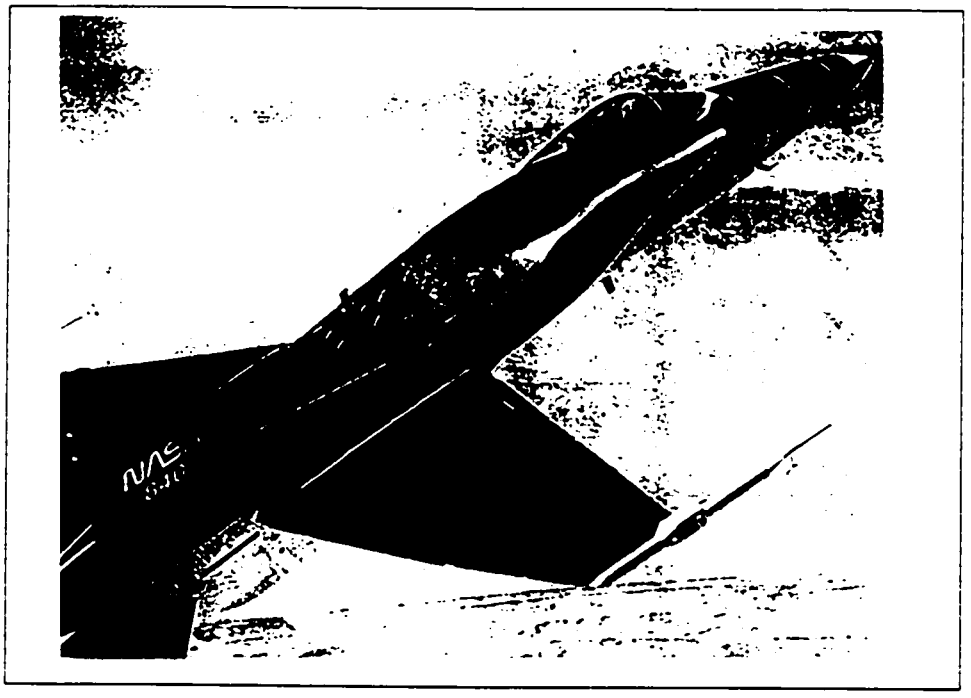

Figure 4: LEX vortex bursting in flight tests (Cummings, 1992).

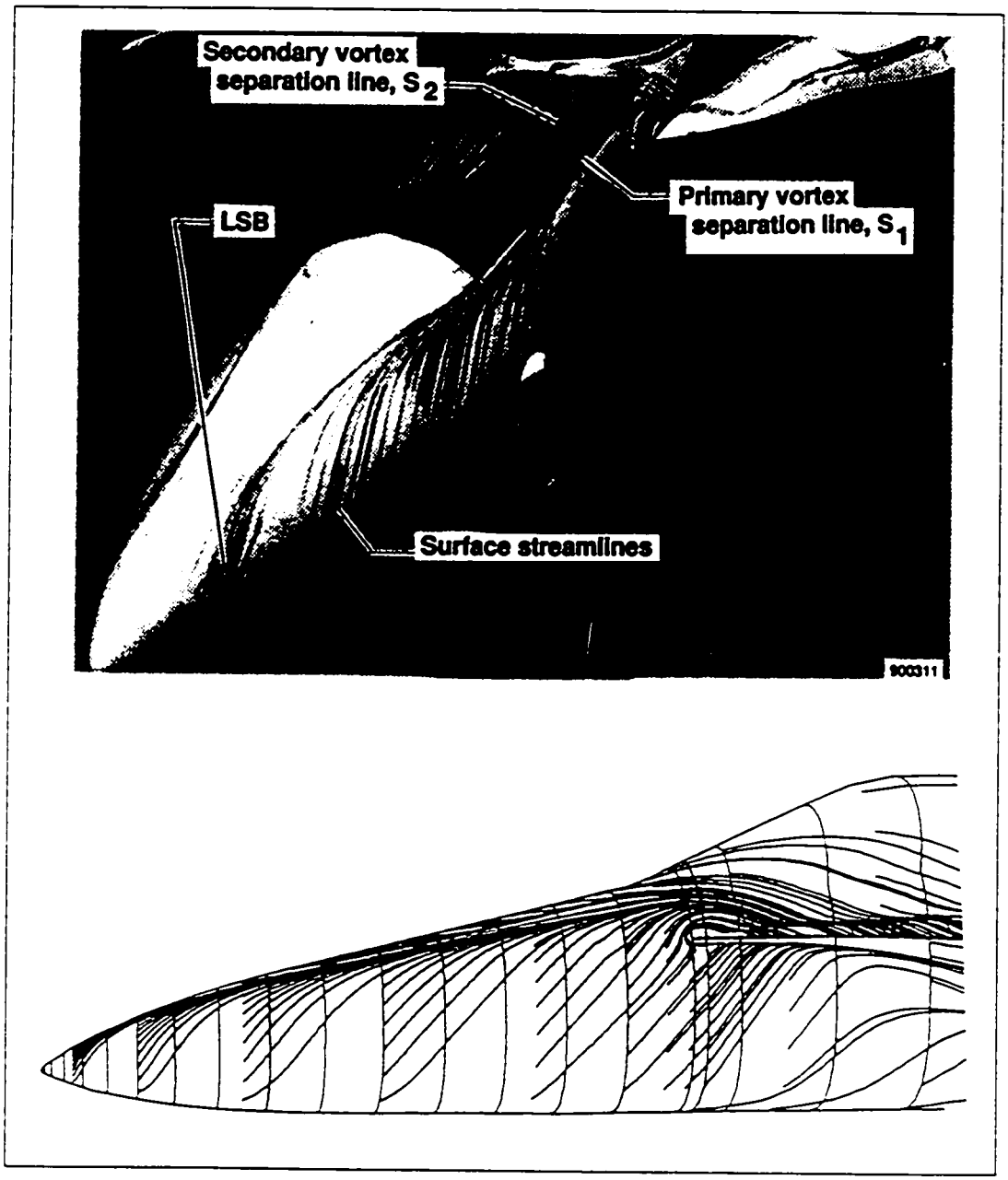

Figure 5: Surface flow visualization of the F-18 forebody, HARV (top, Del Frate et al. 1990) and computational (bottom, Thomas et al. 1989).

Research Facility	Re_c	Model scale, Percent	Fluid Medium
● Flight	8 to 13 x 10^6	–	Air
□ DTRC	1.75 x 10^6	6	Air
◇ BART	1.60 x 10^5	3	Air
△ LSWT	3.60 x 10^5	12	Air
▽ FVF	1.26 x 10^4	3	Water

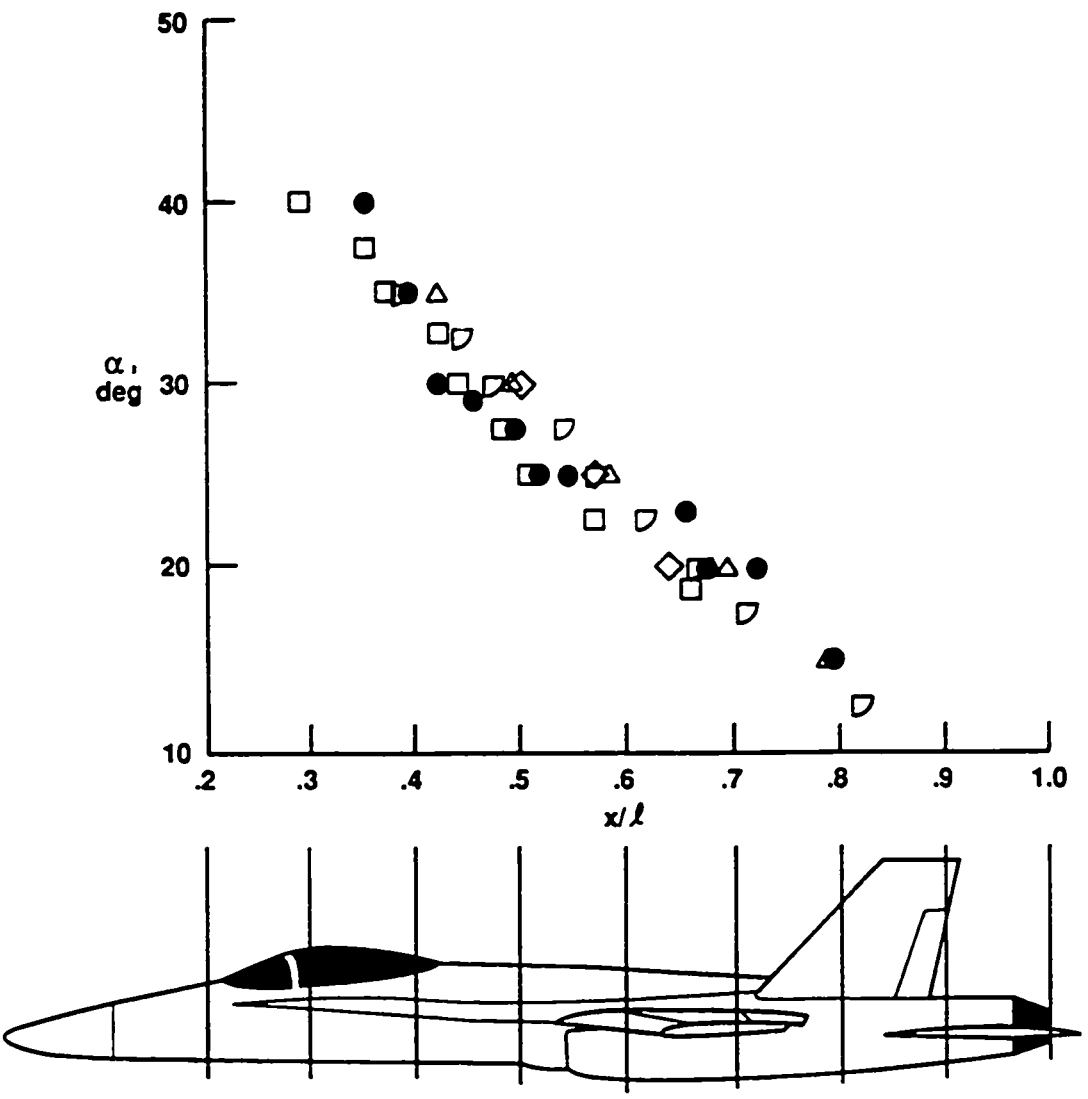

Figure 6: F-18 LEX vortex core breakdown locations at various angles of attack (Del Frate et al, 1990).

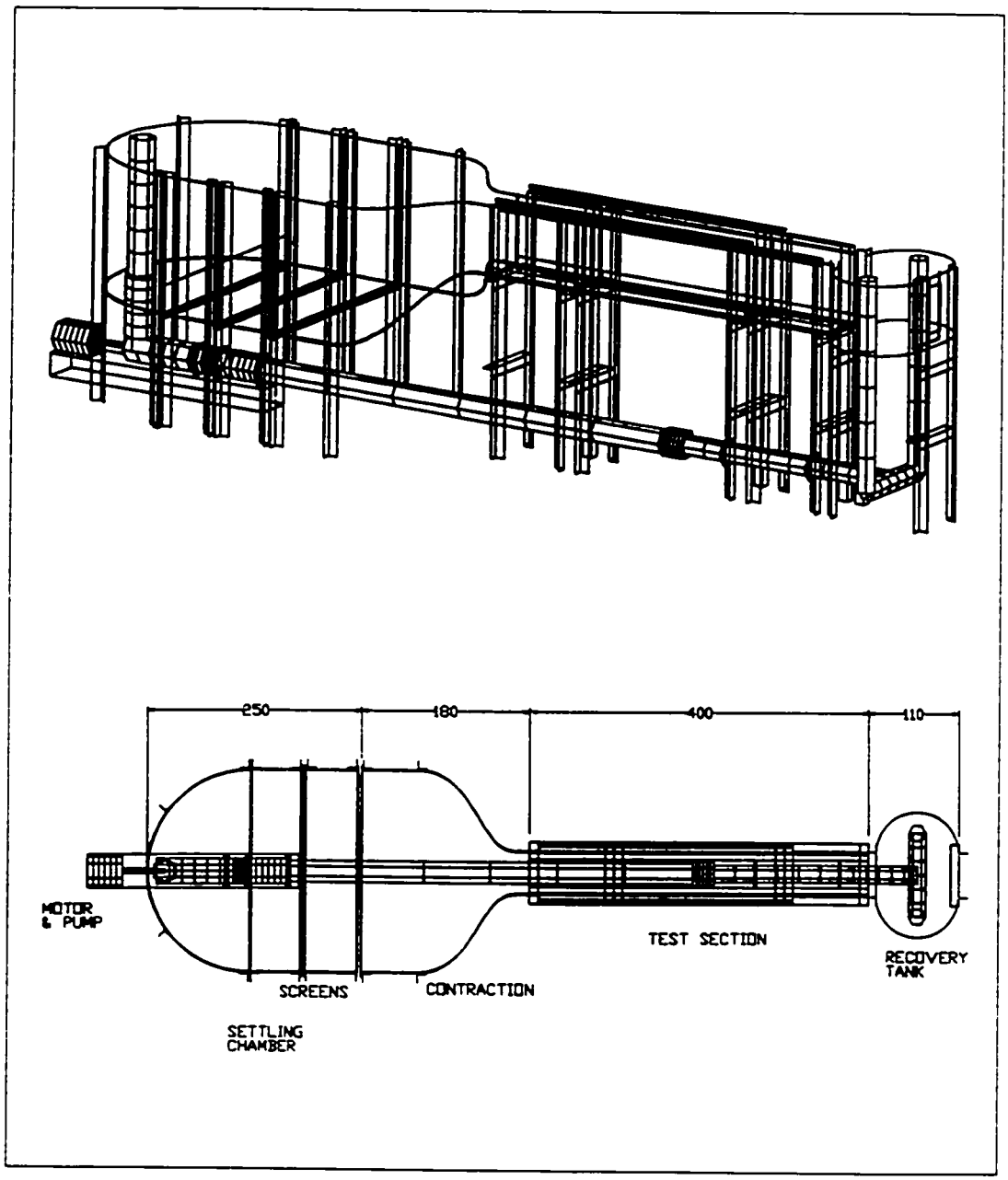

Figure 7: University of Ottawa recirculating water tunnel; dimensions in cm (Kislich-Lemyre, 1997).

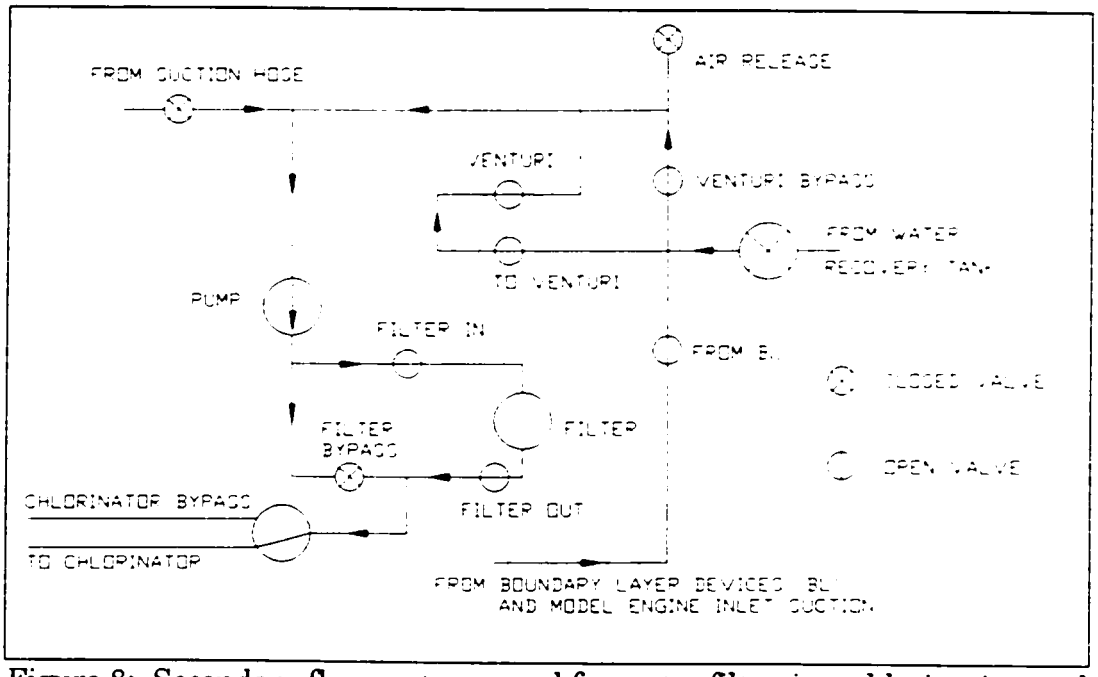

Figure 8: Secondary flow systems used for water filtration, chlorination and suction.

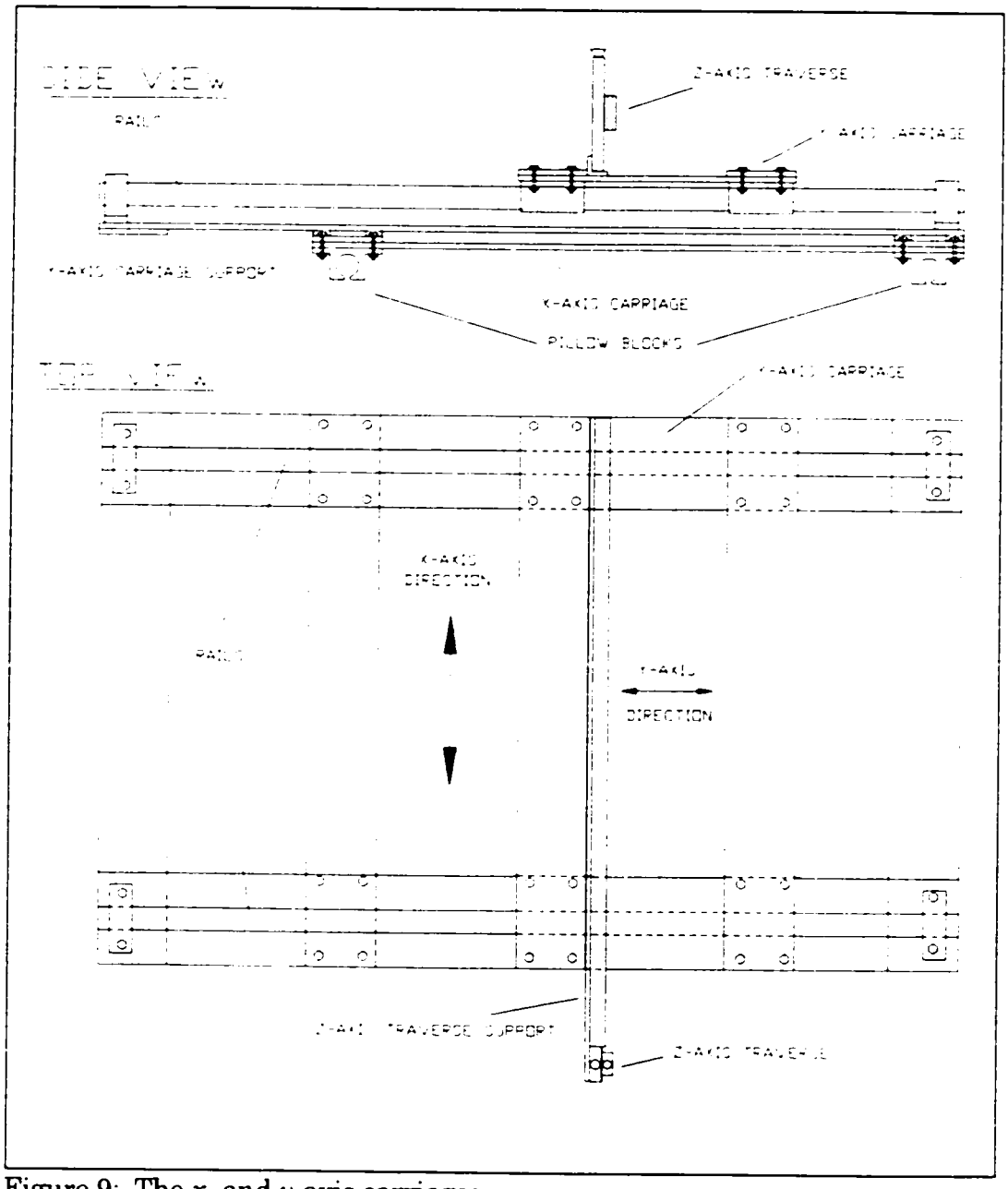

Figure 9: The x- and y-axis carriages.

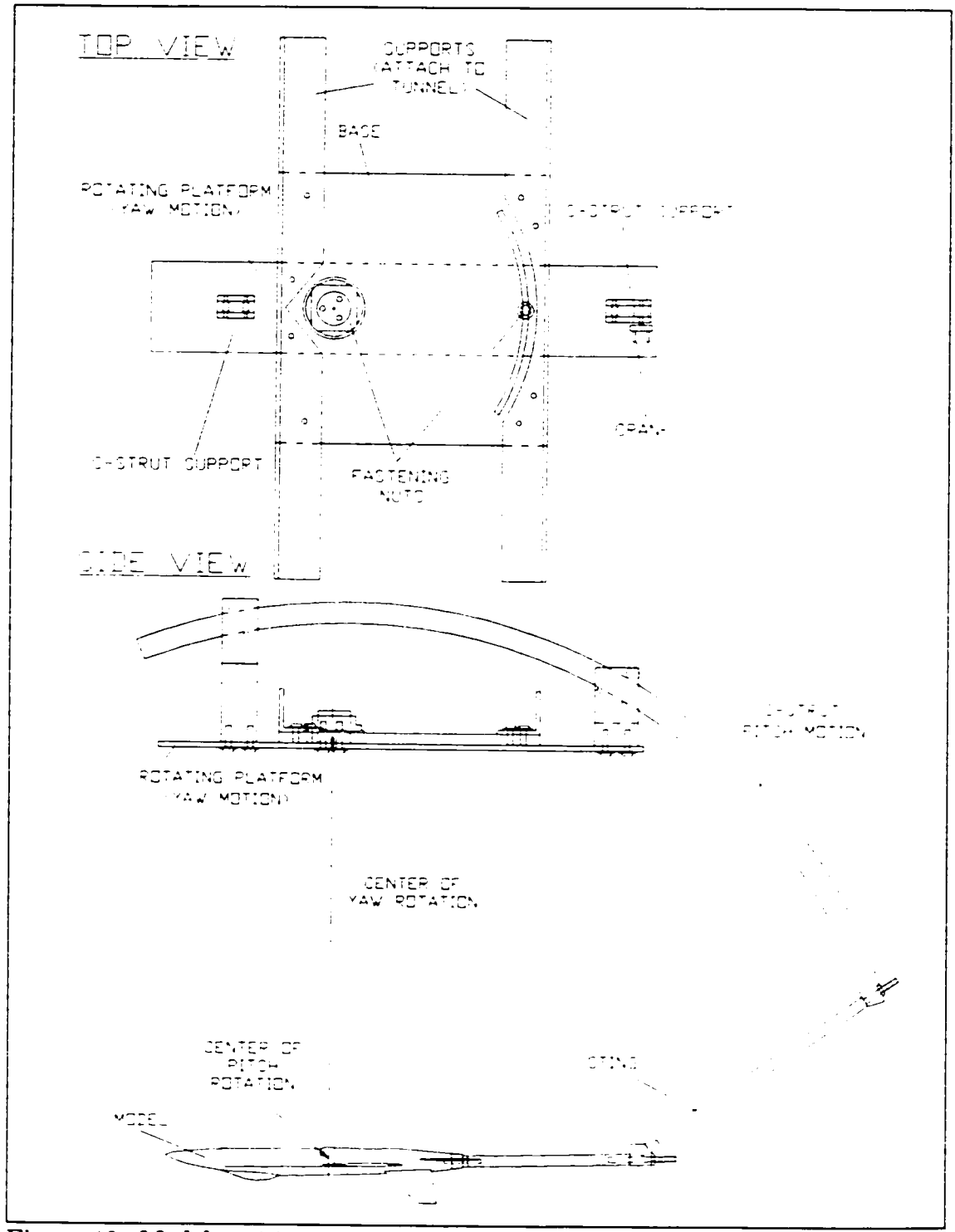

Figure 10: Model positioning system. Note that the C-strut, sting and model are not shown in the top view. Detailed drawings are available in Appendix A.

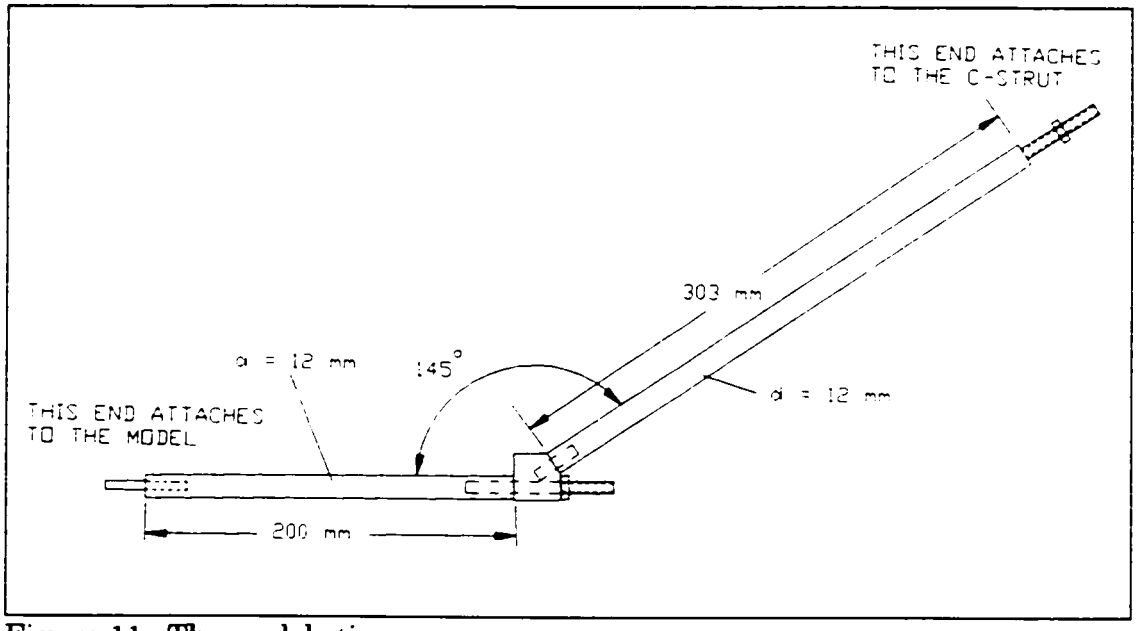

Figure 11: The model sting.

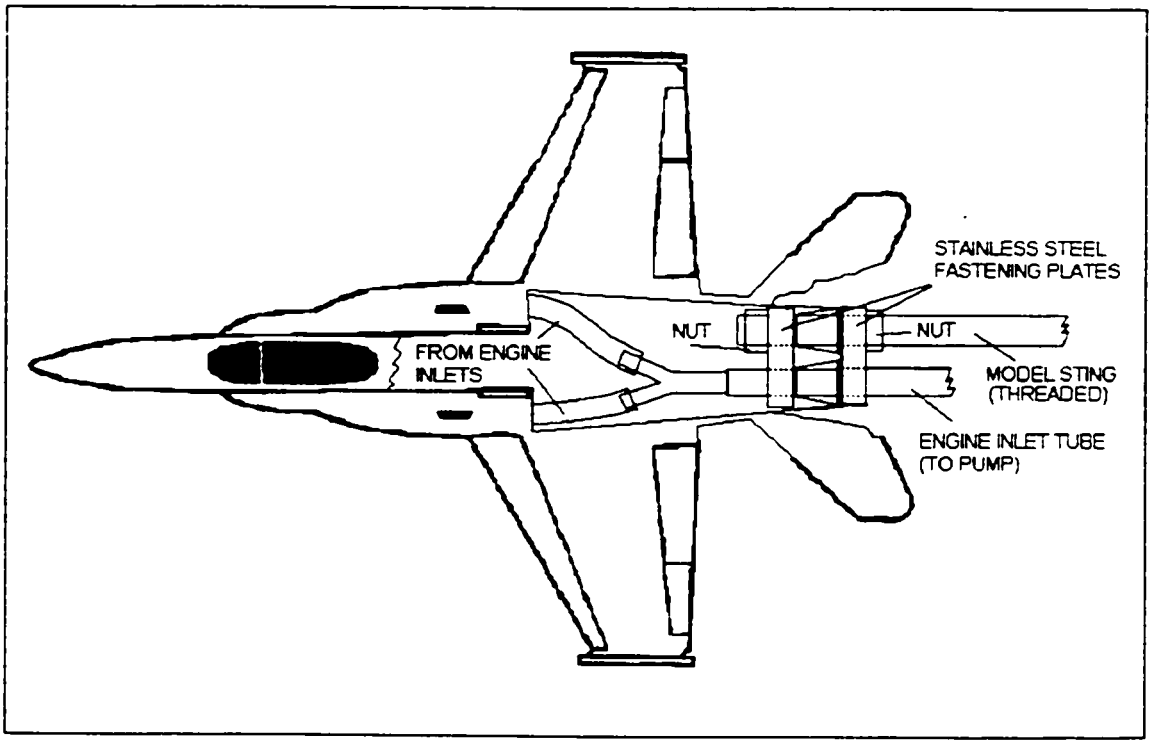

Figure 12: Positioning of the engine flow tubes and the sting as attached inside the model.

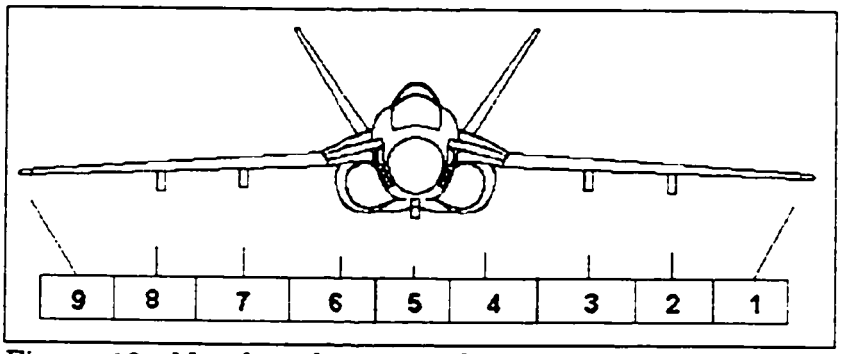

Figure 13: Numbered stations for store placement on the CF-18 aircraft.

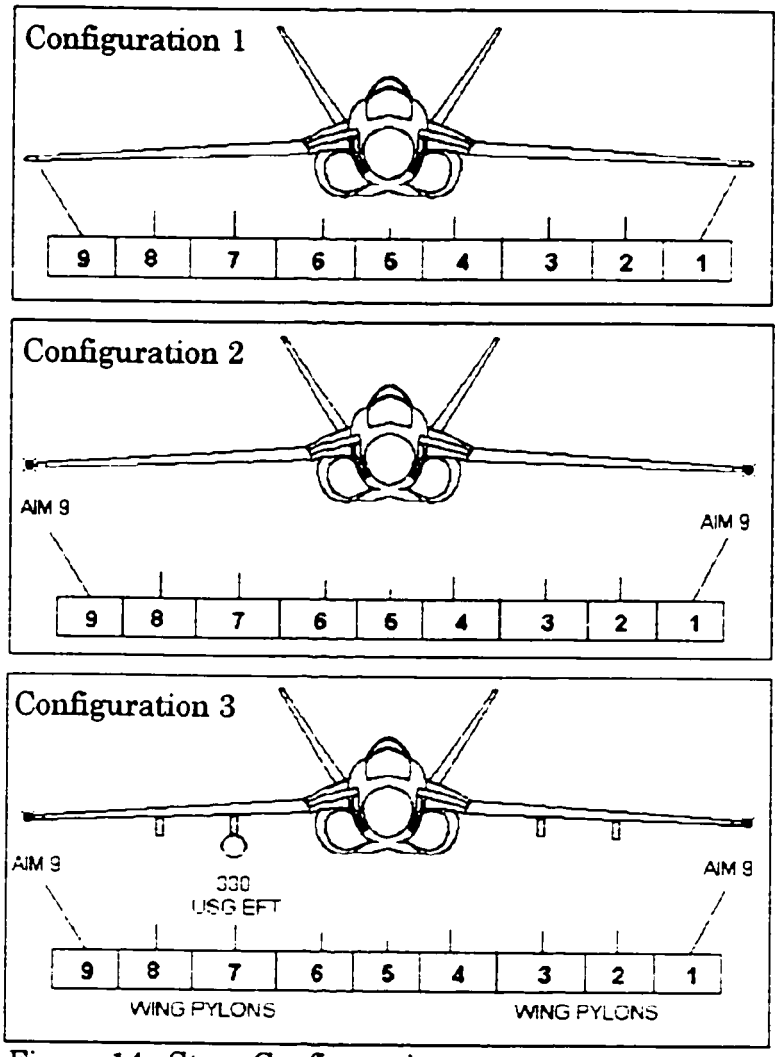

Figure 14: Store Configurations.

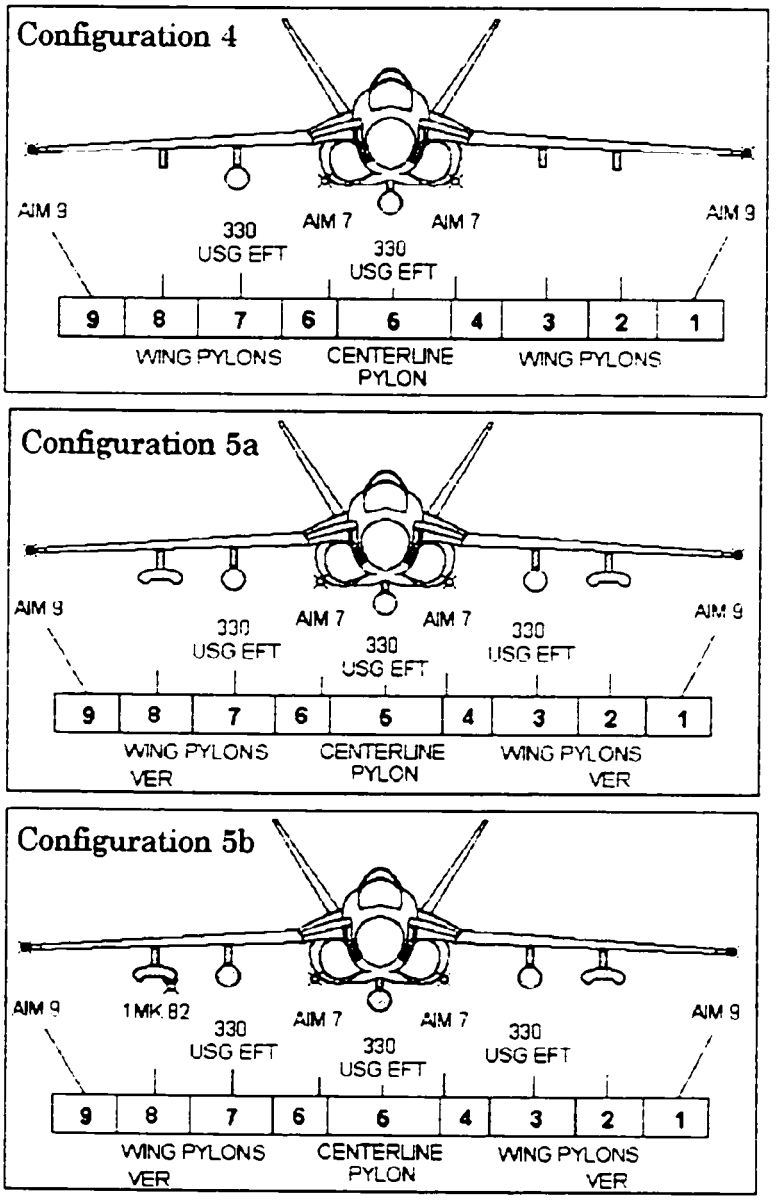

Figure 14 (continued): Store Configurations.

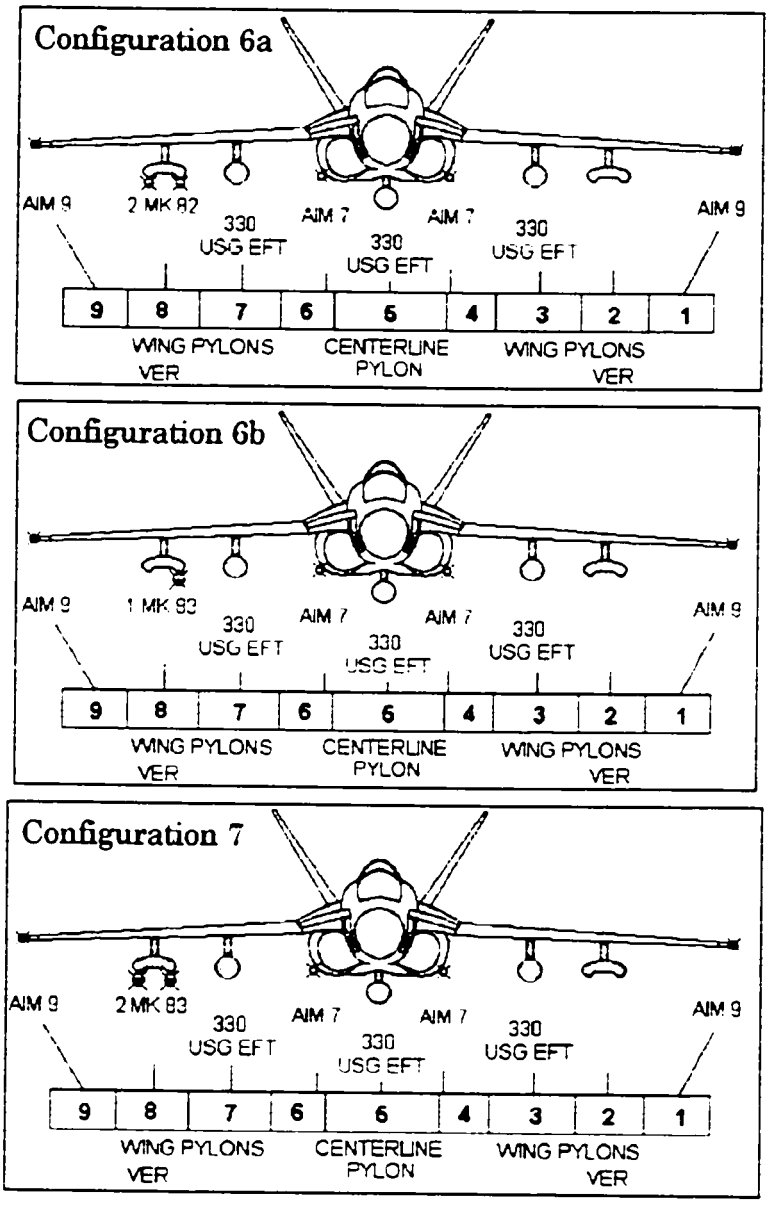

Figure 14 (continued): Store Configurations.

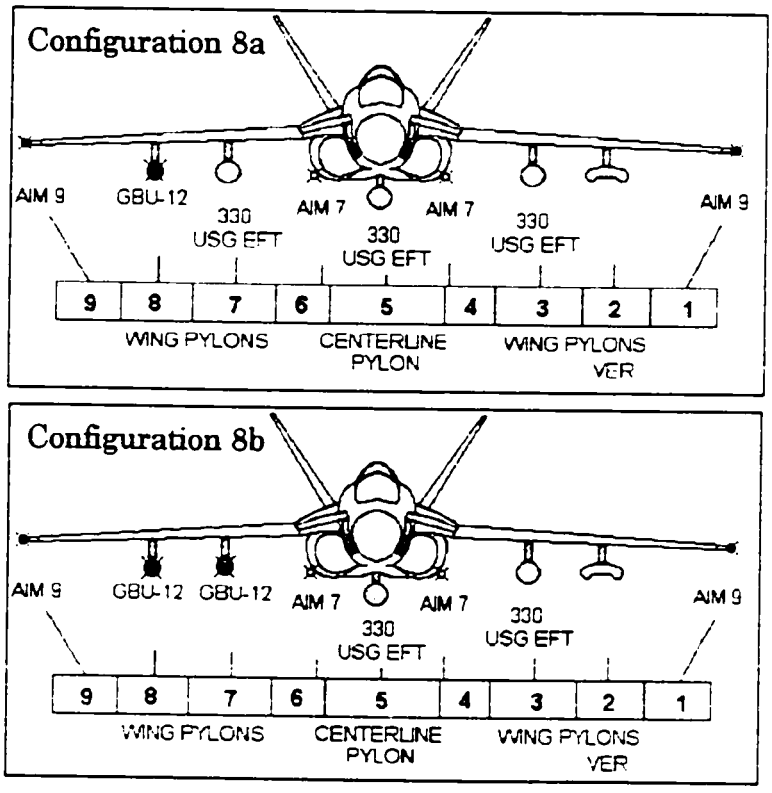

Figure 14 (concluded): Store Configurations.

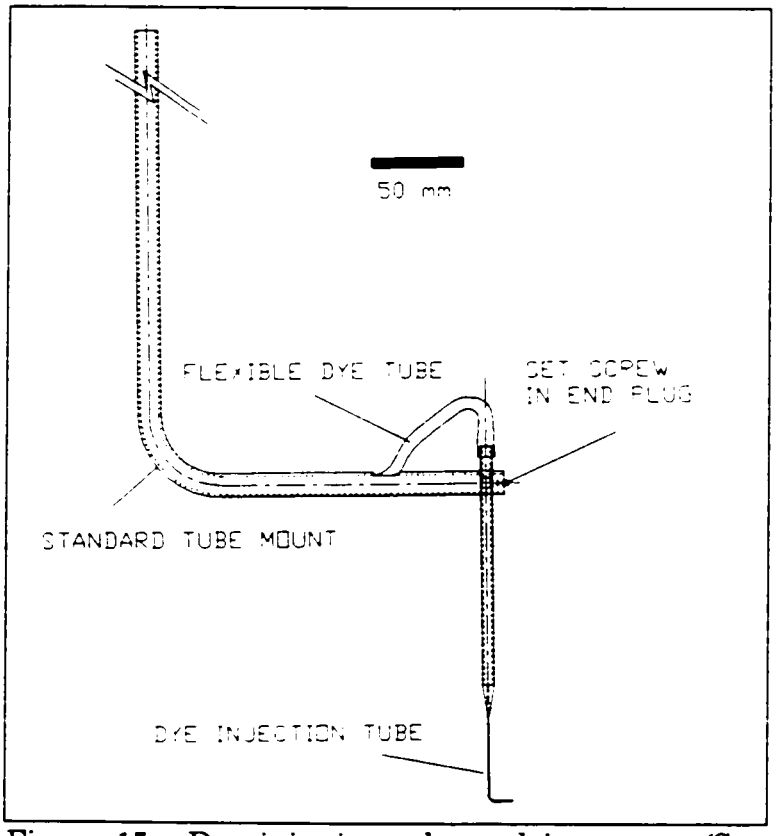

Figure 15: Dye injection tube and its mount (See Appendix A for more detailed drawings).

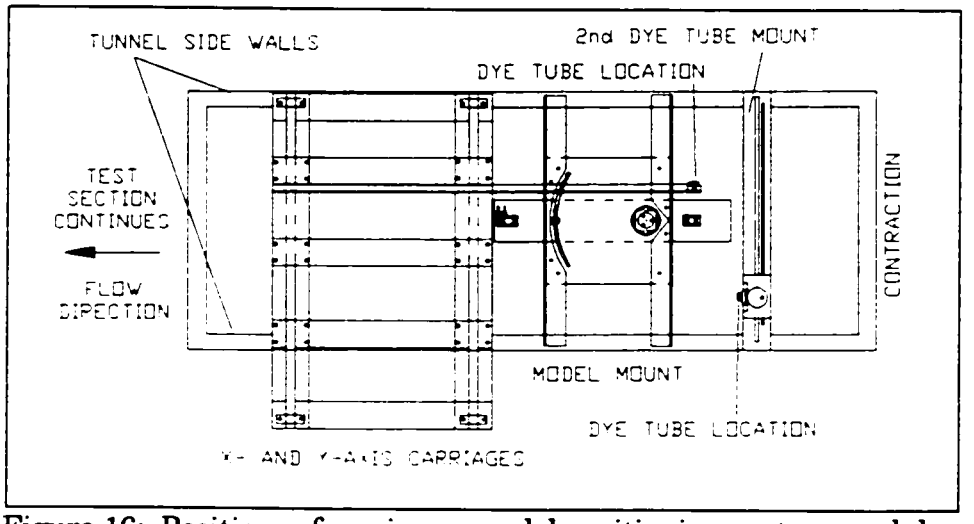

Figure 16: Positions of carriages, model positioning system, and dye tubes above the water tunnel.

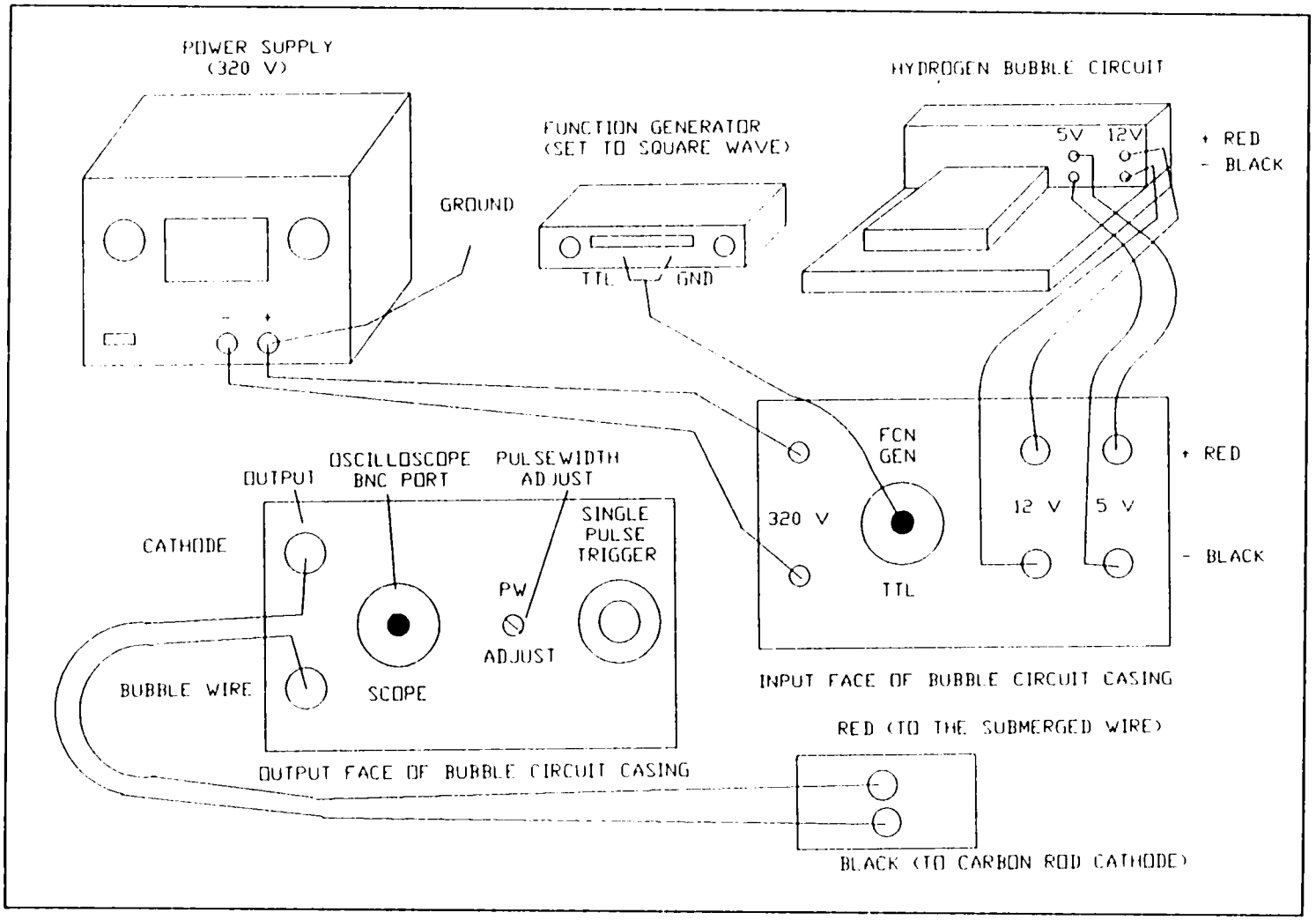

Figure 17: Hydrogen bubble system components and connections.

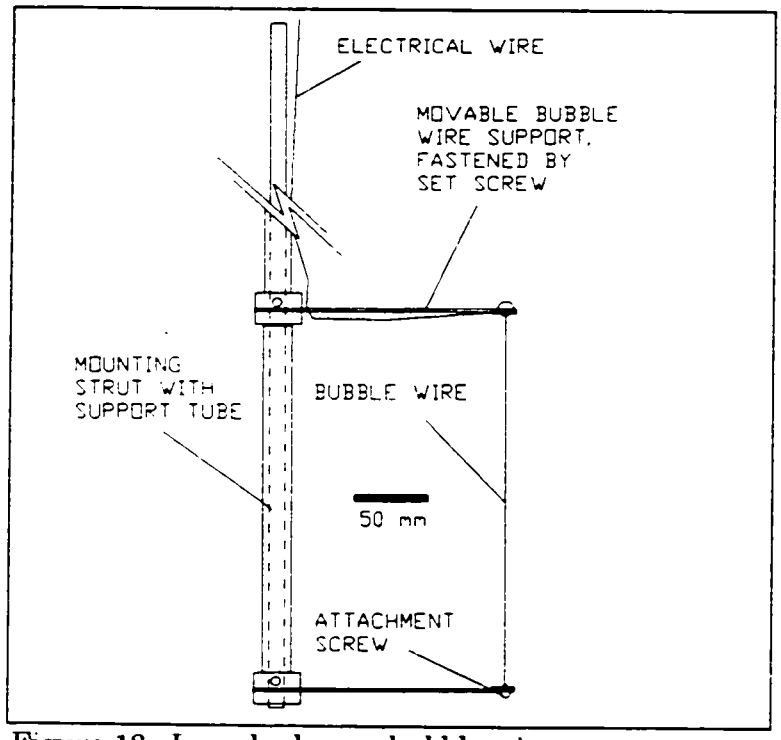

Figure 18: Long hydrogen bubble wire.

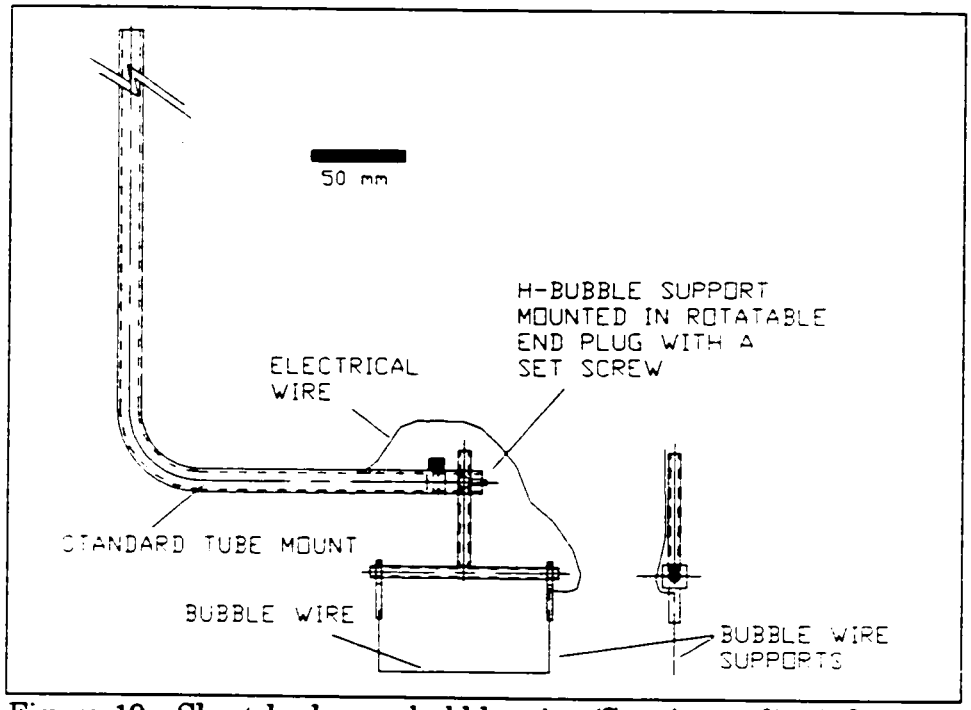

Figure 19: Short hydrogen bubble wire (See Appendix A for more detailed drawings).

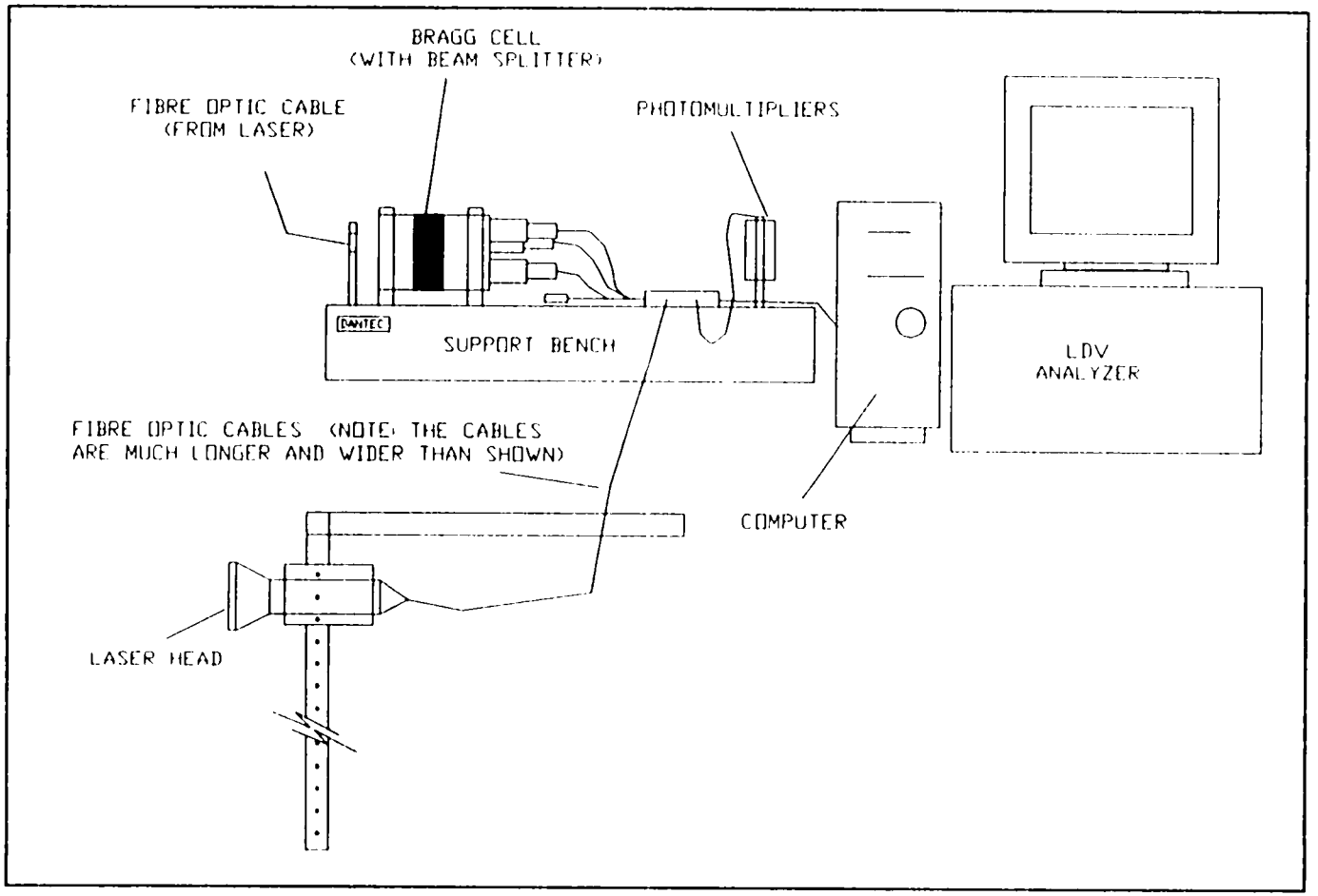

Figure 20: Laser Doppler Velocimetry components and connections.

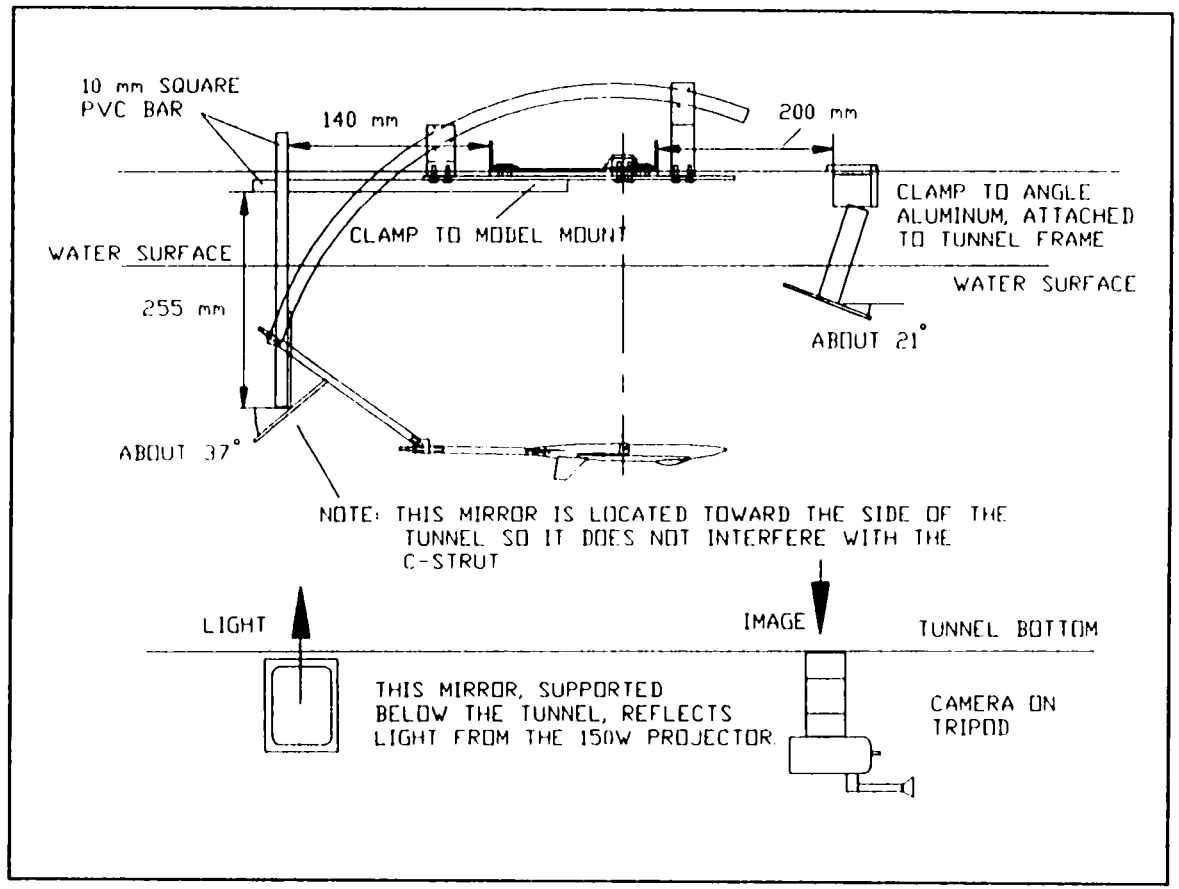

Figure 21: Typical mirror setup for low angle of attack studies.

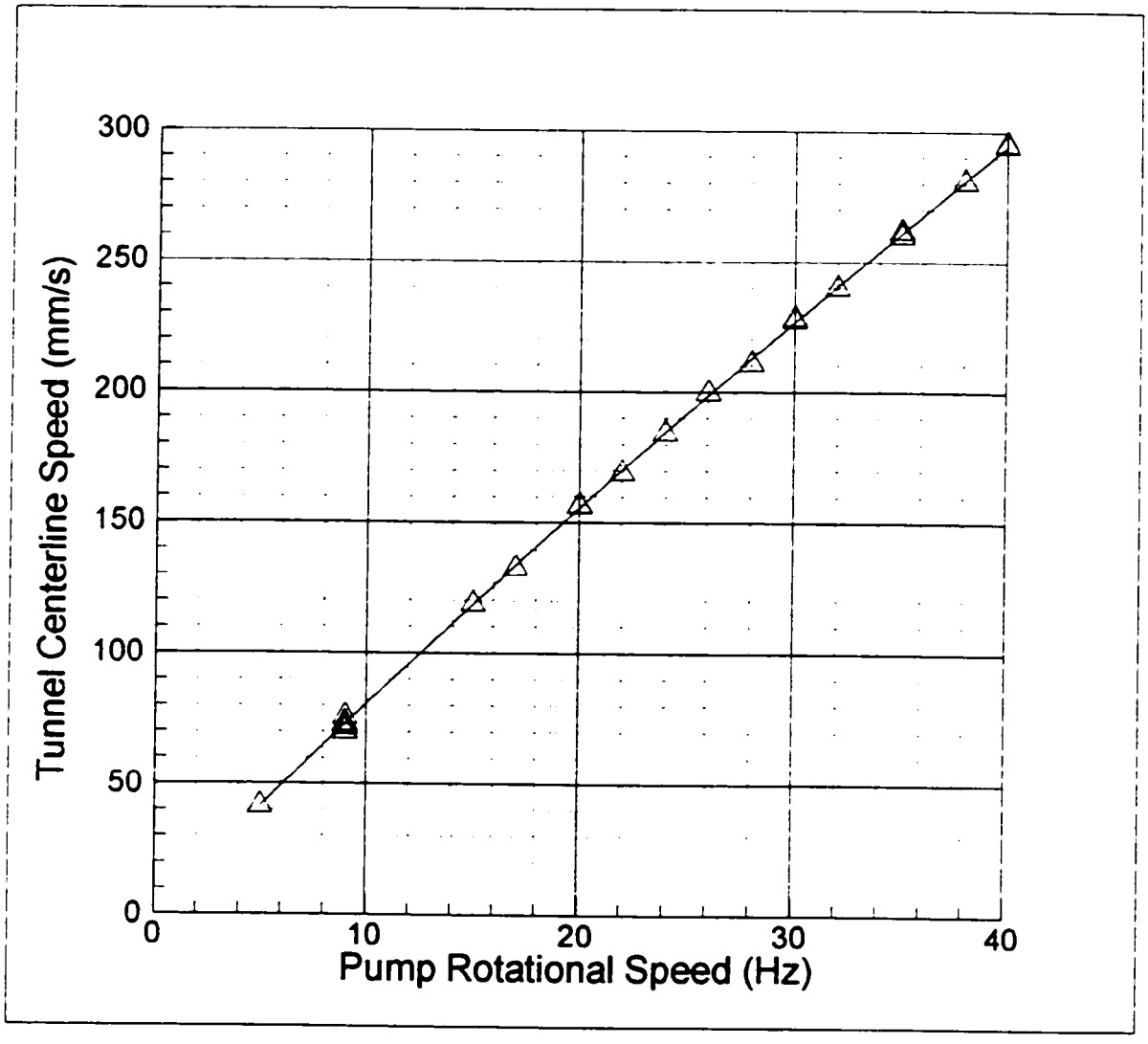

Figure 22: Centerline velocity vs. pump rotational speed (water level at 0.70 m).

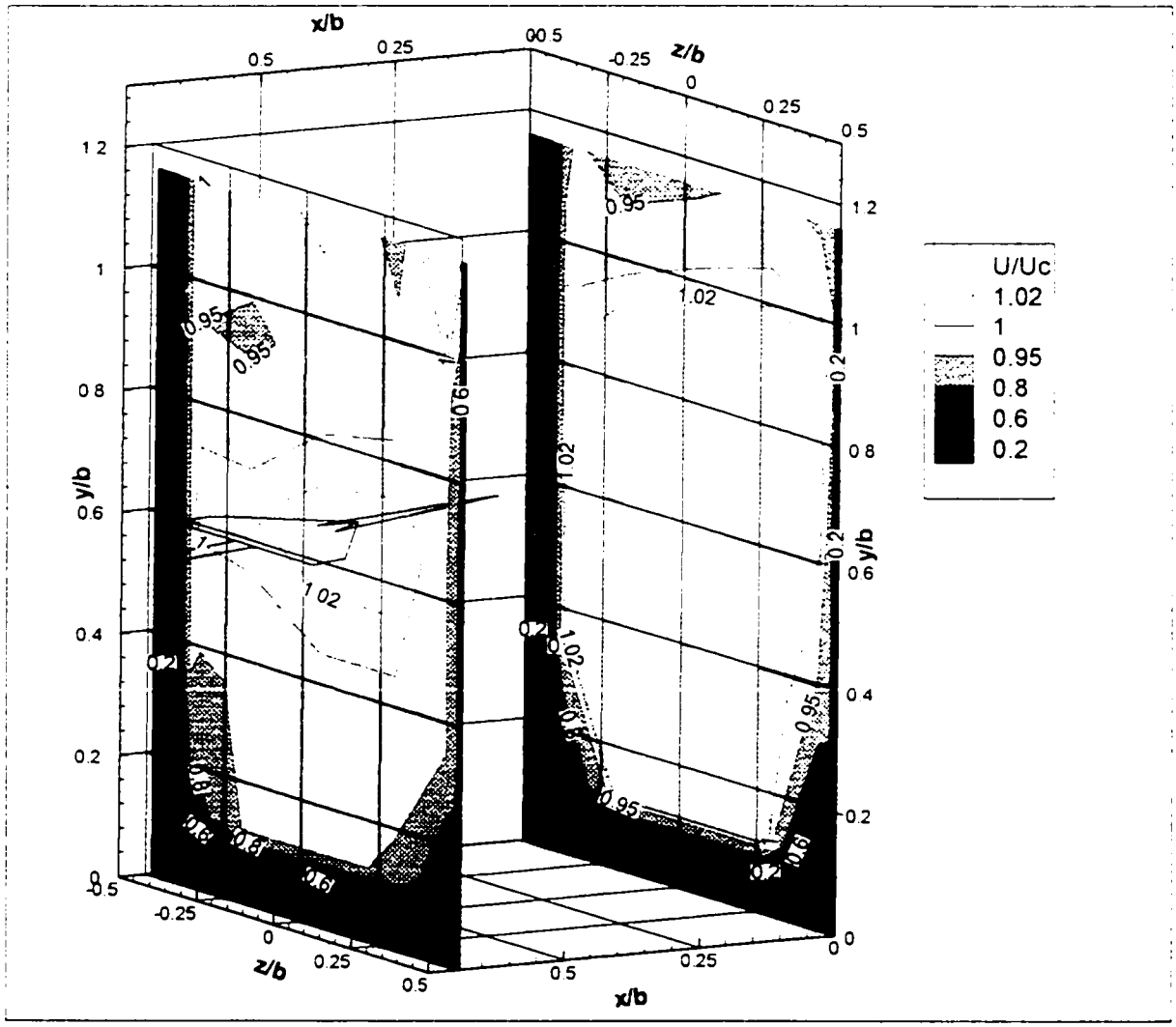

Figure 23: Streamwise velocity contours. Note that x/b = 0 represents the test section entrance. The wire frame on the x/b = 0.70 plane represents the location of the model in the water tunnel.

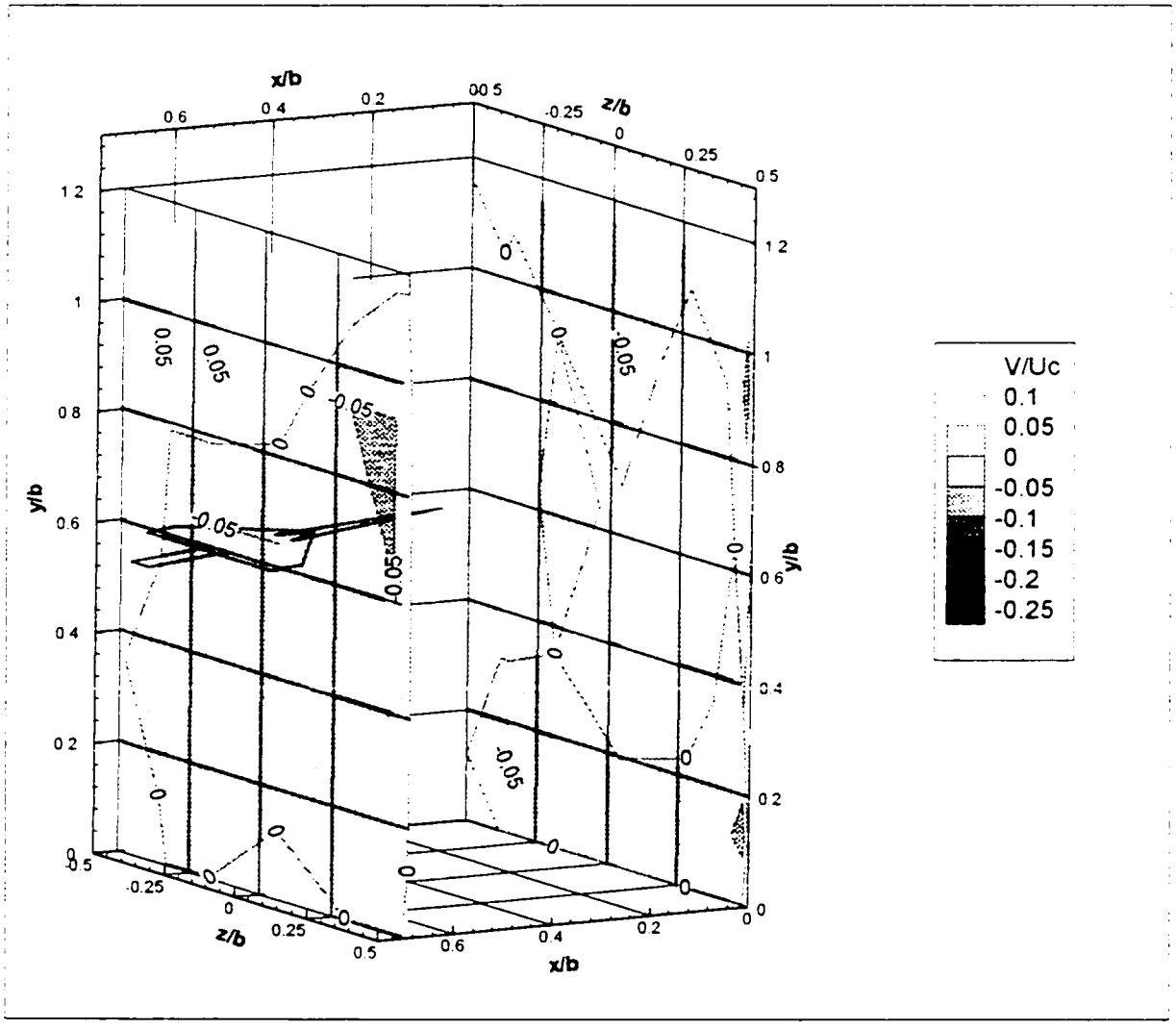

Figure 24. Vertical velocity contours. Note that x/b = 0 represents the test section entrance. The wire frame on the x/b = 0.70 plane represents the location of the model in the water tunnel.

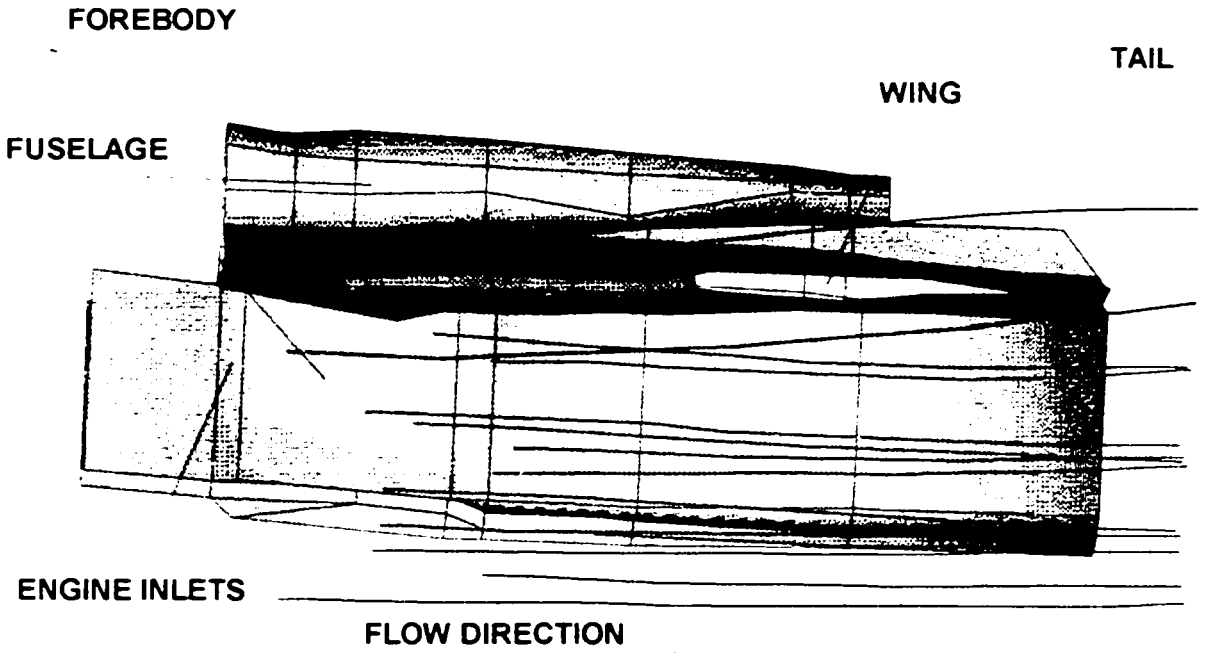

Figure 25: Side view of the fuselage section of the aircraft at the wing, displaying streaklines over the clean wing profile, at $\alpha = 5°$. Note that the green and red lines move around the wing-tip.

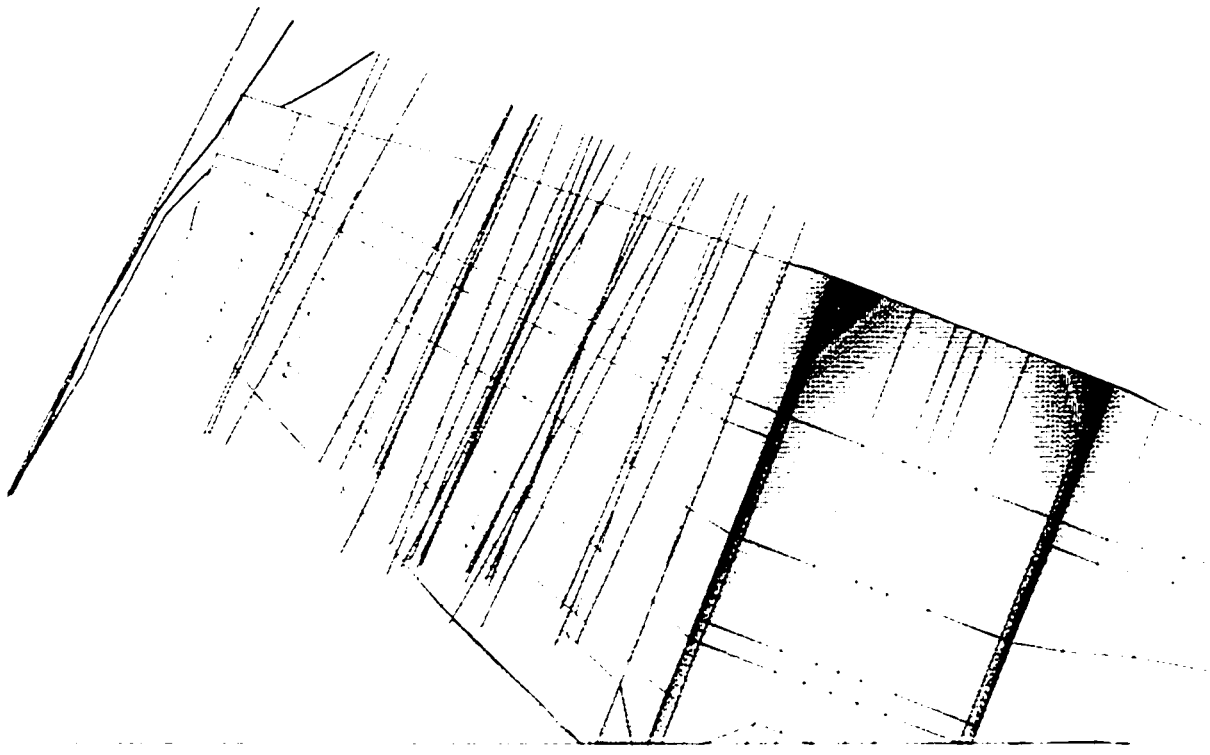

Figure 26: Clean wing streaklines from below the wing, at $\alpha = 5^{\circ}$. Note that the green and red lines move around the wing-tip.

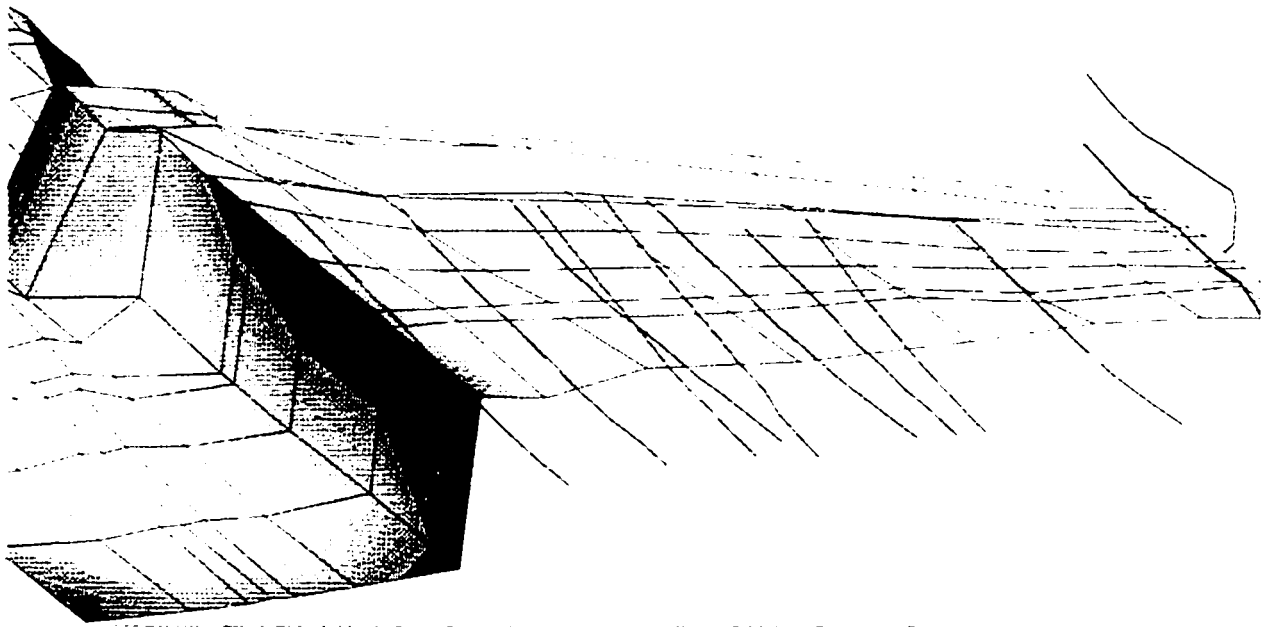

Figure 27: Clean wing streaklines located 0.1c from the lower surface, at $\alpha = 5^{\circ}$.

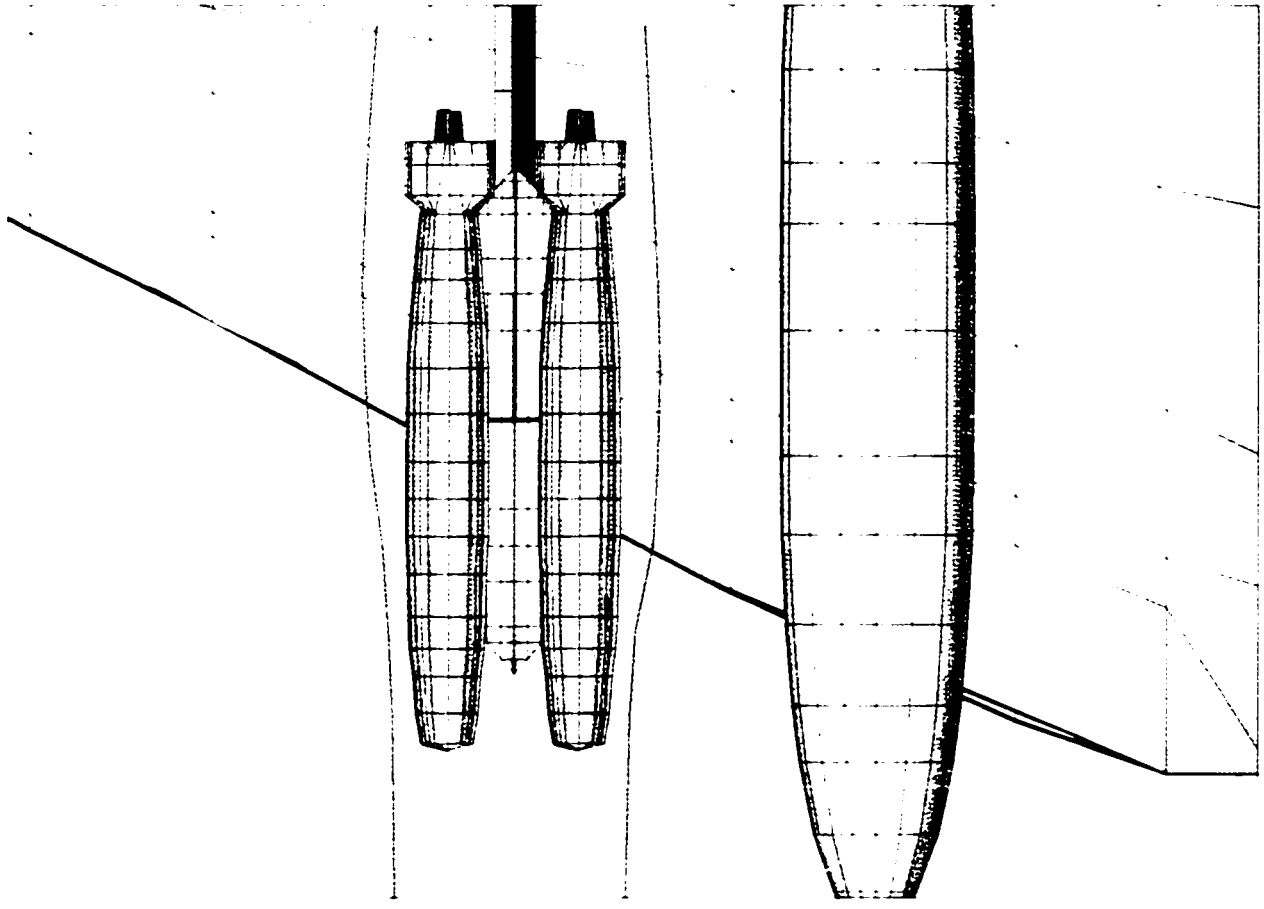

Figure 28: Bottom view of streaklines around two MK-82 bombs mounted at station 8, at $\alpha = 5^{\circ}$.

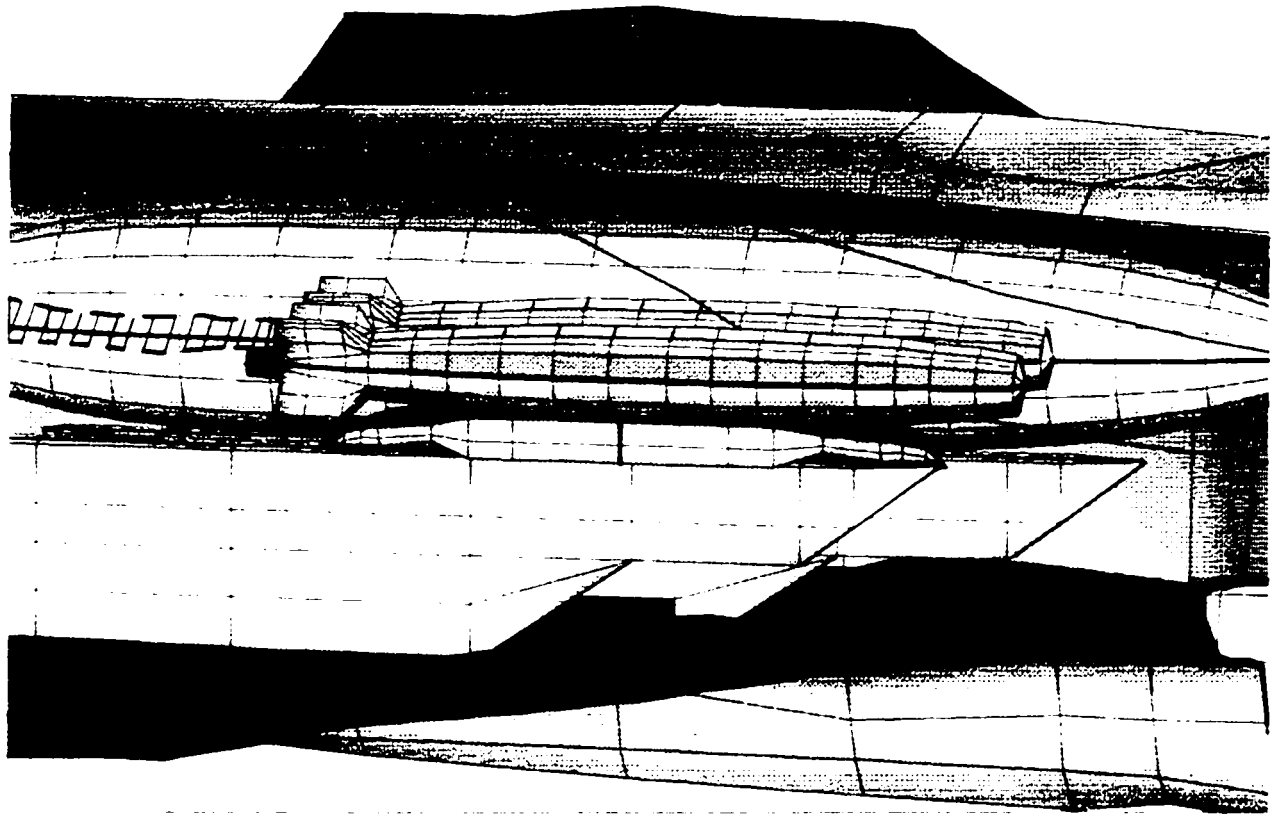

Figure 29: Streaklines located between two the MK-82 bombs mounted at station 8 at $\alpha = 5^{\circ}$. Note that the cross-hatched area represents a region of recirculating flow.

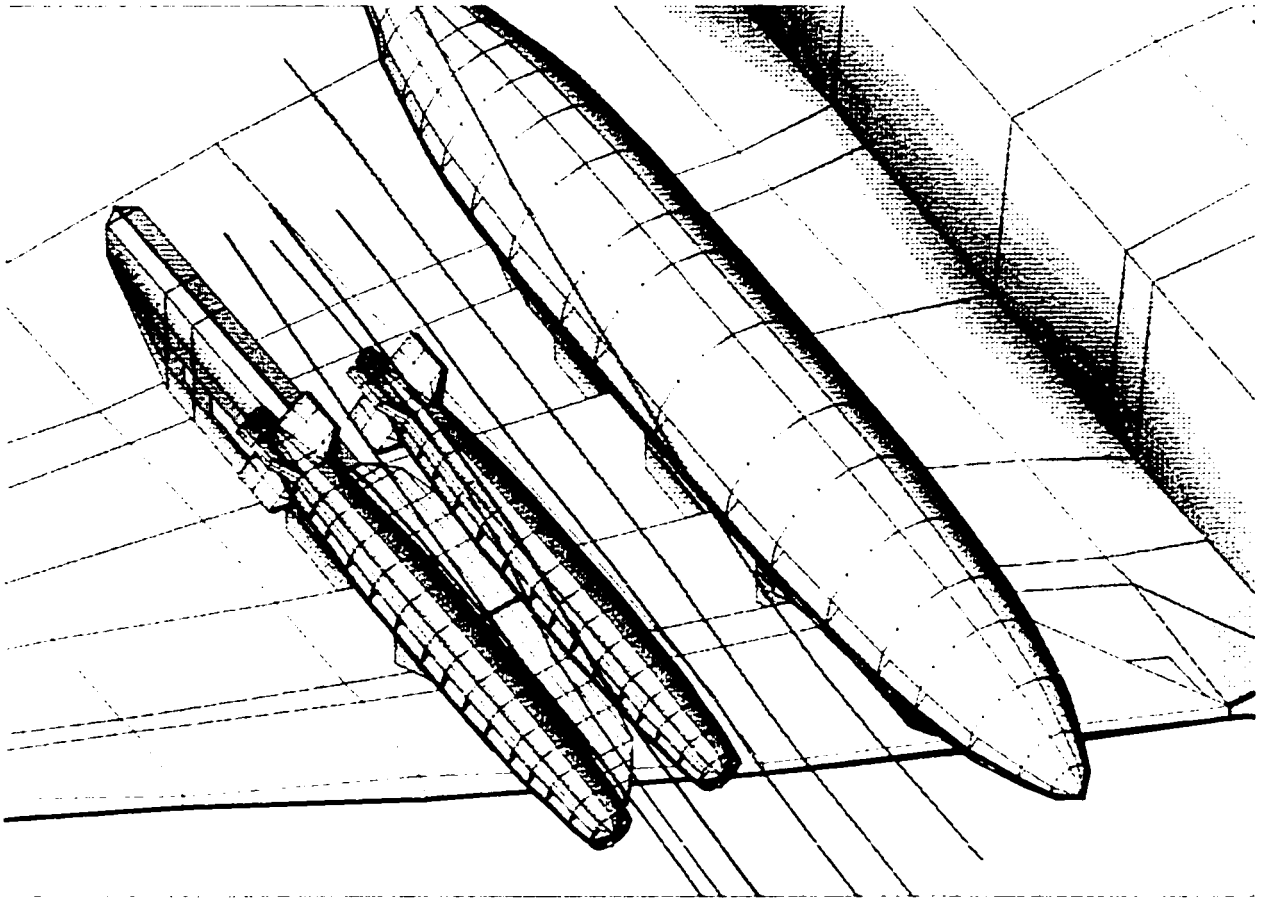

Figure 30: Streaklines between the MK-82s at station 8 and the EFT at station 7. The green lines pass directly over each bomb. The cyan and red streaks pass between them.

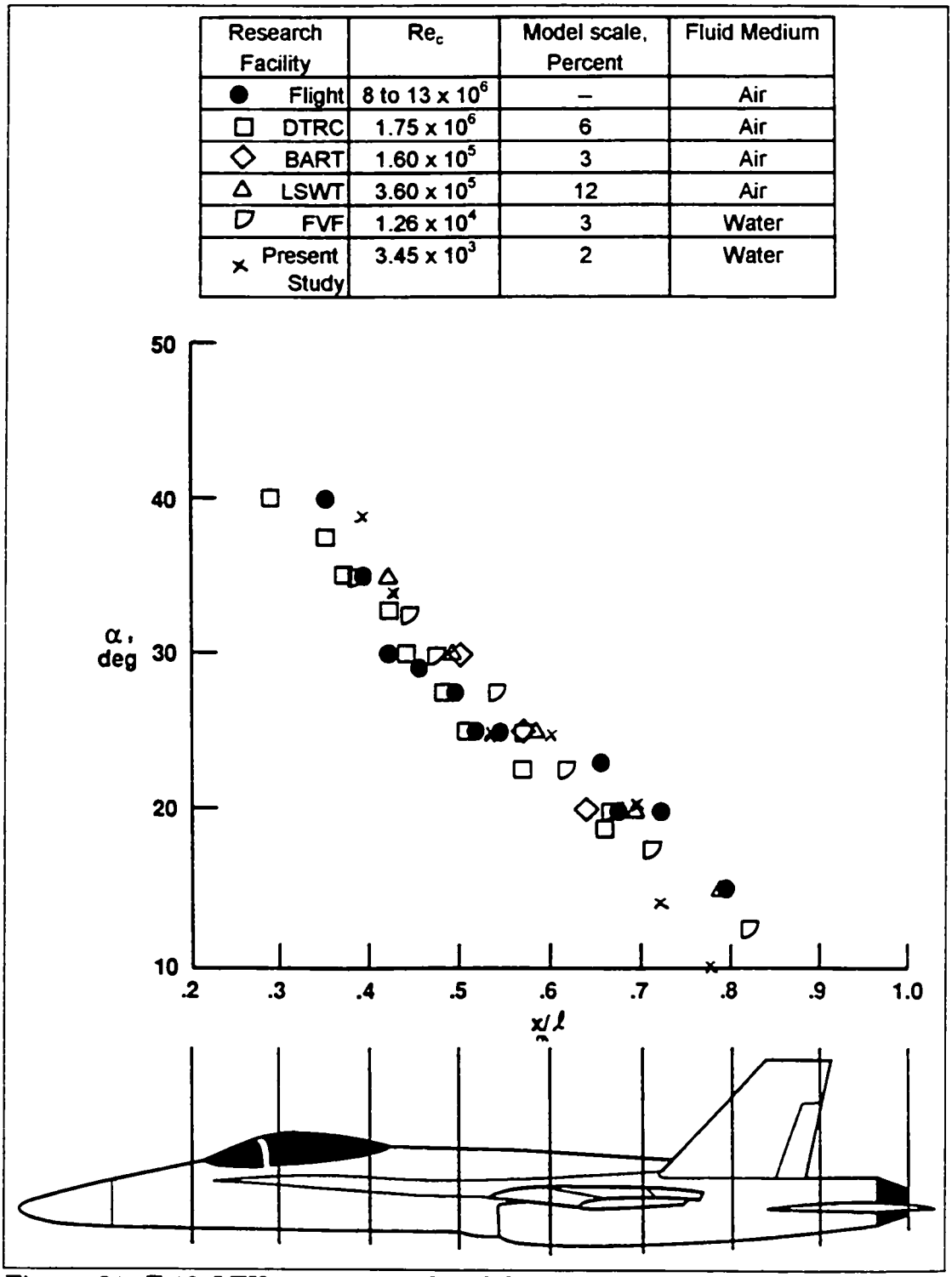

Figure 31: F-18 LEX vortex core breakdown locations at various angles of attack (Del Frate et al, 1990), including results from the present study.

Plates

Plate 1: A flow quality test in the unobstructed water tunnel using a dye streakline.

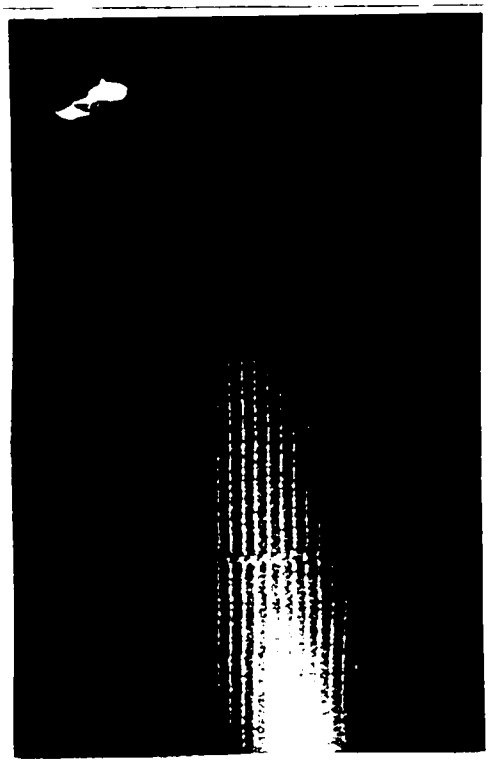

Plate 2: A flow quality test in the unobstructed water tunnel using hydrogen bubble timelines.

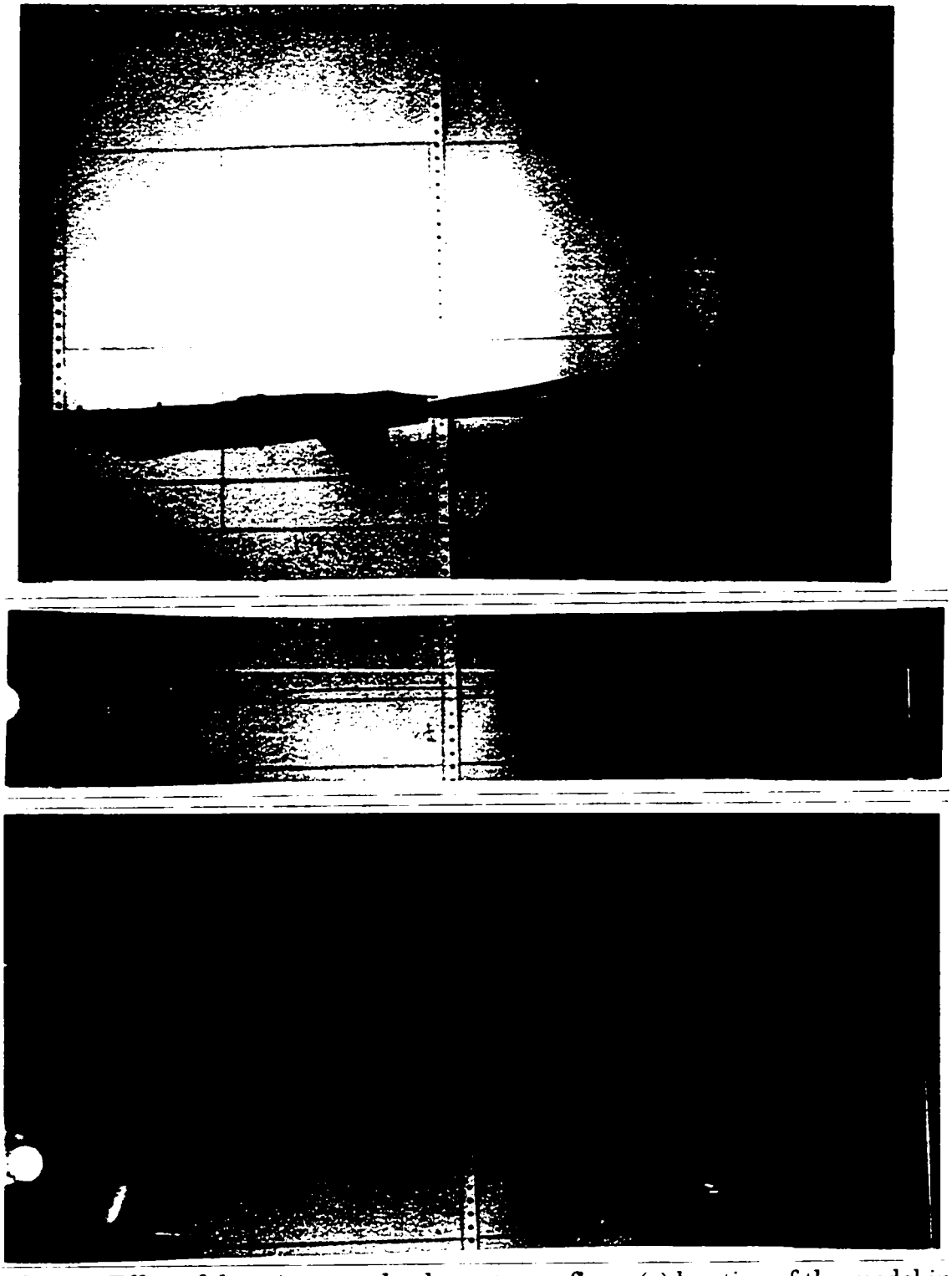

Plate 3: Effect of the mirror on the downstream flow: (a) location of the model in the tunnel, (b) dye streakline in the unobstructed tunnel, and (c) dye streakline with the mirror in the tunnel.

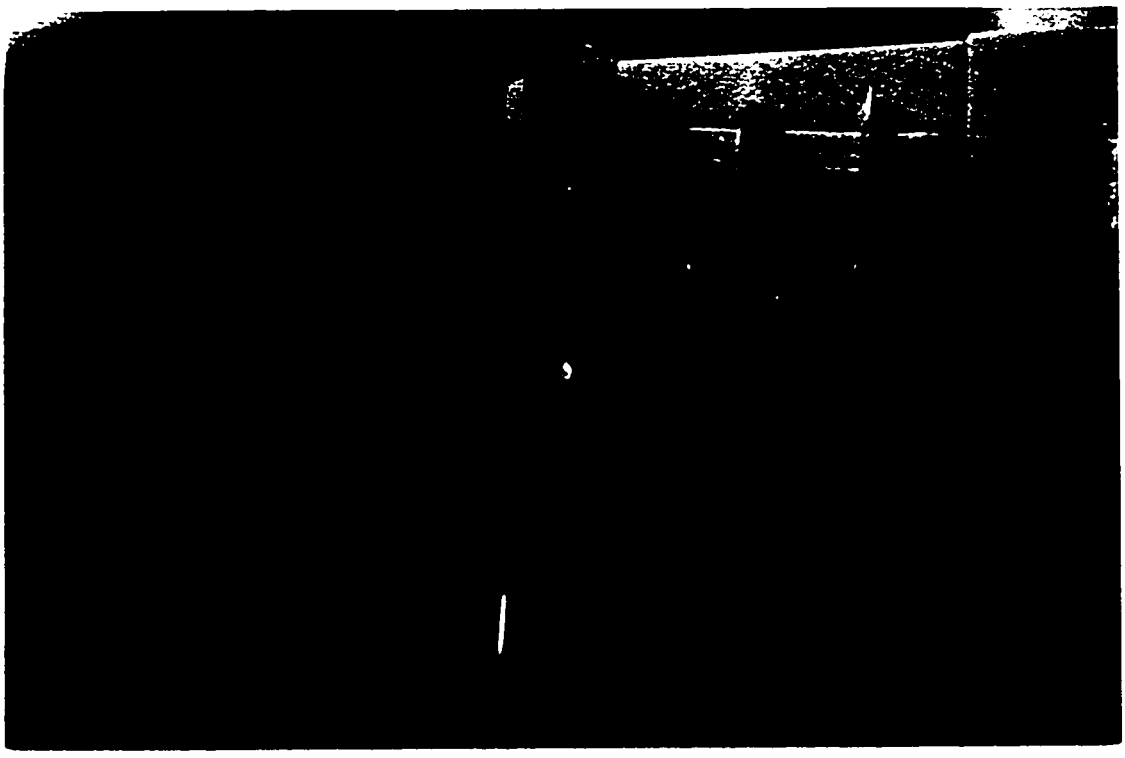

Plate 4: Bottom view of AIM 9 wing-tip missile at $\alpha = 5^{\circ}$.

Plate 5: Side view of AIM 9 wing-tip missile at $\alpha = 5^{\circ}$.

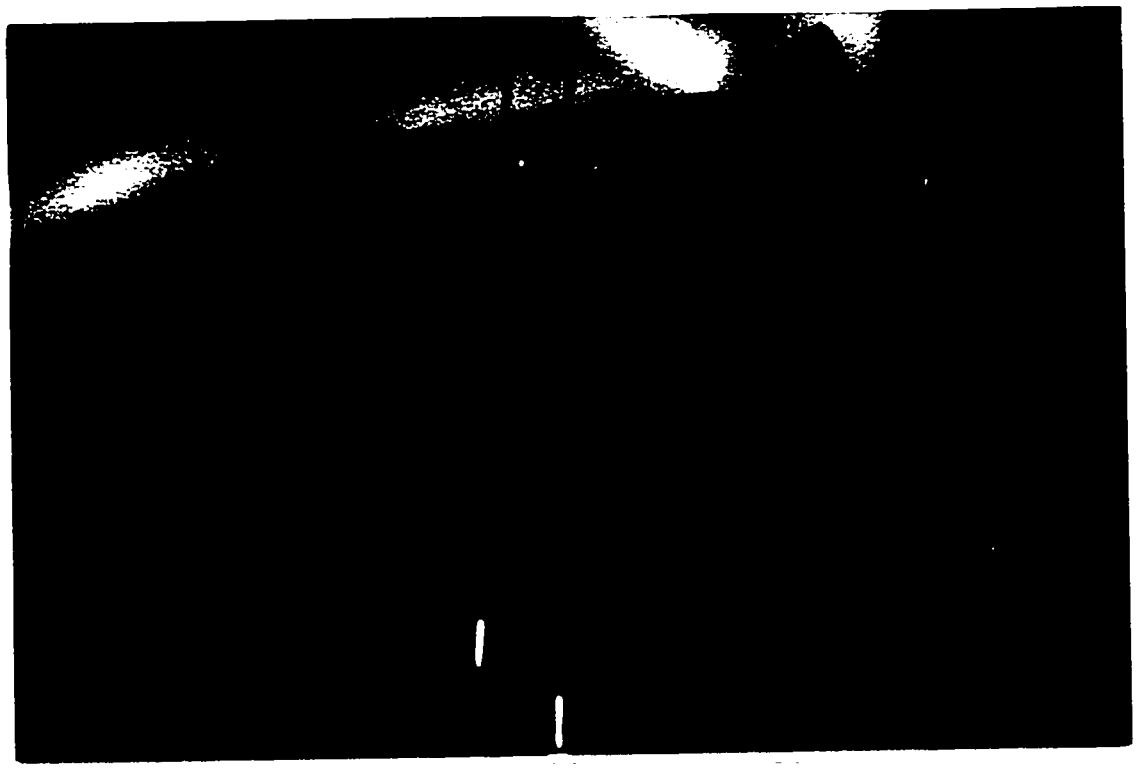

Plate 6: Bottom view of the pylon at station 8 at $\alpha = 5^{\circ}$.

Plate 7: Side view of the VER at station 8 at $\alpha = 5^{\circ}$.

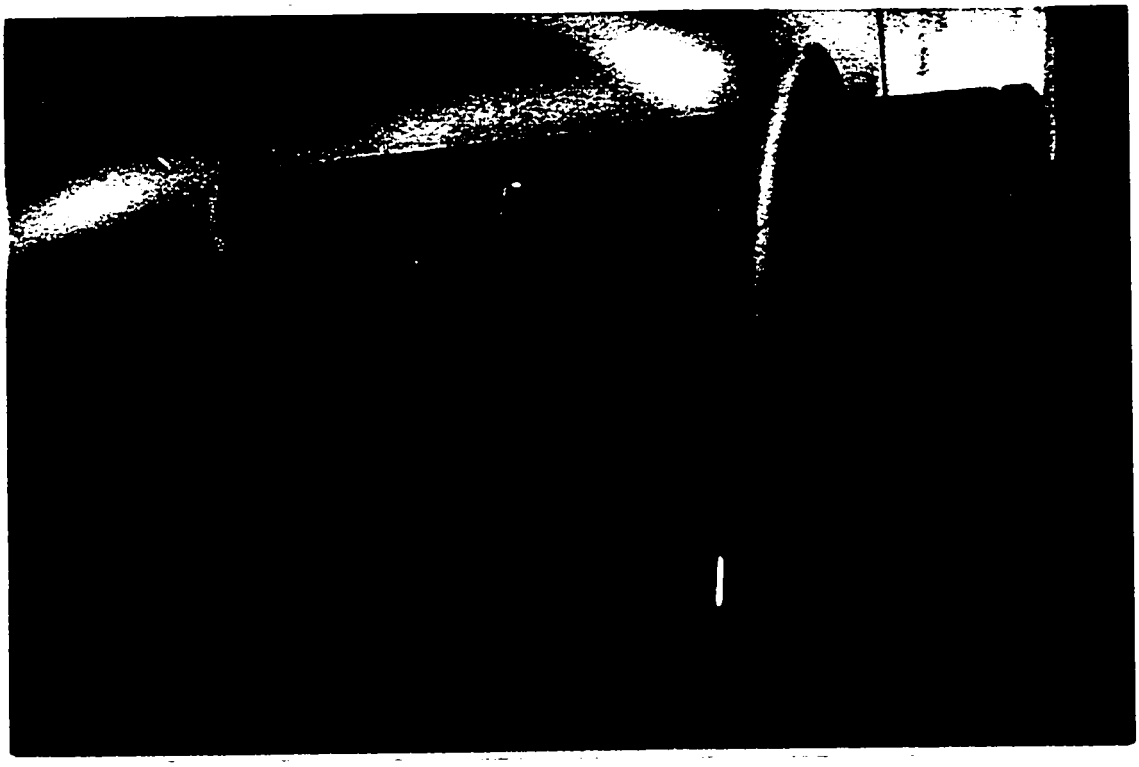

Plate 8: Bottom view of the EFT at station 7 at $\alpha = 5^{\circ}$.

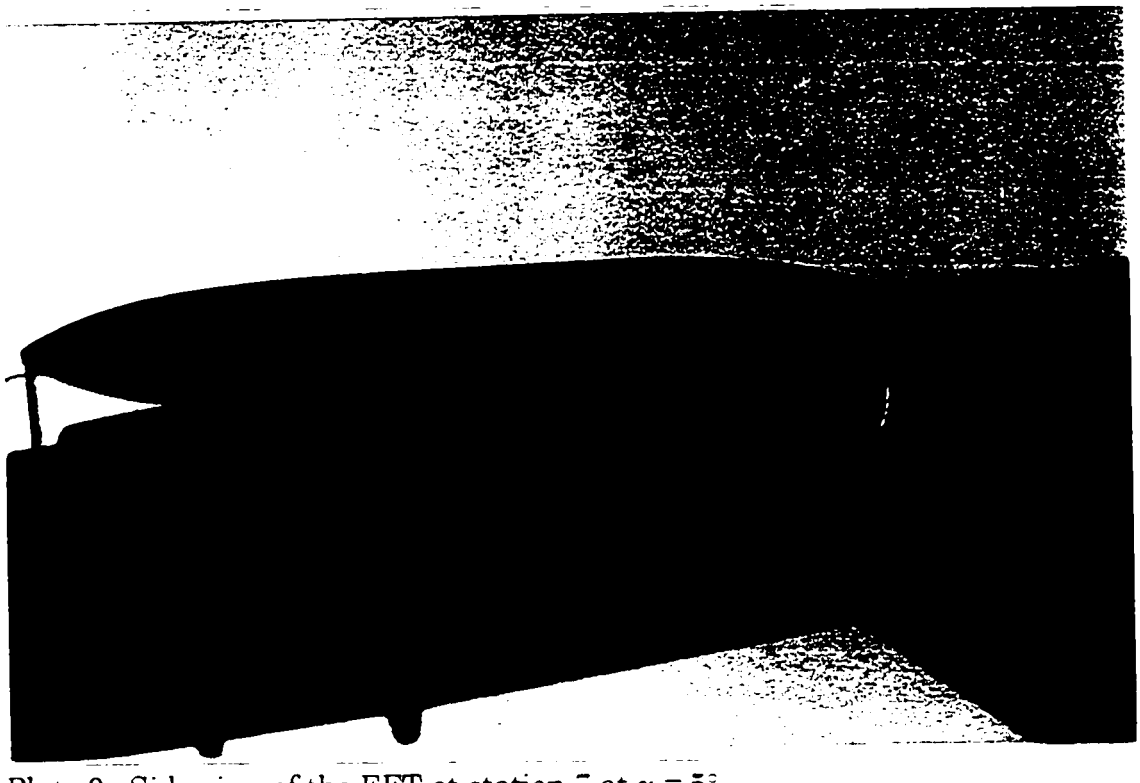

Plate 9: Side view of the EFT at station 7 at $\alpha = 5^{\circ}$

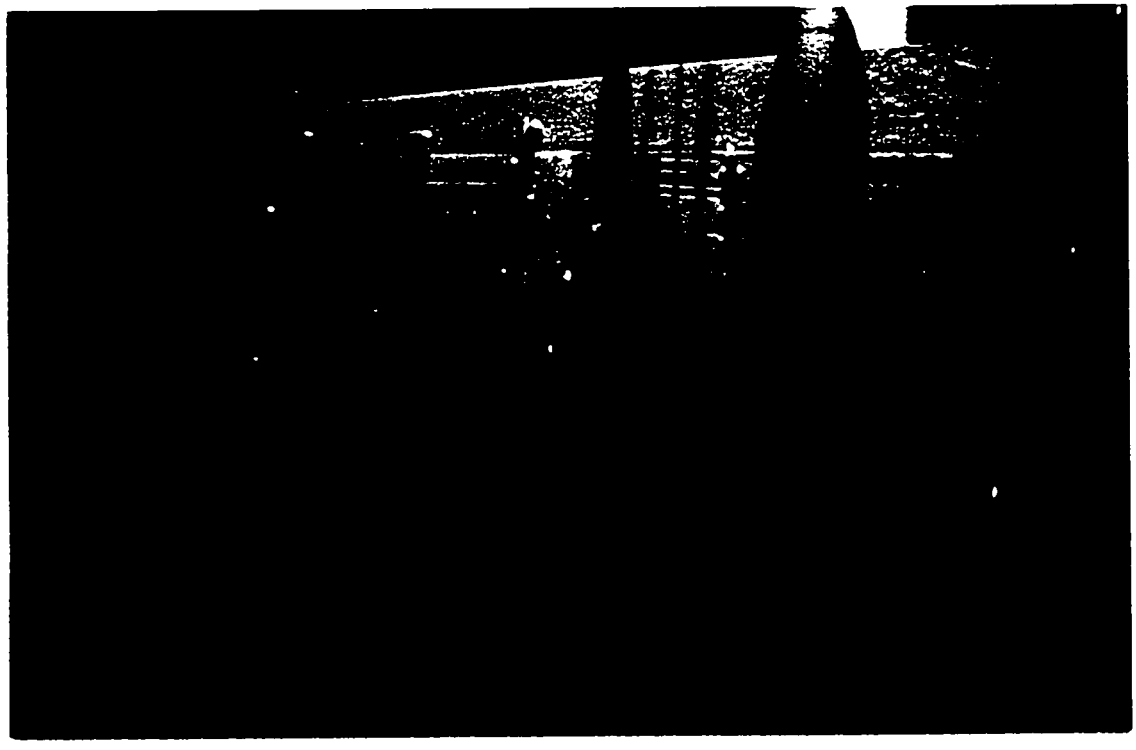

Plate 10: Bottom view of a single MK-82 on the VER at station 8 at $\alpha = 5^{\circ}$.

Plate 11: Side view of a single MK-82 on the VER at station 8 at $\alpha = 5^{\circ}$.

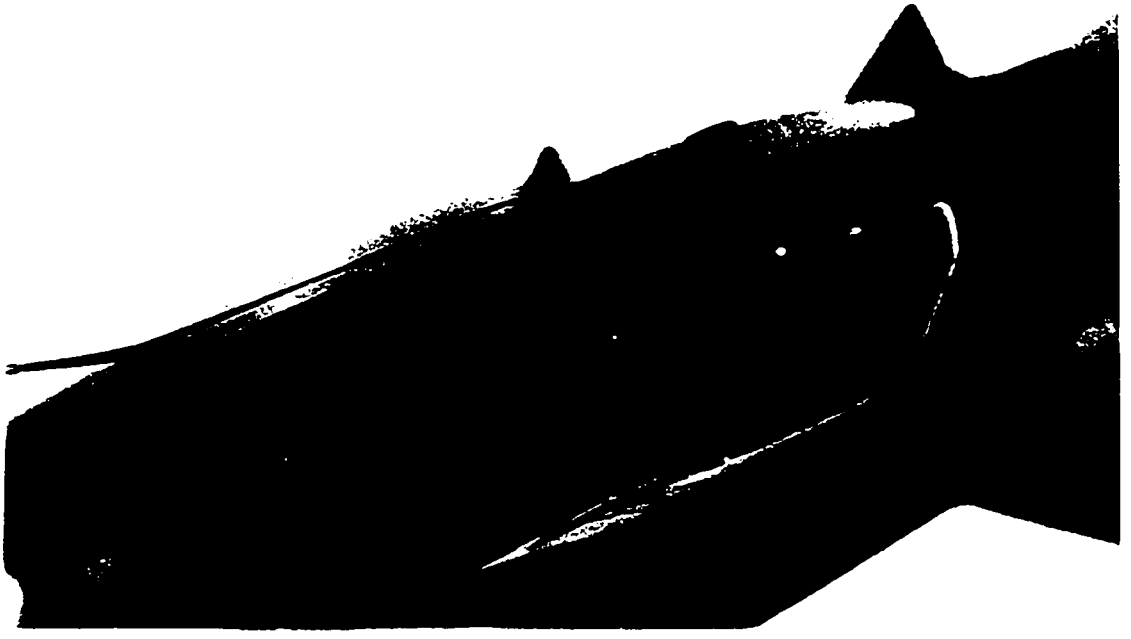

Plate 12: Side view of two MK-83 bombs on the VER at station 8 at $\alpha = 25^{\circ}$.

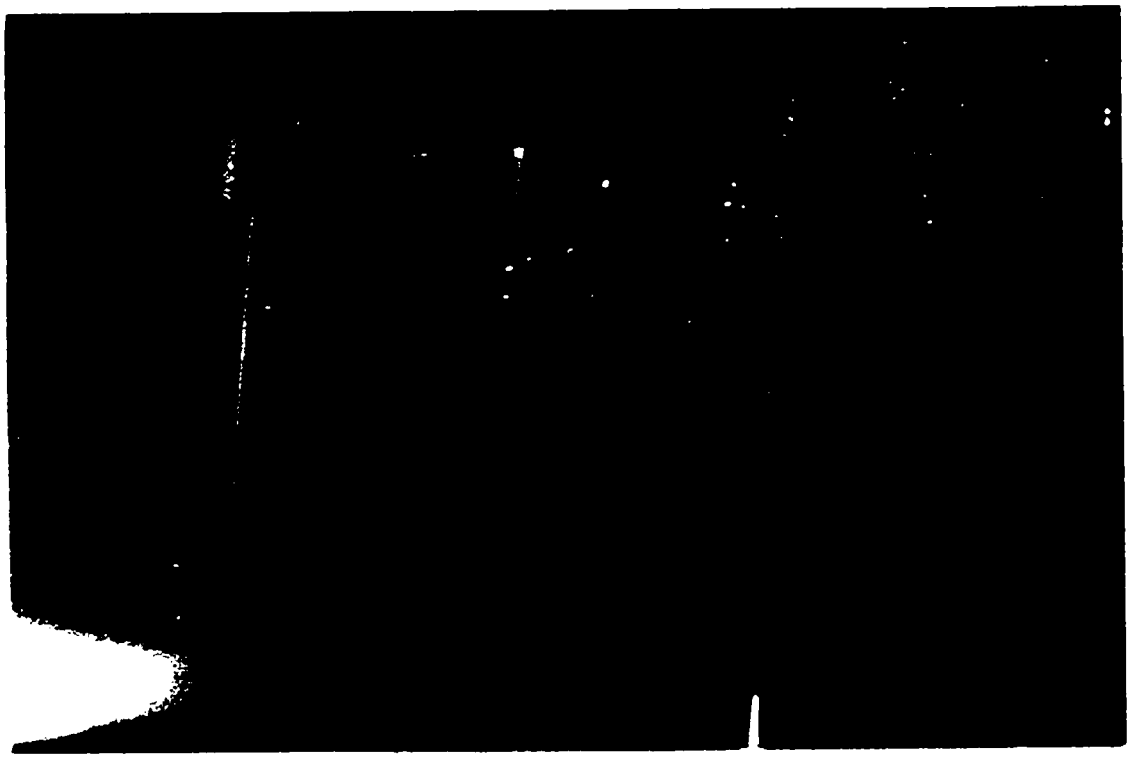

Plate 13: Streakline trajectories between a GBU-12 at station 8 and an EFT at station 7 at $\alpha = 5°$.

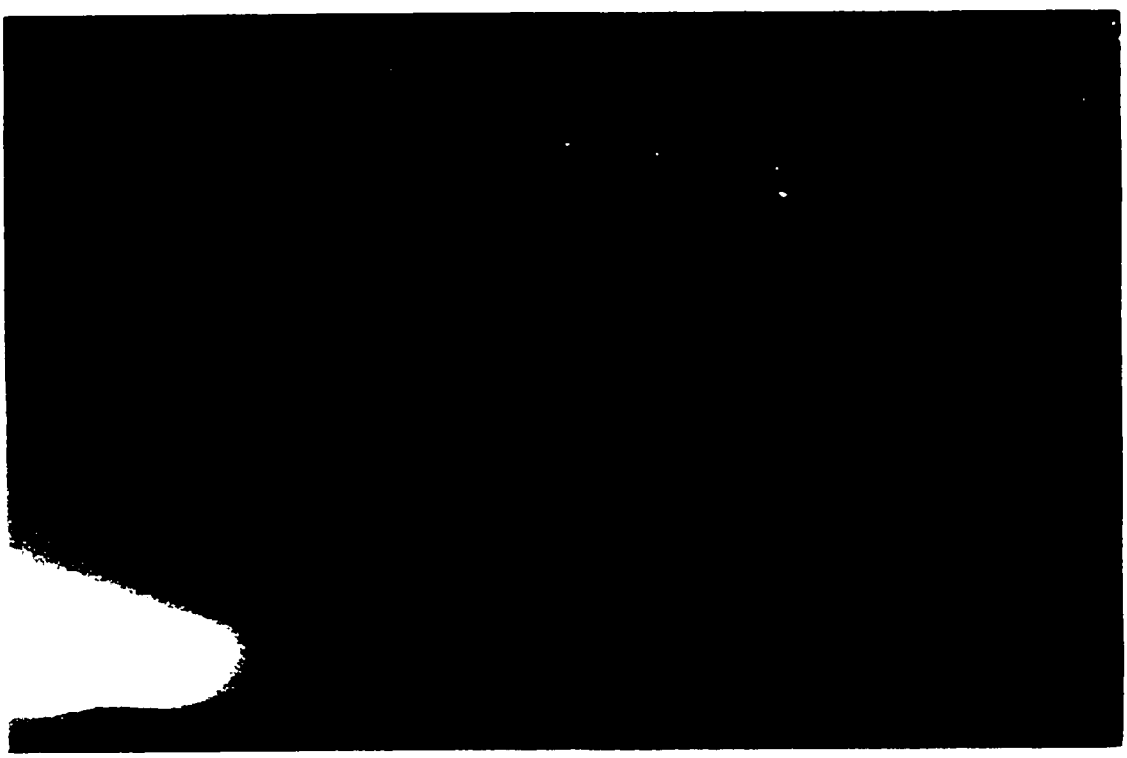

Plate 14: Bottom view of two GBU-12 bombs at $\alpha = 20°$.

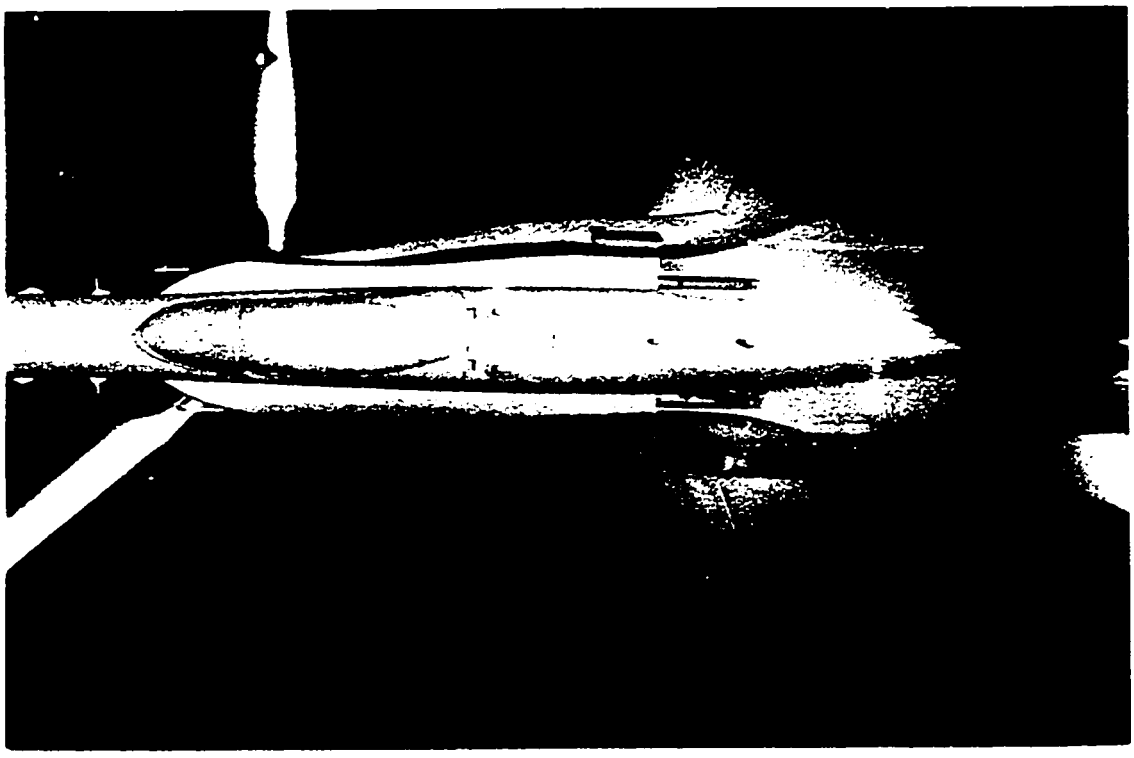

Plate 15: Top view of the LEX vortex at $\alpha = 5^{\circ}$, using the water-based dye.

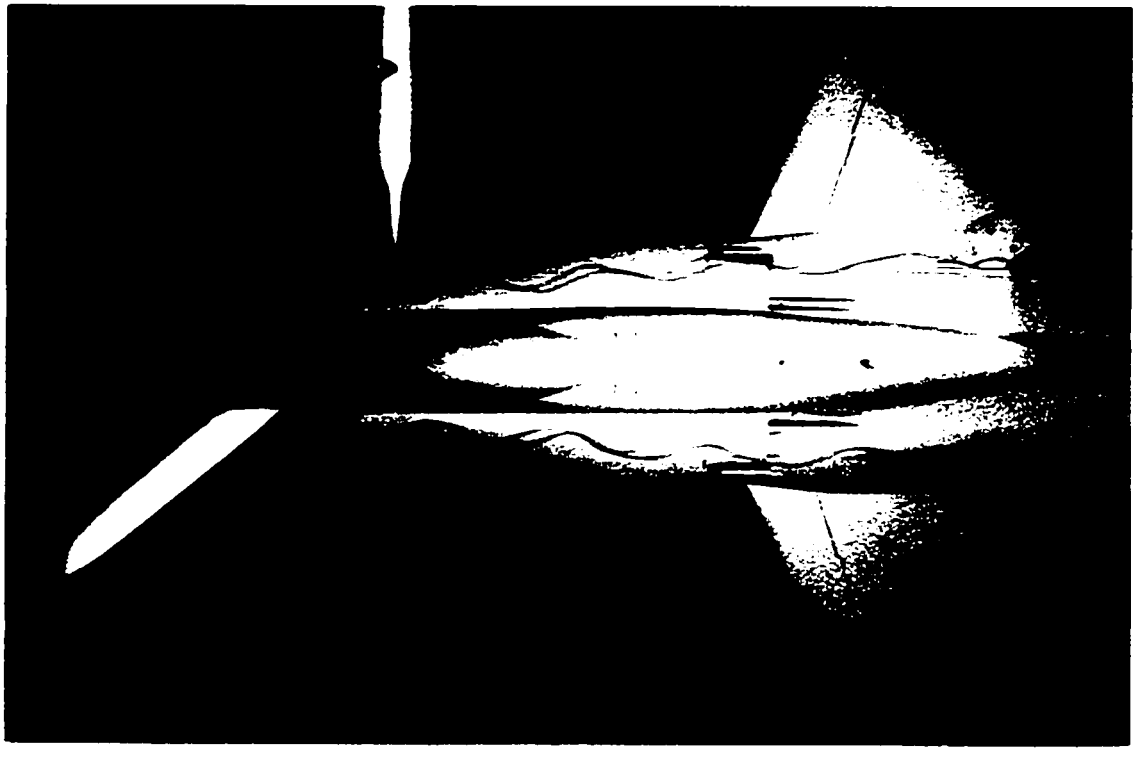

Plate 16: Top view of the LEX vortex at $\alpha = 20^{\circ}$, using the water-based dye.

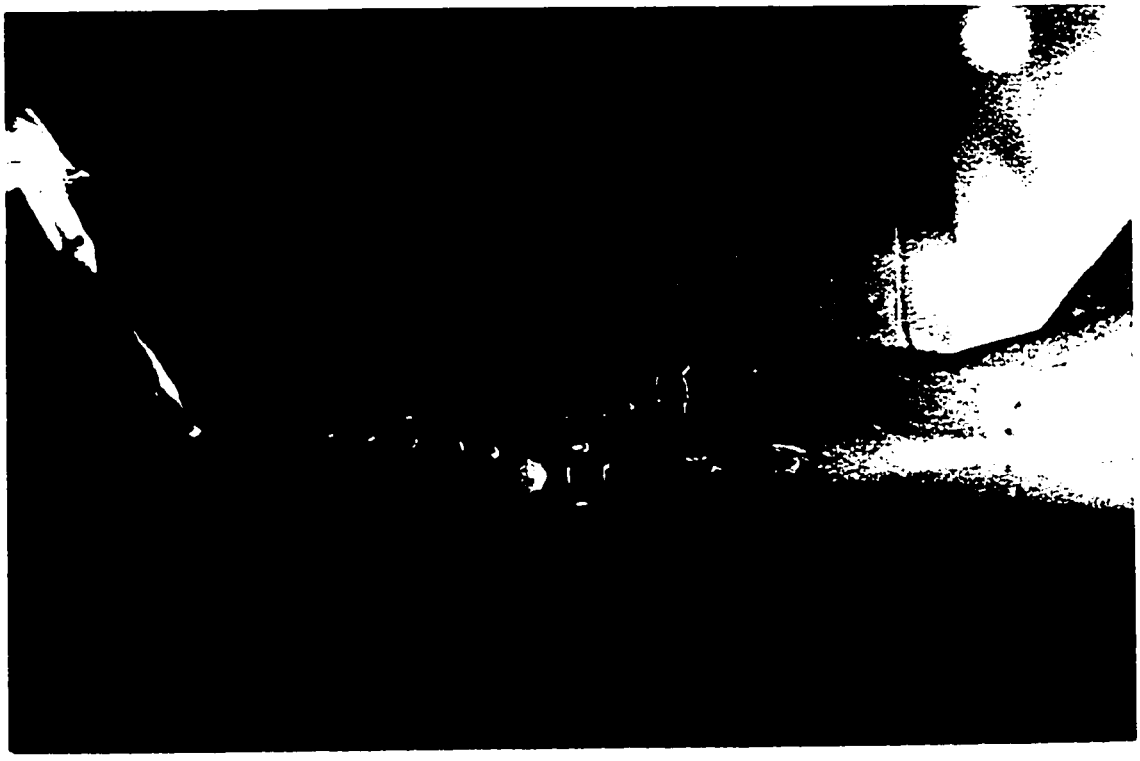

Plate 17: Top view of the LEX vortex at $\alpha = 25^{\circ}$, using hydrogen bubbles.

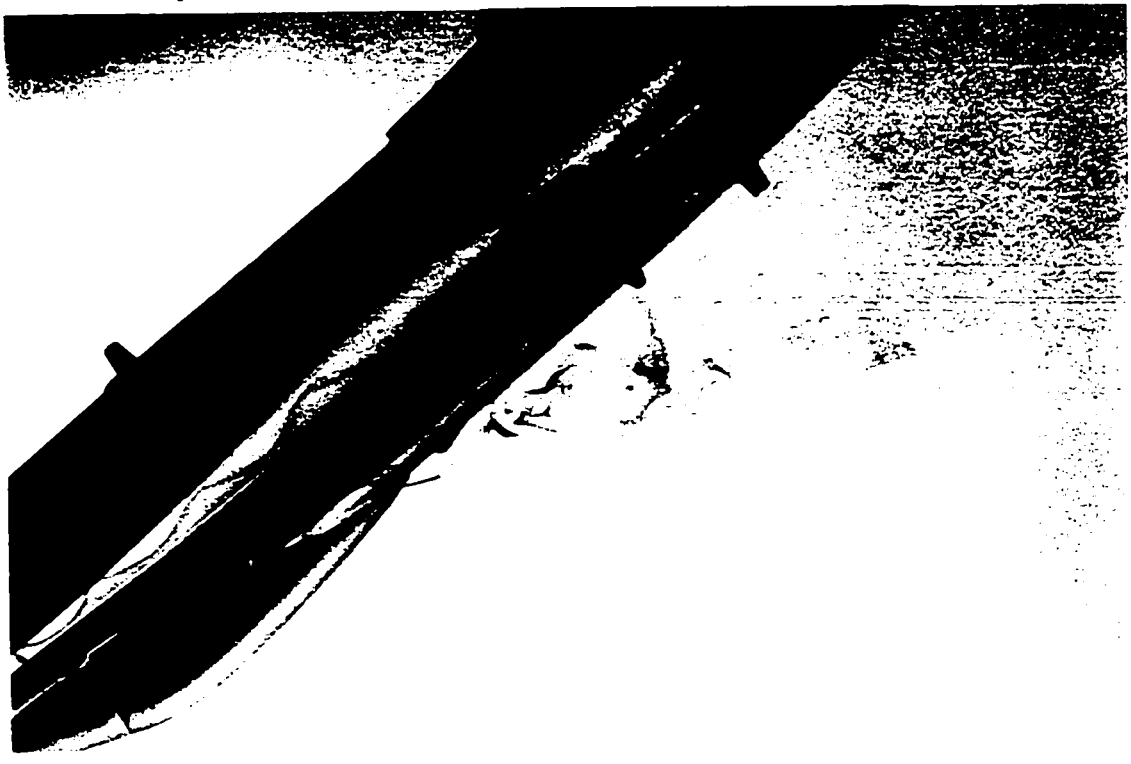

Plate 18: Side view of the LEX vortex at $\alpha = 35^{\circ}$, using the water-based dye.

Plate 19: Side view of the LEX vortex at $\alpha = 35^{\circ}$, using the shear-thickening dye.

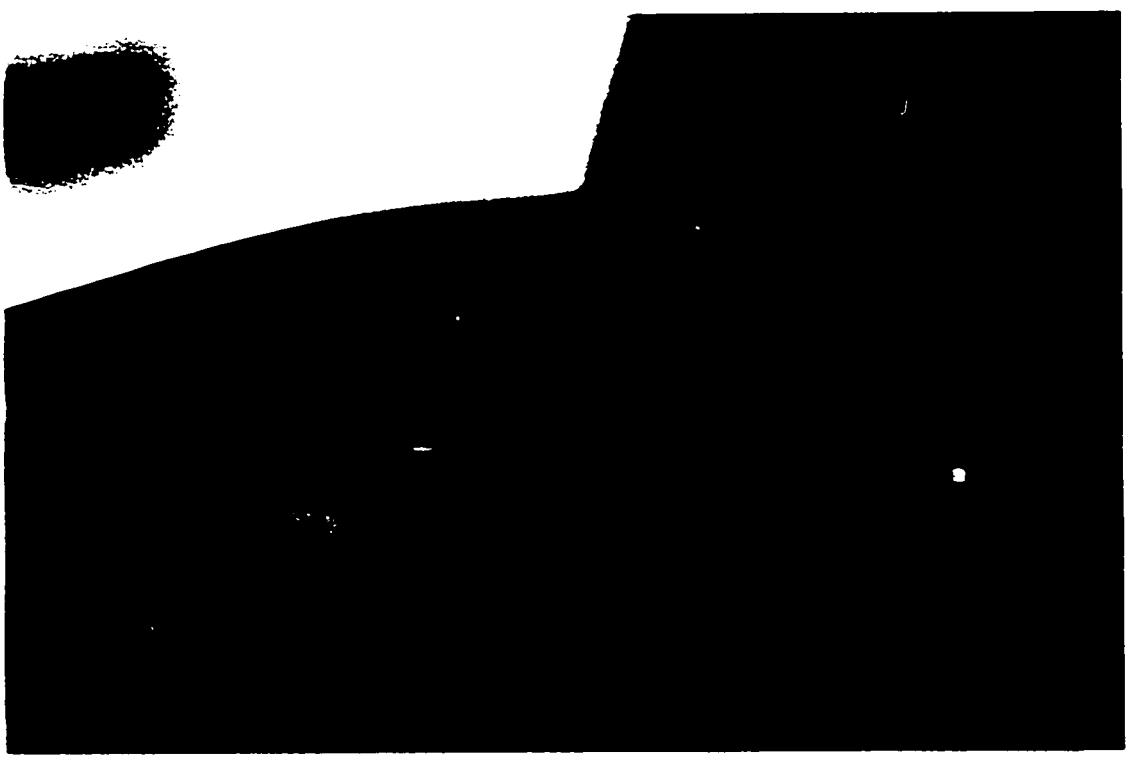

Plate 20: Top view of the LEX vortex at $\alpha = 35^{\circ}$, using the shear-thickening dye.

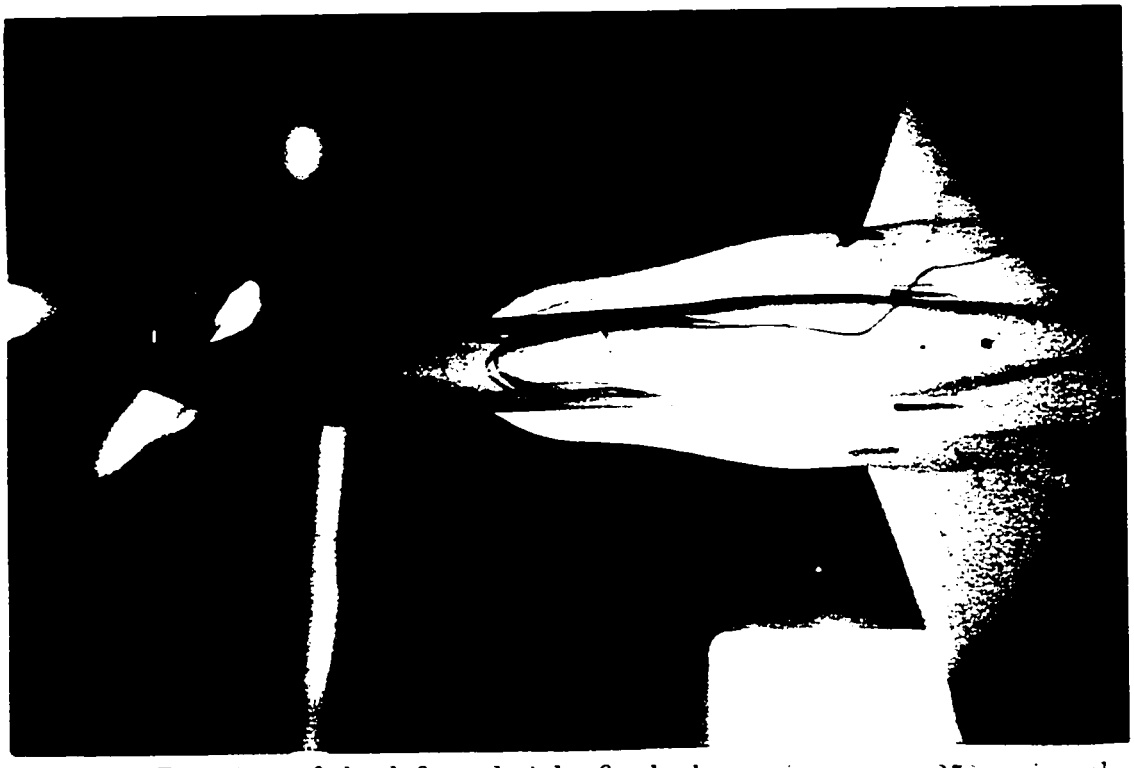

Plate 21: Top view of the left and right forebody vortices at = 25°, using the water-based dye.

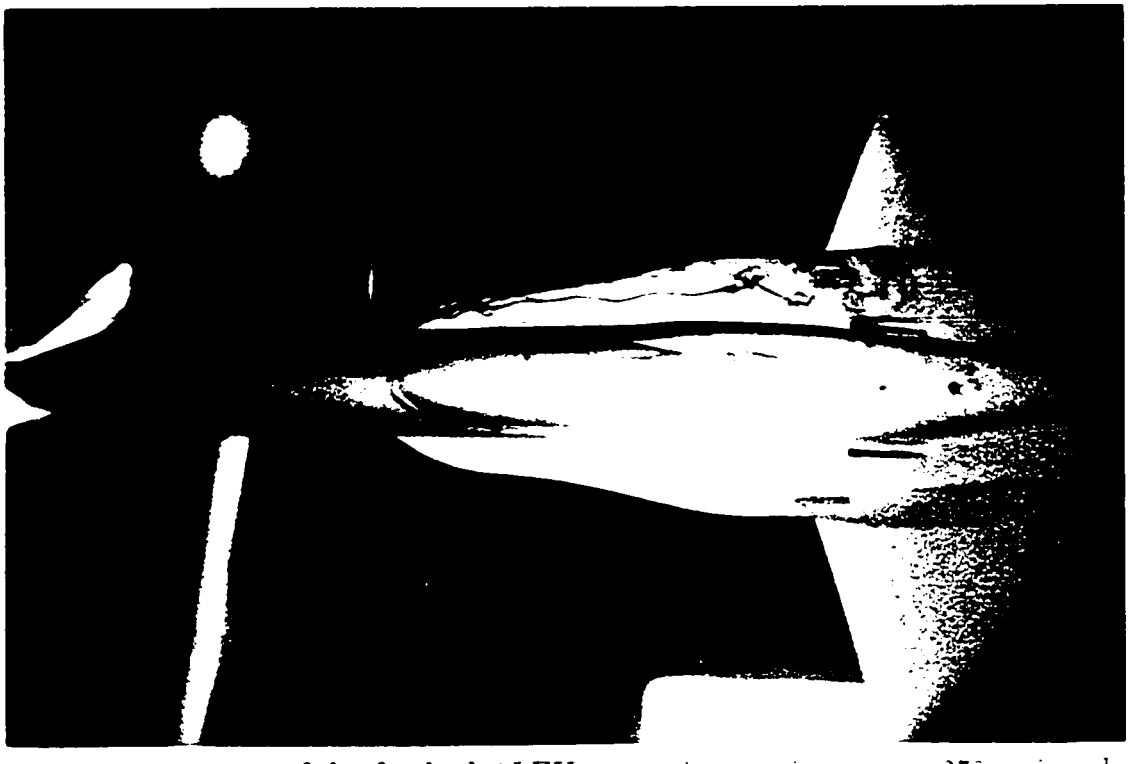

Plate 22: Top view of the forebody/ LEX vortex interaction at α = 25°, using the water-based dye.

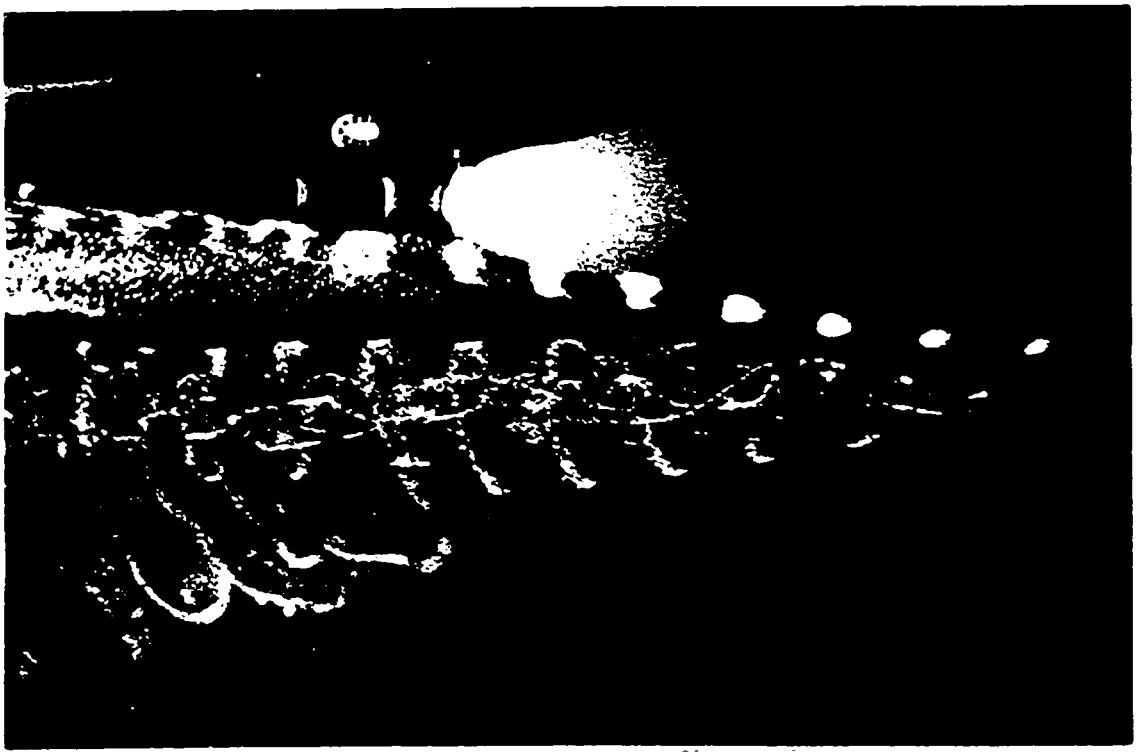

Plate 23: Top view of the LEX vortex at = 25°, using hydrogen bubbles, showing the vortex core.

Appendix A

Yaw & Pitch Positioning System

Page	Parts	Description
A3	1-7,21-22	Assembly drawing of main structure.
A4	1	Structure top plate.
A5	2	Rotating bottom plate.
A6	3,4	Support angle Aluminum sections.
A7	5,6,7	Rotating shaft, nut and washer.
A8	8	C-strut.
A9	9	Back C-strut support.
A10	10	Front C-strut support.
A11	11-14	Drive wheel and crank.

A12	9, 11-19	Assembly of drive wheel and crank.
A13	20	Small rollers with notes.
A14	23, 24	Sting support: Interior block and exterior attachment plate.
A15	25	Dye container support.
A16	26	Block for holding dye/ bubble supports.
A17	27	C-strut pointer.
A18	28, 29	Dye injection tube and support.
A19	30-33	Bubble wire and support.
A20	31, 32	Bubble wire support rotatable plug and strut.
A21	33	Plastic wire holder.

A3

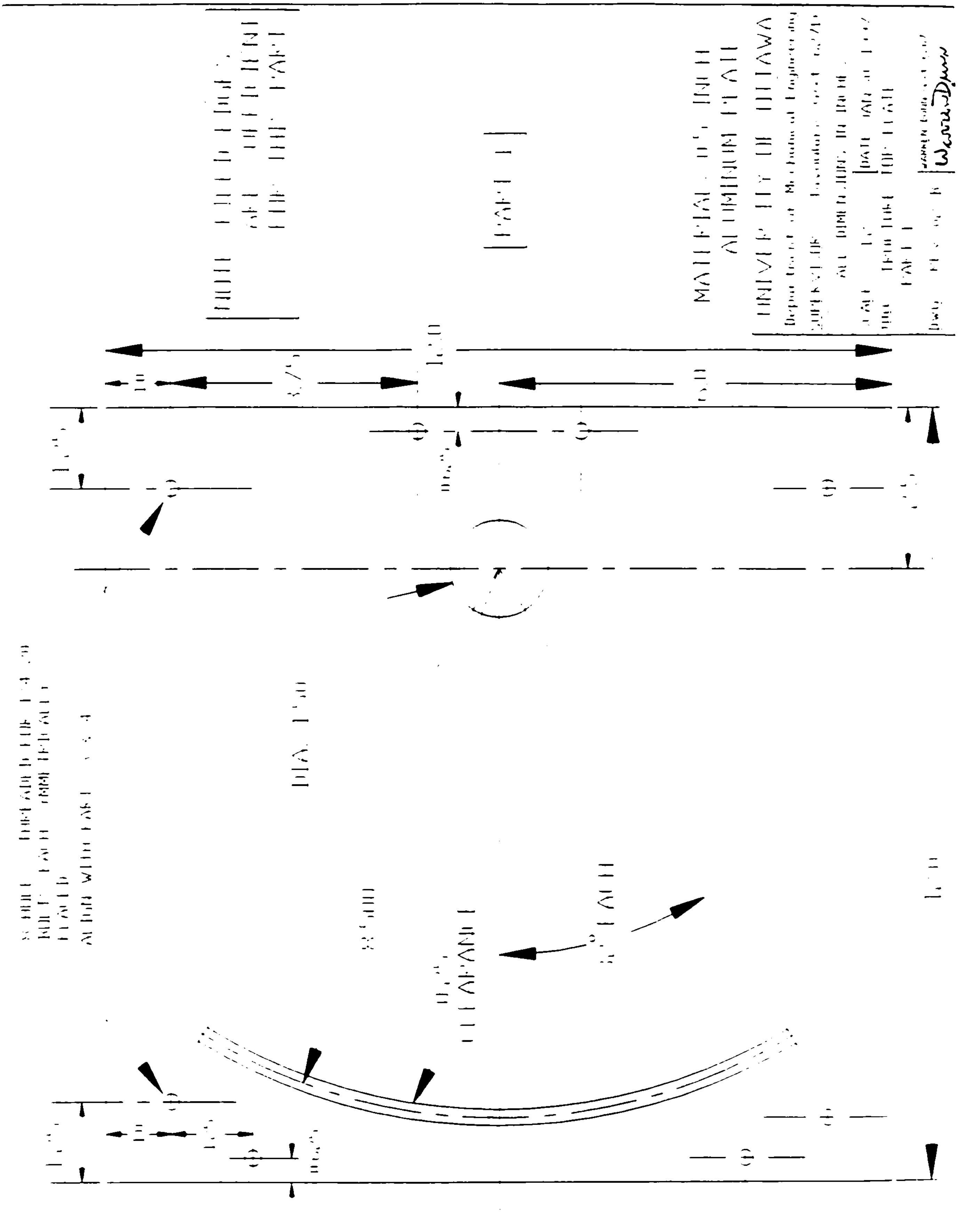

UNIVERSITY OF OTTAWA
PART 1
DIA. 1.50

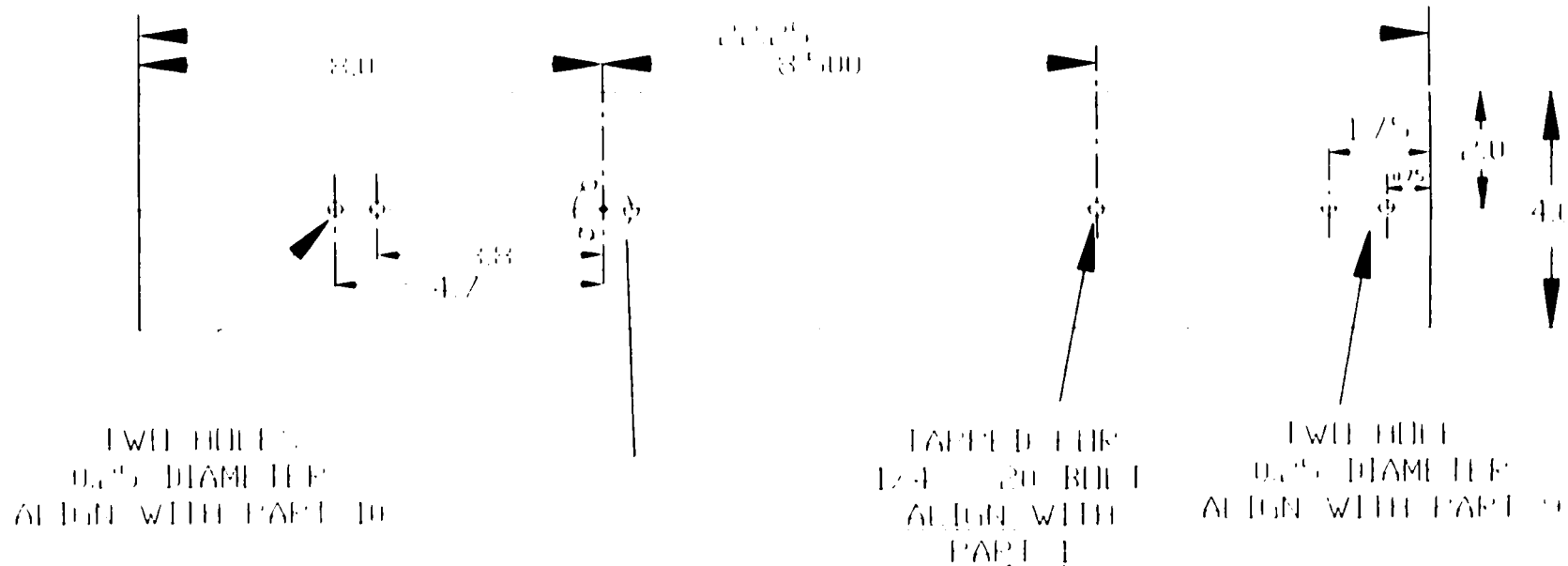

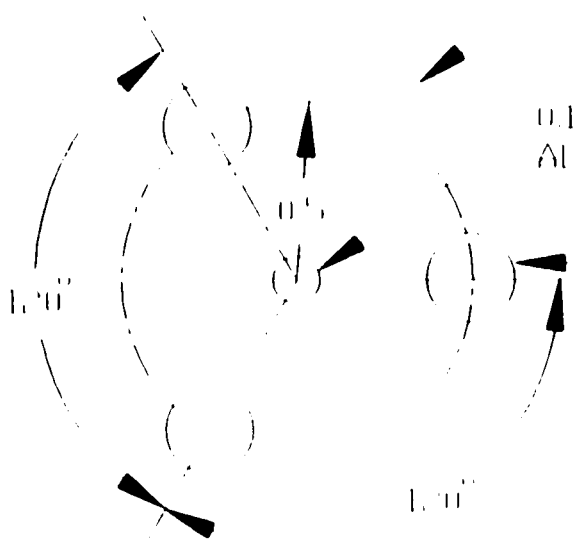

NOTE: TAPPED HOLES ARE THROUGH HOLES IN PART

MATERIAL:
ALUMINUM PLATE

UNIVERSITY OF OTTAWA
Department of Mechanical Engineering
ALL DIMENSIONS IN INCHES
SCALE: 1:1 | DATE: JAN 30, 2007
TITLE: ROTATING BOTTOM PLATE PART 2
DWG REV 03 | Warren Dias

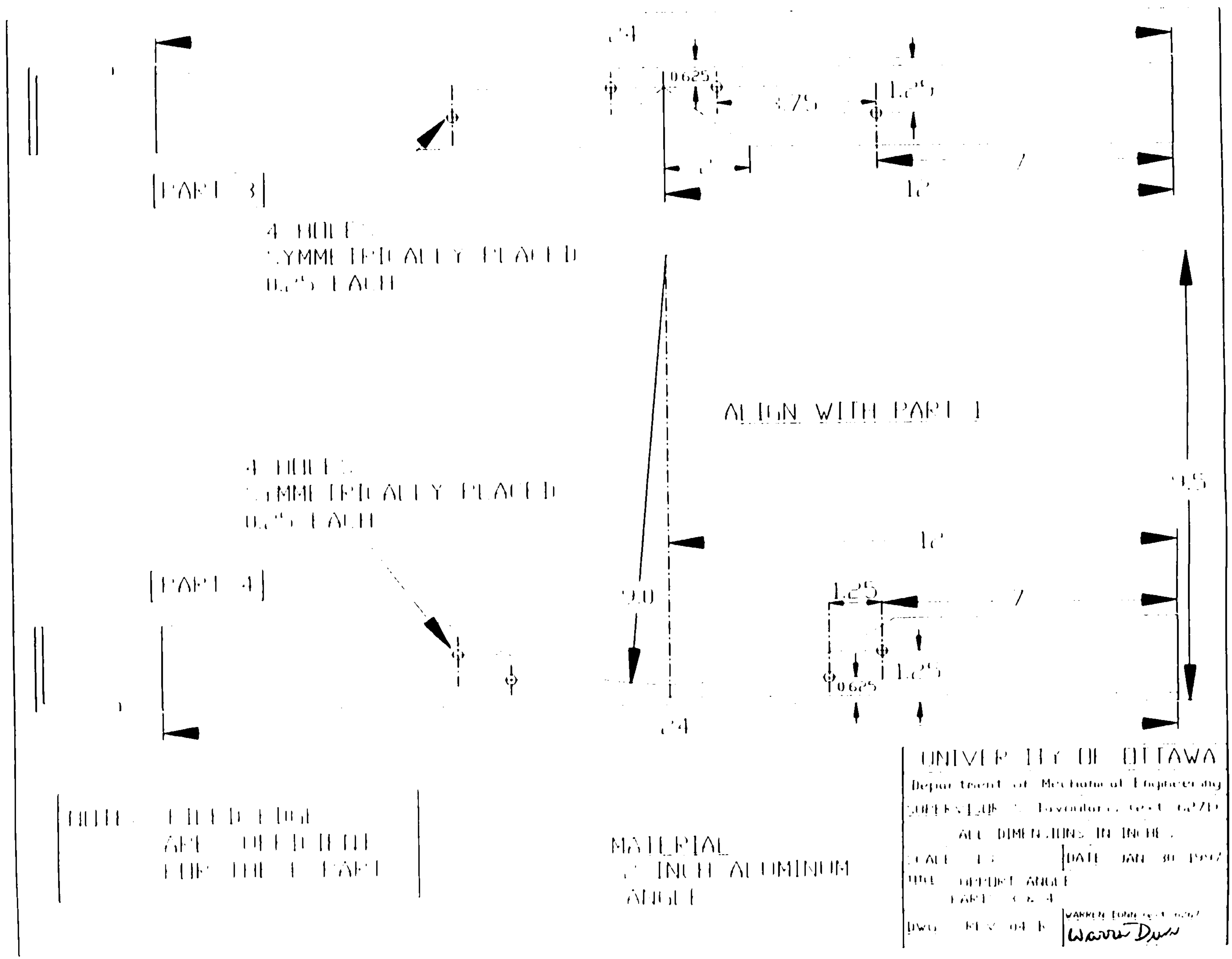
PART 3
4 HOLES
SYMMETRICALLY PLACED
PART 4
ALIGN WITH PART 1
0.625
1.25
9.0
MATERIAL
INCH ALUMINUM
ANGLE
UNIVERSITY OF OTTAWA
Department of Mechanical Engineering
ALL DIMENSIONS IN INCHES
DATE

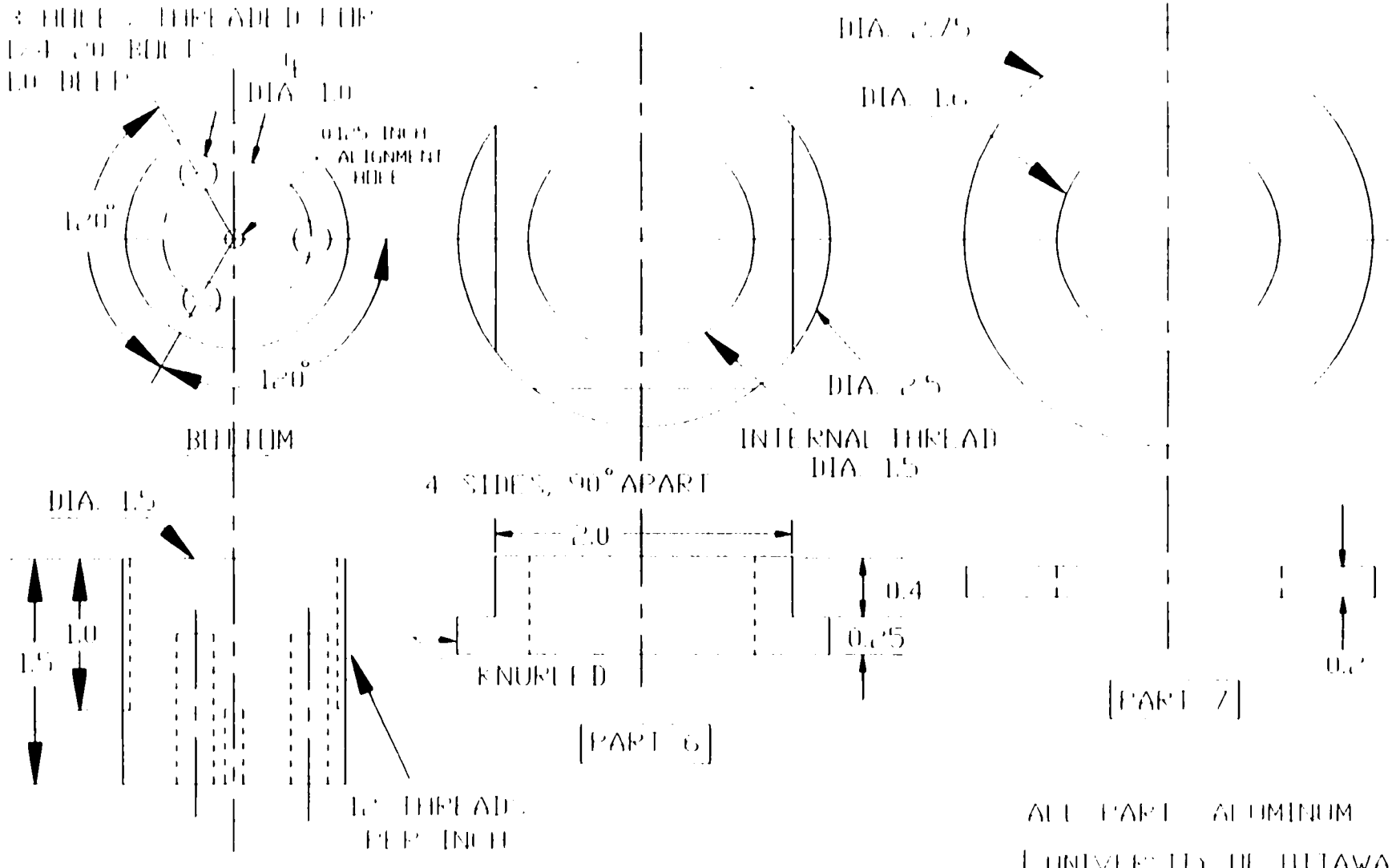
3 HOLES, THREADED FOR
1/4-20 BOLTS
1.0 DEEP
DIA. 1.0
0.125 INCH
ALIGNMENT
HOLE
120°
120°
BOTTOM
DIA. 1.5
1.5
1.0
12 THREADS
PER INCH
[PART 5]
ALIGN WITH
PART 5
DIA. 2.75
DIA. 2.5
DIA. 2.5
INTERNAL THREAD
DIA. 1.5
4 SIDES, 90° APART
2.0
0.4
0.25
KNURLED
[PART 6]
[PART 7]
0.2
ALL PART ALUMINUM
UNIVERSITY OF OTTAWA
Department of Mechanical Engineering
SUPERVISOR: Dr. Ernest A. Vallée
ALL DIMENSIONS IN INCHES
SCALE: 1:1
DATE: JAN 30 1992
DRG: ROTATING SHAFT NUT WASHER
PART 5, 6 & 7
DWG. NO. 2 OF 3
DRAWN BY: Warren Druw
NOTE: PARTS 6 & 7 ACT AS
NUT AND WASHER
RESPECTIVELY FOR
PART 5

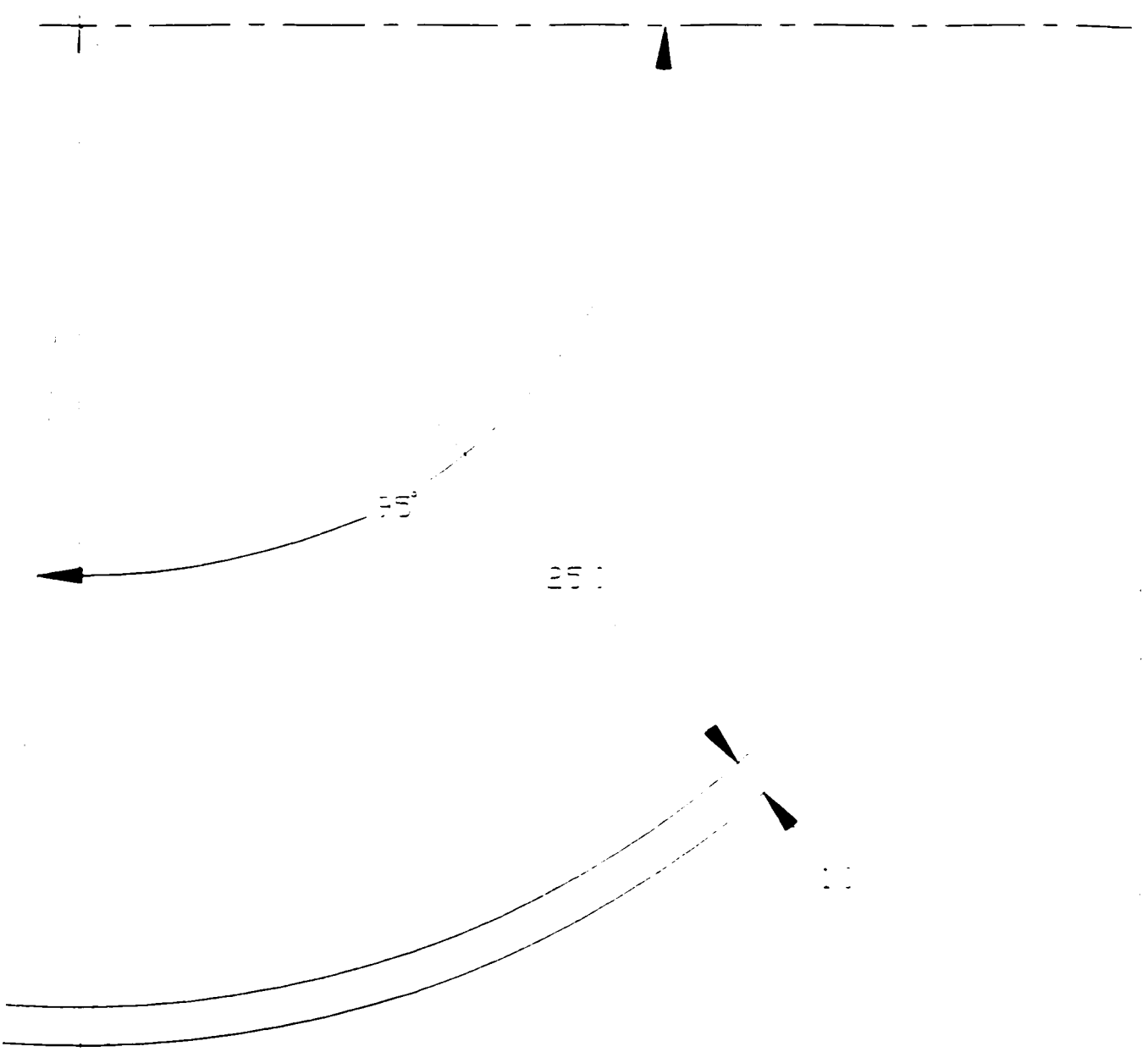

MATERIAL

Department of Mechanical Engineering	
ALL DIMENSIONS IN INCHES	
SCALE	DATE
TITLE: PART 3	
DWG - REV 06-8	WARREN DUNN

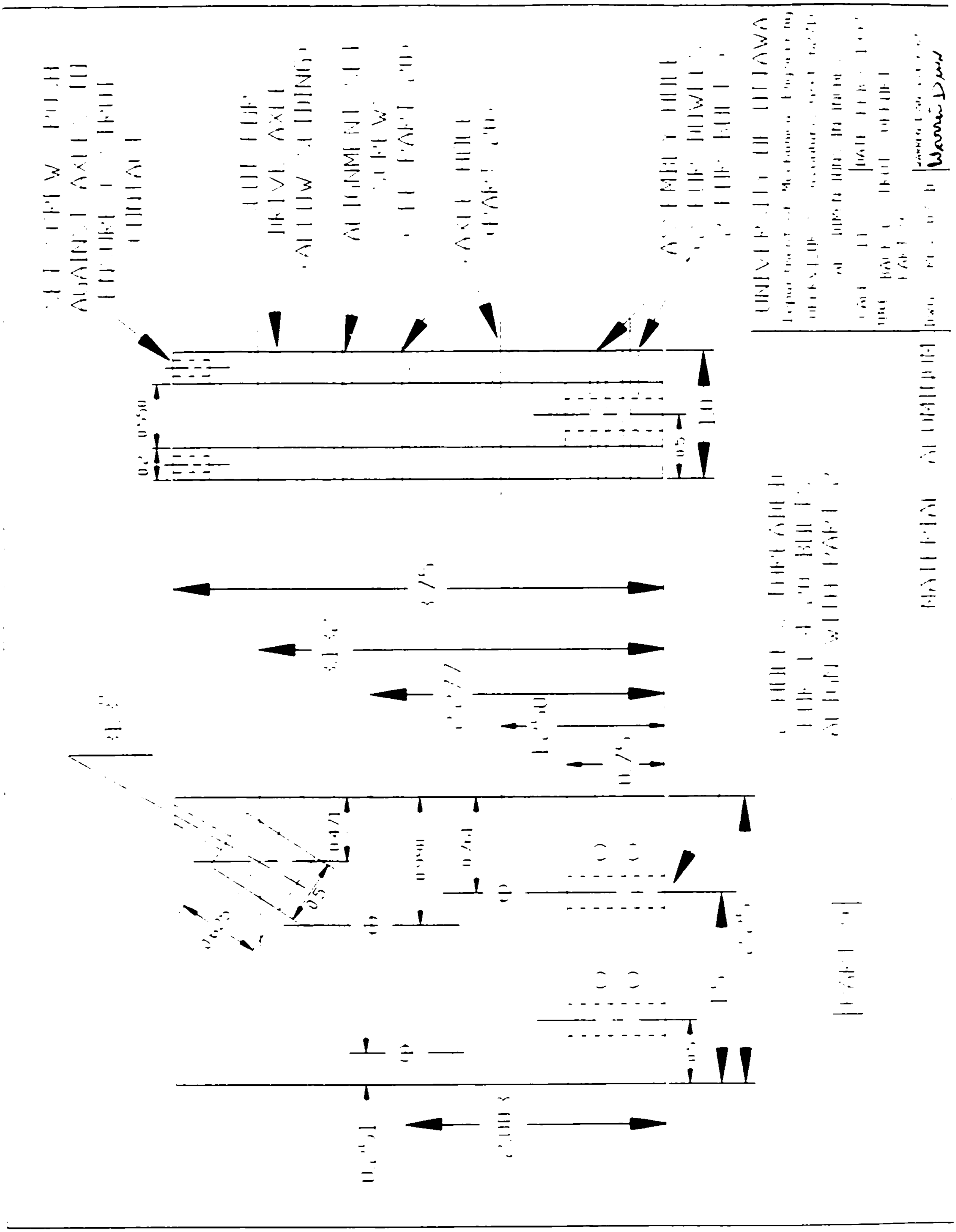
UNIVERSITY OF OTTAWA

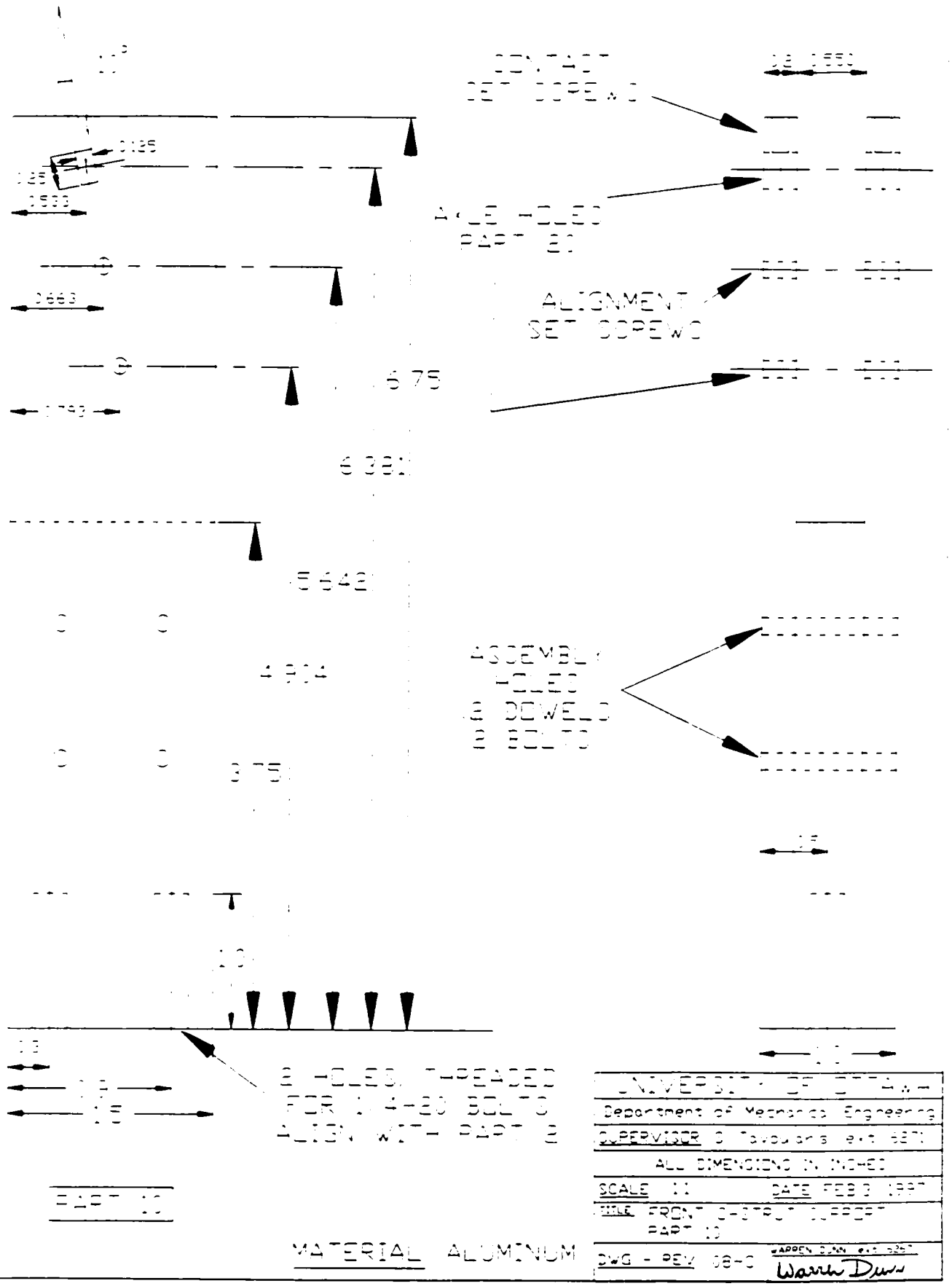

UNIVERSITY OF [illegible]	
Department of Mechanical Engineering	
SUPERVISOR [illegible]	
ALL DIMENSIONS IN INCHES	
SCALE 1:1	DATE FEB 3 1997
TITLE FRONT OUTPUT SLEEVE PART 10	
DWG - REV 08-0	WARREN DUNN [illegible] Warren Dunn

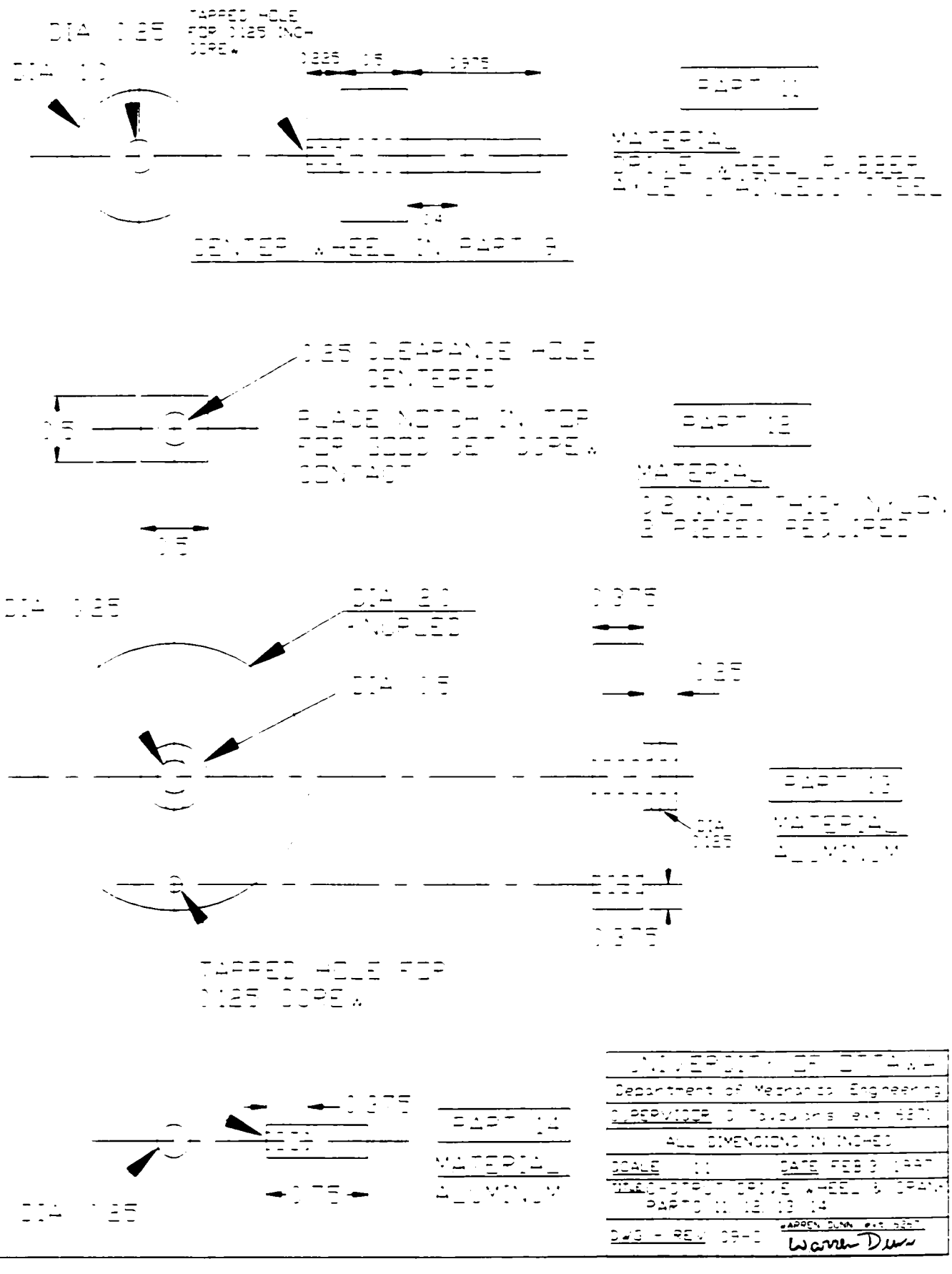
TAPPED HOLE
FOR .125 INCH
DIA .125
DIA .10
.0625 .15 .075
PART 11
MATERIAL
CENTER WHEEL IN PART 9
.125 CLEARANCE HOLE
CENTERED
PLACE NOTCH IN TOP
FOR GOOD GET DOPE &
CONTACT
.15
PART 12
MATERIAL
DIA .125
DIA .30
ANGLED
DIA .15
.075
.125
PART 13
MATERIAL
ALUMINUM
TAPPED HOLE FOR
.125 DOPE &
.075
PART 14
MATERIAL
ALUMINUM
DIA .125
.075
UNIVERSITY OF CALIFORNIA
Department of Mechanical Engineering
DRIVE WHEEL & SPACER
ALL DIMENSIONS IN INCHES
SCALE 1:1
DATE FEB 3 1997
DRAWING DRIVE WHEEL & SPACER
PARTS 11 12 13 14
DWG - REV 09-0
WARREN DUNN ME DEPT
Warren Dunn

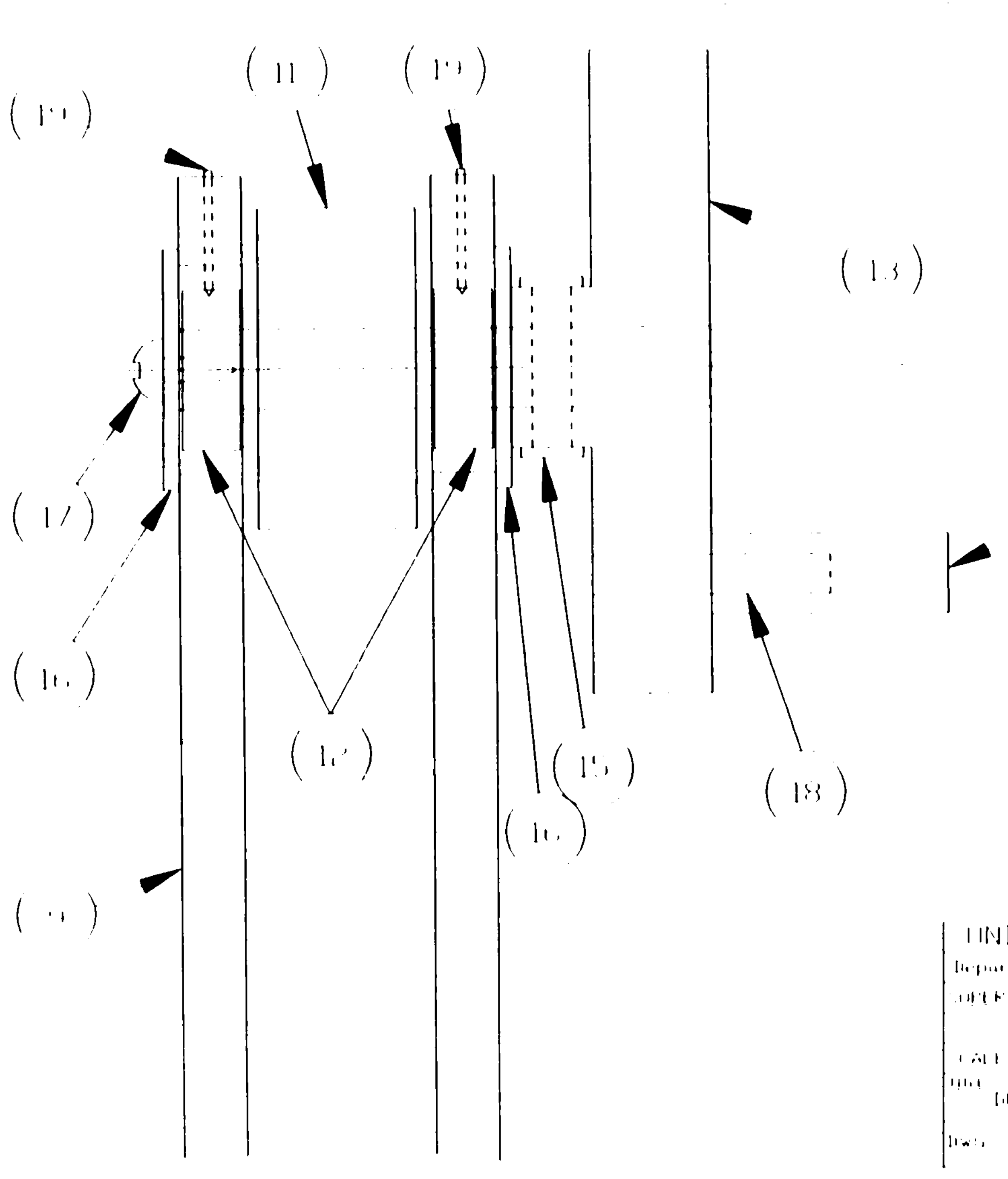

15	HOLDING PIN
16	STAINLESS STEEL WASHER (2)
17	0.25 LONG 1/8 INCH SCREW
18	0.75 LONG THREADED BINDING ROD
19	SET SCREWS (2) 0.75 LONG

UNIVERSITY OF OTTAWA
Department of Mechanical Engineering
SUPERVISOR: [illegible]
ALL DIMENSIONS IN INCHES
SCALE [illegible] | DATE FEB [illegible]
[illegible] WHEEL FRAME ASSEMBLY
DWG [illegible] | WARREN [illegible]

MATERIAL
PC 1 PER 3 INCH OF 1 INCH DIA
ALSO 3 INCHES OF STEEL
4 PIECES REQUIRED

THE ROLLERS MUST MOVE FREELY ON THE AXLES

THE THREE BOTTOM AXLES (2 IN PART 3 AND 1 IN PART 1) ARE TO BE PERMANENTLY MOUNTED. THE TOP AXLE IN PART 1 ALLOWS DECOUPING OF THE CHUTE (PART 3) BY USE OF SET SCREWS. A NOTCH SHOULD BE PLACED ON THE TOP SURFACE OF THE AXLE AT EACH END

ALIGNMENT SET SCREWS

EACH ALIGNMENT SET SCREW WILL HAVE A TEFLON TIP THAT WILL KEEP THE CHUTE FROM MOVING LATERALLY AS SHOWN BELOW

[illegible]	
Department of Mechanical Engineering	
SUPERVISOR [illegible]	
ALL DIMENSIONS IN INCHES	
SCALE 1:1	DATE FEB 3 1997
TITLE SMALL ROLLERS PART 2)	
DWG # REV [illegible]	DRAWN BY Warren Dunn

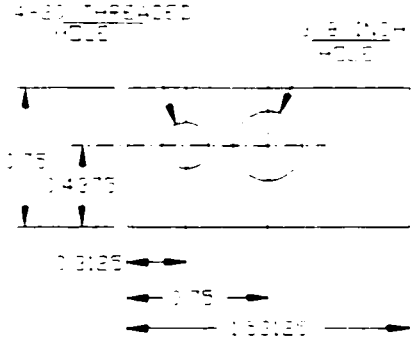

23

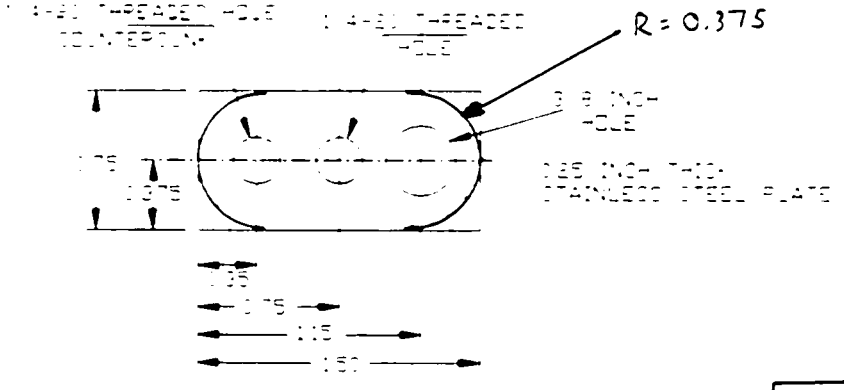

24

[illegible]	[illegible]
Department of Mechanical Engineering	
[illegible]	[illegible]
ALL DIMENSIONS IN INCHES	
SCALE 1:1	DATE APR 29 1997
TITLE STING SUPPORT INSERT BLOCK AND EXIT ATTACHMENT PLATE	
DWG - REV 12-A	WARREN DUNN [illegible]

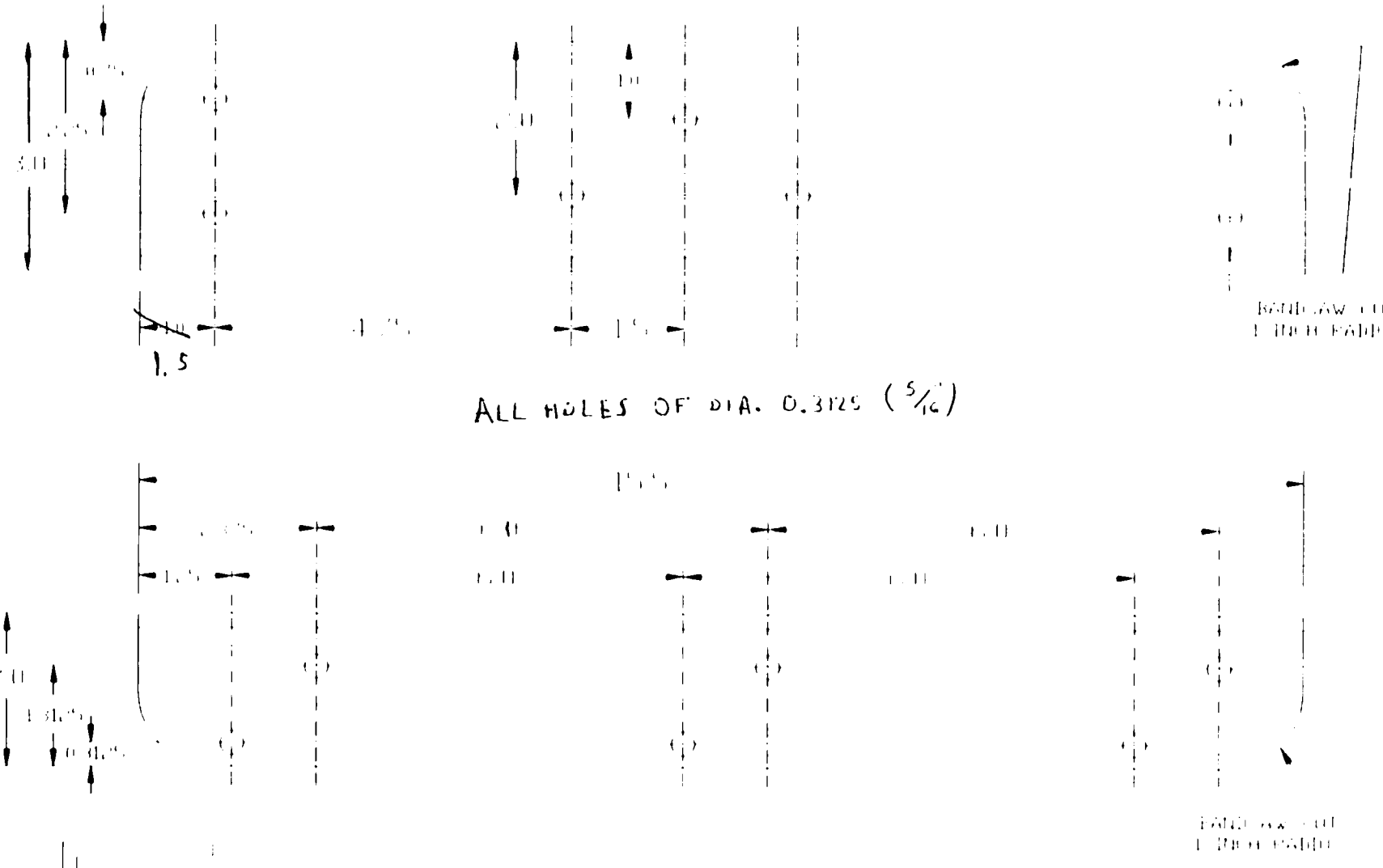

PART 25

Warren Dunn

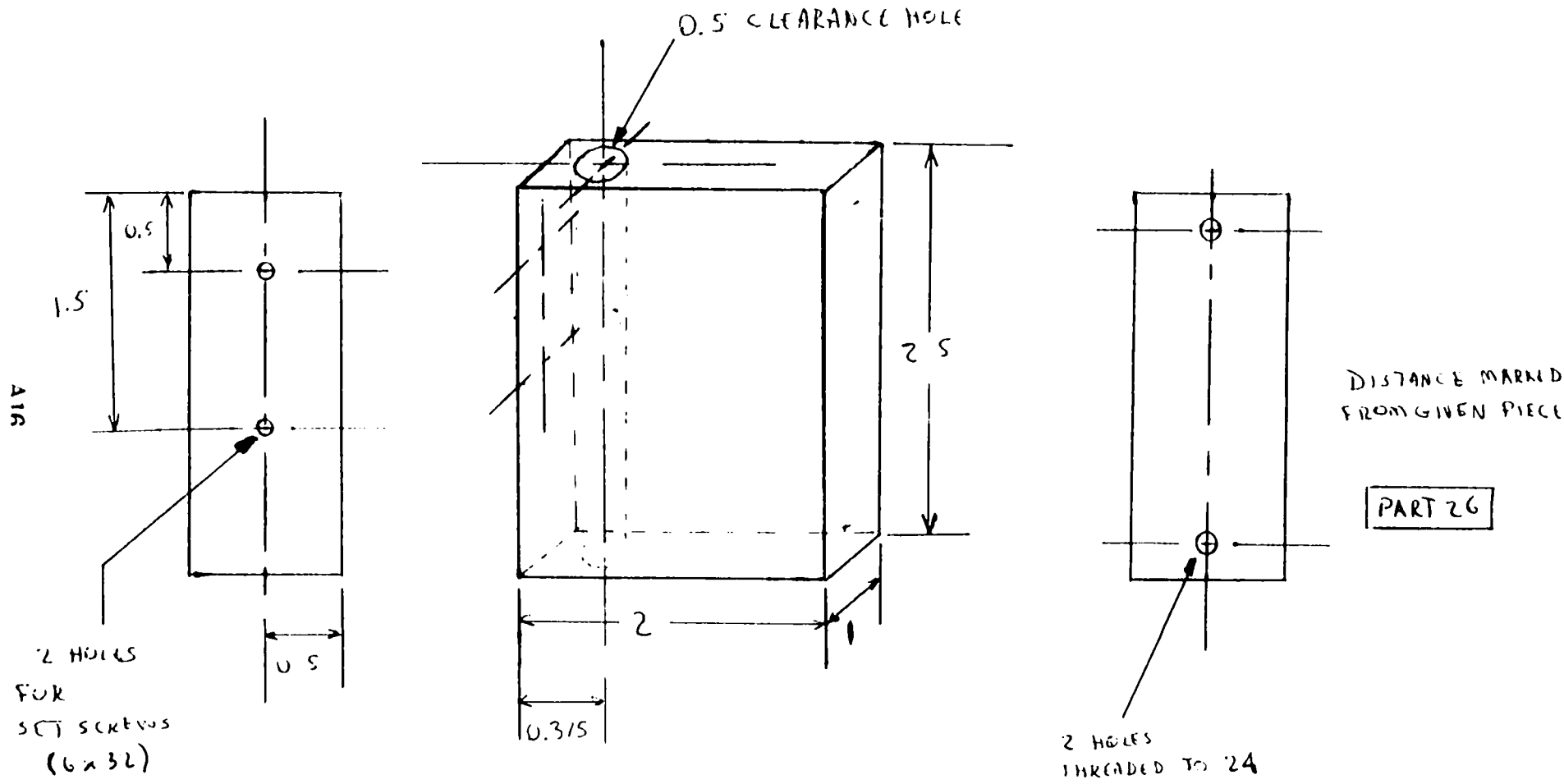

A16

MATERIAL ALUMINUM

LARREN DUNN (GLL)

October 3, 1997

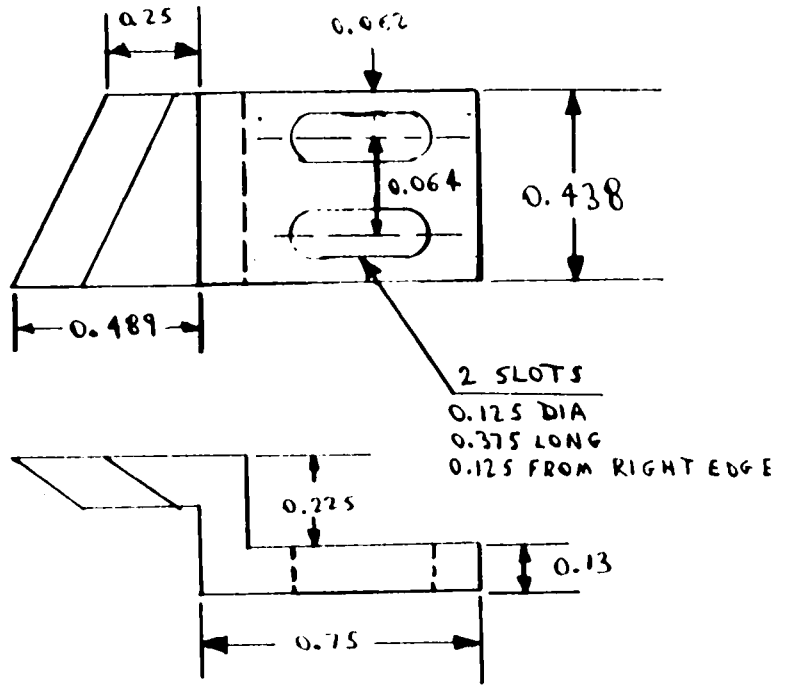

PART 27

MATERIAL: ALUMINUM

WARREN DUNN (6267)
(S. TAVOULARIS) (6271)
MAY 21, 1947

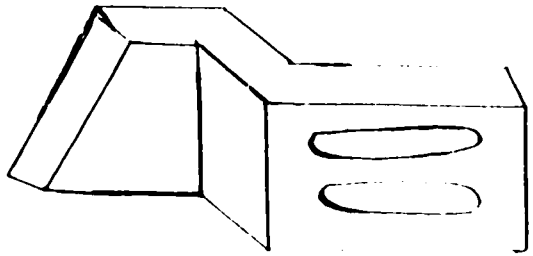

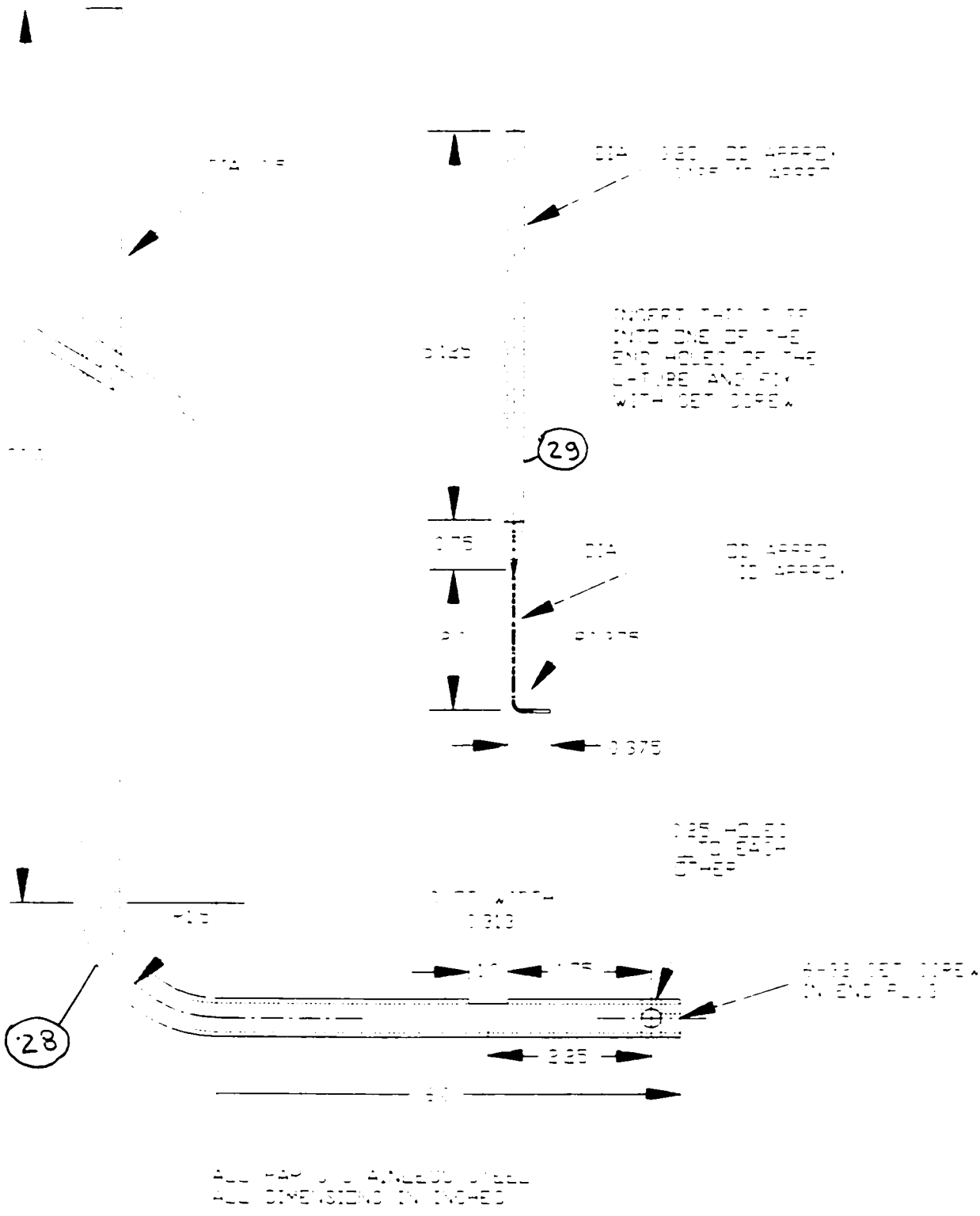
29
0.375
28

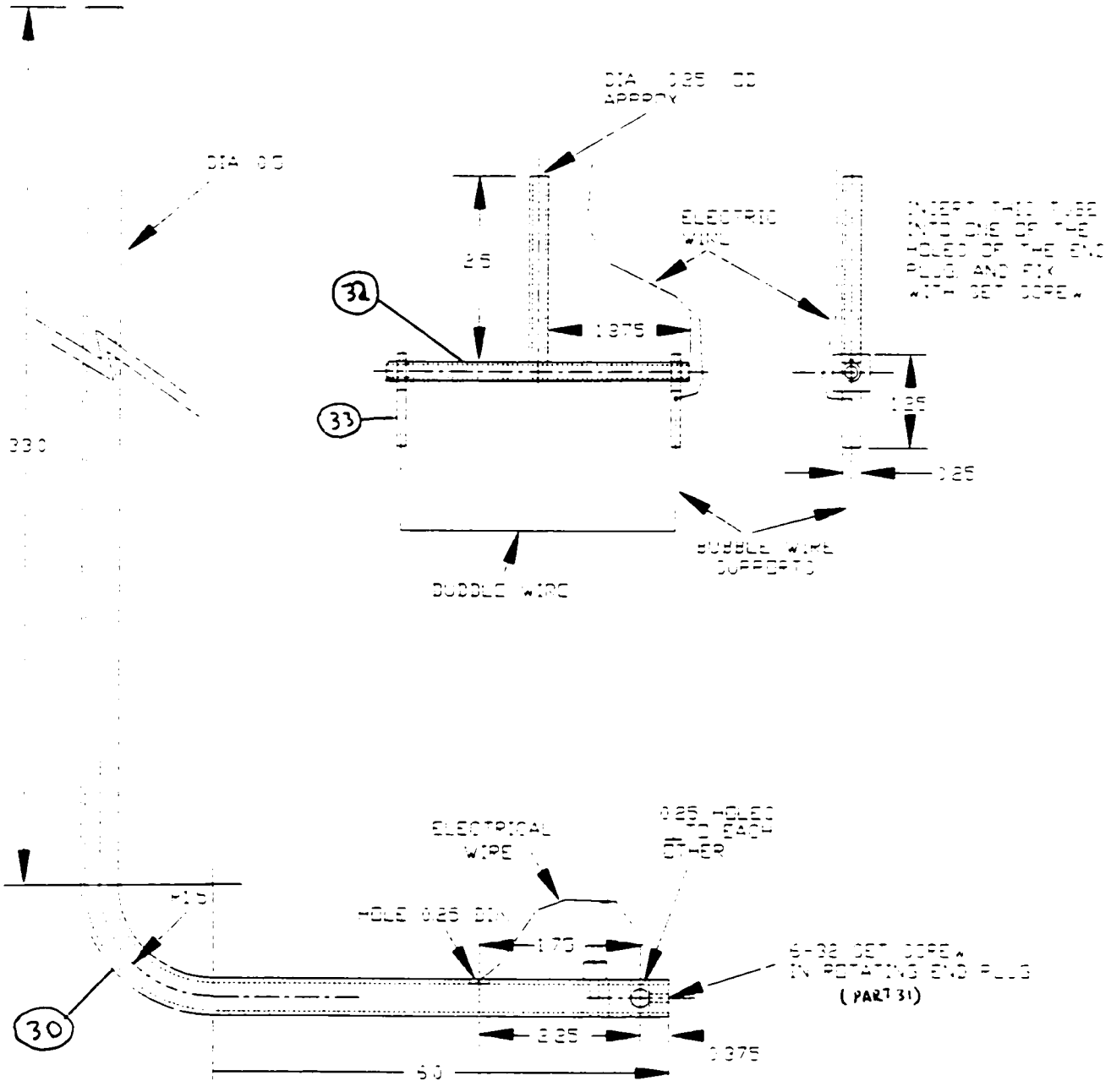
DIA .035 OD
APPROX
DIA .OD
ELECTRIC
WIRE
INSERT THIS TUBE
INTO ONE OF THE
HOLES OF THE END
PLUG AND FIX
WITH SET SCREW
.25
.375
32
33
.125
.25
.330
BUBBLE WIRE
BUBBLE WIRE
SUPPORTS
ELECTRICAL
WIRE
.025 HOLES
TO EACH
OTHER
.15
HOLE .025 DIA
.175
6-32 SET SCREW
IN ROTATING END PLUG
(PART 31)
30
.325
.375
5.0
ALL PARTS STAINLESS STEEL
ALL DIMENSIONS IN INCHES

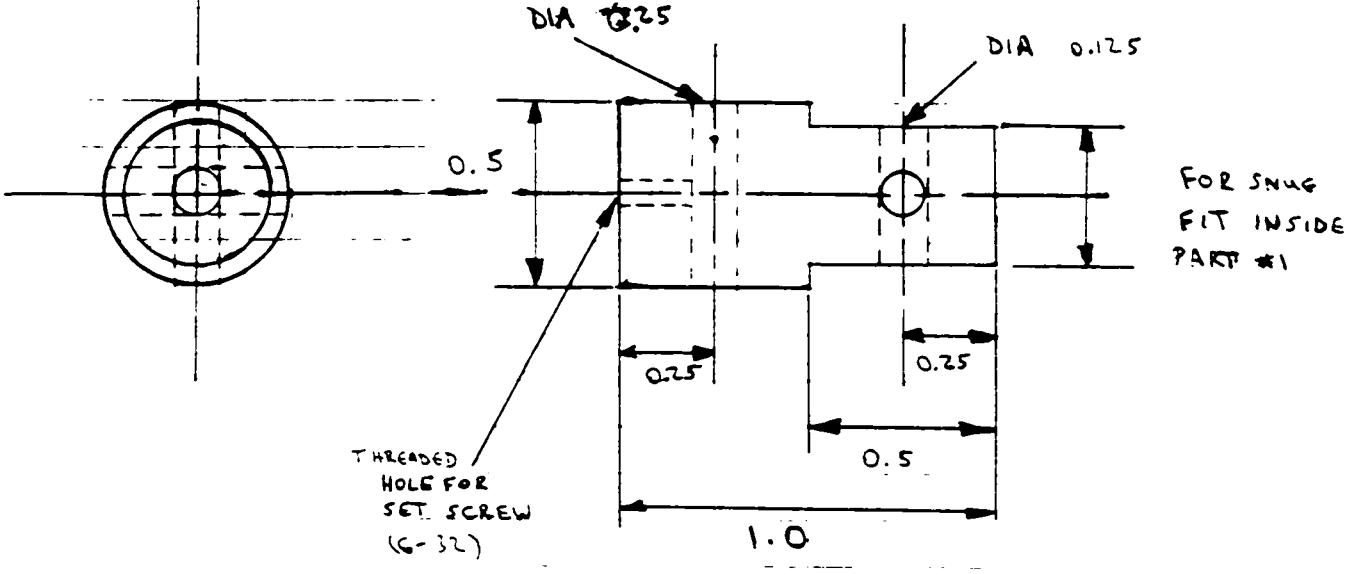

PART #3.1

MATERIAL: STAINLESS STEEL

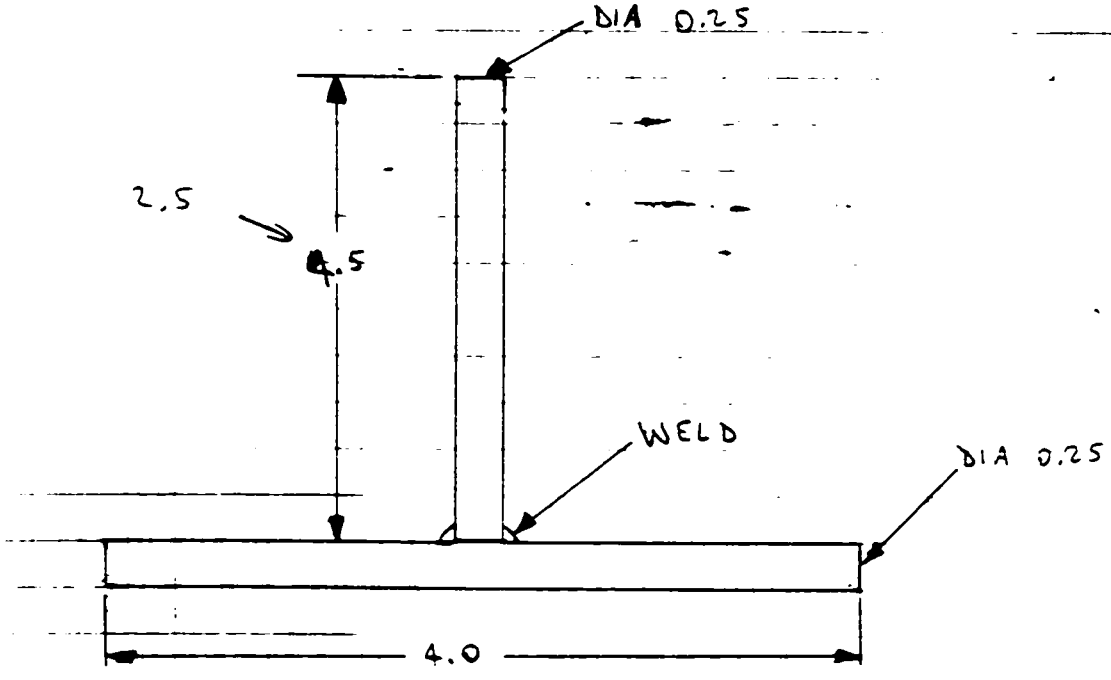

PART #32

MATERIAL: STAINLESS STEEL

Warren Dunn (6267)
S. Tavoularis (6271)
June 11, 1997

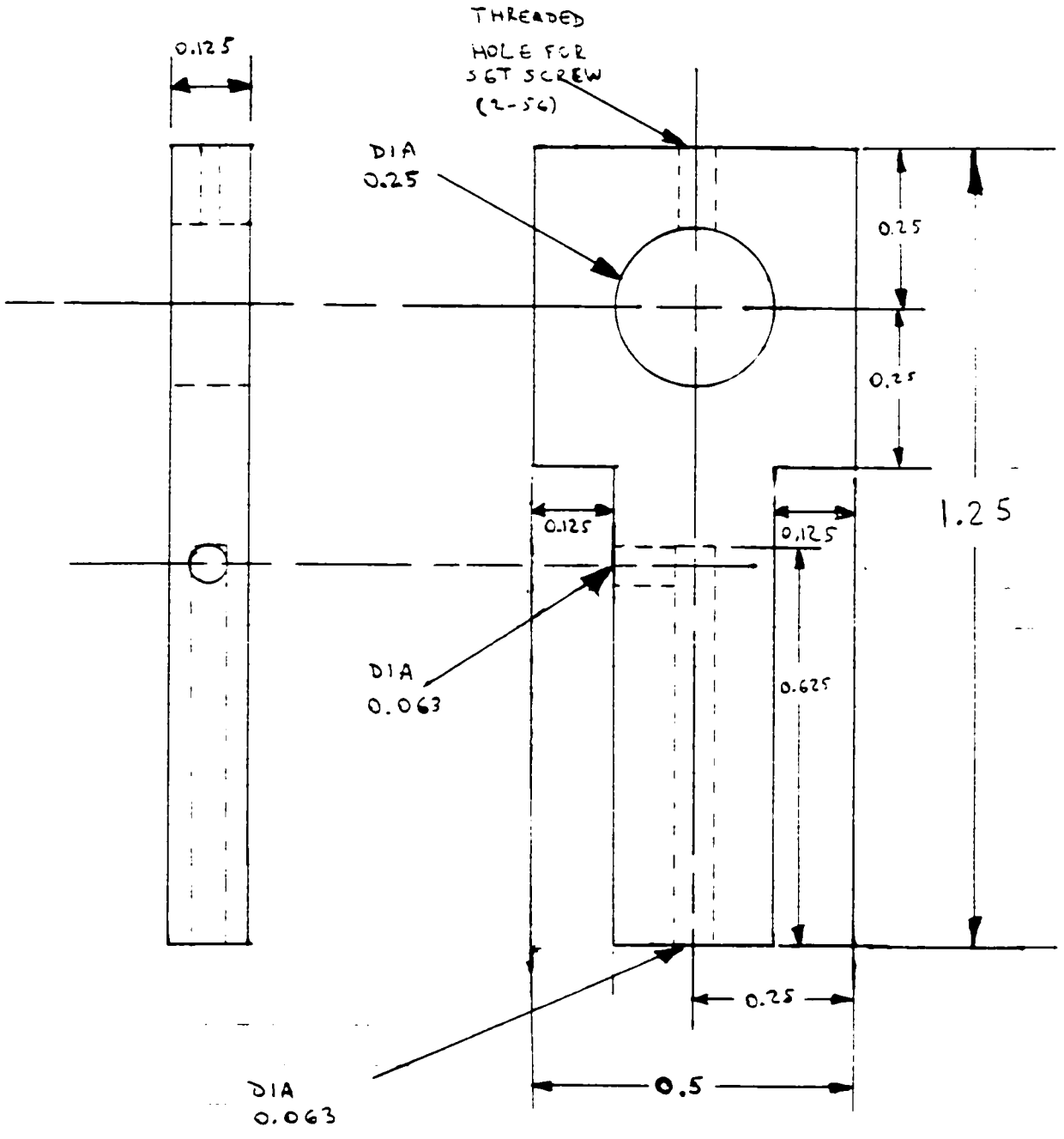

PART #34

MATERIAL:

QTY 2

Warren Dunn (6267)
S. Tavoularis (6271)
June 11, 1997

Appendix B

Water Tunnel Sketches

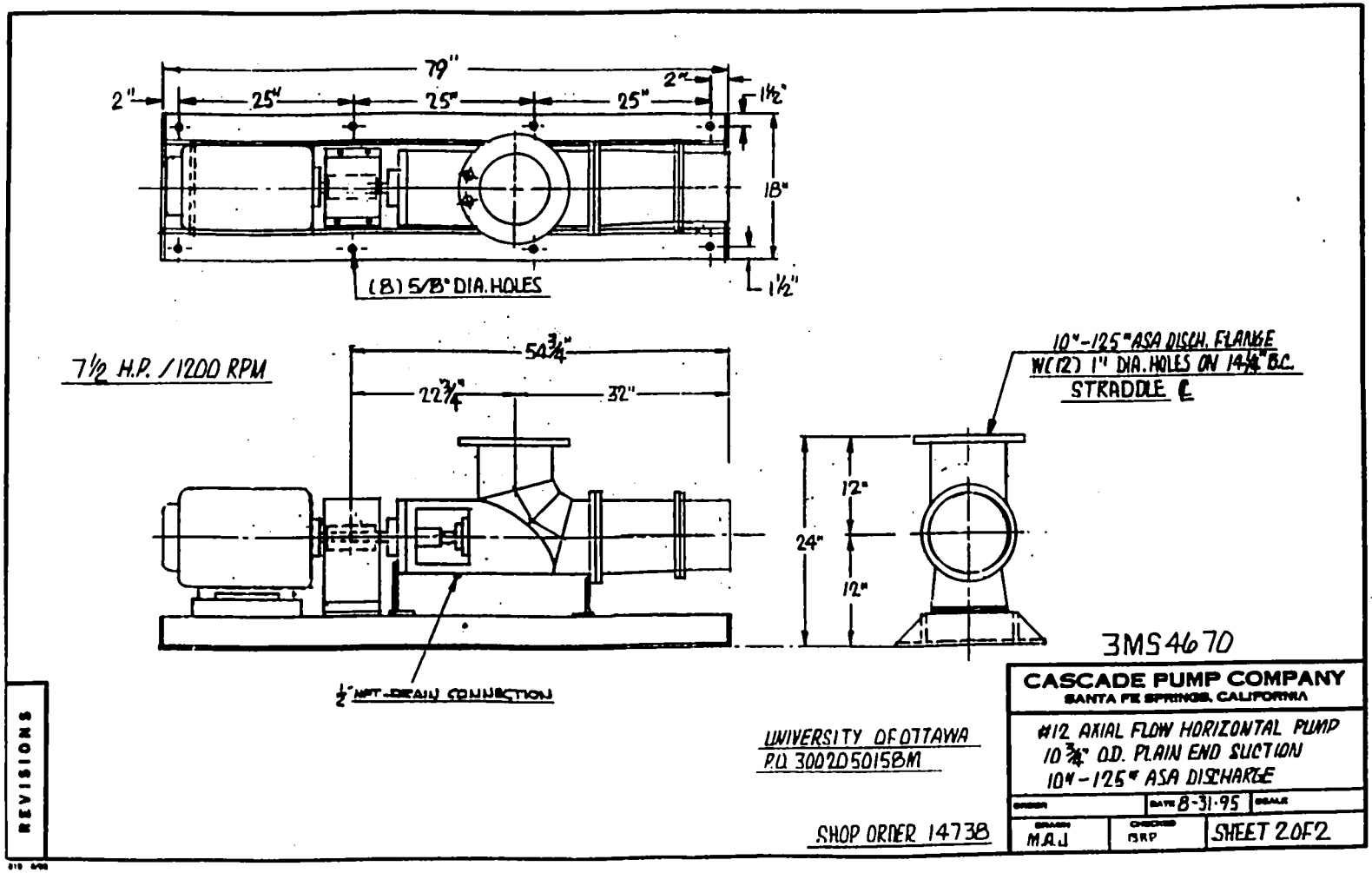
79"
2"
25"
25"
25"
2"
1½"
18"
(8) 5/8" DIA. HOLES
1½"
7½ H.P. / 1200 RPM
54¾"
22¾"
32"
10"-125# ASA DISCH. FLANGE
W/(12) 1" DIA. HOLES ON 14¼" B.C.
STRADDLE ℄
12"
24"
12"
½" NPT-DRAIN CONNECTION
3MS4670
REVISIONS
UNIVERSITY OF OTTAWA
P.O. 300205015BM
SHOP ORDER 14738
CASCADE PUMP COMPANY
SANTA FE SPRINGS, CALIFORNIA
#12 AXIAL FLOW HORIZONTAL PUMP
10¾" O.D. PLAIN END SUCTION
10"-125# ASA DISCHARGE
DATE 8-31-95
DRAWN M.A.J
CHECKED ISRP
SHEET 2 OF 2

B2

ITEM	QTY	DESCRIPTION	MATERIAL	PART NO	ITEM	QTY	DESCRIPTION	MATERIAL	PART NO.
1	1	SUCTION PIPE	FAB. STEEL	14738-2	13	1	PACKING GLAND	BRONZE	C17
					14	1	PUMP SHAFT COUPLING	C 1020 STL	SC 950
3	1	THRUST COLLAR & KEY	416 STN STL	M100C	15	1	BRG. HOUSING SEAL	NATIONAL	470038
4	1	PROPELLER	316 STN. STL	AFC 103	16	1	BEARING HOUSING	STEEL	BH207A
5	1	DISCH. BOWL ENERAC	SAE 660 BRZ	C102	17	1	THRUST BEARING	—	20207
6	1	DISCHARGE BOWL	316 STN. STL	AFC 100C	18	1	LOCK NUT & WASHER	—	STOCK
7	1	DISCH. BOWL	SAE 40 BRZ	C102	19	1	BEARING COVER	STEEL	BC 207
8	1	PUMP SHAFT	416 STN STL	14738-3	20	1	BEARING COVER SEAL	NATIONAL	471354
9	1	DISCHARGE ELBOW	FAB STEEL	14738-1	21	1	HEAD SHAFT	416 STN STL	14738-4
10	1	PKG. BOX BUSHING	SAE 660 BRZ	C26-4	22	1	FLEXIBLE COUPLING	STEEL	STOCK
11	1	PACKING BOX	CAST IRON	C27					
12		PKG. RINGS	TEFLON	STOCK					

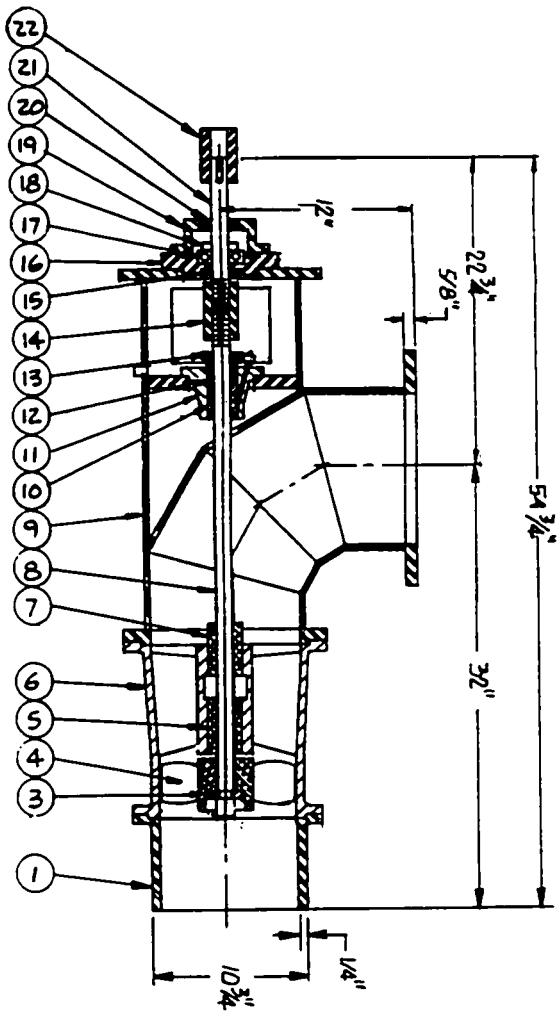

SHOP ORDER 14738

UNIVERSITY OF OTTAWA
P.O. 300205015BM

3MS 46 TD

CASCADE PUMP CO.
SANTA FE SPRINGS, CALIFORNIA

10" AXIAL FLOW PROPELLER PUMP
10 3/4" O.D. PLAIN END SUCTION
10" 125# ASA DISCHARGE

DRAWN M.A.J. 8-31-95 CHECKED E.R.T.

SHEET 1 OF 2

CURVE NO. 14738

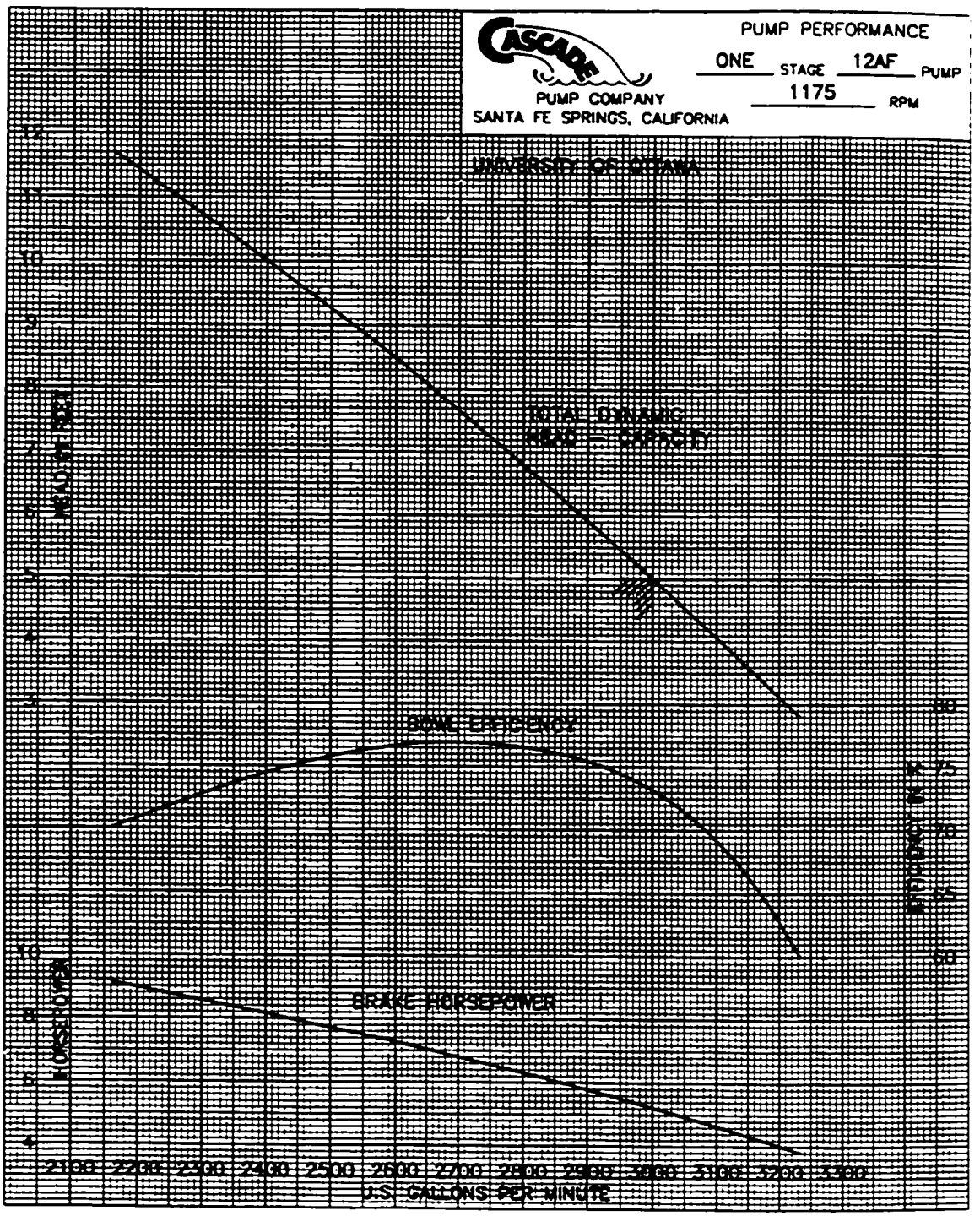

CURVES SHOW APPROXIMATELY THE CHARACTERISTICS WHEN PUMPING CLEAR NON-AERATED WATER NO GUARANTEE IS MADE EXCEPT FOR THE RATED POINT

B5

NOTE 1. CONDUIT BOX MAY BE ASSEMBLED WITH ENTRANCE UP, DOWN OR TO EITHER SIDE.

NOTE 2: F1 ASSEMBLY AS SHOWN. F2 ASSEMBLY CONDUIT BOX ON OPPOSITE SIDE FROM SHOWN LOCATION.

CAD NO	DH250:B5825NAP001
REF.	
PLOT CLASS	100,101,110,150
PLOT SCALE	.3

GE Canada — PETERBOROUGH

TITLE

INDUCTION MOTOR OUTLINE

4002B5825NAP00

FRAME BASE PER FR.K/KS-2501 — STANDARD DRIPPROOF — C.I.R.

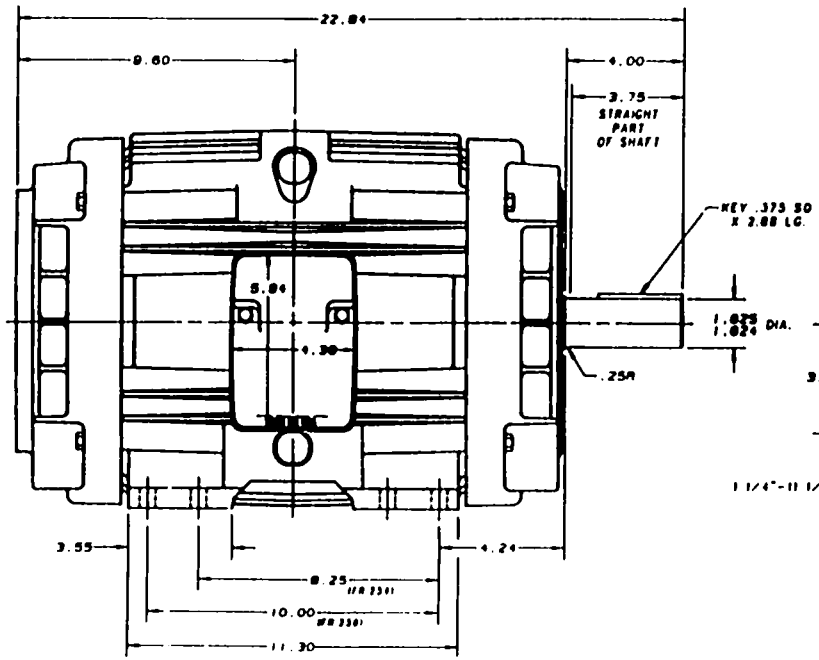

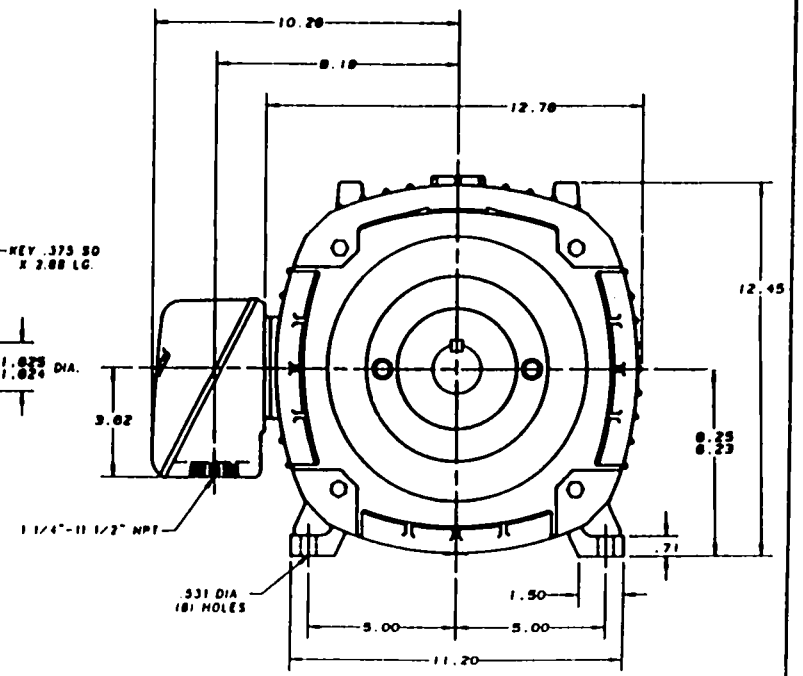

PRINTS TO	
18K15	
NAME	DATE
DRAWN JOHN FERRIER	SEPT 10
ENGINEER JOHN FERRIER	SEPT 10

GENERAL ELECTRIC COMPANY
GE MOTORS & INDUSTRIAL SYSTEMS
2000 TAYLOR STREET - BOX 2205
FORT WAYNE, INDIANA 46801

DATA TRANSMITTAL 9/13/95

CUSTOMER: CASCADE PUMP CO

10107 S NORWALK BLVD

SANTA FE SPRINGS CA 90670

MARKS: S.O.# 14738

CUSTOMER ORDER NO. 37970

G.E. REQN. NO. 694-04455
G.E. ORDER NO. 950908044

"PRINT APPROVAL"

ITEM NO.	1	MODEL NO.	NEW MODEL
TYPE	K	FRAME	254T
HP	7.5	RPM-FL	1170
PHASE	3	VOLTS	575
HZ	60	SERVICE FACTOR	1.15
TIME RATING	CONT	AMB-MAX	40 DEG C
INSUL CLASS	F	NEMA DESIGN	B
CODE	H	AMPS-FL	8.4
NEMA NOM EFF	86.5	MAX KVAR	4.2
BEARING-DE	6309ZC3	BEARING-ODE	6309ZC3
OUTLINE	4002B5825NAP001	DESIGN	25PD3200BA
ENCLOSURE IS	DRIPPROOF		

ADDITIONAL MOTOR DATA:

LOAD%	125	115	100	75	50	25
EFF	85.6	86.3	86.5	87.6	86.5	80.1
P.F.	80.7	79.7	77.5	71.1	59.0	37.9
AMPS	10.1	9.4	8.4	6.8	5.5	4.6

DISTRIBUTION INFORMATION:

4 MDT'S & O/L'S TO CHARGEE, ATTN: BOB BROWN

SAME TO BARRY RITTER, 4-6

TERRI STEWART

W.T. Entrance Section

General Layout.

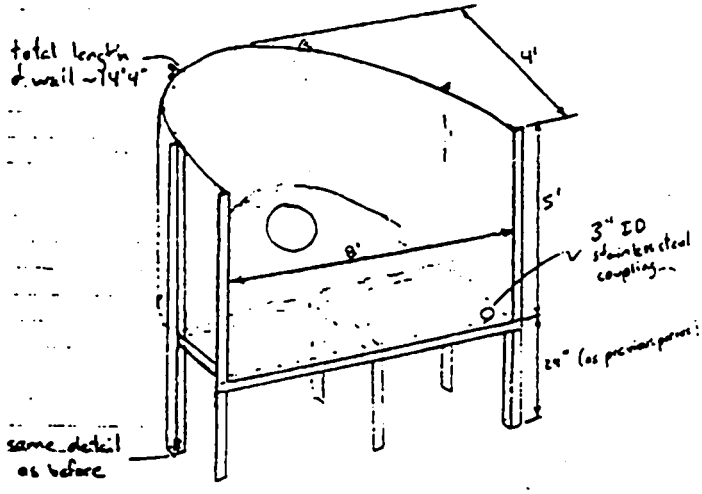

shape of flat bottom w/ holes to be provided on 4'x8' white sheet

use bottom shape as template for curved walls and as guide for erecting support beams.

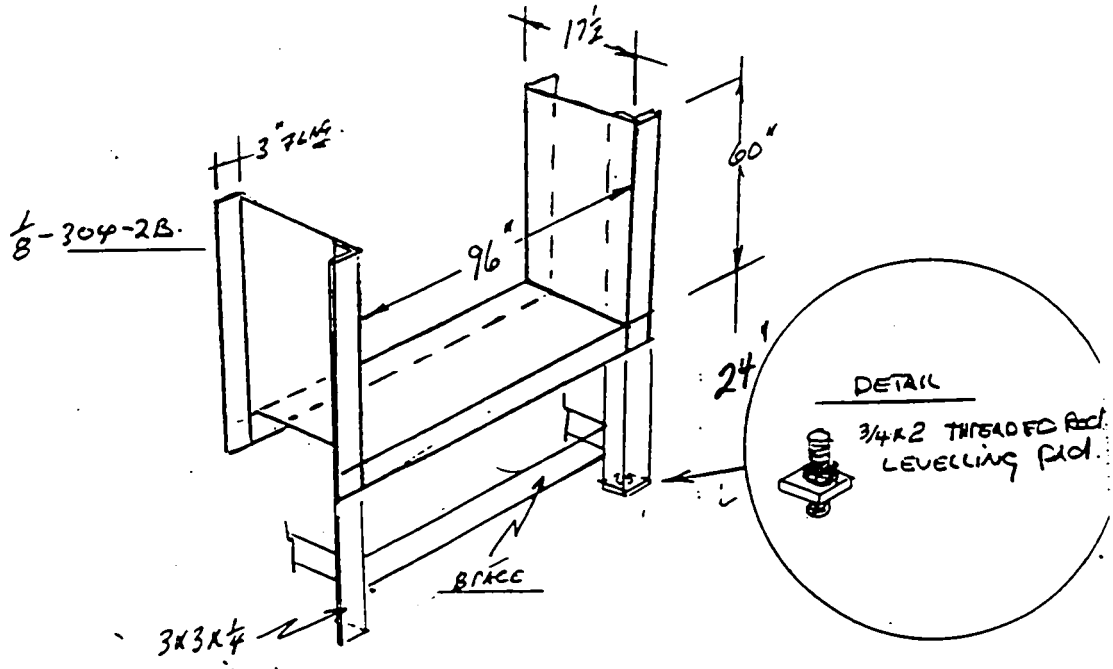

Appendix C

Electronic Circuit Drawings

The following figures are presented in Appendix C:

C1 The hydrogen bubble voltage pulsing circuit, as described in Section 3.4.2 (Budwig and Peattie, 1989).

C2 The circuit for the camera timer power supply, used in conjunction with the camera timer circuit presented in Figure C4.

C3 The camera timer circuit, designed and built by the electronics laboratory at the University of Ottawa.

C4 The solencid valve control box circuit, designed and built by the electronics laboratory at the University of Ottawa, intended for use with the dye injection tubes, as described in Section 3.4.1.

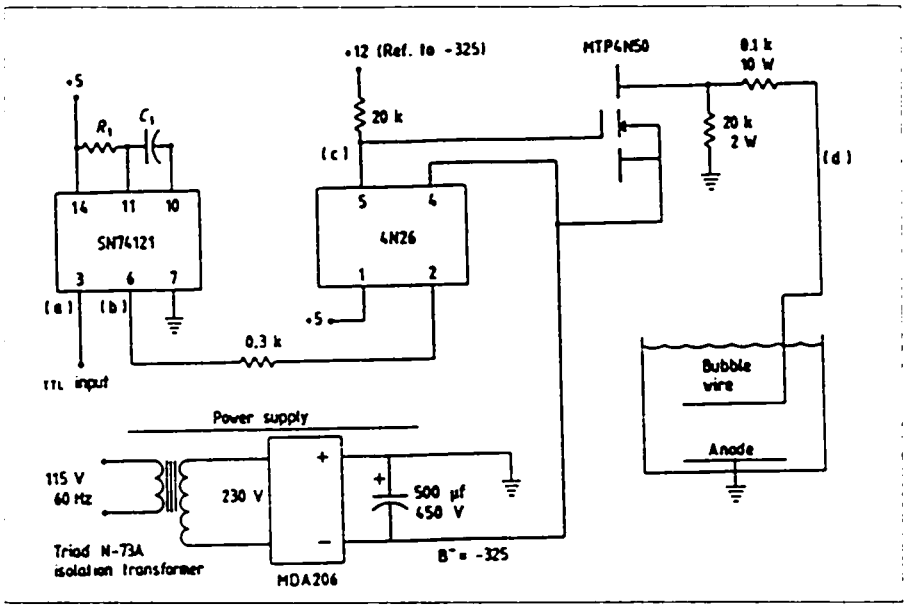

Figure C1: The hydrogen bubble voltage pulsing circuit (Budwig and Peattie, 1989).

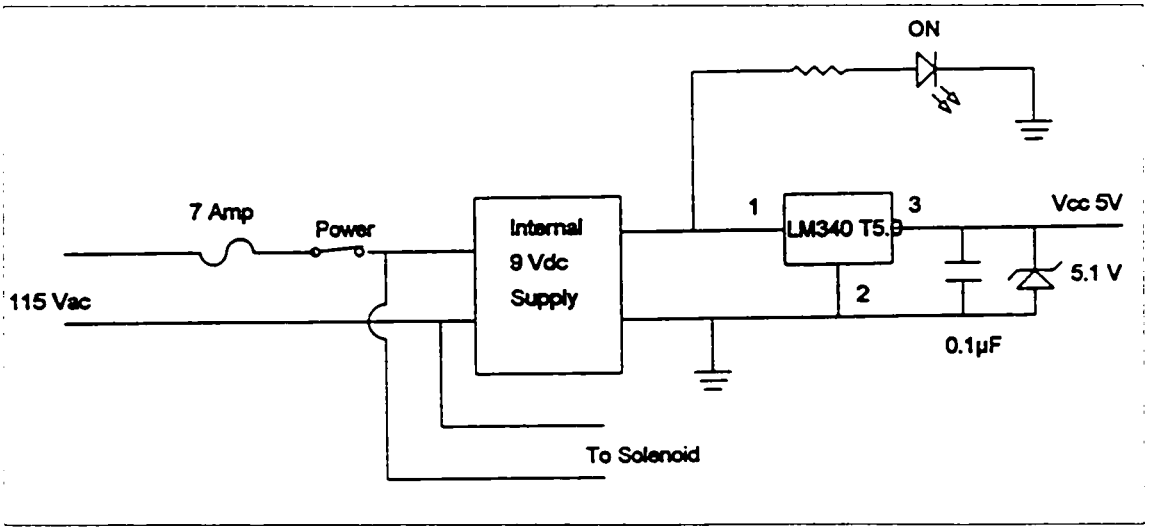

Figure C2: Power supply circuit for the camera timer circuit (see Figure C3).

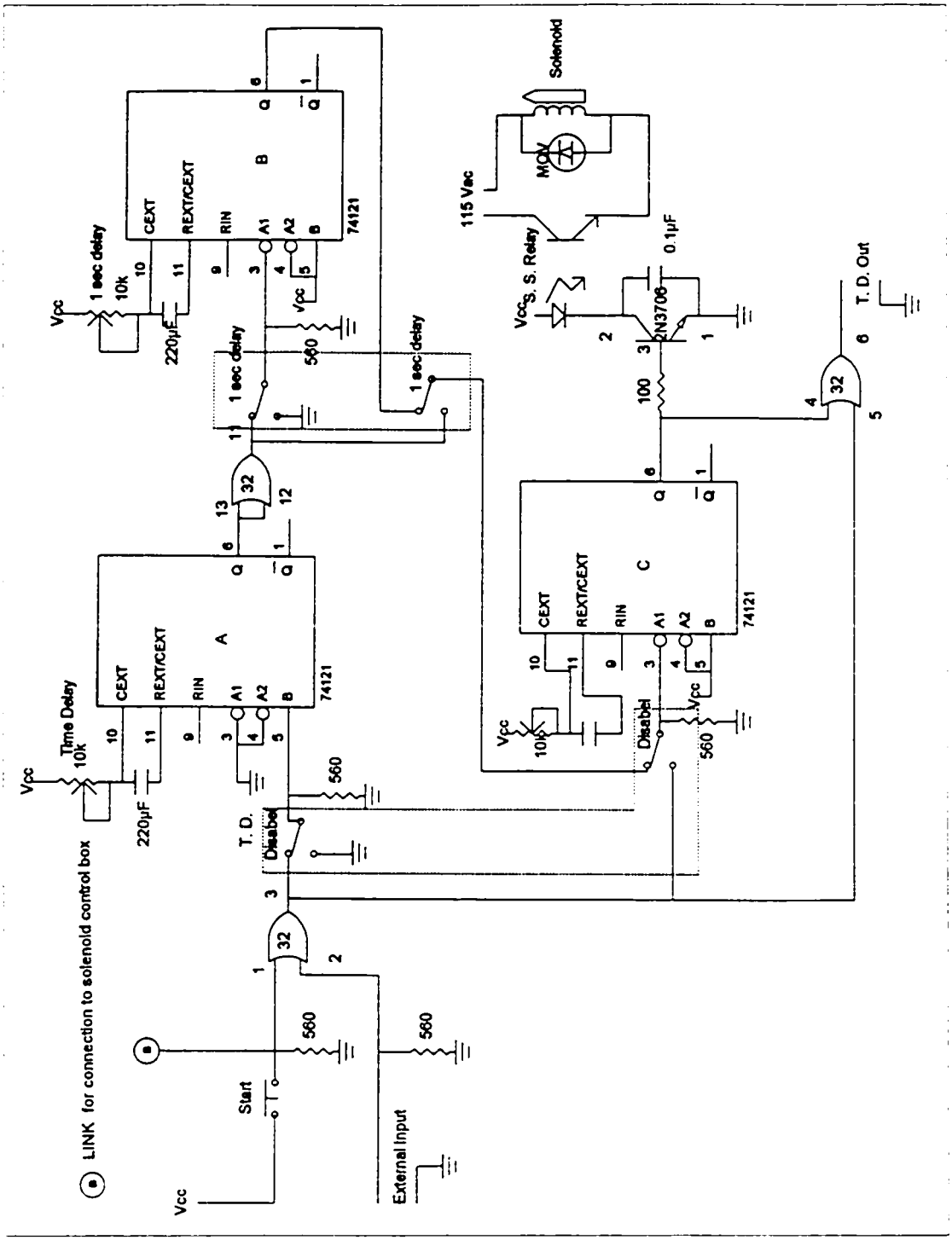

Figure C3: The camera timer circuit.

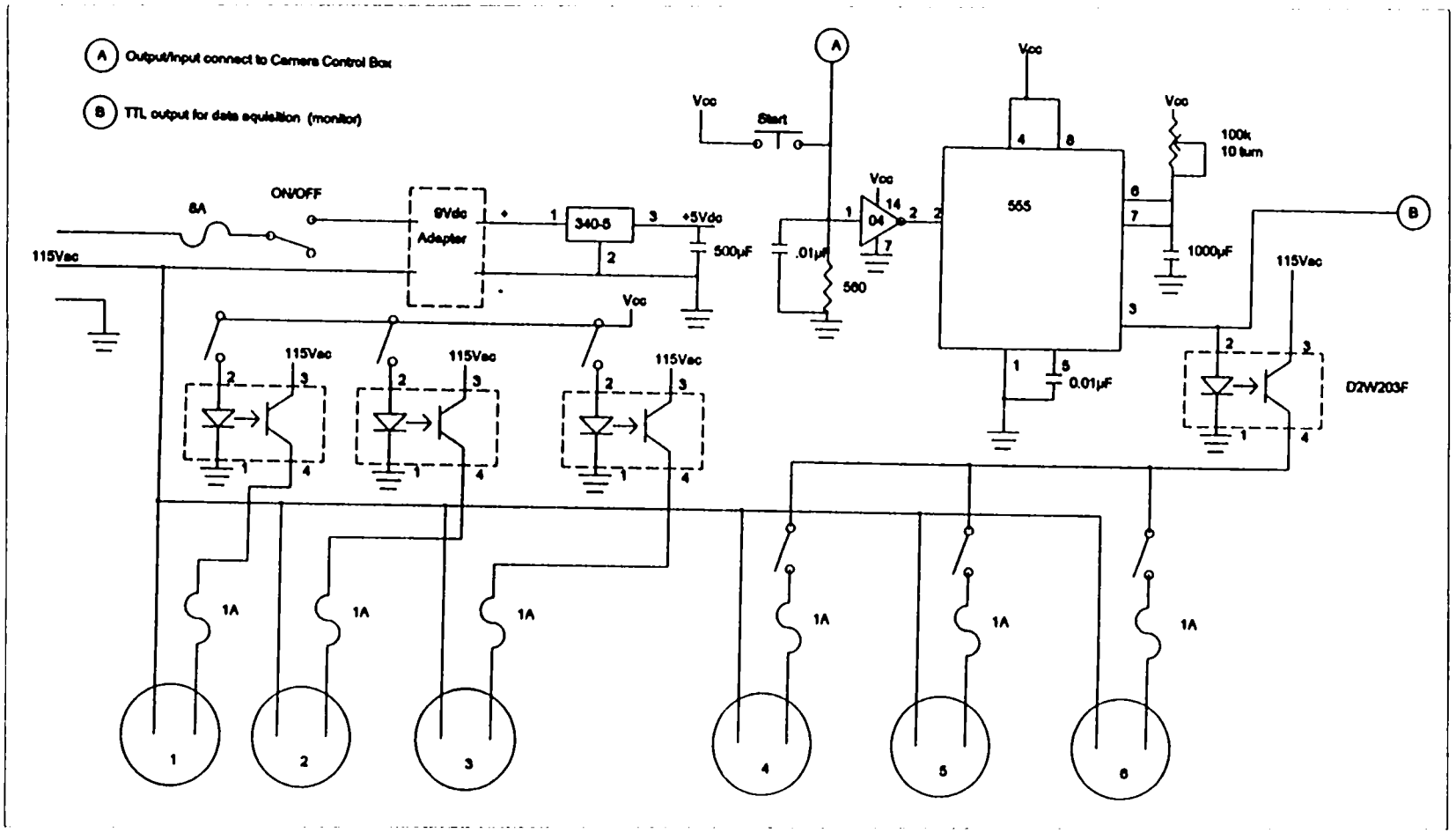

Figure C4: The solenoid valve control box circuit, intended for use with the dye injection system.

Appendix D

Mounting and Dismounting Procedures

For ease of assembly and minimum risk of damaging components or injury trying to avoid this damage, the systems should be set up in the following order: model, dye system or hydrogen bubble wire, lighting, camera. Inevitably, position corrections will be required. It is suggested that positioning should be as close as possible to the desired location before the next system setup is begun, and only minor adjustments be made once all systems have been set up.

D.1 Model

Mounting

1. Submerge the model, allowing as many air bubbles as possible to escape.
2. Remove one nut and washer, insert the sting into the C-strut hole, replace the washer and nut.

3. Tighten the nut at the same time as assuring zero roll angle. This was done by eye by checking the profile of the model against the base of the positioning system, which has two holes precisely located along the centerline for purposes of assembling the mount.
4. Turn the 124 W (1/6 hp) pump off, and open the flow valve, ensuring the engine flow tube is above the waterline.
5. Assure valve and engine flow tubes (one from the model, one from the pump) are full of water, and attach them underwater.
6. Turn the 124 W (1/6 hp) pump on.
7. Close the large valve under the drainage tank, and the 4 boundary layer valves closest to the lab wall for model engine flow. This will give a flow rate of approximately 0.4 gpm on the flow meter.

Dismounting

1. Turn the 124 W (1/6 hp) pump off, and open all the valves.
2. Close flow valve, detach flow tubes; do not allow valve flow tube to fall to the ground, spilling water: wrap it around the carriage or the tunnel frame, out of the way.
3. Loosen and remove the nut and washer on the sting, and remove sting from the C-strut hole. Then replace nut and washer on the sting.
4. Hold the model sting down, nose up above the tunnel to drain the water.

D.2 Dye System

Mounting

1. Mount the stainless steel L-tube in the set screws to the vertical traverse, with the flexible tubing just above the water surface.
2. Mount the injection tube into the L- tube, ensuring all of it is below the water.
3. Purge the injection tube of air by attaching the syringe (modified so that the needle has been removed and replaced with some flexible tubing) to the injection tube base and withdrawing the plunger until it fills with water. Note that filling the syringe with water and then trying to push the air out of the injection tube does not work well.
4. Connect the flexible tube from dye canister to the flexible tube protruding from the stainless steel L- tube above the tunnel.
5. Fill the dye canister with dye, ensuring all exit valves are closed.
6. Open the high pressure supply valve, then the low pressure regulator valve to about 30 kPa.
7. Open the dye canister valve slightly, and connect the flexible tube (which has now been purged of air) to the injection tube. This requires practice: as the dye canister valve is located beneath the tunnel, and the injection tube is inside the tunnel, a lot of dye can be lost into the tunnel before the flexible tube is attached to the injection tube.

8. Position the injection tube at the desired location and reduce the pressure to get the desired dye flow rate. Note: Pressure must first be lowered at the low pressure regulator valve, then in the line by pressing the air release button on the dye canister.

Dismounting

1. Close the high pressure valve, and press the air release button on the dye canister until all the pressure is released.
2. Raise the stainless steel L-tube until the top of the injection tube is out of the water.
3. Remove the flexible tubing from the injection tube, allowing it to drain into the dye canister. It may be necessary to release the pressure a second time for this to happen.
4. Remove the injection tube from the stainless steel L-tube. Purge it of the remaining dye by blowing air into it with the same syringe as above.
5. Disconnect the flexible tubing coming from the dye canister from the flexible tubing in the stainless steel L-tube and remove the L-tube from the system, ensuring any residual dye is not spilled onto the tunnel or floor.

D.3 Hydrogen Bubble Wire

Mounting

1. Mount the wire and frame into the stainless steel L-tube facing sideways (this minimizes the chance of wire breakage during mounting).
2. Mount the stainless steel L-tube to the vertical traverse using the set screws.
3. Arrange the wire and its frame in the orientation and location desired.
4. Plug the bubble wire into negative slot on the connector above the tunnel.
5. Drop the carbon rod (anode) into the water downstream of the model.
6. Plug the connector into the pulsing circuit (the wires are colour coded).
7. Plug in all components, turn the signal generator on (7 Hz was best for this study).
8. Ensure the voltage generator is set to minimum voltage, turn it on, wait 5 to 10 seconds for the startup peak to pass, then set it to about 100 volts. Bubbles should be seen emanating from the wire.

Dismounting

1. Turn all power off and unplug the system. Unplug the connector box from pulsing circuit and the bubble wire from connector box.
2. Remove the carbon anode from the water.
3. Rotate the bubble wire sideways to avoid breakage during dismounting.

4. Remove the bubble wire system from the water.

Note: This procedure is described for the small hydrogen bubble wire. The large bubble wire and frame is mounted in the same way, but the wire can only be oriented in the vertical plane, so steps 1 and 3 in the mounting procedure, as well as step 3 in the dismounting procedure may be disregarded.

Appendix E

Tecplot Data Files

E.1 Wing Surfaces

```
TITLE = "CF-18"
VARIABLES = "Z"
"X"
"Y"
ZONE T="Upper Wing"
I=8, J=16, K=1,F=POINT
DT=(SINGLE SINGLE SINGLE )
0.0000E+000 5.7730E-001 0.0000E+000
7.8900E-002 5.7660E-001 0.0000E+000
1.4540E-001 5.8170E-001 0.0000E+000
2.9300E-001 5.7750E-001 0.0000E+000
4.5680E-001 5.6850E-001 0.0000E+000
6.4040E-001 5.5970E-001 0.0000E+000
7.0630E-001 5.5210E-001 0.0000E+000
7.5200E-001 5.4920E-001 0.0000E+000
0.0000E+000 5.8000E-001 5.7700E-002
7.8900E-002 5.6910E-001 5.5100E-002
1.4540E-001 5.7440E-001 6.2000E-002
2.9300E-001 5.7020E-001 5.5200E-002
4.5680E-001 5.6210E-001 5.8800E-002
6.4040E-001 5.5310E-001 4.9100E-002
7.0630E-001 5.4890E-001 3.9100E-002
7.5200E-001 5.4850E-001 3.9100E-002
0.0000E+000 5.5210E-001 9.9000E-002
7.8900E-002 5.4200E-001 1.0170E-001
1.4540E-001 5.3920E-001 1.0510E-001
2.9300E-001 5.3870E-001 8.6900E-002
4.5680E-001 5.3600E-001 8.7100E-002
6.4040E-001 5.3600E-001 7.8800E-002
7.0630E-001 5.3600E-001 7.3600E-002
7.5200E-001 5.3600E-001 6.5700E-002
0.0000E+000 4.9760E-001 1.2040E-001
7.8900E-002 4.9760E-001 1.2280E-001
1.4540E-001 4.9760E-001 1.1800E-001
2.9300E-001 5.0700E-001 1.0830E-001
4.5680E-001 4.8500E-001 1.0640E-001
6.4040E-001 5.2180E-001 9.7000E-002
7.0630E-001 5.2180E-001 9.3100E-002
7.5200E-001 5.2180E-001 8.5800E-002
0.0000E+000 4.5330E-001 1.3880E-001
7.8900E-002 4.5330E-001 1.3880E-001
1.4540E-001 4.5330E-001 1.3540E-001
2.9300E-001 4.7090E-001 1.2240E-001
4.5680E-001 4.7490E-001 1.2210E-001
6.4040E-001 4.9490E-001 1.0660E-001
7.0630E-001 4.9490E-001 1.0070E-001
7.5200E-001 4.9490E-001 9.7600E-002
0.0000E+000 4.4120E-001 1.8970E-001
7.8900E-002 4.4120E-001 1.8690E-001
1.4980E-001 4.4120E-001 1.8920E-001
3.0400E-001 4.5030E-001 1.8990E-001
4.6710E-001 4.5900E-001 1.9830E-001
6.5160E-001 4.8050E-001 1.9700E-001
7.0630E-001 4.8160E-001 1.9210E-001
7.5200E-001 4.7370E-001 2.8900E-001
0.0000E+000 4.2620E-001 2.7320E-001
9.3600E-002 4.2820E-001 2.7150E-001
1.6620E-001 4.3060E-001 2.7410E-001
3.2520E-001 4.3980E-001 2.7210E-001
4.7780E-001 4.5780E-001 2.8160E-001
6.6370E-001 4.6940E-001 2.8710E-001
7.1010E-001 4.7110E-001 2.8900E-001
9.4600E-001 4.7370E-001 2.8900E-001
0.0000E+000 4.2620E-001 2.7320E-001
9.3600E-002 4.2820E-001 2.7150E-001
1.6620E-001 4.3060E-001 2.7410E-001
3.2520E-001 4.3980E-001 2.7210E-001
4.7780E-001 4.4230E-001 2.8160E-001
6.6370E-001 4.3940E-001 2.8710E-001
7.1010E-001 4.3530E-001 2.8900E-001
1.0000E+000 4.0400E-001 2.8900E-001
0.0000E+000 4.1710E-001 3.1250E-001
9.3600E-002 4.2040E-001 3.1140E-001
1.6620E-001 4.2050E-001 3.1820E-001
3.2520E-001 4.2970E-001 3.2140E-001
4.7780E-001 4.3060E-001 3.3080E-001
6.6370E-001 4.3090E-001 3.3090E-001
7.1010E-001 4.2770E-001 3.3290E-001
1.0000E+000 4.0400E-001 3.2840E-001
0.0000E+000 3.7940E-001 3.6950E-001
8.9700E-002 3.9130E-001 3.6950E-001
2.0240E-001 4.0250E-001 3.6950E-001
3.2350E-001 4.0660E-001 3.6950E-001
4.7950E-001 4.0580E-001 3.7700E-001
6.5710E-001 4.0840E-001 3.7700E-001
7.4780E-001 4.0890E-001 3.7700E-001
9.9220E-001 3.8070E-001 3.7700E-001
4.4800E-002 3.6490E-001 4.9550E-001
1.3740E-001 3.6930E-001 4.9550E-001
2.4880E-001 3.8710E-001 4.9550E-001
3.6050E-001 3.9450E-001 4.9550E-001
4.9300E-001 4.0110E-001 5.0300E-001
6.7190E-001 4.0450E-001 5.2000E-001
7.5280E-001 4.0050E-001 5.2000E-001
9.8400E-001 4.0030E-001 5.2000E-001
1.5350E-001 3.5000E-001 7.3290E-001
2.3210E-001 3.6870E-001 7.3290E-001
3.1870E-001 3.7310E-001 7.3290E-001
4.4290E-001 3.8020E-001 7.3290E-001
5.3880E-001 3.8930E-001 7.3290E-001
6.8370E-001 3.8650E-001 7.3290E-001
7.6330E-001 3.8090E-001 7.3990E-001
9.6900E-001 3.8150E-001 7.3990E-001
2.8570E-001 3.3970E-001 9.8680E-001
3.4460E-001 3.4830E-001 9.8680E-001
4.1950E-001 3.5680E-001 9.8680E-001
5.1740E-001 3.6030E-001 9.8680E-001
5.7810E-001 3.6220E-001 9.8680E-001
7.2880E-001 3.6540E-001 9.8680E-001
7.7920E-001 3.6760E-001 9.8680E-001
9.4400E-001 3.5650E-001 9.8680E-001
3.8450E-001 3.2130E-001 1.1680E+000
4.2530E-001 3.2380E-001 1.1680E+000
4.8940E-001 3.3510E-001 1.1680E+000
5.7080E-001 3.3510E-001 1.1680E+000
6.2180E-001 3.3510E-001 1.1680E+000
7.4940E-001 3.3460E-001 1.1680E+000
7.9240E-001 3.3690E-001 1.1680E+000
9.3220E-001 3.4440E-001 1.1680E+000
4.6100E-001 3.0920E-001 1.3210E+000
4.9740E-001 3.2120E-001 1.3210E+000
5.4390E-001 3.2120E-001 1.3210E+000
6.1570E-001 3.2120E-001 1.3210E+000
6.6280E-001 3.2470E-001 1.3210E+000
7.6550E-001 3.2750E-001 1.3210E+000
7.9900E-001 3.2850E-001 1.3210E+000
9.2480E-001 3.2700E-001 1.3210E+000
5.1670E-001 3.0670E-001 1.4290E+000
5.3700E-001 3.1260E-001 1.4290E+000
5.7990E-001 3.1250E-001 1.4290E+000
6.4790E-001 3.1390E-001 1.4290E+000
6.8230E-001 3.1390E-001 1.4360E+000
7.7380E-001 3.1390E-001 1.4360E+000
8.0410E-001 3.1530E-001 1.4360E+000
9.1410E-001 3.0730E-001 1.4360E+000
ZONE T="Lower Wing"
I=10, J=13, K=1,F=POINT
DT=(SINGLE SINGLE SINGLE )
-1.4800E-001 1.7950E-001 0.0000E+000
-1.4800E-001 1.7950E-001 0.0000E+000
0.0000E+000 1.7540E-001 0.0000E+000
1.6400E-001 1.6630E-001 0.0000E+000
2.6690E-001 1.6010E-001 0.0000E+000
3.0810E-001 1.5540E-001 0.0000E+000
4.7830E-001 1.4380E-001 0.0000E+000
7.2300E-001 1.3760E-001 0.0000E+000
1.0000E+000 1.4180E-001 0.0000E+000
1.0000E+000 1.4180E-001 0.0000E+000
-1.4800E-001 1.9030E-001 6.6500E-002
-1.4800E-001 1.9030E-001 6.6500E-002
0.0000E+000 1.8370E-001 6.6500E-002
1.6400E-001 1.7380E-001 6.0700E-002
2.6690E-001 1.6560E-001 5.3600E-002
3.0810E-001 1.6070E-001 4.4800E-002
4.7830E-001 1.4750E-001 3.1400E-002
7.2300E-001 1.3990E-001 3.1400E-002
1.0000E+000 1.3850E-001 3.1400E-002
1.0000E+000 1.3850E-001 3.1400E-002
-1.4800E-001 1.6730E-001 1.1110E-001
-1.4800E-001 1.6730E-001 1.1110E-001
0.0000E+000 1.6010E-001 1.1110E-001
1.6400E-001 1.6010E-001 1.1110E-001
2.6690E-001 1.5240E-001 1.1110E-001
3.0810E-001 1.3650E-001 1.1580E-001
4.7830E-001 1.3630E-001 1.1580E-001
7.2300E-001 1.3280E-001 1.1580E-001
1.0000E+000 1.4140E-001 1.1580E-001
1.0000E+000 1.4140E-001 1.1580E-001
-1.4800E-001 1.6730E-001 1.1110E-001
-1.4800E-001 1.6730E-001 1.1110E-001
0.0000E+000 1.6010E-001 1.1110E-001
2.6200E-002 1.5030E-001 2.5630E-001
2.6690E-001 1.3660E-001 2.6100E-001
3.0810E-001 1.3760E-001 2.6100E-001
4.7830E-001 1.3670E-001 2.6100E-001
7.2300E-001 1.4400E-001 2.6100E-001
1.0000E+000 1.4580E-001 2.6100E-001
1.0000E+000 1.4580E-001 2.6100E-001
-1.4800E-001 3.9130E-001 2.1360E-001
-1.4800E-001 3.9130E-001 2.1360E-001
0.0000E+000 3.7810E-001 2.1360E-001
2.6200E-002 3.7490E-001 2.7950E-001
2.6690E-001 3.6940E-001 2.8300E-001
3.0810E-001 3.6940E-001 2.8300E-001
4.7830E-001 3.6940E-001 2.8300E-001
7.2300E-001 3.6990E-001 2.8300E-001
1.0000E+000 3.7850E-001 2.8300E-001
1.0000E+000 3.7850E-001 2.8300E-001
0.0000E+000 3.7810E-001 2.1360E-001
0.0000E+000 3.7810E-001 2.1360E-001
1.0000E-004 3.7490E-001 2.7950E-001
1.5670E-001 3.6400E-001 2.8300E-001
2.6690E-001 3.6940E-001 2.8300E-001
4.7830E-001 3.6940E-001 2.8300E-001
6.7380E-001 3.7410E-001 2.8300E-001
7.2300E-001 3.6990E-001 2.8300E-001
1.0000E+000 3.7850E-001 2.8300E-001
1.0000E+000 3.7850E-001 2.8300E-001
0.0000E+000 3.6150E-001 3.6950E-001
0.0000E+000 3.6150E-001 3.6950E-001
1.4050E-001 3.4330E-001 3.6950E-001
1.8260E-001 3.5170E-001 3.6950E-001
3.0810E-001 3.5220E-001 3.6950E-001
4.9760E-001 3.5060E-001 3.7700E-001
6.7380E-001 3.6370E-001 3.7700E-001
7.2300E-001 3.6510E-001 3.7700E-001
9.9250E-001 3.6120E-001 3.7700E-001
```

9.9220E-001 3.8070E-001 3.7700E-001
0.0000E+000 3.7940E-001 3.6950E-001
0 0000E-000 3 6150E-001 3.6950E-001
1.9360E-001 3.2130E-001 4.9550E-001
2.3490E-001 3.3340E-001 4.9550E-001
3.6270E-001 3.3590E-001 4.9550E-001
5 3510E-001 3.4560E-001 5.0300E-001
6.9170E-001 3.5810E-001 5.2000E-001
7.4320E-001 3.5590E-001 5.2000E-001
9.8700E-001 3.7920E-001 5.2000E-001
9 8400E-001 4 0030E-001 5.2000E-001
1.5350E-001 3.5000E-001 7.3290E-001
1.5630E-001 3.3800E-001 7.3290E-001
2.8130E-001 3.2300E-001 7.3290E-001
3 1660E-001 3.2560E-001 7.3290E-001
4.2750E-001 3.2590E-001 7.3290E-001
5.7880E-001 3.3360E-001 7.3290E-001
7.1090E-001 3.4210E-001 7.3290E-001
7 6650E-001 3.4080E-001 7.3990E-001
9.7350E-001 3.5100E-001 7.3990E-001
9.6900E-001 3.8150E-001 7.3990E-001
2.8570E-001 3.3970E-001 9.8680E-001
2.9650E-001 3.1770E-001 9.8680E-001
3.8250E-001 3.0670E-001 9.8680E-001
4.1110E-001 3.1250E-001 9.8680E-001
5.1450E-001 3.1190E-001 9.8680E-001
6.2350E-001 3.1460E-001 9.8680E-001
7.3320E-001 3.2510E-001 9.8680E-001
7.7970E-001 3.3120E-001 9.8680E-001
9.5910E-001 3.3860E-001 9.8680E-001
9.4400E-001 3.5650E-001 9.8680E-001
3.8450E-001 3.2130E-001 1.1680E+000
3.8300E-001 3.0330E-001 1.1680E+000
4.5480E-001 2.9060E-001 1.1680E+000
4.7640E-001 2.9700E-001 1.1680E+000
5.7750E-001 2.9520E-001 1.1680E+000
6.4990E-001 2.9500E-001 1.1680E+000
7.4500E-001 2.9780E-001 1.1680E+000
7.9600E-001 3.0450E-001 1.1680E+000
9.3510E-001 3.2800E-001 1.1680E+000
9.3220E-001 3.4440E-001 1.1680E+000
4.6100E-001 3.0920E-001 1.3210E+000
4.7400E-001 2.9130E-001 1.3210E+000
5.2610E-001 2.9280E-001 1.3210E+000
5.4320E-001 2.9010E-001 1.3210E+000
6.2810E-001 2.8690E-001 1.3210E+000
6.8230E-001 2.9050E-001 1.3210E+000
7.6130E-001 2.9620E-001 1.3210E+000
8.0730E-001 3.0010E-001 1.3210E+000
9.2530E-001 3.0940E-001 1.3210E+000
9.2480E-001 3 2700E-001 1.3210E+000
5.1670E-001 3.0670E-001 1.4290E+000
5.2030E-001 2.9060E-001 1.4290E+000
5.5460E-001 2.8660E-001 1.4290E+000
5.8780E-001 2.8550E-001 1.4290E+000
6.4990E-001 2.8420E-001 1.4290E+000
7.0370E-001 2.8030E-001 1.4360E+000
7.7480E-001 2.8620E-001 1.4360E+000
7.9920E-001 2.9010E-001 1.4360E+000
9 1970E-001 2.9080E-001 1.4360E+000
9.1410E-001 3.0730E-001 1.4360E+000
ZONE T="Mirror of Upper surface"
I=8, J=16, K=1,F=POINT
DT=(SINGLE SINGLE SINGLE)
0.0000E+000 5.7730E-001 0.0000E+000
7.8900E-002 5.7660E-001 0.0000E+000
1.4540E-001 5.8170E-001 0 0000E+000
2.9300E-001 5.7750E-001 0.0000E+000
4.5680E-001 5.6850E-001 0.0000E+000
6.4040E-001 5.5970E-001 0.0000E+000
7.0630E-001 5.5210E-001 0.0000E+000
7.5200E-001 5.4920E-001 0.0000E+000
0.0000E+000 5.8000E-001 -5.7700E-002
7 8900E-002 5.6910E-001 -5 5100E-002
1.4540E-001 5.7440E-001 -6.2000E-002
2.9300E-001 5.7020E-001 -5.5200E-002
4.5680E-001 5.6210E-001 -5.8800E-002
6 4040E-001 5.5310E-001 -4.9100E-002
7.0630E-001 5.4890E-001 -3.9100E-002
7.5200E-001 5.4850E-001 -3.9100E-002
0.0000E+000 5.5210E-001 -9.9000E-002
7 8900E-002 5.4200E-001 -1.0170E-001
1.4540E-001 5.3920E-001 -1.0510E-001
2.9300E-001 5.3870E-001 -8.6900E-002
4.5680E-001 5.3600E-001 -8.7100E-002
6.4040E-001 5.3600E-001 -7.8800E-002
7.0630E-001 5.3600E-001 -7.3600E-002
7.5200E-001 5.3600E-001 -6.5700E-002
0.0000E+000 4.9760E-001 -1.2040E-001
7.8900E-002 4.9760E-001 -1.2280E-001
1.4540E-001 4.9760E-001 -1.1800E-001
2.9300E-001 5.0700E-001 -1.0830E-001
4.5680E-001 4.8500E-001 -1.0640E-001
6.4040E-001 5.2180E-001 -9.7000E-002
7.0630E-001 5.2180E-001 -9.3100E-002
7.5200E-001 5.2180E-001 -8.5800E-002
0.0000E+000 4.5330E-001 -1.3880E-001
7.8900E-002 4.5330E-001 -1.3880E-001
1.4540E-001 4.5330E-001 -1.3540E-001
2.9300E-001 4.7090E-001 -1.2240E-001
4.5680E-001 4.7490E-001 -1.2210E-001
6.4040E-001 4.9490E-001 -1.0660E-001
7.0630E-001 4.9490E-001 -1.0070E-001
7.5200E-001 4.9490E-001 -9.7600E-002
0.0000E+000 4.4120E-001 -1.8970E-001
7.8900E-002 4.4120E-001 -1.8690E-001
1.4980E-001 4.4120E-001 -1.8920E-001
3.0400E-001 4.5030E-001 -1.8990E-001
4.6710E-001 4.5900E-001 -1.9830E-001
6.5160E-001 4.8050E-001 -1.9700E-001
7.0630E-001 4.8160E-001 -1.9210E-001
7.5200E-001 4.7370E-001 -2.8900E-001
0.0000E+000 4.2620E-001 -2.7320E-001
9.3600E-002 4.2820E-001 -2.7150E-001
1.6620E-001 4.3060E-001 -2.7410E-001
3.2520E-001 4.3980E-001 -2.7210E-001
4.7780E-001 4.5780E-001 -2.8160E-001
6.6370E-001 4.6940E-001 -2.8710E-001
7.1010E-001 4.7110E-001 -2.8900E-001
9.4600E-001 4.7370E-001 -2.8900E-001
0.0000E+000 4.2620E-001 -2.7320E-001
9 3600E-002 4.2820E-001 -2.7150E-001
1.6620E-001 4.3060E-001 -2.7410E-001
3.2520E-001 4.3980E-001 -2.7210E-001
4.7780E-001 4.4230E-001 -2.8160E-001
6.6370E-001 4.3940E-001 -2.8710E-001
7.1010E-001 4 3530E-001 -2.8900E-001
1.0000E+000 4.0400E-001 -2.8900E-001
0.0000E+000 4.1710E-001 -3.1250E-001
9.3600E-002 4.2040E-001 -3.1140E-001
1 6620E-001 4.2050E-001 -3.1820E-001
3.2520E-001 4.2970E-001 -3.2140E-001
4.7780E-001 4.3060E-001 -3.3080E-001
6.6370E-001 4.3090E-001 -3.3090E-001
7.1010E-001 4.2770E-001 -3.3290E-001
1.0000E+000 4.0400E-001 -3.2840E-001
0.0000E+000 3.7940E-001 -3.6950E-001
8.9700E-002 3.9130E-001 -3.6950E-001
2.0240E-001 4.0250E-001 -3.6950E-001
3.2350E-001 4.0660E-001 -3.6950E-001
4.7950E-001 4.0580E-001 -3.7700E-001
6.5710E-001 4.0840E-001 -3.7700E-001
7.4780E-001 4.0890E-001 -3.7700E-001
9.9220E-001 3.8070E-001 -3.7700E-001
4 4800E-002 3 6490E-001 -4 9550E-001
1.3740E-001 3.6930E-001 -4.9550E-001
2.4880E-001 3.8710E-001 -4.9550E-001
3.6050E-001 3.9450E-001 -4.9550E-001
4.9300E-001 4.0110E-001 -5 0300E-001
6.7190E-001 4.0450E-001 -5.2000E-001
7.5280E-001 4.0050E-001 -5.2000E-001
9.8400E-001 4.0030E-001 -5.2000E-001
1.5350E-001 3.5000E-001 -7.3290E-001
2.3210E-001 3.6870E-001 -7.3290E-001
3.1870E-001 3.7310E-001 -7.3290E-001
4.4290E-001 3.8020E-001 -7.3290E-001
5.3880E-001 3.8930E-001 -7.3290E-001
6.8370E-001 3.8650E-001 -7.3290E-001
7.6330E-001 3.8090E-001 -7.3990E-001
9.6900E-001 3.8150E-001 -7.3990E-001
2.8570E-001 3.3970E-001 -9.8680E-001
3.4460E-001 3.4830E-001 -9.8680E-001
4.1950E-001 3.5680E-001 -9.8680E-001
5.1740E-001 3.6030E-001 -9.8680E-001
5.7810E-001 3.6220E-001 -9.8680E-001
7.2880E-001 3.6540E-001 -9.8680E-001
7.7920E-001 3.6760E-001 -9.8680E-001
9.4400E-001 3.5650E-001 -9.8680E-001
3.8450E-001 3.2130E-001 -1.1680E+000
4.2530E-001 3.2380E-001 -1.1680E+000
4.8940E-001 3.3510E-001 -1.1680E+000
5.7080E-001 3.3510E-001 -1.1680E+000
6.2180E-001 3.3510E-001 -1.1680E+000
7.4940E-001 3.3460E-001 -1.1680E+000
7.9240E-001 3.3690E-001 -1.1680E+000
9.3220E-001 3.4440E-001 -1.1680E+000
4.6100E-001 3.0920E-001 -1.3210E+000
4.9740E-001 3.2120E-001 -1.3210E+000
5.4390E-001 3.2120E-001 -1.3210E+000
6.1570E-001 3.2120E-001 -1.3210E+000
6.6280E-001 3 2470E-001 -1 3210E+000
7.6550E-001 3.2750E-001 -1.3210E+000
7.9900E-001 3.2850E-001 -1.3210E+000
9.2480E-001 3.2700E-001 -1.3210E+000
5.1670E-001 3.0670E-001 -1.4290E+000
5.3700E-001 3.1260E-001 -1.4290E+000
5.7990E-001 3.1250E-001 -1.4290E+000
6.4790E-001 3.1390E-001 -1.4290E+000
6.8230E-001 3.1390E-001 -1.4360E+000
7.7380E-001 3.1390E-001 -1.4360E+000
8.0410E-001 3.1530E-001 -1.4360E+000
9.1410E-001 3.0730E-001 -1.4360E+000
ZONE T="Mirror of Lower surface"
I=10, J=13, K=1,F=POINT
DT=(SINGLE SINGLE SINGLE)
-1.4800E-001 1.7950E-001 0.0000E+000
-1.4800E-001 1.7950E-001 0 0000E+000
0.0000E+000 1.7540E-001 0.0000E+000
1.6400E-001 1.6630E-001 0.0000E+000
2.6690E-001 1.6010E-001 0.0000E+000
3.0810E-001 1.5540E-001 0.0000E+000
4.7830E-001 1.4380E-001 0 0000E+000
7.2300E-001 1.3760E-001 0.0000E+000
1.0000E+000 1.4180E-001 0.0000E+000
1.0000E+000 1.4180E-001 0.0000E+000
-1.4800E-001 1.9030E-001 -6.6500E-002
-1.4800E-001 1.9030E-001 -6.6500E-002
0.0000E+000 1.8370E-001 -6.6500E-002
1.6400E-001 1.7380E-001 -6 0700E-002
2.6690E-001 1.6560E-001 -5.3600E-002
3.0810E-001 1.6070E-001 -4.4800E-002
4.7830E-001 1.4750E-001 -3.1400E-002
7.2300E-001 1.3990E-001 -3 1400E-002

1.0000E+000 1.3850E-001 -3.1400E-002
1.0000E+000 1.3850E-001 -3.1400E-002
-1.4800E-001 1.6730E-001 -1.1110E-001
-1.4800E-001 1.6730E-001 -1.1110E-001
0.0000E+000 1.6010E-001 -1.1110E-001
1.6400E-001 1.6010E-001 -1.1110E-001
2.6690E-001 1.5240E-001 -1.1110E-001
3.0810E-001 1.3650E-001 -1.1580E-001
4.7830E-001 1.3630E-001 -1.1580E-001
7.2300E-001 1.3280E-001 -1.1580E-001
1.0000E+000 1.4140E-001 -1.1580E-001
1.0000E+000 1.4140E-001 -1.1580E-001
-1.4800E-001 1.6730E-001 -1.1110E-001
-1.4800E-001 1.6730E-001 -1.1110E-001
0.0000E+000 1.6010E-001 -1.1110E-001
2.6200E-002 1.5030E-001 -2.5630E-001
2.6690E-001 1.3660E-001 -2.6100E-001
3.0810E-001 1.3760E-001 -2.6100E-001
4.7830E-001 1.3670E-001 -2.6100E-001
7.2300E-001 1.4400E-001 -2.6100E-001
1.0000E+000 1.4580E-001 -2.6100E-001
1.0000E+000 1.4580E-001 -2.6100E-001
-1.4800E-001 3.9130E-001 -2.1360E-001
-1.4800E-001 3.9130E-001 -2.1360E-001
0.0000E+000 3.7810E-001 -2.1360E-001
2.6200E-002 3.7490E-001 -2.7950E-001
2.6690E-001 3.6940E-001 -2.8300E-001
3.0810E-001 3.6940E-001 -2.8300E-001
4.7830E-001 3.6940E-001 -2.8300E-001
7.2300E-001 3.6990E-001 -2.8300E-001
1.0000E+000 3.7850E-001 -2.8300E-001
1.0000E+000 3.7850E-001 -2.8300E-001
0.0000E+000 3.7810E-001 -2.1360E-001
0.0000E+000 3.7810E-001 -2.1360E-001
1.0000E-004 3.7490E-001 -2.7950E-001
1.5670E-001 3.6400E-001 -2.8300E-001
2.6690E-001 3.6940E-001 -2.8300E-001
4.7830E-001 3.6940E-001 -2.8300E-001
6.7380E-001 3.7410E-001 -2.8300E-001
7.2300E-001 3.6990E-001 -2.8300E-001
1.0000E+000 3.7850E-001 -2.8300E-001
1.0000E+000 3.7850E-001 -2.8300E-001
0.0000E+000 3.6150E-001 -3.6950E-001
0.0000E+000 3.6150E-001 -3.6950E-001
1.4050E-001 3.4330E-001 -3.6950E-001
1.8260E-001 3.5170E-001 -3.6950E-001
3.0810E-001 3.5220E-001 -3.6950E-001
4.9760E-001 3.5060E-001 -3.7700E-001
6.7380E-001 3.6370E-001 -3.7700E-001
7.2300E-001 3.6510E-001 -3.7700E-001
9.9250E-001 3.6120E-001 -3.7700E-001
9.9220E-001 3.8070E-001 -3.7700E-001
0.0000E+000 3.7940E-001 -3.6950E-001
0.0000E+000 3.6150E-001 -3.6950E-001
1.9360E-001 3.2130E-001 -4.9550E-001
2.3490E-001 3.3340E-001 -4.9550E-001
3.6270E-001 3.3590E-001 -4.9550E-001
5.3510E-001 3.4560E-001 -5.0300E-001
6.9170E-001 3.5810E-001 -5.2000E-001
7.4320E-001 3.5590E-001 -5.2000E-001
9.8700E-001 3.7920E-001 -5.2000E-001
9.8400E-001 4.0030E-001 -5.2000E-001
1.5350E-001 3.5000E-001 -7.3290E-001
1.5630E-001 3.3800E-001 -7.3290E-001
2.8130E-001 3.2300E-001 -7.3290E-001
3.1660E-001 3.2560E-001 -7.3290E-001
4.2750E-001 3.2590E-001 -7.3290E-001
5.7880E-001 3.3360E-001 -7.3290E-001
7.1090E-001 3.4210E-001 -7.3290E-001
7.6650E-001 3.4080E-001 -7.3990E-001
9.7350E-001 3.5100E-001 -7.3990E-001
9.6900E-001 3.8150E-001 -7.3990E-001
2.8570E-001 3.3970E-001 -9.8680E-001
2.9650E-001 3.1770E-001 -9.8680E-001
3.8250E-001 3.0670E-001 -9.8680E-001
4.1110E-001 3.1250E-001 -9.8680E-001
5.1450E-001 3.1190E-001 -9.8680E-001
6.2350E-001 3.1460E-001 -9.8680E-001
7.3320E-001 3.2510E-001 -9.8680E-001
7.7970E-001 3.3120E-001 -9.8680E-001
9.5910E-001 3.3860E-001 -9.8680E-001
9.4400E-001 3.5650E-001 -9.8680E-001
3.8450E-001 3.2130E-001 -1.1680E+000
3.8300E-001 3.0330E-001 -1.1680E+000
4.5480E-001 2.9060E-001 -1.1680E+000
4.7640E-001 2.9700E-001 -1.1680E+000
5.7750E-001 2.9520E-001 -1.1680E+000
6.4990E-001 2.9500E-001 -1.1680E+000
7.4500E-001 2.9780E-001 -1.1680E+000
7.9600E-001 3.0450E-001 -1.1680E+000
9.3510E-001 3.2800E-001 -1.1680E+000
9.3220E-001 3.4440E-001 -1.1680E+000
4.6100E-001 3.0920E-001 -1.3210E+000
4.7400E-001 2.9130E-001 -1.3210E+000
5.2610E-001 2.9280E-001 -1.3210E+000
5.4320E-001 2.9010E-001 -1.3210E+000
6.2810E-001 2.8690E-001 -1.3210E+000
6.8230E-001 2.9050E-001 -1.3210E+000
7.6130E-001 2.9620E-001 -1.3210E+000
8.0730E-001 3.0010E-001 -1.3210E+000
9.2530E-001 3.0940E-001 -1.3210E+000
9.2480E-001 3.2700E-001 -1.3210E+000
5.1670E-001 3.0670E-001 -1.4290E+000
5.2030E-001 2.9060E-001 -1.4290E+000
5.5460E-001 2.8660E-001 -1.4290E+000
5.8780E-001 2.8550E-001 -1.4290E+000
6.4990E-001 2.8420E-001 -1.4290E+000
7.0370E-001 2.8030E-001 -1.4360E+000
7.7480E-001 2.8620E-001 -1.4360E+000
7.9920E-001 2.9010E-001 -1.4360E+000
9.1970E-001 2.9080E-001 -1.4360E+000
9.1410E-001 3.0730E-001 -1.4360E+000

E.2 Stores

TITLE = "CF-18"
VARIABLES = "Z"
"X"
"Y"
ZONE T="PylonIn"
I=10, J=14, K=1,F=POINT
DT=(SINGLE SINGLE SINGLE)
-1.0014E-009 2.2690E-001 6.1050E-001
5.5481E-002 2.2690E-001 6.1050E-001
9.2631E-002 2.2690E-001 6.1050E-001
2.1019E-001 2.2690E-001 6.1050E-001
3.2384E-001 2.2690E-001 6.1050E-001
4.8967E-001 2.2690E-001 6.1050E-001
6.2654E-001 2.2690E-001 6.1050E-001
6.6773E-001 2.2690E-001 6.1050E-001
7.5571E-001 2.2690E-001 6.1050E-001
7.6744E-001 2.2690E-001 6.1050E-001
-1.0014E-009 2.2690E-001 6.1050E-001
5.5481E-002 2.6918E-001 5.9345E-001
9.2631E-002 2.9705E-001 5.9284E-001
2.1019E-001 2.9705E-001 5.9278E-001
3.2384E-001 2.9705E-001 5.9327E-001
4.8967E-001 2.9705E-001 5.9339E-001
6.2654E-001 2.9705E-001 5.9339E-001
6.6773E-001 2.9705E-001 5.9339E-001
7.5571E-001 2.6918E-001 5.9388E-001
7.6744E-001 2.2690E-001 6.1050E-001
-1.0014E-009 2.2690E-001 6.1050E-001
5.5481E-002 2.6918E-001 5.9345E-001
9.2631E-002 2.9705E-001 5.9284E-001
2.1019E-001 2.9705E-001 5.9278E-001
3.2384E-001 2.9705E-001 5.9327E-001
4.8967E-001 2.9705E-001 5.9339E-001
6.2654E-001 2.9705E-001 5.9339E-001
6.6773E-001 2.9705E-001 5.9339E-001
7.5571E-001 2.6918E-001 5.9388E-001
7.6744E-001 2.2690E-001 6.1050E-001
-1.0014E-009 2.2690E-001 6.1050E-001
5.5481E-002 2.6918E-001 5.9345E-001
9.2631E-002 2.9705E-001 5.9284E-001
2.1019E-001 2.9705E-001 5.9278E-001
3.2384E-001 3.1501E-001 5.9327E-001
4.8967E-001 3.6768E-001 5.9339E-001
6.2654E-001 3.6462E-001 5.9339E-001
6.6773E-001 3.6438E-001 5.9339E-001
7.5571E-001 2.6918E-001 5.9388E-001
7.6744E-001 2.2690E-001 6.1050E-001
-1.0014E-009 2.2690E-001 6.1050E-001
5.5481E-002 2.6918E-001 6.1050E-001
9.2631E-002 2.9705E-001 6.1050E-001
2.1019E-001 2.9705E-001 6.1050E-001
3.2384E-001 3.7501E-001 6.1050E-001
4.8967E-001 3.6768E-001 6.1050E-001
6.2654E-001 3.6462E-001 6.1050E-001
6.6773E-001 3.6438E-001 6.1050E-001
7.5571E-001 2.6918E-001 6.1050E-001
7.6744E-001 2.2690E-001 6.1050E-001
-1.0014E-009 2.2690E-001 6.1050E-001
5.5481E-002 2.2690E-001 6.1050E-001
9.2631E-002 2.2690E-001 6.1050E-001
2.1019E-001 2.2690E-001 6.1050E-001
3.2384E-001 2.2690E-001 6.1050E-001
4.8967E-001 2.2690E-001 6.1050E-001
6.2654E-001 2.2690E-001 6.1050E-001
6.6773E-001 2.2690E-001 6.1050E-001
7.5571E-001 2.2690E-001 6.1050E-001
7.6744E-001 2.2690E-001 6.1050E-001
-1.0014E-009 2.2690E-001 6.1050E-001
5.5481E-002 2.2690E-001 6.2755E-001
9.2631E-002 2.2690E-001 6.2816E-001
2.1019E-001 2.2690E-001 6.2822E-001
3.2384E-001 2.2690E-001 6.2773E-001
4.8967E-001 2.2690E-001 6.2761E-001
6.2654E-001 2.2690E-001 6.2761E-001
6.6773E-001 2.2690E-001 6.2761E-001
7.5571E-001 2.2690E-001 6.2712E-001

7.6744E-001 2.2690E-001 6.1050E-001
-1.0014E-009 2.2690E-001 6.1050E-001
5.5481E-002 2.6918E-001 6.2755E-001
9.2631E-002 2.6918E-001 6.2816E-001
2.1019E-001 2.6918E-001 6.2822E-001
3.2384E-001 2.6918E-001 6.2773E-001
4.8967E-001 2.6918E-001 6.2761E-001
6.2654E-001 2.6918E-001 6.2761E-001
6.6773E-001 2.6918E-001 6.2761E-001
7.5571E-001 2.6918E-001 6.2712E-001
7.6744E-001 2.2690E-001 6.1050E-001
-1.0014E-009 2.2690E-001 6.1050E-001
5.5481E-002 2.6918E-001 6.2755E-001
9.2631E-002 2.9705E-001 6.2816E-001
2.1019E-001 2.9705E-001 6.2822E-001
3.2384E-001 2.9705E-001 6.2773E-001
4.8967E-001 2.9705E-001 6.2761E-001
6.2654E-001 2.9705E-001 6.2761E-001
6.6773E-001 2.9705E-001 6.2761E-001
7.5571E-001 2.6918E-001 6.2712E-001
7.6744E-001 2.2690E-001 6.1050E-001
-1.0014E-009 2.2690E-001 6.1050E-001
5.5481E-002 2.6918E-001 6.2755E-001
9.2631E-002 2.9705E-001 6.2816E-001
2.1019E-001 2.9705E-001 6.2822E-001
3.2384E-001 3.3126E-001 6.2773E-001
4.8967E-001 3.3126E-001 6.2761E-001
6.2654E-001 3.3126E-001 6.2761E-001
6.6773E-001 3.3126E-001 6.2761E-001
7.5571E-001 2.6918E-001 6.2712E-001
7.6744E-001 2.2690E-001 6.1050E-001
-1.0014E-009 2.2690E-001 6.1050E-001
5.5481E-002 2.6918E-001 6.2755E-001
9.2631E-002 2.9705E-001 6.2816E-001
2.1019E-001 2.9705E-001 6.2822E-001
3.2384E-001 3.7501E-001 6.2773E-001
4.8967E-001 3.6768E-001 6.2761E-001
6.2654E-001 3.6462E-001 6.2761E-001
6.6773E-001 3.6438E-001 6.2761E-001
7.5571E-001 2.6918E-001 6.2712E-001
7.6744E-001 2.2690E-001 6.1050E-001
-1.0014E-009 2.2690E-001 6.1050E-001
5.5481E-002 2.6918E-001 6.1050E-001
9.2631E-002 2.9705E-001 6.1050E-001
2.1019E-001 2.9705E-001 6.1050E-001
3.2384E-001 3.7501E-001 6.1050E-001
4.8967E-001 3.6768E-001 6.1050E-001
6.2654E-001 3.6462E-001 6.1050E-001
6.6773E-001 3.6438E-001 6.1050E-001
7.5571E-001 2.6918E-001 6.1050E-001
7.6744E-001 2.2690E-001 6.1050E-001
ZONE T="PylonOut"
I=10, J=14, K=1,F=POINT
DT=(SINGLE SINGLE SINGLE)
9.0000E-002 1.8000E-001 9.1580E-001
1.4548E-001 1.8000E-001 9.1580E-001
1.8263E-001 1.8000E-001 9.1580E-001
3.0019E-001 1.8000E-001 9.1580E-001
4.1384E-001 1.8000E-001 9.1580E-001
5.7967E-001 1.8000E-001 9.1580E-001
7.1654E-001 1.8000E-001 9.1580E-001
7.5773E-001 1.8000E-001 9.1580E-001
8.4571E-001 1.8000E-001 9.1580E-001
8.5744E-001 1.8000E-001 9.1580E-001
9.0000E-002 1.8000E-001 9.1580E-001
1.4548E-001 1.8000E-001 8.9875E-001
1.8263E-001 1.8000E-001 8.9814E-001
3.0019E-001 1.8000E-001 8.9808E-001
4.1384E-001 1.8000E-001 8.9857E-001
5.7967E-001 1.8000E-001 8.9869E-001
7.1654E-001 1.8000E-001 8.9869E-001
7.5773E-001 1.8000E-001 8.9869E-001
8.4571E-001 1.8000E-001 8.9918E-001
8.5744E-001 1.8000E-001 9.1580E-001
9.0000E-002 1.8000E-001 9.1580E-001
1.4548E-001 2.2228E-001 8.9875E-001
1.8263E-001 2.5015E-001 8.9814E-001
3.0019E-001 2.5015E-001 8.9808E-001
4.1384E-001 2.5015E-001 8.9857E-001
5.7967E-001 2.5015E-001 8.9869E-001
7.1654E-001 2.5015E-001 8.9869E-001
7.5773E-001 2.5015E-001 8.9869E-001
8.4571E-001 2.2228E-001 8.9918E-001
8.5744E-001 1.8000E-001 9.1580E-001
9.0000E-002 1.8000E-001 9.1580E-001
1.4548E-001 2.2228E-001 8.9875E-001
1.8263E-001 2.5015E-001 8.9814E-001
3.0019E-001 2.5015E-001 8.9808E-001
4.1384E-001 2.8436E-001 8.9857E-001
5.7967E-001 2.8436E-001 8.9869E-001
7.1654E-001 2.8436E-001 8.9869E-001
7.5773E-001 2.8436E-001 8.9869E-001
8.4571E-001 2.2228E-001 8.9918E-001
8.5744E-001 1.8000E-001 9.1580E-001
9.0000E-002 1.8000E-001 9.1580E-001
1.4548E-001 2.2228E-001 8.9875E-001
1.8263E-001 2.5015E-001 8.9814E-001
3.0019E-001 2.5015E-001 8.9808E-001
4.1384E-001 2.8111E-001 8.9857E-001
5.7967E-001 3.2078E-001 8.9869E-001
7.1654E-001 3.1772E-001 8.9869E-001
7.5773E-001 3.1748E-001 8.9869E-001
8.4571E-001 2.2228E-001 8.9918E-001
8.5744E-001 1.8000E-001 9.1580E-001
9.0000E-002 1.8000E-001 9.1580E-001
1.4548E-001 2.2228E-001 9.1580E-001
1.8263E-001 2.5015E-001 9.1580E-001
3.0019E-001 2.5015E-001 9.1580E-001
4.1384E-001 3.2811E-001 9.1580E-001
5.7967E-001 3.2078E-001 9.1580E-001
7.1654E-001 3.1772E-001 9.1580E-001
7.5773E-001 3.1748E-001 9.1580E-001
8.4571E-001 2.2228E-001 9.1580E-001
8.5744E-001 1.8000E-001 9.1580E-001
ZONE T="EFT"
I=22, J=20, K=1,F=POINT
DT=(SINGLE SINGLE SINGLE)
-1.5000E-001 1.4500E-001 6.1050E-001
-1.2924E-001 1.6515E-001 6.1050E-001
-1.0031E-001 1.7809E-001 6.1050E-001
-5.1832E-002 1.9585E-001 6.1050E-001
9.3407E-003 2.0849E-001 6.1050E-001
5.7204E-002 2.1484E-001 6.1050E-001
1.2656E-001 2.2058E-001 6.1050E-001
2.0263E-001 2.2437E-001 6.1050E-001
2.6954E-001 2.2522E-001 6.1050E-001
3.7576E-001 2.2546E-001 6.1050E-001
4.6685E-001 2.2571E-001 6.1050E-001
5.1813E-001 2.2504E-001 6.1050E-001
5.9762E-001 2.2479E-001 6.1050E-001
6.5965E-001 2.2192E-001 6.1050E-001
7.1007E-001 2.1869E-001 6.1050E-001
7.5354E-001 2.1191E-001 6.1050E-001

7.9188E-001 2.0288E-001 6.1050E-001 9.2009E-001 1.4500E-001 6.1050E-001 9.3407E-003 1.8990E-001 6.5540E-001
8.3669E-001 1.9353E-001 6.1050E-001 -1.5000E-001 1.4500E-001 6.1050E-001 5.7204E-002 1.9439E-001 6.5989E-001
8.6245E-001 1.8206E-001 6.1050E-001 -1.2924E-001 1.4500E-001 5.9035E-001 1.2656E-001 1.9844E-001 6.6394E-001
8.9249E-001 1.7284E-001 6.1050E-001 -1.0031E-001 1.4500E-001 5.7741E-001 2.0263E-001 2.0112E-001 6.6662E-001
9.0653E-001 1.6472E-001 6.1050E-001 -5.1832E-002 1.4500E-001 5.5965E-001 2.6954E-001 2.0172E-001 6.6722E-001
9.2009E-001 1.4500E-001 6.1050E-001 9.3407E-003 1.4500E-001 5.4701E-001 3.7576E-001 2.0190E-001 6.6740E-001
-1.5000E-001 1.4500E-001 6.1050E-001 5.7204E-002 1.4500E-001 5.4066E-001 4.6685E-001 2.0207E-001 6.6757E-001
-1.2924E-001 1.6361E-001 6.0279E-001 1.2656E-001 1.4500E-001 5.3492E-001 5.1813E-001 2.0159E-001 6.6709E-001
-1.0031E-001 1.7557E-001 5.9784E-001 2.0263E-001 1.4500E-001 5.3113E-001 5.9762E-001 2.0142E-001 6.6692E-001
-5.1832E-002 1.9198E-001 5.9104E-001 2.6954E-001 1.4500E-001 5.3028E-001 6.5965E-001 1.9939E-001 6.6489E-001
9.3407E-003 2.0366E-001 5.8620E-001 3.7576E-001 1.4500E-001 5.3004E-001 7.1007E-001 1.9711E-001 6.6260E-001
5.7204E-002 2.0953E-001 5.8377E-001 4.6685E-001 1.4500E-001 5.2979E-001 7.5354E-001 1.9231E-001 6.5781E-001
1.2656E-001 2.1483E-001 5.8158E-001 5.1813E-001 1.4500E-001 5.3046E-001 7.9188E-001 1.8592E-001 6.5142E-001
2.0263E-001 2.1832E-001 5.8013E-001 5.9762E-001 1.4500E-001 5.3071E-001 8.3669E-001 1.7932E-001 6.4482E-001
2.6954E-001 2.1911E-001 5.7980E-001 6.5965E-001 1.4500E-001 5.3358E-001 8.6245E-001 1.7120E-001 6.3670E-001
3.7576E-001 2.1934E-001 5.7971E-001 7.1007E-001 1.4500E-001 5.3681E-001 8.9249E-001 1.6468E-001 6.3019E-001
4.6685E-001 2.1956E-001 5.7961E-001 7.5354E-001 1.4500E-001 5.4359E-001 9.0653E-001 1.5894E-001 6.2444E-001
5.1813E-001 2.1894E-001 5.7987E-001 7.9188E-001 1.4500E-001 5.5262E-001 9.2009E-001 1.4500E-001 6.1050E-001
5.9762E-001 2.1872E-001 5.7997E-001 8.3669E-001 1.4500E-001 5.6197E-001 -1.5000E-001 1.4500E-001 6.1050E-001
6.5965E-001 2.1607E-001 5.8106E-001 8.6245E-001 1.4500E-001 5.7344E-001 -1.2924E-001 1.5271E-001 6.2911E-001
7.1007E-001 2.1308E-001 5.8230E-001 8.9249E-001 1.4500E-001 5.8266E-001 -1.0031E-001 1.5766E-001 6.4107E-001
7.5354E-001 2.0682E-001 5.8489E-001 9.0653E-001 1.4500E-001 5.9078E-001 -5.1832E-002 1.6446E-001 6.5748E-001
7.9188E-001 1.9847E-001 5.8835E-001 9.2009E-001 1.4500E-001 6.1050E-001 9.3407E-003 1.6930E-001 6.6916E-001
8.3669E-001 1.8984E-001 5.9193E-001 -1.5000E-001 1.4500E-001 6.1050E-001 5.7204E-002 1.7173E-001 6.7503E-001
8.6245E-001 1.7924E-001 5.9632E-001 -1.2924E-001 1.6515E-001 6.1050E-001 1.2656E-001 1.7392E-001 6.8033E-001
8.9249E-001 1.7072E-001 5.9985E-001 -1.0031E-001 1.7809E-001 6.1050E-001 2.0263E-001 1.7537E-001 6.8382E-001
9.0653E-001 1.6322E-001 6.0295E-001 -5.1832E-002 1.9585E-001 6.1050E-001 2.6954E-001 1.7570E-001 6.8461E-001
9.2009E-001 1.4500E-001 6.1050E-001 9.3407E-003 2.0849E-001 6.1050E-001 3.7576E-001 1.7579E-001 6.8484E-001
-1.5000E-001 1.4500E-001 6.1050E-001 5.7204E-002 2.1484E-001 6.1050E-001 4.6685E-001 1.7589E-001 6.8506E-001
-1.2924E-001 1.5925E-001 5.9625E-001 1.2656E-001 2.2058E-001 6.1050E-001 5.1813E-001 1.7563E-001 6.8444E-001
-1.0031E-001 1.6840E-001 5.8710E-001 2.0263E-001 2.2437E-001 6.1050E-001 5.9762E-001 1.7553E-001 6.8422E-001
-5.1832E-002 1.8096E-001 5.7454E-001 2.6954E-001 2.2522E-001 6.1050E-001 6.5965E-001 1.7444E-001 6.8157E-001
9.3407E-003 1.8990E-001 5.6560E-001 3.7576E-001 2.2546E-001 6.1050E-001 7.1007E-001 1.7320E-001 6.7858E-001
5.7204E-002 1.9439E-001 5.6111E-001 4.6685E-001 2.2571E-001 6.1050E-001 7.5354E-001 1.7061E-001 6.7232E-001
1.2656E-001 1.9844E-001 5.5706E-001 5.1813E-001 2.2504E-001 6.1050E-001 7.9188E-001 1.6715E-001 6.6397E-001
2.0263E-001 2.0112E-001 5.5438E-001 5.9762E-001 2.2479E-001 6.1050E-001 8.3669E-001 1.6357E-001 6.5534E-001
2.6954E-001 2.0172E-001 5.5378E-001 6.5965E-001 2.2192E-001 6.1050E-001 8.6245E-001 1.5918E-001 6.4474E-001
3.7576E-001 2.0190E-001 5.5360E-001 7.1007E-001 2.1869E-001 6.1050E-001 8.9249E-001 1.5565E-001 6.3622E-001
4.6685E-001 2.0207E-001 5.5343E-001 7.5354E-001 2.1191E-001 6.1050E-001 9.0653E-001 1.5255E-001 6.2872E-001
5.1813E-001 2.0159E-001 5.5391E-001 7.9188E-001 2.0288E-001 6.1050E-001 9.2009E-001 1.4500E-001 6.1050E-001
5.9762E-001 2.0142E-001 5.5408E-001 8.3669E-001 1.9353E-001 6.1050E-001 -1.5000E-001 1.4500E-001 6.1050E-001
6.5965E-001 1.9939E-001 5.5611E-001 8.6245E-001 1.8206E-001 6.1050E-001 -1.2924E-001 1.4500E-001 6.3065E-001
7.1007E-001 1.9711E-001 5.5839E-001 8.9249E-001 1.7284E-001 6.1050E-001 -1.0031E-001 1.4500E-001 6.4359E-001
7.5354E-001 1.9231E-001 5.6319E-001 9.0653E-001 1.6472E-001 6.1050E-001 -5.1832E-002 1.4500E-001 6.6135E-001
7.9188E-001 1.8592E-001 5.6958E-001 9.2009E-001 1.4500E-001 6.1050E-001 9.3407E-003 1.4500E-001 6.7399E-001
8.3669E-001 1.7932E-001 5.7618E-001 -1.5000E-001 1.4500E-001 6.1050E-001 5.7204E-002 1.4500E-001 6.8034E-001
8.6245E-001 1.7120E-001 5.8430E-001 -1.2924E-001 1.6361E-001 6.1821E-001 1.2656E-001 1.4500E-001 6.8608E-001
8.9249E-001 1.6468E-001 5.9082E-001 -1.0031E-001 1.7557E-001 6.2316E-001 2.0263E-001 1.4500E-001 6.8987E-001
9.0653E-001 1.5894E-001 5.9656E-001 -5.1832E-002 1.9198E-001 6.2996E-001 2.6954E-001 1.4500E-001 6.9072E-001
9.2009E-001 1.4500E-001 6.1050E-001 9.3407E-003 2.0366E-001 6.3480E-001 3.7576E-001 1.4500E-001 6.9096E-001
-1.5000E-001 1.4500E-001 6.1050E-001 5.7204E-002 2.0953E-001 6.3723E-001 4.6685E-001 1.4500E-001 6.9121E-001
-1.2924E-001 1.5271E-001 5.9189E-001 1.2656E-001 2.1483E-001 6.3942E-001 5.1813E-001 1.4500E-001 6.9054E-001
-1.0031E-001 1.5766E-001 5.7993E-001 2.0263E-001 2.1832E-001 6.4087E-001 5.9762E-001 1.4500E-001 6.9029E-001
-5.1832E-002 1.6446E-001 5.6352E-001 2.6954E-001 2.1911E-001 6.4120E-001 6.5965E-001 1.4500E-001 6.8742E-001
9.3407E-003 1.6930E-001 5.5184E-001 3.7576E-001 2.1934E-001 6.4129E-001 7.1007E-001 1.4500E-001 6.8419E-001
5.7204E-002 1.7173E-001 5.4597E-001 4.6685E-001 2.1956E-001 6.4139E-001 7.5354E-001 1.4500E-001 6.7741E-001
1.2656E-001 1.7392E-001 5.4067E-001 5.1813E-001 2.1894E-001 6.4113E-001 7.9188E-001 1.4500E-001 6.6838E-001
2.0263E-001 1.7537E-001 5.3718E-001 5.9762E-001 2.1872E-001 6.4103E-001 8.3669E-001 1.4500E-001 6.5903E-001
2.6954E-001 1.7570E-001 5.3639E-001 6.5965E-001 2.1607E-001 6.3994E-001 8.6245E-001 1.4500E-001 6.4756E-001
3.7576E-001 1.7579E-001 5.3616E-001 7.1007E-001 2.1308E-001 6.3870E-001 8.9249E-001 1.4500E-001 6.3834E-001
4.6685E-001 1.7589E-001 5.3594E-001 7.5354E-001 2.0682E-001 6.3611E-001 9.0653E-001 1.4500E-001 6.3022E-001
5.1813E-001 1.7563E-001 5.3656E-001 7.9188E-001 1.9847E-001 6.3265E-001 9.2009E-001 1.4500E-001 6.1050E-001
5.9762E-001 1.7553E-001 5.3678E-001 8.3669E-001 1.8984E-001 6.2907E-001 -1.5000E-001 1.4500E-001 6.1050E-001
6.5965E-001 1.7444E-001 5.3943E-001 8.6245E-001 1.7924E-001 6.2468E-001 -1.2924E-001 1.2485E-001 6.1050E-001
7.1007E-001 1.7320E-001 5.4242E-001 8.9249E-001 1.7072E-001 6.2115E-001 -1.0031E-001 1.1191E-001 6.1050E-001
7.5354E-001 1.7061E-001 5.4868E-001 9.0653E-001 1.6322E-001 6.1805E-001 -5.1832E-002 9.4145E-002 6.1050E-001
7.9188E-001 1.6715E-001 5.5703E-001 9.2009E-001 1.4500E-001 6.1050E-001 9.3407E-003 8.1508E-002 6.1050E-001
8.3669E-001 1.6357E-001 5.6566E-001 -1.5000E-001 1.4500E-001 6.1050E-001 5.7204E-002 7.5159E-002 6.1050E-001
8.6245E-001 1.5918E-001 5.7626E-001 -1.2924E-001 1.5925E-001 6.2475E-001 1.2656E-001 6.9420E-002 6.1050E-001
8.9249E-001 1.5565E-001 5.8478E-001 -1.0031E-001 1.6840E-001 6.3390E-001 2.0263E-001 6.5635E-002 6.1050E-001
9.0653E-001 1.5255E-001 5.9228E-001 -5.1832E-002 1.8096E-001 6.4646E-001 2.6954E-001 6.4780E-002 6.1050E-001

```
3.7576E-001 6.4536E-002 6.1050E-001
4.6685E-001 6.4292E-002 6.1050E-001
5.1813E-001 6.4963E-002 6.1050E-001
5.9762E-001 6.5208E-002 6.1050E-001
6.5965E-001 6.8077E-002 6.1050E-001
7.1007E-001 7.1313E-002 6.1050E-001
7.5354E-001 7.8089E-002 6.1050E-001
7.9188E-001 8.7125E-002 6.1050E-001
8.3669E-001 9.6465E-002 6.1050E-001
8.6245E-001 1.0794E-001 6.1050E-001
8.9249E-001 1.1716E-001 6.1050E-001
9.0653E-001 1.2528E-001 6.1050E-001
9.2009E-001 1.4500E-001 6.1050E-001
-1.5000E-001 1.4500E-001 6.1050E-001
-1.2924E-001 1.2639E-001 6.0279E-001
-1.0031E-001 1.1443E-001 5.9784E-001
-5.1832E-002 9.8016E-002 5.9104E-001
9.3407E-003 8.6341E-002 5.8620E-001
5.7204E-002 8.0475E-002 5.8377E-001
1.2656E-001 7.5173E-002 5.8158E-001
2.0263E-001 7.1676E-002 5.8013E-001
2.6954E-001 7.0886E-002 5.7980E-001
3.7576E-001 7.0661E-002 5.7971E-001
4.6685E-001 7.0436E-002 5.7961E-001
5.1813E-001 7.1056E-002 5.7987E-001
5.9762E-001 7.1281E-002 5.7997E-001
6.5965E-001 7.3933E-002 5.8106E-001
7.1007E-001 7.6922E-002 5.8230E-001
7.5354E-001 8.3182E-002 5.8489E-001
7.9188E-001 9.1530E-002 5.8835E-001
8.3669E-001 1.0016E-001 5.9193E-001
8.6245E-001 1.1076E-001 5.9632E-001
8.9249E-001 1.1928E-001 5.9985E-001
9.0653E-001 1.2678E-001 6.0295E-001
9.2009E-001 1.4500E-001 6.1050E-001
-1.5000E-001 1.4500E-001 6.1050E-001
-1.2924E-001 1.3075E-001 5.9625E-001
-1.0031E-001 1.2160E-001 5.8710E-001
-5.1832E-002 1.0904E-001 5.7454E-001
9.3407E-003 1.0010E-001 5.6560E-001
5.7204E-002 9.5614E-002 5.6111E-001
1.2656E-001 9.1557E-002 5.5706E-001
2.0263E-001 8.8880E-002 5.5438E-001
2.6954E-001 8.8276E-002 5.5378E-001
3.7576E-001 8.8104E-002 5.5360E-001
4.6685E-001 8.7930E-002 5.5343E-001
5.1813E-001 8.8405E-002 5.5391E-001
5.9762E-001 8.8579E-002 5.5408E-001
6.5965E-001 9.0607E-002 5.5611E-001
7.1007E-001 9.2895E-002 5.5839E-001
7.5354E-001 9.7687E-002 5.6319E-001
7.9188E-001 1.0408E-001 5.6958E-001
8.3669E-001 1.1068E-001 5.7618E-001
8.6245E-001 1.1880E-001 5.8430E-001
8.9249E-001 1.2532E-001 5.9082E-001
9.0653E-001 1.3106E-001 5.9656E-001
9.2009E-001 1.4500E-001 6.1050E-001
-1.5000E-001 1.4500E-001 6.1050E-001
-1.2924E-001 1.3729E-001 5.9189E-001
-1.0031E-001 1.3234E-001 5.7993E-001
-5.1832E-002 1.2554E-001 5.6352E-001
9.3407E-003 1.2070E-001 5.5184E-001
5.7204E-002 1.1827E-001 5.4597E-001
1.2656E-001 1.1608E-001 5.4067E-001
2.0263E-001 1.1463E-001 5.3718E-001
2.6954E-001 1.1430E-001 5.3639E-001
3.7576E-001 1.1421E-001 5.3616E-001
4.6685E-001 1.1411E-001 5.3594E-001
5.1813E-001 1.1437E-001 5.3656E-001
5.9762E-001 1.1447E-001 5.3678E-001
6.5965E-001 1.1556E-001 5.3943E-001
7.1007E-001 1.1680E-001 5.4242E-001
7.5354E-001 1.1939E-001 5.4868E-001
7.9188E-001 1.2285E-001 5.5703E-001
8.3669E-001 1.2643E-001 5.6566E-001
8.6245E-001 1.3082E-001 5.7626E-001
8.9249E-001 1.3435E-001 5.8478E-001
9.0653E-001 1.3745E-001 5.9228E-001
9.2009E-001 1.4500E-001 6.1050E-001
-1.5000E-001 1.4500E-001 6.1050E-001
-1.2924E-001 1.4500E-001 5.9035E-001
-1.0031E-001 1.4500E-001 5.7741E-001
-5.1832E-002 1.4500E-001 5.5965E-001
9.3407E-003 1.4500E-001 5.4701E-001
5.7204E-002 1.4500E-001 5.4066E-001
1.2656E-001 1.4500E-001 5.3492E-001
2.0263E-001 1.4500E-001 5.3113E-001
2.6954E-001 1.4500E-001 5.3028E-001
3.7576E-001 1.4500E-001 5.3004E-001
4.6685E-001 1.4500E-001 5.2979E-001
5.1813E-001 1.4500E-001 5.3046E-001
5.9762E-001 1.4500E-001 5.3071E-001
6.5965E-001 1.4500E-001 5.3358E-001
7.1007E-001 1.4500E-001 5.3681E-001
7.5354E-001 1.4500E-001 5.4359E-001
7.9188E-001 1.4500E-001 5.5262E-001
8.3669E-001 1.4500E-001 5.6197E-001
8.6245E-001 1.4500E-001 5.7344E-001
8.9249E-001 1.4500E-001 5.8266E-001
9.0653E-001 1.4500E-001 5.9078E-001
9.2009E-001 1.4500E-001 6.1050E-001
-1.5000E-001 1.4500E-001 6.1050E-001
-1.2924E-001 1.2485E-001 6.1050E-001
-1.0031E-001 1.1191E-001 6.1050E-001
-5.1832E-002 9.4145E-002 6.1050E-001
9.3407E-003 8.1508E-002 6.1050E-001
5.7204E-002 7.5159E-002 6.1050E-001
1.2656E-001 6.9420E-002 6.1050E-001
2.0263E-001 6.5635E-002 6.1050E-001
2.6954E-001 6.4780E-002 6.1050E-001
3.7576E-001 6.4536E-002 6.1050E-001
4.6685E-001 6.4292E-002 6.1050E-001
5.1813E-001 6.4963E-002 6.1050E-001
5.9762E-001 6.5208E-002 6.1050E-001
6.5965E-001 6.8077E-002 6.1050E-001
7.1007E-001 7.1313E-002 6.1050E-001
7.5354E-001 7.8089E-002 6.1050E-001
7.9188E-001 8.7125E-002 6.1050E-001
8.3669E-001 9.6465E-002 6.1050E-001
8.6245E-001 1.0794E-001 6.1050E-001
8.9249E-001 1.1716E-001 6.1050E-001
9.0653E-001 1.2528E-001 6.1050E-001
9.2009E-001 1.4500E-001 6.1050E-001
-1.5000E-001 1.4500E-001 6.1050E-001
-1.2924E-001 1.2639E-001 6.1821E-001
-1.0031E-001 1.1443E-001 6.2316E-001
-5.1832E-002 9.8016E-002 6.2996E-001
9.3407E-003 8.6341E-002 6.3480E-001
5.7204E-002 8.0475E-002 6.3723E-001
1.2656E-001 7.5173E-002 6.3942E-001
2.0263E-001 7.1676E-002 6.4087E-001
2.6954E-001 7.0886E-002 6.4120E-001
3.7576E-001 7.0661E-002 6.4129E-001
4.6685E-001 7.0436E-002 6.4139E-001
5.1813E-001 7.1056E-002 6.4113E-001
5.9762E-001 7.1281E-002 6.4103E-001
6.5965E-001 7.3933E-002 6.3994E-001
7.1007E-001 7.6922E-002 6.3870E-001
7.5354E-001 8.3182E-002 6.3611E-001
7.9188E-001 9.1530E-002 6.3265E-001
8.3669E-001 1.0016E-001 6.2907E-001
8.6245E-001 1.1076E-001 6.2468E-001
8.9249E-001 1.1928E-001 6.2115E-001
9.0653E-001 1.2678E-001 6.1805E-001
9.2009E-001 1.4500E-001 6.1050E-001
-1.5000E-001 1.4500E-001 6.1050E-001
-1.2924E-001 1.3075E-001 6.2475E-001
-1.0031E-001 1.2160E-001 6.3390E-001
-5.1832E-002 1.0904E-001 6.4646E-001
9.3407E-003 1.0010E-001 6.5540E-001
5.7204E-002 9.5614E-002 6.5989E-001
1.2656E-001 9.1557E-002 6.6394E-001
2.0263E-001 8.8880E-002 6.6662E-001
2.6954E-001 8.8276E-002 6.6722E-001
3.7576E-001 8.8104E-002 6.6740E-001
4.6685E-001 8.7930E-002 6.6757E-001
5.1813E-001 8.8405E-002 6.6709E-001
5.9762E-001 8.8579E-002 6.6692E-001
6.5965E-001 9.0607E-002 6.6489E-001
7.1007E-001 9.2895E-002 6.6260E-001
7.5354E-001 9.7687E-002 6.5781E-001
7.9188E-001 1.0408E-001 6.5142E-001
8.3669E-001 1.1068E-001 6.4482E-001
8.6245E-001 1.1880E-001 6.3670E-001
8.9249E-001 1.2532E-001 6.3019E-001
9.0653E-001 1.3106E-001 6.2444E-001
9.2009E-001 1.4500E-001 6.1050E-001
-1.5000E-001 1.4500E-001 6.1050E-001
-1.2924E-001 1.3729E-001 6.2911E-001
-1.0031E-001 1.3234E-001 6.4107E-001
-5.1832E-002 1.2554E-001 6.5748E-001
9.3407E-003 1.2070E-001 6.6916E-001
5.7204E-002 1.1827E-001 6.7503E-001
1.2656E-001 1.1608E-001 6.8033E-001
2.0263E-001 1.1463E-001 6.8382E-001
2.6954E-001 1.1430E-001 6.8461E-001
3.7576E-001 1.1421E-001 6.8484E-001
4.6685E-001 1.1411E-001 6.8506E-001
5.1813E-001 1.1437E-001 6.8444E-001
5.9762E-001 1.1447E-001 6.8422E-001
6.5965E-001 1.1556E-001 6.8157E-001
7.1007E-001 1.1680E-001 6.7858E-001
7.5354E-001 1.1939E-001 6.7232E-001
7.9188E-001 1.2285E-001 6.6397E-001
8.3669E-001 1.2643E-001 6.5534E-001
8.6245E-001 1.3082E-001 6.4474E-001
8.9249E-001 1.3435E-001 6.3622E-001
9.0653E-001 1.3745E-001 6.2872E-001
9.2009E-001 1.4500E-001 6.1050E-001
-1.5000E-001 1.4500E-001 6.1050E-001
-1.2924E-001 1.4500E-001 6.3065E-001
-1.0031E-001 1.4500E-001 6.4359E-001
-5.1832E-002 1.4500E-001 6.6135E-001
9.3407E-003 1.4500E-001 6.7399E-001
5.7204E-002 1.4500E-001 6.8034E-001
1.2656E-001 1.4500E-001 6.8608E-001
2.0263E-001 1.4500E-001 6.8987E-001
2.6954E-001 1.4500E-001 6.9072E-001
3.7576E-001 1.4500E-001 6.9096E-001
4.6685E-001 1.4500E-001 6.9121E-001
5.1813E-001 1.4500E-001 6.9054E-001
5.9762E-001 1.4500E-001 6.9029E-001
6.5965E-001 1.4500E-001 6.8742E-001
7.1007E-001 1.4500E-001 6.8419E-001
7.5354E-001 1.4500E-001 6.7741E-001
7.9188E-001 1.4500E-001 6.6838E-001
8.3669E-001 1.4500E-001 6.5903E-001
8.6245E-001 1.4500E-001 6.4756E-001
8.9249E-001 1.4500E-001 6.3834E-001
9.0653E-001 1.4500E-001 6.3022E-001
9.2009E-001 1.4500E-001 6.1050E-001
ZONE T="VER"
I=8, J=68, K=1,F=POINT
```

DT=(SINGLE SINGLE SINGLE)

5.1465E-001 1.8000E-001 9.1500E-001
5.0317E-001 1.6472E-001 9.1500E-001
4.8901E-001 1.6065E-001 9.1500E-001
4.7521E-001 1.5580E-001 9.1500E-001
4.3736E-001 1.5337E-001 9.1500E-001
4.0720E-001 1.5016E-001 9.1500E-001
3.7570E-001 1.5016E-001 9.1500E-001
3.0000E-001 1.5016E-001 9.1500E-001
5.1465E-001 1.8000E-001 9.1500E-001
5.0317E-001 1.6472E-001 9.0352E-001
4.8901E-001 1.6065E-001 9.0352E-001
4.7521E-001 1.5580E-001 9.0352E-001
4.3736E-001 1.5337E-001 9.0352E-001
4.0720E-001 1.5016E-001 9.0352E-001
3.7570E-001 1.5016E-001 9.0352E-001
3.0000E-001 1.5016E-001 9.0352E-001
5.1465E-001 1.8000E-001 9.1500E-001
5.0317E-001 1.6472E-001 9.0352E-001
4.8901E-001 1.6065E-001 8.9180E-001
4.7521E-001 1.5580E-001 8.9180E-001
4.3736E-001 1.5337E-001 8.9180E-001
4.0720E-001 1.5016E-001 8.9180E-001
3.7570E-001 1.5016E-001 8.9180E-001
3.0000E-001 1.5016E-001 8.9180E-001
5.1465E-001 1.8000E-001 9.1500E-001
5.0317E-001 1.6472E-001 9.0352E-001
4.8901E-001 1.6065E-001 8.9180E-001
4.7521E-001 1.5580E-001 8.8228E-001
4.3736E-001 1.5337E-001 8.8228E-001
4.0720E-001 1.5016E-001 8.8228E-001
3.7570E-001 1.5016E-001 8.8228E-001
3.0000E-001 1.5016E-001 8.8228E-001
5.1465E-001 1.8000E-001 9.1500E-001
5.0317E-001 1.6472E-001 9.0352E-001
4.8901E-001 1.6065E-001 8.9180E-001
4.7521E-001 1.5580E-001 8.8228E-001
4.3736E-001 1.5337E-001 8.7434E-001
4.0720E-001 1.5016E-001 8.7434E-001
3.7570E-001 1.5016E-001 8.7434E-001
3.0000E-001 1.5016E-001 8.7434E-001
5.1465E-001 1.8000E-001 9.1500E-001
5.0317E-001 1.6444E-001 9.0352E-001
4.8901E-001 1.5930E-001 8.9180E-001
4.7521E-001 1.5708E-001 8.8228E-001
4.3736E-001 1.5280E-001 8.7434E-001
4.0720E-001 1.4345E-001 8.7434E-001
3.7570E-001 1.4345E-001 8.7434E-001
3.0000E-001 1.4345E-001 8.7434E-001
5.1465E-001 1.8000E-001 9.1500E-001
5.0317E-001 1.6444E-001 9.0352E-001
4.8901E-001 1.5930E-001 8.9180E-001
4.7521E-001 1.5708E-001 8.8228E-001
4.3736E-001 1.5280E-001 8.7434E-001
4.0720E-001 1.4345E-001 8.6103E-001
3.7570E-001 1.4345E-001 8.6103E-001
3.0000E-001 1.4345E-001 8.6103E-001
5.1465E-001 1.8000E-001 9.1500E-001
5.0317E-001 1.6444E-001 9.0352E-001
4.8901E-001 1.5930E-001 8.9180E-001
4.7521E-001 1.5708E-001 8.8228E-001
4.3736E-001 1.5280E-001 8.7434E-001
4.0720E-001 1.4345E-001 8.4980E-001
3.7570E-001 1.4345E-001 8.4980E-001
3.0000E-001 1.4345E-001 8.4980E-001
5.1465E-001 1.8000E-001 9.1500E-001
5.0317E-001 1.7186E-001 9.0352E-001
4.8901E-001 1.6736E-001 8.9180E-001
4.7521E-001 1.6586E-001 8.8228E-001
4.3736E-001 1.6101E-001 8.7434E-001
4.0720E-001 1.5994E-001 8.4980E-001
3.7570E-001 1.5994E-001 8.4980E-001
3.0000E-001 1.5994E-001 8.4980E-001
5.1465E-001 1.8000E-001 9.1500E-001
5.0317E-001 1.7522E-001 9.0352E-001
4.8901E-001 1.7379E-001 8.9180E-001
4.7521E-001 1.7379E-001 8.8753E-001
4.3736E-001 1.6601E-001 8.7434E-001
4.0720E-001 1.7257E-001 8.6103E-001
3.7570E-001 1.7257E-001 8.6103E-001
3.0000E-001 1.7257E-001 8.6103E-001
5.1465E-001 1.8000E-001 9.1500E-001
5.0317E-001 1.7522E-001 9.0352E-001
4.8901E-001 1.7379E-001 8.9180E-001
4.7521E-001 1.7379E-001 8.8753E-001
4.3736E-001 1.6601E-001 8.7434E-001
4.0720E-001 1.7257E-001 8.7434E-001
3.7570E-001 1.7257E-001 8.7434E-001
3.0000E-001 1.7257E-001 8.7434E-001
5.1465E-001 1.8000E-001 9.1500E-001
5.0317E-001 1.7822E-001 9.0352E-001
4.8901E-001 1.7379E-001 8.9180E-001
4.7521E-001 1.7379E-001 8.8753E-001
4.3736E-001 1.6601E-001 8.7434E-001
4.0720E-001 1.6601E-001 8.7434E-001
3.7570E-001 1.6601E-001 8.7434E-001
3.0000E-001 1.6601E-001 8.7434E-001
5.1465E-001 1.8000E-001 9.1500E-001
5.0317E-001 1.7822E-001 9.0352E-001
4.8901E-001 1.7607E-001 8.9180E-001
4.7521E-001 1.7479E-001 8.8753E-001
4.3736E-001 1.7286E-001 8.8753E-001
4.0720E-001 1.7186E-001 8.8753E-001
3.7570E-001 1.7186E-001 8.8753E-001
3.0000E-001 1.7186E-001 8.8753E-001
5.1465E-001 1.8000E-001 9.1500E-001
5.0317E-001 1.7822E-001 9.0352E-001
4.8901E-001 1.7714E-001 9.0352E-001
4.7521E-001 1.7536E-001 9.0352E-001
4.3736E-001 1.7500E-001 9.0352E-001
4.0720E-001 1.7457E-001 9.0352E-001
3.7570E-001 1.7457E-001 9.0352E-001
3.0000E-001 1.7457E-001 9.0352E-001
5.1465E-001 1.8000E-001 9.1500E-001
5.0317E-001 1.7886E-001 9.1500E-001
4.8901E-001 1.7814E-001 9.1500E-001
4.7521E-001 1.7750E-001 9.1500E-001
4.3736E-001 1.7679E-001 9.1500E-001
4.0720E-001 1.7457E-001 9.0352E-001
3.7570E-001 1.8000E-001 9.0352E-001
3.0000E-001 1.8000E-001 9.0352E-001
5.1465E-001 1.8000E-001 9.1500E-001
5.0317E-001 1.7886E-001 9.1500E-001
4.8901E-001 1.7814E-001 9.1500E-001
4.7521E-001 1.7750E-001 9.1500E-001
4.3736E-001 1.7679E-001 9.1500E-001
4.0720E-001 1.7457E-001 9.1500E-001
3.7570E-001 1.8000E-001 9.1500E-001
3.0000E-001 1.8000E-001 9.1500E-001
5.1465E-001 1.8000E-001 9.1500E-001
5.0317E-001 1.6472E-001 9.1500E-001
4.8901E-001 1.6065E-001 9.1500E-001
4.7521E-001 1.5580E-001 9.1500E-001
4.3736E-001 1.5337E-001 9.1500E-001
4.0720E-001 1.5016E-001 9.1500E-001
3.7570E-001 1.5016E-001 9.1500E-001
3.0000E-001 1.5016E-001 9.1500E-001
5.1465E-001 1.8000E-001 9.1500E-001
5.0317E-001 1.6472E-001 9.0352E-001
4.8901E-001 1.6065E-001 9.0352E-001
4.7521E-001 1.5580E-001 9.0352E-001
4.3736E-001 1.5337E-001 9.0352E-001
4.0720E-001 1.5016E-001 9.0352E-001
3.7570E-001 1.5016E-001 9.0352E-001
3.0000E-001 1.5016E-001 9.0352E-001
5.1465E-001 1.8000E-001 9.1500E-001
5.0317E-001 1.6472E-001 9.0352E-001
4.8901E-001 1.6065E-001 8.9180E-001
4.7521E-001 1.5580E-001 8.9180E-001
4.3736E-001 1.5337E-001 8.9180E-001
4.0720E-001 1.5016E-001 8.9180E-001
3.7570E-001 1.5016E-001 8.9180E-001
3.0000E-001 1.5016E-001 8.9180E-001
5.1465E-001 1.8000E-001 9.1500E-001
5.0317E-001 1.6472E-001 9.0352E-001
4.8901E-001 1.6065E-001 8.9180E-001
4.7521E-001 1.5580E-001 8.8228E-001
4.3736E-001 1.5337E-001 8.8228E-001
4.0720E-001 1.5016E-001 8.8228E-001
3.7570E-001 1.5016E-001 8.8228E-001
3.0000E-001 1.5016E-001 8.8228E-001
5.1465E-001 1.8000E-001 9.1500E-001
5.0317E-001 1.6472E-001 9.0352E-001
4.8901E-001 1.6065E-001 8.9180E-001
4.7521E-001 1.5580E-001 8.8228E-001
4.3736E-001 1.5337E-001 8.7434E-001
4.0720E-001 1.5016E-001 8.7434E-001
3.7570E-001 1.5016E-001 8.7434E-001
3.0000E-001 1.5016E-001 8.7434E-001
5.1465E-001 1.8000E-001 9.1500E-001
5.0317E-001 1.6444E-001 9.0352E-001
4.8901E-001 1.5930E-001 8.9180E-001
4.7521E-001 1.5708E-001 8.8228E-001
4.3736E-001 1.5280E-001 8.7434E-001
4.0720E-001 1.4345E-001 8.7434E-001
3.7570E-001 1.4345E-001 8.7434E-001
3.0000E-001 1.4345E-001 8.7434E-001
5.1465E-001 1.8000E-001 9.1500E-001
5.0317E-001 1.6444E-001 9.0352E-001
4.8901E-001 1.5930E-001 8.9180E-001
4.7521E-001 1.5708E-001 8.8228E-001
4.3736E-001 1.5280E-001 8.7434E-001
4.0720E-001 1.4345E-001 8.6103E-001
3.7570E-001 1.4345E-001 8.6103E-001
3.0000E-001 1.4345E-001 8.6103E-001
5.1465E-001 1.8000E-001 9.1500E-001
5.0317E-001 1.6444E-001 9.0352E-001
4.8901E-001 1.5930E-001 8.9180E-001
4.7521E-001 1.5708E-001 8.8228E-001
4.3736E-001 1.5280E-001 8.7434E-001
4.0720E-001 1.4345E-001 8.4980E-001
3.7570E-001 1.4345E-001 8.4980E-001
3.0000E-001 1.4345E-001 8.4980E-001
5.1465E-001 1.8000E-001 9.1500E-001
5.0317E-001 1.7186E-001 9.0352E-001
4.8901E-001 1.6736E-001 8.9180E-001
4.7521E-001 1.6586E-001 8.8228E-001
4.3736E-001 1.6101E-001 8.7434E-001
4.0720E-001 1.5994E-001 8.4980E-001

3.7570E-001 1.5994E-001 8.4980E-001
3.0000E-001 1.5994E-001 8.4980E-001
5.1465E-001 1.8000E-001 9.1500E-001
5.0317E-001 1.7522E-001 9.0352E-001
4.8901E-001 1.7379E-001 8.9180E-001
4.7521E-001 1.7379E-001 8.8753E-001
4.3736E-001 1.6601E-001 8.7434E-001
4.0720E-001 1.7257E-001 8.6103E-001
3.7570E-001 1.7257E-001 8.6103E-001
3.0000E-001 1.7257E-001 8.6103E-001
5.1465E-001 1.8000E-001 9.1500E-001
5.0317E-001 1.7522E-001 9.0352E-001
4.8901E-001 1.7379E-001 8.9180E-001
4.7521E-001 1.7379E-001 8.8753E-001
4.3736E-001 1.6601E-001 8.7434E-001
4.0720E-001 1.7257E-001 8.7434E-001
3.7570E-001 1.7257E-001 8.7434E-001
3.0000E-001 1.7257E-001 8.7434E-001
5.1465E-001 1.8000E-001 9.1500E-001
5.0317E-001 1.7822E-001 9.0352E-001
4.8901E-001 1.7379E-001 8.9180E-001
4.7521E-001 1.7379E-001 8.8753E-001
4.3736E-001 1.6601E-001 8.7434E-001
4.0720E-001 1.6601E-001 8.7434E-001
3.7570E-001 1.6601E-001 8.7434E-001
3.0000E-001 1.6601E-001 8.7434E-001
5.1465E-001 1.8000E-001 9.1500E-001
5.0317E-001 1.7822E-001 9.0352E-001
4.8901E-001 1.7607E-001 8.9180E-001
4.7521E-001 1.7479E-001 8.8753E-001
4.3736E-001 1.7286E-001 8.8753E-001
4.0720E-001 1.7186E-001 8.8753E-001
3.7570E-001 1.7186E-001 8.8753E-001
3.0000E-001 1.7186E-001 8.8753E-001
5.1465E-001 1.8000E-001 9.1500E-001
5.0317E-001 1.7822E-001 9.0352E-001
4.8901E-001 1.7714E-001 9.0352E-001
4.7521E-001 1.7536E-001 9.0352E-001
4.3736E-001 1.7500E-001 9.0352E-001
4.0720E-001 1.7457E-001 9.0352E-001
3.7570E-001 1.7457E-001 9.0352E-001
3.0000E-001 1.7457E-001 9.0352E-001
5.1465E-001 1.8000E-001 9.1500E-001
5.0317E-001 1.7886E-001 9.1500E-001
4.8901E-001 1.7814E-001 9.1500E-001
4.7521E-001 1.7750E-001 9.1500E-001
4.3736E-001 1.7679E-001 9.1500E-001
4.0720E-001 1.7457E-001 9.0352E-001
3.7570E-001 1.8000E-001 9.0352E-001
3.0000E-001 1.8000E-001 9.0352E-001
5.1465E-001 1.8000E-001 9.1500E-001
5.0317E-001 1.7886E-001 9.1500E-001
4.8901E-001 1.7814E-001 9.1500E-001
4.7521E-001 1.7750E-001 9.1500E-001
4.3736E-001 1.7679E-001 9.1500E-001
4.0720E-001 1.7457E-001 9.1500E-001
3.7570E-001 1.8000E-001 9.1500E-001
3.0000E-001 1.8000E-001 9.1500E-001
5.1465E-001 1.8000E-001 9.1500E-001
5.0317E-001 1.6472E-001 9.1500E-001
4.8901E-001 1.6065E-001 9.1500E-001
4.7521E-001 1.5580E-001 9.1500E-001
4.3736E-001 1.5337E-001 9.1500E-001

4.0720E-001 1.5016E-001 9.1500E-001
3.7570E-001 1.5016E-001 9.1500E-001
3.0000E-001 1.5016E-001 9.1500E-001
5.1465E-001 1.8000E-001 9.1500E-001
5.0317E-001 1.6472E-001 9.0352E-001
4.8901E-001 1.6065E-001 9.0352E-001
4.7521E-001 1.5580E-001 9.0352E-001
4.3736E-001 1.5337E-001 9.0352E-001
4.0720E-001 1.5016E-001 9.0352E-001
3.7570E-001 1.5016E-001 9.0352E-001
3.0000E-001 1.5016E-001 9.0352E-001
5.1465E-001 1.8000E-001 9.1500E-001
5.0317E-001 1.6472E-001 9.0352E-001
4.8901E-001 1.6065E-001 8.9180E-001
4.7521E-001 1.5580E-001 8.9180E-001
4.3736E-001 1.5337E-001 8.9180E-001
4.0720E-001 1.5016E-001 8.9180E-001
3.7570E-001 1.5016E-001 8.9180E-001
3.0000E-001 1.5016E-001 8.9180E-001
5.1465E-001 1.8000E-001 9.1500E-001
5.0317E-001 1.6472E-001 9.0352E-001
4.8901E-001 1.6065E-001 8.9180E-001
4.7521E-001 1.5580E-001 8.8228E-001
4.3736E-001 1.5337E-001 8.8228E-001
4.0720E-001 1.5016E-001 8.8228E-001
3.7570E-001 1.5016E-001 8.8228E-001
3.0000E-001 1.5016E-001 8.8228E-001
5.1465E-001 1.8000E-001 9.1500E-001
5.0317E-001 1.6472E-001 9.0352E-001
4.8901E-001 1.6065E-001 8.9180E-001
4.7521E-001 1.5580E-001 8.8228E-001
4.3736E-001 1.5337E-001 8.7434E-001
4.0720E-001 1.5016E-001 8.7434E-001
3.7570E-001 1.5016E-001 8.7434E-001
3.0000E-001 1.5016E-001 8.7434E-001
5.1465E-001 1.8000E-001 9.1500E-001
5.0317E-001 1.6444E-001 9.0352E-001
4.8901E-001 1.5930E-001 8.9180E-001
4.7521E-001 1.5708E-001 8.8228E-001
4.3736E-001 1.5280E-001 8.7434E-001
4.0720E-001 1.4345E-001 8.7434E-001
3.7570E-001 1.4345E-001 8.7434E-001
3.0000E-001 1.4345E-001 8.7434E-001
5.1465E-001 1.8000E-001 9.1500E-001
5.0317E-001 1.6444E-001 9.0352E-001
4.8901E-001 1.5930E-001 8.9180E-001
4.7521E-001 1.5708E-001 8.8228E-001
4.3736E-001 1.5280E-001 8.7434E-001
4.0720E-001 1.4345E-001 8.6103E-001
3.7570E-001 1.4345E-001 8.6103E-001
3.0000E-001 1.4345E-001 8.6103E-001
5.1465E-001 1.8000E-001 9.1500E-001
5.0317E-001 1.6444E-001 9.0352E-001
4.8901E-001 1.5930E-001 8.9180E-001
4.7521E-001 1.5708E-001 8.8228E-001
4.3736E-001 1.5280E-001 8.7434E-001
4.0720E-001 1.4345E-001 8.4980E-001
3.7570E-001 1.4345E-001 8.4980E-001
3.0000E-001 1.4345E-001 8.4980E-001
5.1465E-001 1.8000E-001 9.1500E-001
5.0317E-001 1.7186E-001 9.0352E-001
4.8901E-001 1.6736E-001 8.9180E-001
4.7521E-001 1.6586E-001 8.8228E-001
4.3736E-001 1.6101E-001 8.7434E-001
4.0720E-001 1.5994E-001 8.4980E-001

4.3736E-001 1.6601E-001 9.5566E-001	1.2479E-001 1.5580E-001 9.0352E-001	1.1099E-001 1.7379E-001 8.9180E-001
4.0720E-001 1.7257E-001 9.8020E-001	1.6264E-001 1.5337E-001 9.0352E-001	1.2479E-001 1.7379E-001 8 8753E-001
3 7570E-001 1.7257E-001 9.8020E-001	1.9280E-001 1 5016E-001 9.0352E-001	1 6264E-001 1 6601E-001 8 7434E-001
3.0000E-001 1.7257E-001 9.8020E-001	2.2430E-001 1.5016E-001 9.0352E-001	1.9280E-001 1.7257E-001 8.6103E-001
5.1465E-001 1.8000E-001 9.1500E-001	3.0000E-001 1.5016E-001 9.0352E-001	2.2430E-001 1.7257E-001 8.6103E-001
5.0317E-001 1.7522E-001 9.2648E-001	8.5348E-002 1.8000E-001 9.1500E-001	3.0000E-001 1.7257E-001 8.6103E-001
4 8901E-001 1.7379E-001 9.3820E-001	9.6825E-002 1.6472E-001 9.0352E-001	8.5348E-002 1.8000E-001 9 1500E-001
4.7521E-001 1.7379E-001 9.4247E-001	1.1099E-001 1.6065E-001 8.9180E-001	9.6825E-002 1.7522E-001 9.0352E-001
4.3736E-001 1.6601E-001 9.5566E-001	1.2479E-001 1.5580E-001 8.9180E-001	1.1099E-001 1.7379E-001 8.9180E-001
4.0720E-001 1.7257E-001 9.6897E-001	1.6264E-001 1.5337E-001 8.9180E-001	1.2479E-001 1.7379E-001 8.8753E-001
3.7570E-001 1.7257E-001 9.6897E-001	1.9280E-001 1.5016E-001 8.9180E-001	1 6264E-001 1 6601E-001 8 7434E-001
3.0000E-001 1.7257E-001 9.6897E-001	2.2430E-001 1.5016E-001 8.9180E-001	1.9280E-001 1.7257E-001 8.7434E-001
5.1465E-001 1.8000E-001 9.1500E-001	3.0000E-001 1.5016E-001 8.9180E-001	2.2430E-001 1.7257E-001 8.7434E-001
5.0317E-001 1.7522E-001 9.2648E-001	8.5348E-002 1.8000E-001 9.1500E-001	3.0000E-001 1.7257E-001 8.7434E-001
4.8901E-001 1.7379E-001 9.3820E-001	9.6825E-002 1.6472E-001 9.0352E-001	8.5348E-002 1.8000E-001 9 1500E-001
4.7521E-001 1.7379E-001 9.4247E-00i	1.1099E-001 1.6065E-001 8.9180E-001	9.6825E-002 1.7822E-001 9.0352E-001
4.3736E-001 1.6601E-001 9.5566E-001	1.2479E-001 1.5580E-001 8.8228E-001	1.1099E-001 1.7379E-001 8.9180E-001
4.0720E-001 1.7257E-001 9.5566E-001	1.6264E-001 1.5337E-001 8.8228E-001	1.2479E-001 1.7379E-001 8.8753E-001
3.7570E-001 1.7257E-001 9.5566E-001	1.9280E-001 1.5016E-001 8.8228E-001	1.6264E-001 1.6601E-001 8 7434E-001
3.0000E-001 1.7257E-001 9.5566E-001	2.2430E-001 1.5016E-001 8.8228E-001	1.9280E-001 1.6601E-001 8.7434E-001
5.1465E-001 1.8000E-001 9.1500E-001	3.0000E-001 1.5016E-001 8.8228E-001	2.2430E-001 1.6601E-001 8.7434E-001
5.0317E-001 1.7822E-001 9.2648E-001	8.5348E-002 1.8000E-001 9.1500E-001	3.0000E-001 1.6601E-001 8.7434E-001
4.8901E-001 1.7379E-001 9.3820E-001	9.6825E-002 1.6472E-001 9.0352E-001	8.5348E-002 1.8000E-001 9 1500E-001
4.7521E-001 1.7379E-001 9.4247E-001	1.1099E-001 1.6065E-001 8.9180E-001	9.6825E-002 1.7822E-001 9.0352E-001
4.3736E-001 1.6601E-001 9.5566E-001	1.2479E-001 1.5580E-001 8.8228E-001	1.1099E-001 1.7607E-001 8.9180E-001
4.0720E-001 1.6601E-001 9.5566E-001	1.6264E-001 1.5337E-001 8.7434E-001	1.2479E-001 1.7479E-001 8.8753E-001
3.7570E-001 1.6601E-001 9.5566E-001	1.9280E-001 1.5016E-001 8.7434E-001	1.6264E-001 1 7286E-001 8.8753E-001
3.0000E-001 1.6601E-001 9.5566E-001	2.2430E-001 1.5016E-001 8.7434E-001	1.9280E-001 1.7186E-001 8.8753E-001
5.1465E-001 1.8000E-001 9.1500E-001	3.0000E-001 1.5016E-001 8.7434E-001	2.2430E-001 1.7186E-001 8.8753E-001
5.0317E-001 1.7822E-001 9.2648E-001	8.5348E-002 1.8000E-001 9.1500E-001	3.0000E-001 1.7186E-001 8.8753E-001
4.8901E-001 1.7607E-001 9.3820E-001	9.6825E-002 1.6444E-001 9.0352E-001	8.5348E-002 1.8000E-001 9 1500E-001
4.7521E-001 1.7479E-001 9.4247E-001	1.1099E-001 1.5930E-001 8.9180E-001	9.6825E-002 1.7822E-001 9.0352E-001
4.3736E-001 1.7286E-001 9.4247E-001	1.2479E-001 1.5708E-001 8.8228E-001	1.1099E-001 1.7714E-001 9.0352E-001
4.0720E-001 1.7186E-001 9.4247E-001	1.6264E-001 1.5280E-001 8.7434E-001	1.2479E-001 1 7536E-001 9.0352E-001
3.7570E-001 1.7186E-001 9.4247E-001	1.9280E-001 1.4345E-001 8.7434E-001	1.6264E-001 1.7500E-001 9.0352E-001
3.0000E-001 1.7186E-001 9.4247E-001	2.2430E-001 1.4345E-001 8.7434E-001	1.9280E-001 1.7457E-001 9.0352E-001
5.1465E-001 1.8000E-001 9.1500E-001	3.0000E-001 1.4345E-001 8.7434E-001	2.2430E-001 1.7457E-001 9.0352E-001
5.0317E-001 1.7822E-001 9.2648E-001	8.5348E-002 1.8000E-001 9.1500E-001	3.0000E-001 1.7457E-001 9.0352E-001
4.8901E-001 1.7714E-001 9.2648E-001	9.6825E-002 1.6444E-001 9.0352E-001	8.5348E-002 1.8000E-001 9.1500E-001
4.7521E-001 1.7536E-001 9.2648E-001	1.1099E-001 1.5930E-001 8.9180E-001	9.6825E-002 1.7886E-001 9.1500E-001
4.3736E-001 1.7500E-001 9.2648E-001	1.2479E-001 1.5708E-001 8.8228E-001	1.1099E-001 1.7814E-001 9.1500E-001
4.0720E-001 1.7457E-001 9.2648E-001	1.6264E-001 1.5280E-001 8.7434E-001	1.2479E-001 1.7750E-001 9.1500E-001
3.7570E-001 1.7457E-001 9.2648E-001	1.9280E-001 1.4345E-001 8.6103E-001	1.6264E-001 1.7679E-001 9.1500E-001
3.0000E-001 1.7457E-001 9.2648E-001	2.2430E-001 1.4345E-001 8.6103E-001	1.9280E-001 1.7457E-001 9.0352E-001
5.1465E-001 1.8000E-001 9.1500E-001	3.0000E-001 1.4345E-001 8.6103E-001	2.2430E-001 1.8000E-001 9.0352E-001
5.0317E-001 1.7886E-001 9.1500E-001	8.5348E-002 1.8000E-001 9.1500E-001	3.0000E-001 1.8000E-001 9.0352E-001
4.8901E-001 1.7814E-001 9.1500E-001	9.6825E-002 1.6444E-001 9.0352E-001	8.5348E-002 1.8000E-001 9.1500E-001
4.7521E-001 1.7750E-001 9.1500E-001	1.1099E-001 1.5930E-001 8.9180E-001	9.6825E-002 1.7886E-001 9.1500E-001
4.3736E-001 1.7679E-001 9.1500E-001	1.2479E-001 1.5708E-001 8.8228E-001	1.1099E-001 1.7814E-001 9.1500E-001
4.0720E-001 1.7457E-001 9.2648E-001	1.6264E-001 1.5280E-001 8.7434E-001	1.2479E-001 1.7750E-001 9.1500E-001
3.7570E-001 1.8000E-001 9.2648E-001	1.9280E-001 1.4345E-001 8.4980E-001	1.6264E-001 1.7679E-001 9.1500E-001
3.0000E-001 1.8000E-001 9.2648E-001	2.2430E-001 1.4345E-001 8.4980E-001	1.9280E-001 1.7457E-001 9.1500E-001
5.1465E-001 1.8000E-001 9.1500E-001	3.0000E-001 1.4345E-001 8.4980E-001	2.2430E-001 1.8000E-001 9.1500E-001
5.0317E-001 1.7886E-001 9.1500E-001	8.5348E-002 1.8000E-001 9.1500E-001	3.0000E-001 1.8000E-001 9.1500E-001
4.8901E-001 1.7814E-001 9.1500E-001	9.6825E-002 1.7186E-001 9.0352E-001	8.5348E-002 1.8000E-001 9.1500E-001
4.7521E-001 1.7750E-001 9.1500E-001	1.1099E-001 1.6736E-001 8.9180E-001	9.6825E-002 1.6472E-001 9.1500E-001
4.3736E-001 1.7679E-001 9.1500E-001	1.2479E-001 1.6586E-001 8.8228E-001	1.1099E-001 1.6065E-001 9.1500E-001
4.0720E-001 1.7457E-001 9.1500E-001	1.6264E-001 1.6101E-001 8.7434E-001	1.2479E-001 1.5580E-001 9.1500E-001
3.7570E-001 1.8000E-001 9.1500E-001	1.9280E-001 1.5994E-001 8.4980E-001	1.6264E-001 1.5337E-001 9 1500E-001
3.0000E-001 1.8000E-001 9.1500E-001	2.2430E-001 1.5994E-001 8.4980E-001	1.9280E-001 1.5016E-001 9.1500E-001
8.5348E-002 1.8000E-001 9.1500E-001	3.0000E-001 1.5994E-001 8.4980E-001	2.2430E-001 1.5016E-001 9.1500E-001
9.6825E-002 1.6472E-001 9.1500E-001	8.5348E-002 1.8000E-001 9.1500E-001	3.0000E-001 1.5016E-001 9.1500E-001
1.1099E-001 1.6065E-001 9.1500E-001	9.6825E-002 1.7522E-001 9.0352E-001	8.5348E-002 1.8000E-001 9 1500E-001
1.2479E-001 1.5580E-001 9.1500E-001	1.1099E-001 1.7379E-001 8.9180E-001	9.6825E-002 1.6472E-001 9.2648E-001
1.6264E-001 1.5337E-001 9.1500E-001	1.2479E-001 1.7379E-001 8.8753E-001	1.1099E-001 1.6065E-001 9.2648E-001
1.9280E-001 1.5016E-001 9.1500E-001	1.6264E-001 1.6601E-001 8.7434E-001	1.2479E-001 1.5580E-001 9.2648E-001
2.2430E-001 1.5016E-001 9.1500E-001	1.9280E-001 1.7257E-001 8.4980E-001	1.6264E-001 1.5337E-001 9.2648E-001
3.0000E-001 1.5016E-001 9.1500E-001	2.2430E-001 1.7257E-001 8.4980E-001	1.9280E-001 1.5016E-001 9.2648E-001
8.5348E-002 1.8000E-001 9.1500E-001	3.0000E-001 1.7257E-001 8.4980E-001	2.2430E-001 1.5016E-001 9.2648E-001
9.6825E-002 1.6472E-001 9.0352E-001	8.5348E-002 1.8000E-001 9.1500E-001	3.0000E-001 1.5016E-001 9.2648E-001
1.1099E-001 1.6065E-001 9.0352E-001	9.6825E-002 1.7522E-001 9.0352E-001	8.5348E-002 1.8000E-001 9.1500E-001

9.6825E-002 1.6472E-001 9.2648E-001
1.1099E-001 1.6065E-001 9.3820E-001
1.2479E-001 1.5580E-001 9.3820E-001
1.6264E-001 1.5337E-001 9.3820E-001
1.9280E-001 1.5016E-001 9.3820E-001
2.2430E-001 1.5016E-001 9.3820E-001
3.0000E-001 1.5016E-001 9.3820E-001
8.5348E-002 1.8000E-001 9.1500E-001
9.6825E-002 1.6472E-001 9.2648E-001
1.1099E-001 1.6065E-001 9.3820E-001
1.2479E-001 1.5580E-001 9.4772E-001
1.6264E-001 1.5337E-001 9.4772E-001
1.9280E-001 1.5016E-001 9.4772E-001
2.2430E-001 1.5016E-001 9.4772E-001
3.0000E-001 1.5016E-001 9.4772E-001
8.5348E-002 1.8000E-001 9.1500E-001
9.6825E-002 1.6472E-001 9.2648E-001
1.1099E-001 1.6065E-001 9.3820E-001
1.2479E-001 1.5580E-001 9.4772E-001
1.6264E-001 1.5337E-001 9.5566E-001
1.9280E-001 1.5016E-001 9.5566E-001
2.2430E-001 1.5016E-001 9.5566E-001
3.0000E-001 1.5016E-001 9.5566E-001
8.5348E-002 1.8000E-001 9.1500E-001
9.6825E-002 1.6444E-001 9.2648E-001
1.1099E-001 1.5930E-001 9.3820E-001
1.2479E-001 1.5708E-001 9.4772E-001
1.6264E-001 1.5280E-001 9.5566E-001
1.9280E-001 1.4345E-001 9.5566E-001
2.2430E-001 1.4345E-001 9.5566E-001
3.0000E-001 1.4345E-001 9.5566E-001
8.5348E-002 1.8000E-001 9.1500E-001
9.6825E-002 1.6444E-001 9.2648E-001
1.1099E-001 1.5930E-001 9.3820E-001
1.2479E-001 1.5708E-001 9.4772E-001
1.6264E-001 1.5280E-001 9.5566E-001
1.9280E-001 1.4345E-001 9.6897E-001
2.2430E-001 1.4345E-001 9.6897E-001
3.0000E-001 1.4345E-001 9.6897E-001
8.5348E-002 1.8000E-001 9.1500E-001
9.6825E-002 1.6444E-001 9.2648E-001
1.1099E-001 1.5930E-001 9.3820E-001
1.2479E-001 1.5708E-001 9.4772E-001
1.6264E-001 1.5280E-001 9.5566E-001
1.9280E-001 1.4345E-001 9.8020E-001
2.2430E-001 1.4345E-001 9.8020E-001
3.0000E-001 1.4345E-001 9.8020E-001
8.5348E-002 1.8000E-001 9.1500E-001
9.6825E-002 1.7186E-001 9.2648E-001
1.1099E-001 1.6736E-001 9.3820E-001
1.2479E-001 1.6586E-001 9.4772E-001
1.6264E-001 1.6101E-001 9.5566E-001
1.9280E-001 1.5994E-001 9.8020E-001
2.2430E-001 1.5994E-001 9.8020E-001
3.0000E-001 1.5994E-001 9.8020E-001
8.5348E-002 1.8000E-001 9.1500E-001
9.6825E-002 1.7522E-001 9.2648E-001
1.1099E-001 1.7379E-001 9.3820E-001
1.2479E-001 1.7379E-001 9.4247E-001
1.6264E-001 1.6601E-001 9.5566E-001
1.9280E-001 1.7257E-001 9.8020E-001
2.2430E-001 1.7257E-001 9.8020E-001
3.0000E-001 1.7257E-001 9.8020E-001
8.5348E-002 1.8000E-001 9.1500E-001
9.6825E-002 1.7522E-001 9.2648E-001
1.1099E-001 1.7379E-001 9.3820E-001
1.2479E-001 1.7379E-001 9.4247E-001
1.6264E-001 1.6601E-001 9.5566E-001
1.9280E-001 1.7257E-001 9.6897E-001
2.2430E-001 1.7257E-001 9.6897E-001
3.0000E-001 1.7257E-001 9.6897E-001
8.5348E-002 1.8000E-001 9.1500E-001
9.6825E-002 1.7522E-001 9.2648E-001
1.1099E-001 1.7379E-001 9.3820E-001
1.2479E-001 1.7379E-001 9.4247E-001
1.6264E-001 1.6601E-001 9.5566E-001
1.9280E-001 1.6601E-001 9.5566E-001
2.2430E-001 1.6601E-001 9.5566E-001
3.0000E-001 1.6601E-001 9.5566E-001
8.5348E-002 1.8000E-001 9.1500E-001
9.6825E-002 1.7822E-001 9.2648E-001
1.1099E-001 1.7607E-001 9.3820E-001
1.2479E-001 1.7479E-001 9.4247E-001
1.6264E-001 1.7286E-001 9.4247E-001
1.9280E-001 1.7186E-001 9.4247E-001
2.2430E-001 1.7186E-001 9.4247E-001
3.0000E-001 1.7186E-001 9.4247E-001
8.5348E-002 1.8000E-001 9.1500E-001
9.6825E-002 1.7822E-001 9.2648E-001
1.1099E-001 1.7714E-001 9.2648E-001
1.2479E-001 1.7536E-001 9.2648E-001
1.6264E-001 1.7500E-001 9.2648E-001
1.9280E-001 1.7457E-001 9.2648E-001
2.2430E-001 1.7457E-001 9.2648E-001
3.0000E-001 1.7457E-001 9.2648E-001
8.5348E-002 1.8000E-001 9.1500E-001
9.6825E-002 1.7886E-001 9.1500E-001
1.1099E-001 1.7814E-001 9.1500E-001
1.2479E-001 1.7750E-001 9.1500E-001
1.6264E-001 1.7679E-001 9.1500E-001
1.9280E-001 1.7457E-001 9.2648E-001
2.2430E-001 1.8000E-001 9.2648E-001
3.0000E-001 1.8000E-001 9.2648E-001
8.5348E-002 1.8000E-001 9.1500E-001
9.6825E-002 1.7886E-001 9.1500E-001
1.1099E-001 1.7814E-001 9.1500E-001
1.2479E-001 1.7750E-001 9.1500E-001
1.6264E-001 1.7679E-001 9.1500E-001
1.9280E-001 1.7457E-001 9.1500E-001
2.2430E-001 1.8000E-001 9.1500E-001
3.0000E-001 1.8000E-001 9.1500E-001
ZONE T="MK82in"
I=22, J=36, K=1,F=POINT
DT=(SINGLE SINGLE SINGLE)
2.0000E-002 1.1000E-001 8.6000E-001
2.5130E-002 1.3080E-001 8.6000E-001
5.1100E-002 1.3500E-001 8.6000E-001
8.2300E-002 1.3720E-001 8.6000E-001
1.0600E-001 1.4020E-001 8.6000E-001
1.3300E-001 1.4140E-001 8.6000E-001
1.6900E-001 1.4190E-001 8.6000E-001
2.0100E-001 1.4350E-001 8.6000E-001
2.3300E-001 1.4350E-001 8.6000E-001
2.6400E-001 1.4350E-001 8.6000E-001
3.0500E-001 1.4300E-001 8.6000E-001
3.4400E-001 1.4280E-001 8.6000E-001
3.8200E-001 1.4090E-001 8.6000E-001
4.1900E-001 1.3770E-001 8.6000E-001
4.4500E-001 1.3600E-001 8.6000E-001
4.7500E-001 1.3300E-001 8.6000E-001
4.9100E-001 1.2940E-001 8.6000E-001
5.1700E-001 1.2580E-001 8.6000E-001
5.3700E-001 1.2150E-001 8.6000E-001
5.3700E-001 1.2150E-001 8.6000E-001
5.6200E-001 1.1934E-001 8.6000E-001
5.6200E-001 1.1000E-001 8.6000E-001
2.0000E-002 1.1000E-001 8.6000E-001
2.5130E-002 1.2780E-001 8.4930E-001
5.1100E-002 1.3140E-001 8.4710E-001
8.2300E-002 1.3330E-001 8.4600E-001
1.0600E-001 1.3590E-001 8.4440E-001
1.3300E-001 1.3690E-001 8.4380E-001
1.6900E-001 1.3740E-001 8.4360E-001
2.0100E-001 1.3870E-001 8.4280E-001
2.3300E-001 1.3870E-001 8.4270E-001
2.6400E-001 1.3870E-001 8.4280E-001
3.0500E-001 1.3830E-001 8.4300E-001
3.4400E-001 1.3820E-001 8.4310E-001
3.8200E-001 1.3650E-001 8.4410E-001
4.1900E-001 1.3380E-001 8.4570E-001
4.4500E-001 1.3230E-001 8.4660E-001
4.7500E-001 1.2970E-001 8.4820E-001
4.9100E-001 1.2710E-001 8.5087E-001
5.1700E-001 1.2450E-001 8.5379E-001
5.3700E-001 1.2110E-001 8.5701E-001
5.3700E-001 1.2110E-001 8.5701E-001
5.6200E-001 1.1801E-001 8.5519E-001
5.6200E-001 1.1000E-001 8.6000E-001
2.0000E-002 1.1000E-001 8.6000E-001
2.5130E-002 1.2780E-001 8.4930E-001
5.1100E-002 1.3140E-001 8.4710E-001
8.2300E-002 1.3330E-001 8.4600E-001
1.0600E-001 1.3590E-001 8.4440E-001
1.3300E-001 1.3690E-001 8.4380E-001
1.6900E-001 1.3740E-001 8.4360E-001
2.0100E-001 1.3870E-001 8.4280E-001
2.3300E-001 1.3870E-001 8.4270E-001
2.6400E-001 1.3870E-001 8.4280E-001
3.0500E-001 1.3830E-001 8.4300E-001
3.4400E-001 1.3820E-001 8.4310E-001
3.8200E-001 1.3650E-001 8.4410E-001
4.1900E-001 1.3380E-001 8.4570E-001
4.4500E-001 1.3230E-001 8.4660E-001
4.7500E-001 1.2970E-001 8.4820E-001
4.9100E-001 1.4650E-001 8.2850E-001
5.1700E-001 1.4630E-001 8.2870E-001
5.3700E-001 1.4680E-001 8.2840E-001
5.3700E-001 1.2110E-001 8.5701E-001
5.6200E-001 1.1801E-001 8.5519E-001
5.6200E-001 1.1000E-001 8.6000E-001
2.0000E-002 1.1000E-001 8.6000E-001
2.5130E-002 1.2470E-001 8.4530E-001
5.1100E-002 1.2770E-001 8.4230E-001

8.2300E-002 1.2930E-001 8.4070E-001	2.3300E-001 1.2730E-001 8.3130E-001	4.1900E-001 8.6200E-002 8.4570E-001
1.0600E-001 1.3140E-001 8.3860E-001	2.6400E-001 1.2720E-001 8.3130E-001	4.4500E-001 8.7700E-002 8.4660E-001
1.3300E-001 1.3220E-001 8.3780E-001	3.0500E-001 1.2700E-001 8.3170E-001	4.7500E-001 9.0300E-002 8.4820E-001
1.6900E-001 1.3260E-001 8.3740E-001	3.4400E-001 1.2690E-001 8.3180E-001	4.9100E-001 9.2900E-002 8.5087E-001
2.0100E-001 1.3370E-001 8.3630E-001	3.8200E-001 1.2590E-001 8.3350E-001	5.1700E-001 9.5500E-002 8.5379E-001
2.3300E-001 1.3370E-001 8.3630E-001	4.1900E-001 1.2430E-001 8.3620E-001	5.3700E-001 9.8900E-002 8.5701E-001
2.6400E-001 1.3370E-001 8.3630E-001	4.4500E-001 1.2340E-001 8.3770E-001	5.3700E-001 9.8900E-002 8.5701E-001
3.0500E-001 1.3340E-001 8.3660E-001	4.7500E-001 1.2180E-001 8.4030E-001	5.6200E-001 1.0199E-001 8.5519E-001
3.4400E-001 1.3320E-001 8.3680E-001	4.9100E-001 1.1913E-001 8.4290E-001	5.6200E-001 1.1000E-001 8.6000E-001
3.8200E-001 1.3180E-001 8.3820E-001	5.1700E-001 1.1621E-001 8.4550E-001	2.0000E-002 1.1000E-001 8.6000E-001
4.1900E-001 1.2960E-001 8.4040E-001	5.3700E-001 1.1299E-001 8.4890E-001	2.5130E-002 9.2200E-002 8.4930E-001
4.4500E-001 1.2840E-001 8.4160E-001	5.3700E-001 1.1299E-001 8.4890E-001	5.1100E-002 8.8600E-002 8.4710E-001
4.7500E-001 1.2620E-001 8.4380E-001	5.6200E-001 1.1481E-001 8.5199E-001	8.2300E-002 8.6700E-002 8.4600E-001
4.9100E-001 1.4400E-001 8.2600E-001	5.6200E-001 1.1000E-001 8.6000E-001	1.0600E-001 8.4100E-002 8.4440E-001
5.1700E-001 1.4380E-001 8.2620E-001	2.0000E-002 1.1000E-001 8.6000E-001	1.3300E-001 8.3100E-002 8.4380E-001
5.3700E-001 1.4420E-001 8.2580E-001	2.5130E-002 1.1000E-001 8.3920E-001	1.6900E-001 8.2600E-002 8.4360E-001
5.3700E-001 1.1812E-001 8.5188E-001	5.1100E-002 1.1000E-001 8.3500E-001	2.0100E-001 8.1300E-002 8.4280E-001
5.6200E-001 1.1660E-001 8.5340E-001	8.2300E-002 1.1000E-001 8.3280E-001	2.3300E-001 8.1300E-002 8.4270E-001
5.6200E-001 1.1000E-001 8.6000E-001	1.0600E-001 1.1000E-001 8.2980E-001	2.6400E-001 8.1300E-002 8.4280E-001
2.0000E-002 1.1000E-001 8.6000E-001	1.3300E-001 1.1000E-001 8.2860E-001	3.0500E-001 8.1700E-002 8.4300E-001
2.5130E-002 1.2070E-001 8.4220E-001	1.6900E-001 1.1000E-001 8.2810E-001	3.4400E-001 8.1800E-002 8.4310E-001
5.1100E-002 1.2290E-001 8.3860E-001	2.0100E-001 1.1000E-001 8.2650E-001	3.8200E-001 8.3500E-002 8.4410E-001
8.2300E-002 1.2400E-001 8.3670E-001	2.3300E-001 1.1000E-001 8.2650E-001	4.1900E-001 8.6200E-002 8.4570E-001
1.0600E-001 1.2560E-001 8.3410E-001	2.6400E-001 1.1000E-001 8.2650E-001	4.4500E-001 8.7700E-002 8.4660E-001
1.3300E-001 1.2620E-001 8.3310E-001	3.0500E-001 1.1000E-001 8.2700E-001	4.7500E-001 9.0300E-002 8.4820E-001
1.6900E-001 1.2640E-001 8.3260E-001	3.4400E-001 1.1000E-001 8.2720E-001	4.9100E-001 8.4300E-002 8.4100E-001
2.0100E-001 1.2720E-001 8.3130E-001	3.8200E-001 1.1000E-001 8.2910E-001	5.1700E-001 8.4300E-002 8.4130E-001
2.3300E-001 1.2730E-001 8.3130E-001	4.1900E-001 1.1000E-001 8.3230E-001	5.3700E-001 8.5000E-002 8.4250E-001
2.6400E-001 1.2720E-001 8.3130E-001	4.4500E-001 1.1000E-001 8.3400E-001	5.3700E-001 9.8900E-002 8.5701E-001
3.0500E-001 1.2700E-001 8.3170E-001	4.7500E-001 1.1000E-001 8.3700E-001	5.6200E-001 1.0199E-001 8.5519E-001
3.4400E-001 1.2690E-001 8.3180E-001	4.9100E-001 1.1000E-001 8.4060E-001	5.6200E-001 1.1000E-001 8.6000E-001
3.8200E-001 1.2590E-001 8.3350E-001	5.1700E-001 1.1000E-001 8.4420E-001	2.0000E-002 1.1000E-001 8.6000E-001
4.1900E-001 1.2430E-001 8.3620E-001	5.3700E-001 1.1000E-001 8.4850E-001	2.5130E-002 9.2200E-002 8.4930E-001
4.4500E-001 1.2340E-001 8.3770E-001	5.3700E-001 1.1000E-001 8.4850E-001	5.1100E-002 8.8600E-002 8.4710E-001
4.7500E-001 1.2180E-001 8.4030E-001	5.6200E-001 1.1000E-001 8.5066E-001	8.2300E-002 8.6700E-002 8.4600E-001
4.9100E-001 1.4150E-001 8.2350E-001	5.6200E-001 1.1000E-001 8.6000E-001	1.0600E-001 8.4100E-002 8.4440E-001
5.1700E-001 1.4130E-001 8.2370E-001	2.0000E-002 1.1000E-001 8.6000E-001	1.3300E-001 8.3100E-002 8.4380E-001
5.3700E-001 1.4160E-001 8.2320E-001	2.5130E-002 8.9200E-002 8.6000E-001	1.6900E-001 8.2600E-002 8.4360E-001
5.3700E-001 1.1299E-001 8.4890E-001	5.1100E-002 8.5000E-002 8.6000E-001	2.0100E-001 8.1300E-002 8.4280E-001
5.6200E-001 1.1481E-001 8.5199E-001	8.2300E-002 8.2800E-002 8.6000E-001	2.3300E-001 8.1300E-002 8.4270E-001
5.6200E-001 1.1000E-001 8.6000E-001	1.0600E-001 7.9800E-002 8.6000E-001	2.6400E-001 8.1300E-002 8.4280E-001
2.0000E-002 1.1000E-001 8.6000E-001	1.3300E-001 7.8600E-002 8.6000E-001	3.0500E-001 8.1700E-002 8.4300E-001
2.5130E-002 1.2070E-001 8.4220E-001	1.6900E-001 7.8100E-002 8.6000E-001	3.4400E-001 8.1800E-002 8.4310E-001
5.1100E-002 1.2290E-001 8.3860E-001	2.0100E-001 7.6500E-002 8.6000E-001	3.8200E-001 8.3500E-002 8.4410E-001
8.2300E-002 1.2400E-001 8.3670E-001	2.3300E-001 7.6500E-002 8.6000E-001	4.1900E-001 8.6200E-002 8.4570E-001
1.0600E-001 1.2560E-001 8.3410E-001	2.6400E-001 7.6500E-002 8.6000E-001	4.4500E-001 8.7700E-002 8.4660E-001
1.3300E-001 1.2620E-001 8.3310E-001	3.0500E-001 7.7000E-002 8.6000E-001	4.7500E-001 9.0300E-002 8.4820E-001
1.6900E-001 1.2640E-001 8.3260E-001	3.4400E-001 7.7200E-002 8.6000E-001	4.9100E-001 7.3500E-002 8.2850E-001
2.0100E-001 1.2720E-001 8.3130E-001	3.8200E-001 7.9100E-002 8.6000E-001	5.1700E-001 7.3700E-002 8.2870E-001
2.3300E-001 1.2730E-001 8.3130E-001	4.1900E-001 8.2300E-002 8.6000E-001	5.3700E-001 7.3200E-002 8.2840E-001
2.6400E-001 1.2720E-001 8.3130E-001	4.4500E-001 8.4000E-002 8.6000E-001	5.3700E-001 9.8900E-002 8.5701E-001
3.0500E-001 1.2700E-001 8.3170E-001	4.7500E-001 8.7000E-002 8.6000E-001	5.6200E-001 1.0199E-001 8.5519E-001
3.4400E-001 1.2690E-001 8.3180E-001	4.9100E-001 9.0600E-002 8.6000E-001	5.6200E-001 1.1000E-001 8.6000E-001
3.8200E-001 1.2590E-001 8.3350E-001	5.1700E-001 9.4200E-002 8.6000E-001	2.0000E-002 1.1000E-001 8.6000E-001
4.1900E-001 1.2430E-001 8.3620E-001	5.3700E-001 9.8500E-002 8.6000E-001	2.5130E-002 9.5300E-002 8.4530E-001
4.4500E-001 1.2340E-001 8.3770E-001	5.3700E-001 9.8500E-002 8.6000E-001	5.1100E-002 9.2300E-002 8.4230E-001
4.7500E-001 1.2180E-001 8.4030E-001	5.6200E-001 1.0066E-001 8.6000E-001	8.2300E-002 9.0700E-002 8.4070E-001
4.9100E-001 1.2900E-001 8.3430E-001	5.6200E-001 1.1000E-001 8.6000E-001	1.0600E-001 8.8600E-002 8.3860E-001
5.1700E-001 1.2870E-001 8.3430E-001	2.0000E-002 1.1000E-001 8.6000E-001	1.3300E-001 8.7800E-002 8.3780E-001
5.3700E-001 1.2750E-001 8.3500E-001	2.5130E-002 9.2200E-002 8.4930E-001	1.6900E-001 8.7400E-002 8.3740E-001
5.3700E-001 1.1299E-001 8.4890E-001	5.1100E-002 8.8600E-002 8.4710E-001	2.0100E-001 8.6300E-002 8.3630E-001
5.6200E-001 1.1481E-001 8.5199E-001	8.2300E-002 8.6700E-002 8.4600E-001	2.3300E-001 8.6300E-002 8.3630E-001
5.6200E-001 1.1000E-001 8.6000E-001	1.0600E-001 8.4100E-002 8.4440E-001	2.6400E-001 8.6300E-002 8.3630E-001
2.0000E-002 1.1000E-001 8.6000E-001	1.3300E-001 8.3100E-002 8.4380E-001	3.0500E-001 8.6600E-002 8.3660E-001
2.5130E-002 1.2070E-001 8.4220E-001	1.6900E-001 8.2600E-002 8.4360E-001	3.4400E-001 8.6800E-002 8.3680E-001
5.1100E-002 1.2290E-001 8.3860E-001	2.0100E-001 8.1300E-002 8.4280E-001	3.8200E-001 8.8200E-002 8.3820E-001
8.2300E-002 1.2400E-001 8.3670E-001	2.3300E-001 8.1300E-002 8.4270E-001	4.1900E-001 9.0400E-002 8.4040E-001
1.0600E-001 1.2560E-001 8.3410E-001	2.6400E-001 8.1300E-002 8.4280E-001	4.4500E-001 9.1600E-002 8.4160E-001
1.3300E-001 1.2620E-001 8.3310E-001	3.0500E-001 8.1700E-002 8.4300E-001	4.7500E-001 9.3800E-002 8.4380E-001
1.6900E-001 1.2640E-001 8.3260E-001	3.4400E-001 8.1800E-002 8.4310E-001	4.9100E-001 7.6000E-002 8.2600E-001
2.0100E-001 1.2720E-001 8.3130E-001	3.8200E-001 8.3500E-002 8.4410E-001	5.1700E-001 7.6200E-002 8.2620E-001

5.3700E-001 7.5800E-002 8.2580E-001	2.5130E-002 1.1000E-001 8.3920E-001	1.6900E-001 1.3740E-001 8.7640E-001
5.3700E-001 1.0188E-001 8.5188E-001	5.1100E-002 1.1000E-001 8.3500E-001	2.0100E-001 1.3870E-001 8.7720E-001
5.6200E-001 1.0340E-001 8.5340E-001	8.2300E-002 1.1000E-001 8.3280E-001	2.3300E-001 1.3870E-001 8.7730E-001
5.6200E-001 1.1000E-001 8.6000E-001	1.0600E-001 1.1000E-001 8.2980E-001	2.6400E-001 1.3870E-001 8.7720E-001
2.0000E-002 1.1000E-001 8.6000E-001	1.3300E-001 1.1000E-001 8.2860E-001	3.0500E-001 1.3830E-001 8.7700E-001
2.5130E-002 9.9300E-002 8.4220E-001	1.6900E-001 1.1000E-001 8.2810E-001	3.4400E-001 1.3820E-001 8.7690E-001
5.1100E-002 9.7100E-002 8.3860E-001	2.0100E-001 1.1000E-001 8.2650E-001	3.8200E-001 1.3650E-001 8.7590E-001
8.2300E-002 9.6000E-002 8.3670E-001	2.3300E-001 1.1000E-001 8.2650E-001	4.1900E-001 1.3380E-001 8.7430E-001
1.0600E-001 9.4400E-002 8.3410E-001	2.6400E-001 1.1000E-001 8.2650E-001	4.4500E-001 1.3230E-001 8.7340E-001
1.3300E-001 9.3800E-002 8.3310E-001	3.0500E-001 1.1000E-001 8.2700E-001	4.7500E-001 1.2970E-001 8.7180E-001
1.6900E-001 9.3600E-002 8.3260E-001	3.4400E-001 1.1000E-001 8.2720E-001	4.9100E-001 1.3570E-001 8.7900E-001
2.0100E-001 9.2800E-002 8.3130E-001	3.8200E-001 1.1000E-001 8.2910E-001	5.1700E-001 1.3570E-001 8.7870E-001
2.3300E-001 9.2700E-002 8.3130E-001	4.1900E-001 1.1000E-001 8.3230E-001	5.3700E-001 1.3500E-001 8.7750E-001
2.6400E-001 9.2800E-002 8.3130E-001	4.4500E-001 1.1000E-001 8.3400E-001	5.3700E-001 1.2110E-001 8.6299E-001
3.0500E-001 9.3000E-002 8.3170E-001	4.7500E-001 1.1000E-001 8.3700E-001	5.6200E-001 1.1801E-001 8.6481E-001
3.4400E-001 9.3100E-002 8.3180E-001	4.9100E-001 1.1000E-001 8.4060E-001	5.6200E-001 1.1000E-001 8.6000E-001
3.8200E-001 9.4100E-002 8.3350E-001	5.1700E-001 1.1000E-001 8.4420E-001	2.0000E-002 1.1000E-001 8.6000E-001
4.1900E-001 9.5700E-002 8.3620E-001	5.3700E-001 1.1000E-001 8.4850E-001	2.5130E-002 1.2780E-001 8.7070E-001
4.4500E-001 9.6600E-002 8.3770E-001	5.3700E-001 1.1000E-001 8.4850E-001	5.1100E-002 1.3140E-001 8.7290E-001
4.7500E-001 9.8200E-002 8.4030E-001	5.6200E-001 1.1000E-001 8.5066E-001	8.2300E-002 1.3330E-001 8.7400E-001
4.9100E-001 7.8500E-002 8.2350E-001	5.6200E-001 1.1000E-001 8.6000E-001	1.0600E-001 1.3590E-001 8.7560E-001
5.1700E-001 7.8700E-002 8.2370E-001	2.0000E-002 1.1000E-001 8.6000E-001	1.3300E-001 1.3690E-001 8.7620E-001
5.3700E-001 7.8400E-002 8.2320E-001	2.5130E-002 1.3080E-001 8.6000E-001	1.6900E-001 1.3740E-001 8.7640E-001
5.3700E-001 1.0701E-001 8.4890E-001	5.1100E-002 1.3500E-001 8.6000E-001	2.0100E-001 1.3870E-001 8.7720E-001
5.6200E-001 1.0519E-001 8.5199E-001	8.2300E-002 1.3720E-001 8.6000E-001	2.3300E-001 1.3870E-001 8.7730E-001
5.6200E-001 1.1000E-001 8.6000E-001	1.0600E-001 1.4020E-001 8.6000E-001	2.6400E-001 1.3870E-001 8.7720E-001
2.0000E-002 1.1000E-001 8.6000E-001	1.3300E-001 1.4140E-001 8.6000E-001	3.0500E-001 1.3830E-001 8.7700E-001
2.5130E-002 9.9300E-002 8.4220E-001	1.6900E-001 1.4190E-001 8.6000E-001	3.4400E-001 1.3820E-001 8.7690E-001
5.1100E-002 9.7100E-002 8.3860E-001	2.0100E-001 1.4350E-001 8.6000E-001	3.8200E-001 1.3650E-001 8.7590E-001
8.2300E-002 9.6000E-002 8.3670E-001	2.3300E-001 1.4350E-001 8.6000E-001	4.1900E-001 1.3380E-001 8.7430E-001
1.0600E-001 9.4400E-002 8.3410E-001	2.6400E-001 1.4350E-001 8.6000E-001	4.4500E-001 1.3230E-001 8.7340E-001
1.3300E-001 9.3800E-002 8.3310E-001	3.0500E-001 1.4300E-001 8.6000E-001	4.7500E-001 1.2970E-001 8.7180E-001
1.6900E-001 9.3600E-002 8.3260E-001	3.4400E-001 1.4280E-001 8.6000E-001	4.9100E-001 1.4650E-001 8.9150E-001
2.0100E-001 9.2800E-002 8.3130E-001	3.8200E-001 1.4090E-001 8.6000E-001	5.1700E-001 1.4630E-001 8.9130E-001
2.3300E-001 9.2700E-002 8.3130E-001	4.1900E-001 1.3770E-001 8.6000E-001	5.3700E-001 1.4680E-001 8.9160E-001
2.6400E-001 9.2800E-002 8.3130E-001	4.4500E-001 1.3600E-001 8.6000E-001	5.3700E-001 1.2110E-001 8.6299E-001
3.0500E-001 9.3000E-002 8.3170E-001	4.7500E-001 1.3300E-001 8.6000E-001	5.6200E-001 1.1801E-001 8.6481E-001
3.4400E-001 9.3100E-002 8.3180E-001	4.9100E-001 1.2940E-001 8.6000E-001	5.6200E-001 1.1000E-001 8.6000E-001
3.8200E-001 9.4100E-002 8.3350E-001	5.1700E-001 1.2580E-001 8.6000E-001	2.0000E-002 1.1000E-001 8.6000E-001
4.1900E-001 9.5700E-002 8.3620E-001	5.3700E-001 1.2150E-001 8.6000E-001	2.5130E-002 1.2470E-001 8.7470E-001
4.4500E-001 9.6600E-002 8.3770E-001	5.3700E-001 1.2150E-001 8.6000E-001	5.1100E-002 1.2770E-001 8.7770E-001
4.7500E-001 9.8200E-002 8.4030E-001	5.6200E-001 1.1934E-001 8.6000E-001	8.2300E-002 1.2930E-001 8.7930E-001
4.9100E-001 9.1000E-002 8.3430E-001	5.6200E-001 1.1000E-001 8.6000E-001	1.0600E-001 1.3140E-001 8.8140E-001
5.1700E-001 9.1300E-002 8.3430E-001	2.0000E-002 1.1000E-001 8.6000E-001	1.3300E-001 1.3220E-001 8.8220E-001
5.3700E-001 9.2500E-002 8.3500E-001	2.5130E-002 1.2780E-001 8.7070E-001	1.6900E-001 1.3260E-001 8.8260E-001
5.3700E-001 1.0701E-001 8.4890E-001	5.1100E-002 1.3140E-001 8.7290E-001	2.0100E-001 1.3370E-001 8.8370E-001
5.6200E-001 1.0519E-001 8.5199E-001	8.2300E-002 1.3330E-001 8.7400E-001	2.3300E-001 1.3370E-001 8.8370E-001
5.6200E-001 1.1000E-001 8.6000E-001	1.0600E-001 1.3590E-001 8.7560E-001	2.6400E-001 1.3370E-001 8.8370E-001
2.0000E-002 1.1000E-001 8.6000E-001	1.3300E-001 1.3690E-001 8.7620E-001	3.0500E-001 1.3340E-001 8.8340E-001
2.5130E-002 9.9300E-002 8.4220E-001	1.6900E-001 1.3740E-001 8.7640E-001	3.4400E-001 1.3320E-001 8.8320E-001
5.1100E-002 9.7100E-002 8.3860E-001	2.0100E-001 1.3870E-001 8.7720E-001	3.8200E-001 1.3180E-001 8.8180E-001
8.2300E-002 9.6000E-002 8.3670E-001	2.3300E-001 1.3870E-001 8.7730E-001	4.1900E-001 1.2960E-001 8.7960E-001
1.0600E-001 9.4400E-002 8.3410E-001	2.6400E-001 1.3870E-001 8.7720E-001	4.4500E-001 1.2840E-001 8.7840E-001
1.3300E-001 9.3800E-002 8.3310E-001	3.0500E-001 1.3830E-001 8.7700E-001	4.7500E-001 1.2620E-001 8.7620E-001
1.6900E-001 9.3600E-002 8.3260E-001	3.4400E-001 1.3820E-001 8.7690E-001	4.9100E-001 1.4400E-001 8.9400E-001
2.0100E-001 9.2800E-002 8.3130E-001	3.8200E-001 1.3650E-001 8.7590E-001	5.1700E-001 1.4380E-001 8.9380E-001
2.3300E-001 9.2700E-002 8.3130E-001	4.1900E-001 1.3380E-001 8.7430E-001	5.3700E-001 1.4420E-001 8.9420E-001
2.6400E-001 9.2800E-002 8.3130E-001	4.4500E-001 1.3230E-001 8.7340E-001	5.3700E-001 1.1812E-001 8.6812E-001
3.0500E-001 9.3000E-002 8.3170E-001	4.7500E-001 1.2970E-001 8.7180E-001	5.6200E-001 1.1660E-001 8.6660E-001
3.4400E-001 9.3100E-002 8.3180E-001	4.9100E-001 1.2710E-001 8.6913E-001	5.6200E-001 1.1000E-001 8.6000E-001
3.8200E-001 9.4100E-002 8.3350E-001	5.1700E-001 1.2450E-001 8.6621E-001	2.0000E-002 1.1000E-001 8.6000E-001
4.1900E-001 9.5700E-002 8.3620E-001	5.3700E-001 1.2110E-001 8.6299E-001	2.5130E-002 1.2070E-001 8.7780E-001
4.4500E-001 9.6600E-002 8.3770E-001	5.3700E-001 1.2110E-001 8.6299E-001	5.1100E-002 1.2290E-001 8.8140E-001
4.7500E-001 9.8200E-002 8.4030E-001	5.6200E-001 1.1801E-001 8.6481E-001	8.2300E-002 1.2400E-001 8.8330E-001
4.9100E-001 1.0087E-001 8.4290E-001	5.6200E-001 1.1000E-001 8.6000E-001	1.0600E-001 1.2560E-001 8.8590E-001
5.1700E-001 1.0379E-001 8.4550E-001	2.0000E-002 1.1000E-001 8.6000E-001	1.3300E-001 1.2620E-001 8.8690E-001
5.3700E-001 1.0701E-001 8.4890E-001	2.5130E-002 1.2780E-001 8.7070E-001	1.6900E-001 1.2640E-001 8.8740E-001
5.3700E-001 1.0701E-001 8.4890E-001	5.1100E-002 1.3140E-001 8.7290E-001	2.0100E-001 1.2720E-001 8.8870E-001
5.6200E-001 1.0519E-001 8.5199E-001	8.2300E-002 1.3330E-001 8.7400E-001	2.3300E-001 1.2730E-001 8.8870E-001
5.6200E-001 1.1000E-001 8.6000E-001	1.0600E-001 1.3590E-001 8.7560E-001	2.6400E-001 1.2720E-001 8.8870E-001
2.0000E-002 1.1000E-001 8.6000E-001	1.3300E-001 1.3690E-001 8.7620E-001	3.0500E-001 1.2700E-001 8.8830E-001

3.4400E-001 1.2690E-001 8.8820E-001	4.9100E-001 1.1000E-001 8.7940E-001	5.6200E-001 1.1000E-001 8.6000E-001
3.8200E-001 1.2590E-001 8.8650E-001	5.1700E-001 1.1000E-001 8.7580E-001	2.0000E-002 1.1000E-001 8.6000E-001
4.1900E-001 1.2430E-001 8.8380E-001	5.3700E-001 1.1000E-001 8.7150E-001	2.5130E-002 9.2200E-002 8.7070E-001
4.4500E-001 1.2340E-001 8.8230E-001	5.3700E-001 1.1000E-001 8.7150E-001	5.1100E-002 8.8600E-002 8.7290E-001
4.7500E-001 1.2180E-001 8.7970E-001	5.6200E-001 1.1000E-001 8.6934E-001	8.2300E-002 8.6700E-002 8.7400E-001
4.9100E-001 1.4150E-001 8.9650E-001	5.6200E-001 1.1000E-001 8.6000E-001	1.0600E-001 8.4100E-002 8.7560E-001
5.1700E-001 1.4130E-001 8.9630E-001	2.0000E-002 1.1000E-001 8.6000E-001	1.3300E-001 8.3100E-002 8.7620E-001
5.3700E-001 1.4160E-001 8.9680E-001	2.5130E-002 8.9200E-002 8.6000E-001	1.6900E-001 8.2600E-002 8.7640E-001
5.3700E-001 1.1299E-001 8.7110E-001	5.1100E-002 8.5000E-002 8.6000E-001	2.0100E-001 8.1300E-002 8.7720E-001
5.6200E-001 1.1481E-001 8.6801E-001	8.2300E-002 8.2800E-002 8.6000E-001	2.3300E-001 8.1300E-002 8.7730E-001
5.6200E-001 1.1000E-001 8.6000E-001	1.0600E-001 7.9800E-002 8.6000E-001	2.6400E-001 8.1300E-002 8.7720E-001
2.0000E-002 1.1000E-001 8.6000E-001	1.3300E-001 7.8600E-002 8.6000E-001	3.0500E-001 8.1700E-002 8.7700E-001
2.5130E-002 1.2070E-001 8.7780E-001	1.6900E-001 7.8100E-002 8.6000E-001	3.4400E-001 8.1800E-002 8.7690E-001
5.1100E-002 1.2290E-001 8.8140E-001	2.0100E-001 7.6500E-002 8.6000E-001	3.8200E-001 8.3500E-002 8.7590E-001
8.2300E-002 1.2400E-001 8.8330E-001	2.3300E-001 7.6500E-002 8.6000E-001	4.1900E-001 8.6200E-002 8.7430E-001
1.0600E-001 1.2560E-001 8.8590E-001	2.6400E-001 7.6500E-002 8.6000E-001	4.4500E-001 8.7700E-002 8.7340E-001
1.3300E-001 1.2620E-001 8.8690E-001	3.0500E-001 7.7000E-002 8.6000E-001	4.7500E-001 9.0300E-002 8.7180E-001
1.6900E-001 1.2640E-001 8.8740E-001	3.4400E-001 7.7200E-002 8.6000E-001	4.9100E-001 7.3500E-002 8.9150E-001
2.0100E-001 1.2720E-001 8.8870E-001	3.8200E-001 7.9100E-002 8.6000E-001	5.1700E-001 7.3700E-002 8.9130E-001
2.3300E-001 1.2730E-001 8.8870E-001	4.1900E-001 8.2300E-002 8.6000E-001	5.3700E-001 7.3200E-002 8.9160E-001
2.6400E-001 1.2720E-001 8.8870E-001	4.4500E-001 8.4000E-002 8.6000E-001	5.3700E-001 9.8900E-002 8.6299E-001
3.0500E-001 1.2700E-001 8.8830E-001	4.7500E-001 8.7000E-002 8.6000E-001	5.6200E-001 1.0199E-001 8.6481E-001
3.4400E-001 1.2690E-001 8.8820E-001	4.9100E-001 9.0600E-002 8.6000E-001	5.6200E-001 1.1000E-001 8.6000E-001
3.8200E-001 1.2590E-001 8.8650E-001	5.1700E-001 9.4200E-002 8.6000E-001	2.0000E-002 1.1000E-001 8.6000E-001
4.1900E-001 1.2430E-001 8.8380E-001	5.3700E-001 9.8500E-002 8.6000E-001	2.5130E-002 9.5300E-002 8.7470E-001
4.4500E-001 1.2340E-001 8.8230E-001	5.3700E-001 9.8500E-002 8.6000E-001	5.1100E-002 9.2300E-002 8.7770E-001
4.7500E-001 1.2180E-001 8.7970E-001	5.6200E-001 1.0066E-001 8.6000E-001	8.2300E-002 9.0700E-002 8.7930E-001
4.9100E-001 1.2900E-001 8.8570E-001	5.6200E-001 1.1000E-001 8.6000E-001	1.0600E-001 8.8600E-002 8.8140E-001
5.1700E-001 1.2870E-001 8.8570E-001	2.0000E-002 1.1000E-001 8.6000E-001	1.3300E-001 8.7800E-002 8.8220E-001
5.3700E-001 1.2750E-001 8.8500E-001	2.5130E-002 9.2200E-002 8.7070E-001	1.6900E-001 8.7400E-002 8.8260E-001
5.3700E-001 1.1299E-001 8.7110E-001	5.1100E-002 8.8600E-002 8.7290E-001	2.0100E-001 8.6300E-002 8.8370E-001
5.6200E-001 1.1481E-001 8.6801E-001	8.2300E-002 8.6700E-002 8.7400E-001	2.3300E-001 8.6300E-002 8.8370E-001
5.6200E-001 1.1000E-001 8.6000E-001	1.0600E-001 8.4100E-002 8.7560E-001	2.6400E-001 8.5300E-002 8.8370E-001
2.0000E-002 1.1000E-001 8.6000E-001	1.3300E-001 8.3100E-002 8.7620E-001	3.0500E-001 8.6600E-002 8.8340E-001
2.5130E-002 1.2070E-001 8.7780E-001	1.6900E-001 8.2600E-002 8.7640E-001	3.4400E-001 8.6800E-002 8.8320E-001
5.1100E-002 1.2290E-001 8.8140E-001	2.0100E-001 8.1300E-002 8.7720E-001	3.8200E-001 8.8200E-002 8.8180E-001
8.2300E-002 1.2400E-001 8.8330E-001	2.3300E-001 8.1300E-002 8.7730E-001	4.1900E-001 9.0400E-002 8.7960E-001
1.0600E-001 1.2560E-001 8.8590E-001	2.6400E-001 8.1300E-002 8.7720E-001	4.4500E-001 9.1600E-002 8.7840E-001
1.3300E-001 1.2620E-001 8.8690E-001	3.0500E-001 8.1700E-002 8.7700E-001	4.7500E-001 9.3800E-002 8.7620E-001
1.6900E-001 1.2640E-001 8.8740E-001	3.4400E-001 8.1800E-002 8.7690E-001	4.9100E-001 7.6000E-002 8.9400E-001
2.0100E-001 1.2720E-001 8.8870E-001	3.8200E-001 8.3500E-002 8.7590E-001	5.1700E-001 7.6200E-002 8.9380E-001
2.3300E-001 1.2730E-001 8.8870E-001	4.1900E-001 8.6200E-002 8.7430E-001	5.3700E-001 7.5800E-002 8.9420E-001
2.6400E-001 1.2720E-001 8.8870E-001	4.4500E-001 8.7700E-002 8.7340E-001	5.3700E-001 1.0188E-001 8.6812E-001
3.0500E-001 1.2700E-001 8.8830E-001	4.7500E-001 9.0300E-002 8.7180E-001	5.6200E-001 1.0340E-001 8.6660E-001
3.4400E-001 1.2690E-001 8.8820E-001	4.9100E-001 9.2900E-002 8.6913E-001	5.6200E-001 1.1000E-001 8.6000E-001
3.8200E-001 1.2590E-001 8.8650E-001	5.1700E-001 9.5500E-002 8.6621E-001	2.0000E-002 1.1000E-001 8.6000E-001
4.1900E-001 1.2430E-001 8.8380E-001	5.3700E-001 9.8900E-002 8.6299E-001	2.5130E-002 9.9300E-002 8.7780E-001
4.4500E-001 1.2340E-001 8.8230E-001	5.3700E-001 9.8900E-002 8.6299E-001	5.1100E-002 9.7100E-002 8.8140E-001
4.7500E-001 1.2180E-001 8.7970E-001	5.6200E-001 1.0199E-001 8.6481E-001	8.2300E-002 9.6000E-002 8.8330E-001
4.9100E-001 1.1913E-001 8.7710E-001	5.6200E-001 1.1000E-001 8.6000E-001	1.0600E-001 9.4400E-002 8.8590E-001
5.1700E-001 1.1621E-001 8.7450E-001	2.0000E-002 1.1000E-001 8.6000E-001	1.3300E-001 9.3800E-002 8.8690E-001
5.3700E-001 1.1299E-001 8.7110E-001	2.5130E-002 9.2200E-002 8.7070E-001	1.6900E-001 9.3600E-002 8.8740E-001
5.3700E-001 1.1299E-001 8.7110E-001	5.1100E-002 8.8600E-002 8.7290E-001	2.0100E-001 9.2800E-002 8.8870E-001
5.6200E-001 1.1481E-001 8.6801E-001	8.2300E-002 8.6700E-002 8.7400E-001	2.3300E-001 9.2700E-002 8.8870E-001
5.6200E-001 1.1000E-001 8.6000E-001	1.0600E-001 8.4100E-002 8.7560E-001	2.6400E-001 9.2800E-002 8.8870E-001
2.0000E-002 1.1000E-001 8.6000E-001	1.3300E-001 8.3100E-002 8.7620E-001	3.0500E-001 9.3000E-002 8.8830E-001
2.5130E-002 1.1000E-001 8.8080E-001	1.6900E-001 8.2600E-002 8.7640E-001	3.4400E-001 9.3100E-002 8.8820E-001
5.1100E-002 1.1000E-001 8.8500E-001	2.0100E-001 8.1300E-002 8.7720E-001	3.8200E-001 9.4100E-002 8.8650E-001
8.2300E-002 1.1000E-001 8.8720E-001	2.3300E-001 8.1300E-002 8.7730E-001	4.1900E-001 9.5700E-002 8.8380E-001
1.0600E-001 1.1000E-001 8.9020E-001	2.6400E-001 8.1300E-002 8.7720E-001	4.4500E-001 9.6600E-002 8.8230E-001
1.3300E-001 1.1000E-001 8.9140E-001	3.0500E-001 8.1700E-002 8.7700E-001	4.7500E-001 9.8200E-002 8.7970E-001
1.6900E-001 1.1000E-001 8.9190E-001	3.4400E-001 8.1800E-002 8.7690E-001	4.9100E-001 7.8500E-002 8.9650E-001
2.0100E-001 1.1000E-001 8.9350E-001	3.8200E-001 8.3500E-002 8.7590E-001	5.1700E-001 7.8700E-002 8.9630E-001
2.3300E-001 1.1000E-001 8.9350E-001	4.1900E-001 8.6200E-002 8.7430E-001	5.3700E-001 7.8400E-002 8.9680E-001
2.6400E-001 1.1000E-001 8.9350E-001	4.4500E-001 8.7700E-002 8.7340E-001	5.3700E-001 1.0701E-001 8.7110E-001
3.0500E-001 1.1000E-001 8.9300E-001	4.7500E-001 9.0300E-002 8.7180E-001	5.6200E-001 1.0519E-001 8.6801E-001
3.4400E-001 1.1000E-001 8.9280E-001	4.9100E-001 8.4300E-002 8.7900E-001	5.6200E-001 1.1000E-001 8.6000E-001
3.8200E-001 1.1000E-001 8.9090E-001	5.1700E-001 8.4300E-002 8.7870E-001	2.0000E-002 1.1000E-001 8.6000E-001
4.1900E-001 1.1000E-001 8.8770E-001	5.3700E-001 8.5000E-002 8.7750E-001	2.5130E-002 9.9300E-002 8.7780E-001
4.4500E-001 1.1000E-001 8.8600E-001	5.3700E-001 9.8900E-002 8.6299E-001	5.1100E-002 9.7100E-002 8.8140E-001
4.7500E-001 1.1000E-001 8.8300E-001	5.6200E-001 1.0199E-001 8.6481E-001	8.2300E-002 9.6000E-002 8.8330E-001

1.0600E-001 9.4400E-002 8.8590E-001
1.3300E-001 9.3800E-002 8.8690E-001
1.6900E-001 9.3600E-002 8.8740E-001
2.0100E-001 9.2800E-002 8.8870E-001
2.3300E-001 9.2700E-002 8.8870E-001
2.6400E-001 9.2800E-002 8.8870E-001
3.0500E-001 9.3000E-002 8.8830E-001
3.4400E-001 9.3100E-002 8.8820E-001
3.8200E-001 9.4100E-002 8.8650E-001
4.1900E-001 9.5700E-002 8.8380E-001
4.4500E-001 9.6600E-002 8.8230E-001
4.7500E-001 9.8200E-002 8.7970E-001
4.9100E-001 9.1000E-002 8.8570E-001
5.1700E-001 9.1300E-002 8.8570E-001
5.3700E-001 9.2500E-002 8.8500E-001
5.3700E-001 1.0701E-001 8.7110E-001
5.6200E-001 1.0519E-001 8.6801E-001
5.6200E-001 1.1000E-001 8.6000E-001
2.0000E-002 1.1000E-001 8.6000E-001
2.5130E-002 9.9300E-002 8.7780E-001
5.1100E-002 9.7100E-002 8.8140E-001
8.2300E-002 9.6000E-002 8.8330E-001
1.0600E-001 9.4400E-002 8.8590E-001
1.3300E-001 9.3800E-002 8.8690E-001
1.6900E-001 9.3600E-002 8.8740E-001
2.0100E-001 9.2800E-002 8.8870E-001
2.3300E-001 9.2700E-002 8.8870E-001
2.6400E-001 9.2800E-002 8.8870E-001
3.0500E-001 9.3000E-002 8.8830E-001
3.4400E-001 9.3100E-002 8.8820E-001
3.8200E-001 9.4100E-002 8.8650E-001
4.1900E-001 9.5700E-002 8.8380E-001
4.4500E-001 9.6600E-002 8.8230E-001
4.7500E-001 9.8200E-002 8.7970E-001
4.9100E-001 1.0087E-001 8.7710E-001
5.1700E-001 1.0379E-001 8.7450E-001
5.3700E-001 1.0701E-001 8.7110E-001
5.3700E-001 1.0701E-001 8.7110E-001
5.6200E-001 1.0519E-001 8.6801E-001
5.6200E-001 1.1000E-001 8.6000E-001
2.0000E-002 1.1000E-001 8.6000E-001
2.5130E-002 1.1000E-001 8.8080E-001
5.1100E-002 1.1000E-001 8.8500E-001
8.2300E-002 1.1000E-001 8.8720E-001
1.0600E-001 1.1000E-001 8.9020E-001
1.3300E-001 1.1000E-001 8.9140E-001
1.6900E-001 1.1000E-001 8.9190E-001
2.0100E-001 1.1000E-001 8.9350E-001
2.3300E-001 1.1000E-001 8.9350E-001
2.6400E-001 1.1000E-001 8.9350E-001
3.0500E-001 1.1000E-001 8.9300E-001
3.4400E-001 1.1000E-001 8.9280E-001
3.8200E-001 1.1000E-001 8.9090E-001
4.1900E-001 1.1000E-001 8.8770E-001
4.4500E-001 1.1000E-001 8.8600E-001
4.7500E-001 1.1000E-001 8.8300E-001
4.9100E-001 1.1000E-001 8.7940E-001
5.1700E-001 1.1000E-001 8.7580E-001
5.3700E-001 1.1000E-001 8.7150E-001
5.3700E-001 1.1000E-001 8.7150E-001
5.6200E-001 1.1000E-001 8.6934E-001
5.6200E-001 1.1000E-001 8.6000E-001
ZONE T="MK82out"
I=22, J=36, K=1,F=POINT
DT=(SINGLE SINGLE SINGLE)
2.0000E-002 1.1000E-001 9.7000E-001
2.5130E-002 1.3080E-001 9.7000E-001
5.1100E-002 1.3500E-001 9.7000E-001
8.2300E-002 1.3720E-001 9.7000E-001
1.0600E-001 1.4020E-001 9.7000E-001
1.3300E-001 1.4140E-001 9.7000E-001
1.6900E-001 1.4190E-001 9.7000E-001
2.0100E-001 1.4350E-001 9.7000E-001
2.3300E-001 1.4350E-001 9.7000E-001
2.6400E-001 1.4350E-001 9.7000E-001
3.0500E-001 1.4300E-001 9.7000E-001
3.4400E-001 1.4280E-001 9.7000E-001
3.8200E-001 1.4090E-001 9.7000E-001
4.1900E-001 1.3770E-001 9.7000E-001
4.4500E-001 1.3600E-001 9.7000E-001
4.7500E-001 1.3300E-001 9.7000E-001
4.9100E-001 1.2940E-001 9.7000E-001
5.1700E-001 1.2580E-001 9.7000E-001
5.3700E-001 1.2150E-001 9.7000E-001
5.3700E-001 1.2150E-001 9.7000E-001
5.6200E-001 1.1934E-001 9.7000E-001
5.6200E-001 1.1000E-001 9.7000E-001
2.0000E-002 1.1000E-001 9.7000E-001
2.5130E-002 1.2780E-001 9.5930E-001
5.1100E-002 1.3140E-001 9.5710E-001
8.2300E-002 1.3330E-001 9.5600E-001
1.0600E-001 1.3590E-001 9.5440E-001
1.3300E-001 1.3690E-001 9.5380E-001
1.6900E-001 1.3740E-001 9.5360E-001
2.0100E-001 1.3870E-001 9.5280E-001
2.3300E-001 1.3870E-001 9.5270E-001
2.6400E-001 1.3870E-001 9.5280E-001
3.0500E-001 1.3830E-001 9.5300E-001
3.4400E-001 1.3820E-001 9.5310E-001
3.8200E-001 1.3650E-001 9.5410E-001
4.1900E-001 1.3380E-001 9.5570E-001
4.4500E-001 1.3230E-001 9.5660E-001
4.7500E-001 1.2970E-001 9.5820E-001
4.9100E-001 1.2710E-001 9.6087E-001
5.1700E-001 1.2450E-001 9.6379E-001
5.3700E-001 1.2110E-001 9.6701E-001
5.3700E-001 1.2110E-001 9.6701E-001
5.6200E-001 1.1801E-001 9.6519E-001
5.6200E-001 1.1000E-001 9.7000E-001
2.0000E-002 1.1000E-001 9.7000E-001
2.5130E-002 1.2780E-001 9.5930E-001
5.1100E-002 1.3140E-001 9.5710E-001
8.2300E-002 1.3330E-001 9.5600E-001
1.0600E-001 1.3590E-001 9.5440E-001
1.3300E-001 1.3690E-001 9.5380E-001
1.6900E-001 1.3740E-001 9.5360E-001
2.0100E-001 1.3870E-001 9.5280E-001
2.3300E-001 1.3870E-001 9.5270E-001
2.6400E-001 1.3870E-001 9.5280E-001
3.0500E-001 1.3830E-001 9.5300E-001
3.4400E-001 1.3820E-001 9.5310E-001
3.8200E-001 1.3650E-001 9.5410E-001
4.1900E-001 1.3380E-001 9.5570E-001
4.4500E-001 1.3230E-001 9.5660E-001
4.7500E-001 1.2970E-001 9.5820E-001
4.9100E-001 1.3570E-001 9.5100E-001
5.1700E-001 1.3570E-001 9.5130E-001
5.3700E-001 1.3500E-001 9.5250E-001
5.3700E-001 1.2110E-001 9.6701E-001
5.6200E-001 1.1801E-001 9.6519E-001
5.6200E-001 1.1000E-001 9.7000E-001
2.0000E-002 1.1000E-001 9.7000E-001
2.5130E-002 1.2780E-001 9.5930E-001
5.1100E-002 1.3140E-001 9.5710E-001
8.2300E-002 1.3330E-001 9.5600E-001
1.0600E-001 1.3590E-001 9.5440E-001
1.3300E-001 1.3690E-001 9.5380E-001
1.6900E-001 1.3740E-001 9.5360E-001
2.0100E-001 1.3870E-001 9.5280E-001
2.3300E-001 1.3870E-001 9.5270E-001
2.6400E-001 1.3870E-001 9.5280E-001
3.0500E-001 1.3830E-001 9.5300E-001
3.4400E-001 1.3820E-001 9.5310E-001
3.8200E-001 1.3650E-001 9.5410E-001
4.1900E-001 1.3380E-001 9.5570E-001
4.4500E-001 1.3230E-001 9.5660E-001
4.7500E-001 1.2970E-001 9.5820E-001
4.9100E-001 1.4400E-001 9.3600E-001
5.1700E-001 1.4380E-001 9.3620E-001
5.3700E-001 1.4420E-001 9.3580E-001
5.3700E-001 1.1812E-001 9.6188E-001
5.6200E-001 1.1660E-001 9.6340E-001
5.6200E-001 1.1000E-001 9.7000E-001
2.0000E-002 1.1000E-001 9.7000E-001
2.5130E-002 1.2070E-001 9.5220E-001
5.1100E-002 1.2290E-001 9.4860E-001
8.2300E-002 1.2400E-001 9.4670E-001
1.0600E-001 1.2560E-001 9.4410E-001
1.3300E-001 1.2620E-001 9.4310E-001
1.6900E-001 1.2640E-001 9.4260E-001
2.0100E-001 1.2720E-001 9.4130E-001
2.3300E-001 1.2730E-001 9.4130E-001
2.6400E-001 1.2720E-001 9.4130E-001
3.0500E-001 1.2700E-001 9.4170E-001
3.4400E-001 1.2690E-001 9.4180E-001
3.8200E-001 1.2590E-001 9.4350E-001
4.1900E-001 1.2430E-001 9.4620E-001
4.4500E-001 1.2340E-001 9.4770E-001
4.7500E-001 1.2180E-001 9.5030E-001
4.9100E-001 1.4150E-001 9.3350E-001
5.1700E-001 1.4130E-001 9.3370E-001
5.3700E-001 1.4160E-001 9.3320E-001
5.3700E-001 1.1299E-001 9.5890E-001
5.6200E-001 1.1481E-001 9.6199E-001
5.6200E-001 1.1000E-001 9.7000E-001
2.0000E-002 1.1000E-001 9.7000E-001
2.5130E-002 1.2070E-001 9.5220E-001
5.1100E-002 1.2290E-001 9.4860E-001
8.2300E-002 1.2400E-001 9.4670E-001
1.0600E-001 1.2560E-001 9.4410E-001
1.3300E-001 1.2620E-001 9.4310E-001
1.6900E-001 1.2640E-001 9.4260E-001
2.0100E-001 1.2720E-001 9.4130E-001
2.3300E-001 1.2730E-001 9.4130E-001
2.6400E-001 1.2720E-001 9.4130E-001
3.0500E-001 1.2700E-001 9.4170E-001
3.4400E-001 1.2690E-001 9.4180E-001
3.8200E-001 1.2590E-001 9.4350E-001
4.1900E-001 1.2430E-001 9.4620E-001
4.4500E-001 1.2340E-001 9.4770E-001
4.7500E-001 1.2180E-001 9.5030E-001

4.9100E-001	1.2900E-001	9.4430E-001	5.6200E-001	1.1000E-001	9.7000E-001	1.0600E-001	8.8600E-002	9.4860E-001
5.1700E-001	1.2870E-001	9.4430E-001	2.0000E-002	1.1000E-001	9.7000E-001	1.3300E-001	8.7800E-002	9.4780E-001
5.3700E-001	1.2750E-001	9.4500E-001	2.5130E-002	9.2200E-002	9.5930E-001	1.6900E-001	8.7400E-002	9.4740E-001
5.3700E-001	1.1299E-001	9.5890E-001	5.1100E-002	8.8600E-002	9.5710E-001	2.0100E-001	8.6300E-002	9.4630E-001
5.6200E-001	1.1481E-001	9.6199E-001	8.2300E-002	8.6700E-002	9.5600E-001	2.3300E-001	8.6300E-002	9.4630E-001
5.6200E-001	1.1000E-001	9.7000E-001	1.0600E-001	8.4100E-002	9.5440E-001	2.6400E-001	8.6300E-002	9.4630E-001
2.0000E-002	1.1000E-001	9.7000E-001	1.3300E-001	8.3100E-002	9.5380E-001	3.0500E-001	8.6600E-002	9.4660E-001
2.5130E-002	1.2070E-001	9.5220E-001	1.6900E-001	8.2600E-002	9.5360E-001	3.4400E-001	8.6800E-002	9.4680E-001
5.1100E-002	1.2290E-001	9.4860E-001	2.0100E-001	8.1300E-002	9.5280E-001	3.8200E-001	8.8200E-002	9.4820E-001
8.2300E-002	1.2400E-001	9.4670E-001	2.3300E-001	8.1300E-002	9.5270E-001	4.1900E-001	9.0400E-002	9.5040E-001
1.0600E-001	1.2560E-001	9.4410E-001	2.6400E-001	8.1300E-002	9.5280E-001	4.4500E-001	9.1600E-002	9.5160E-001
1.3300E-001	1.2620E-001	9.4310E-001	3.0500E-001	8.1700E-002	9.5300E-001	4.7500E-001	9.3800E-002	9.5380E-001
1.6900E-001	1.2640E-001	9.4260E-001	3.4400E-001	8.1800E-002	9.5310E-001	4.9100E-001	7.6000E-002	9.3600E-001
2.0100E-001	1.2720E-001	9.4130E-001	3.8200E-001	8.3500E-002	9.5410E-001	5.1700E-001	7.6200E-002	9.3620E-001
2.3300E-001	1.2730E-001	9.4130E-001	4.1900E-001	8.6200E-002	9.5570E-001	5.3700E-001	7.5800E-002	9.3580E-001
2.6400E-001	1.2720E-001	9.4130E-001	4.4500E-001	8.7700E-002	9.5660E-001	5.3700E-001	1.0188E-001	9.6188E-001
3.0500E-001	1.2700E-001	9.4170E-001	4.7500E-001	9.0300E-002	9.5820E-001	5.6200E-001	1.0340E-001	9.6340E-001
3.4400E-001	1.2690E-001	9.4180E-001	4.9100E-001	9.2900E-002	9.6087E-001	5.6200E-001	1.1000E-001	9.7000E-001
3.8200E-001	1.2590E-001	9.4350E-001	5.1700E-001	9.5500E-002	9.6379E-001	2.0000E-002	1.1000E-001	9.7000E-001
4.1900E-001	1.2430E-001	9.4620E-001	5.3700E-001	9.8900E-002	9.6701E-001	2.5130E-002	9.9300E-002	9.5220E-001
4.4500E-001	1.2340E-001	9.4770E-001	5.3700E-001	9.8900E-002	9.6701E-001	5.1100E-002	9.7100E-002	9.4860E-001
4.7500E-001	1.2180E-001	9.5030E-001	5.6200E-001	1.0199E-001	9.6519E-001	8.2300E-002	9.6000E-002	9.4670E-001
4.9100E-001	1.1913E-001	9.5290E-001	5.6200E-001	1.1000E-001	9.7000E-001	1.0600E-001	9.4400E-002	9.4410E-001
5.1700E-001	1.1621E-001	9.5550E-001	2.0000E-002	1.1000E-001	9.7000E-001	1.3300E-001	9.3800E-002	9.4310E-001
5.3700E-001	1.1299E-001	9.5890E-001	2.5130E-002	9.2200E-002	9.5930E-001	1.6900E-001	9.3600E-002	9.4260E-001
5.3700E-001	1.1299E-001	9.5890E-001	5.1100E-002	8.8600E-002	9.5710E-001	2.0100E-001	9.2800E-002	9.4130E-001
5.6200E-001	1.1481E-001	9.6199E-001	8.2300E-002	8.6700E-002	9.5600E-001	2.3300E-001	9.2700E-002	9.4130E-001
5.6200E-001	1.1000E-001	9.7000E-001	1.0600E-001	8.4100E-002	9.5440E-001	2.6400E-001	9.2800E-002	9.4130E-001
2.0000E-002	1.1000E-001	9.7000E-001	1.3300E-001	8.3100E-002	9.5380E-001	3.0500E-001	9.3000E-002	9.4170E-001
2.5130E-002	1.1000E-001	9.4920E-001	1.6900E-001	8.2600E-002	9.5360E-001	3.4400E-001	9.3100E-002	9.4180E-001
5.1100E-002	1.1000E-001	9.4500E-001	2.0100E-001	8.1300E-002	9.5280E-001	3.8200E-001	9.4100E-002	9.4350E-001
8.2300E-002	1.1000E-001	9.4280E-001	2.3300E-001	8.1300E-002	9.5270E-001	4.1900E-001	9.5700E-002	9.4620E-001
1.0600E-001	1.1000E-001	9.3980E-001	2.6400E-001	8.1300E-002	9.5280E-001	4.4500E-001	9.6600E-002	9.4770E-001
1.3300E-001	1.1000E-001	9.3860E-001	3.0500E-001	8.1700E-002	9.5300E-001	4.7500E-001	9.8200E-002	9.5030E-001
1.6900E-001	1.1000E-001	9.3810E-001	3.4400E-001	8.1800E-002	9.5310E-001	4.9100E-001	7.8500E-002	9.3350E-001
2.0100E-001	1.1000E-001	9.3650E-001	3.8200E-001	8.3500E-002	9.5410E-001	5.1700E-001	7.8700E-002	9.3370E-001
2.3300E-001	1.1000E-001	9.3650E-001	4.1900E-001	8.6200E-002	9.5570E-001	5.3700E-001	7.8400E-002	9.3320E-001
2.6400E-001	1.1000E-001	9.3650E-001	4.4500E-001	8.7700E-002	9.5660E-001	5.3700E-001	1.0701E-001	9.5890E-001
3.0500E-001	1.1000E-001	9.3700E-001	4.7500E-001	9.0300E-002	9.5820E-001	5.6200E-001	1.0519E-001	9.6199E-001
3.4400E-001	1.1000E-001	9.3720E-001	4.9100E-001	8.4300E-002	9.5100E-001	5.6200E-001	1.1000E-001	9.7000E-001
3.8200E-001	1.1000E-001	9.3910E-001	5.1700E-001	8.4300E-002	9.5130E-001	2.0000E-002	1.1000E-001	9.7000E-001
4.1900E-001	1.1000E-001	9.4230E-001	5.3700E-001	8.5000E-002	9.5250E-001	2.5130E-002	9.9300E-002	9.5220E-001
4.4500E-001	1.1000E-001	9.4400E-001	5.3700E-001	9.8900E-002	9.6701E-001	5.1100E-002	9.7100E-002	9.4860E-001
4.7500E-001	1.1000E-001	9.4700E-001	5.6200E-001	1.0199E-001	9.6519E-001	8.2300E-002	9.6000E-002	9.4670E-001
4.9100E-001	1.1000E-001	9.5060E-001	5.6200E-001	1.1000E-001	9.7000E-001	1.0600E-001	9.4400E-002	9.4410E-001
5.1700E-001	1.1000E-001	9.5420E-001	2.0000E-002	1.1000E-001	9.7000E-001	1.3300E-001	9.3800E-002	9.4310E-001
5.3700E-001	1.1000E-001	9.5850E-001	2.5130E-002	9.2200E-002	9.5930E-001	1.6900E-001	9.3600E-002	9.4260E-001
5.3700E-001	1.1000E-001	9.5850E-001	5.1100E-002	8.8600E-002	9.5710E-001	2.0100E-001	9.2800E-002	9.4130E-001
5.6200E-001	1.1000E-001	9.6066E-001	8.2300E-002	8.6700E-002	9.5600E-001	2.3300E-001	9.2700E-002	9.4130E-001
5.6200E-001	1.1000E-001	9.7000E-001	1.0600E-001	8.4100E-002	9.5440E-001	2.6400E-001	9.2800E-002	9.4130E-001
2.0000E-002	1.1000E-001	9.7000E-001	1.3300E-001	8.3100E-002	9.5380E-001	3.0500E-001	9.3000E-002	9.4170E-001
2.5130E-002	8.9200E-002	9.7000E-001	1.6900E-001	8.2600E-002	9.5360E-001	3.4400E-001	9.3100E-002	9.4180E-001
5.1100E-002	8.5000E-002	9.7000E-001	2.0100E-001	8.1300E-002	9.5280E-001	3.8200E-001	9.4100E-002	9.4350E-001
8.2300E-002	8.2800E-002	9.7000E-001	2.3300E-001	8.1300E-002	9.5270E-001	4.1900E-001	9.5700E-002	9.4620E-001
1.0600E-001	7.9800E-002	9.7000E-001	2.6400E-001	8.1300E-002	9.5280E-001	4.4500E-001	9.6600E-002	9.4770E-001
1.3300E-001	7.8600E-002	9.7000E-001	3.0500E-001	8.1700E-002	9.5300E-001	4.7500E-001	9.8200E-002	9.5030E-001
1.6900E-001	7.8100E-002	9.7000E-001	3.4400E-001	8.1800E-002	9.5310E-001	4.9100E-001	9.1000E-002	9.4430E-001
2.0100E-001	7.6500E-002	9.7000E-001	3.8200E-001	8.3500E-002	9.5410E-001	5.1700E-001	9.1300E-002	9.4430E-001
2.3300E-001	7.6500E-002	9.7000E-001	4.1900E-001	8.6200E-002	9.5570E-001	5.3700E-001	9.2500E-002	9.4590E-001
2.6400E-001	7.6500E-002	9.7000E-001	4.4500E-001	8.7700E-002	9.5660E-001	5.3700E-001	1.0701E-001	9.5890E-001
3.0500E-001	7.7000E-002	9.7000E-001	4.7500E-001	9.0300E-002	9.5820E-001	5.6200E-001	1.0519E-001	9.6199E-001
3.4400E-001	7.7200E-002	9.7000E-001	4.9100E-001	7.3500E-002	9.3850E-001	5.6200E-001	1.1000E-001	9.7000E-001
3.8200E-001	7.9100E-002	9.7000E-001	5.1700E-001	7.3700E-002	9.3870E-001	2.0000E-002	1.1000E-001	9.7000E-001
4.1900E-001	8.2300E-002	9.7000E-001	5.3700E-001	7.3200E-002	9.3840E-001	2.5130E-002	9.9300E-002	9.5220E-001
4.4500E-001	8.4000E-002	9.7000E-001	5.3700E-001	9.8900E-002	9.6701E-001	5.1100E-002	9.7100E-002	9.4860E-001
4.7500E-001	8.7000E-002	9.7000E-001	5.6200E-001	1.0199E-001	9.6519E-001	8.2300E-002	9.6000E-002	9.4670E-001
4.9100E-001	9.0600E-002	9.7000E-001	5.6200E-001	1.1000E-001	9.7000E-001	1.0600E-001	9.4400E-002	9.4410E-001
5.1700E-001	9.4200E-002	9.7000E-001	2.0000E-002	1.1000E-001	9.7000E-001	1.3300E-001	9.3800E-002	9.4310E-001
5.3700E-001	9.8500E-002	9.7000E-001	2.5130E-002	9.5300E-002	9.5530E-001	1.6900E-001	9.3600E-002	9.4260E-001
5.3700E-001	9.8500E-002	9.7000E-001	5.1100E-002	9.2300E-002	9.5230E-001	2.0100E-001	9.2800E-002	9.4130E-001
5.6200E-001	1.0066E-001	9.7000E-001	8.2300E-002	9.0700E-002	9.5070E-001	2.3300E-001	9.2700E-002	9.4130E-001

2.6400E-001 9.2800E-002 9.4130E-001
3.0500E-001 9.3000E-002 9.4170E-001
3.4400E-001 9.3100E-002 9.4180E-001
3.8200E-001 9.4100E-002 9.4350E-001
4.1900E-001 9.5700E-002 9.4620E-001
4.4500E-001 9.6600E-002 9.4770E-001
4.7500E-001 9.8200E-002 9.5030E-001
4.9100E-001 1.0087E-001 9.5290E-001
5.1700E-001 1.0379E-001 9.5550E-001
5.3700E-001 1.0701E-001 9.5890E-001
5.3700E-001 1.0701E-001 9.5890E-001
5.6200E-001 1.0519E-001 9.6199E-001
5.6200E-001 1.1000E-001 9.7000E-001
2.0000E-002 1.1000E-001 9.7000E-001
2.5130E-002 1.1000E-001 9.4920E-001
5.1100E-002 1.1000E-001 9.4500E-001
8.2300E-002 1.1000E-001 9.4280E-001
1.0600E-001 1.1000E-001 9.3980E-001
1.3300E-001 1.1000E-001 9.3860E-001
1.6900E-001 1.1000E-001 9.3810E-001
2.0100E-001 1.1000E-001 9.3650E-001
2.3300E-001 1.1000E-001 9.3650E-001
2.6400E-001 1.1000E-001 9.3650E-001
3.0500E-001 1.1000E-001 9.3700E-001
3.4400E-001 1.1000E-001 9.3720E-001
3.8200E-001 1.1000E-001 9.3910E-001
4.1900E-001 1.1000E-001 9.4230E-001
4.4500E-001 1.1000E-001 9.4400E-001
4.7500E-001 1.1000E-001 9.4700E-001
4.9100E-001 1.1000E-001 9.5060E-001
5.1700E-001 1.1000E-001 9.5420E-001
5.3700E-001 1.1000E-001 9.5850E-001
5.3700E-001 1.1000E-001 9.5850E-001
5.6200E-001 1.1000E-001 9.6066E-001
5.6200E-001 1.1000E-001 9.7000E-001
2.0000E-002 1.1000E-001 9.7000E-001
2.5130E-002 1.3080E-001 9.7000E-001
5.1100E-002 1.3500E-001 9.7000E-001
8.2300E-002 1.3720E-001 9.7000E-001
1.0600E-001 1.4020E-001 9.7000E-001
1.3300E-001 1.4140E-001 9.7000E-001
1.6900E-001 1.4190E-001 9.7000E-001
2.0100E-001 1.4350E-001 9.7000E-001
2.3300E-001 1.4350E-001 9.7000E-001
2.6400E-001 1.4350E-001 9.7000E-001
3.0500E-001 1.4300E-001 9.7000E-001
3.4400E-001 1.4280E-001 9.7000E-001
3.8200E-001 1.4090E-001 9.7000E-001
4.1900E-001 1.3770E-001 9.7000E-001
4.4500E-001 1.3600E-001 9.7000E-001
4.7500E-001 1.3300E-001 9.7000E-001
4.9100E-001 1.2940E-001 9.7000E-001
5.1700E-001 1.2580E-001 9.7000E-001
5.3700E-001 1.2150E-001 9.7000E-001
5.3700E-001 1.2150E-001 9.7000E-001
5.6200E-001 1.1934E-001 9.7000E-001
5.6200E-001 1.1000E-001 9.7000E-001
2.0000E-002 1.1000E-001 9.7000E-001
2.5130E-002 1.2780E-001 9.8070E-001
5.1100E-002 1.3140E-001 9.8290E-001
8.2300E-002 1.3330E-001 9.8400E-001
1.0600E-001 1.3590E-001 9.8560E-001
1.3300E-001 1.3690E-001 9.8620E-001
1.6900E-001 1.3740E-001 9.8640E-001
2.0100E-001 1.3870E-001 9.8720E-001
2.3300E-001 1.3870E-001 9.8730E-001
2.6400E-001 1.3870E-001 9.8720E-001
3.0500E-001 1.3830E-001 9.8700E-001
3.4400E-001 1.3820E-001 9.8690E-001
3.8200E-001 1.3650E-001 9.8590E-001
4.1900E-001 1.3380E-001 9.8430E-001
4.4500E-001 1.3230E-001 9.8340E-001
4.7500E-001 1.2970E-001 9.8180E-001
4.9100E-001 1.2710E-001 9.7913E-001
5.1700E-001 1.2450E-001 9.7621E-001
5.3700E-001 1.2110E-001 9.7299E-001
5.3700E-001 1.2110E-001 9.7299E-001
5.6200E-001 1.1801E-001 9.7481E-001
5.6200E-001 1.1000E-001 9.7000E-001
2.0000E-002 1.1000E-001 9.7000E-001
2.5130E-002 1.2780E-001 9.8070E-001
5.1100E-002 1.3140E-001 9.8290E-001
8.2300E-002 1.3330E-001 9.8400E-001
1.0600E-001 1.3590E-001 9.8560E-001
1.3300E-001 1.3690E-001 9.8620E-001
1.6900E-001 1.3740E-001 9.8640E-001
2.0100E-001 1.3870E-001 9.8720E-001
2.3300E-001 1.3870E-001 9.8730E-001
2.6400E-001 1.3870E-001 9.8720E-001
3.0500E-001 1.3830E-001 9.8700E-001
3.4400E-001 1.3820E-001 9.8690E-001
3.8200E-001 1.3650E-001 9.8590E-001
4.1900E-001 1.3380E-001 9.8430E-001
4.4500E-001 1.3230E-001 9.8340E-001
4.7500E-001 1.2970E-001 9.8180E-001
4.9100E-001 1.3570E-001 9.8900E-001
5.1700E-001 1.3570E-001 9.8870E-001
5.3700E-001 1.3500E-001 9.8750E-001
5.3700E-001 1.2110E-001 9.7299E-001
5.6200E-001 1.1801E-001 9.7481E-001
5.6200E-001 1.1000E-001 9.7000E-001
2.0000E-002 1.1000E-001 9.7000E-001
2.5130E-002 1.2780E-001 9.8070E-001
5.1100E-002 1.3140E-001 9.8290E-001
8.2300E-002 1.3330E-001 9.8400E-001
1.0600E-001 1.3590E-001 9.8560E-001
1.3300E-001 1.3690E-001 9.8620E-001
1.6900E-001 1.3740E-001 9.8640E-001
2.0100E-001 1.3870E-001 9.8720E-001
2.3300E-001 1.3870E-001 9.8730E-001
2.6400E-001 1.3870E-001 9.8720E-001
3.0500E-001 1.3830E-001 9.8700E-001
3.4400E-001 1.3820E-001 9.8690E-001
3.8200E-001 1.3650E-001 9.8590E-001
4.1900E-001 1.3380E-001 9.8430E-001
4.4500E-001 1.3230E-001 9.8340E-001
4.7500E-001 1.2970E-001 9.8180E-001
4.9100E-001 1.4650E-001 1.0015E-000
5.1700E-001 1.4630E-001 1.0013E-000
5.3700E-001 1.4680E-001 1.0016E-000
5.3700E-001 1.2110E-001 9.7299E-001
5.6200E-001 1.1801E-001 9.7481E-001
5.6200E-001 1.1000E-001 9.7000E-001
2.0000E-002 1.1000E-001 9.7000E-001
2.5130E-002 1.2470E-001 9.8470E-001
5.1100E-002 1.2770E-001 9.8770E-001
8.2300F-002 1.2930E-001 9.8930E-001
1.0600E-001 1.3140E-001 9.9140E-001
1.3300E-001 1.3220E-001 9.9220E-001
1.6900E-001 1.3260E-001 9.9260E-001
2.0100E-001 1.3370E-001 9.9370E-001
2.3300E-001 1.3370E-001 9.9370E-001
2.6400E-001 1.3370E-001 9.9370E-001
3.0500E-001 1.3340E-001 9.9340E-001
3.4400E-001 1.3320E-001 9.9320E-001
3.8200E-001 1.3180E-001 9.9180E-001
4.1900E-001 1.2960E-001 9.8960E-001
4.4500E-001 1.2840E-001 9.8840E-001
4.7500E-001 1.2620E-001 9.8620E-001
4.9100E-001 1.4400E-001 1.0040E-000
5.1700E-001 1.4380E-001 1.0038E-000
5.3700E-001 1.4420E-001 1.0042E-000
5.3700E-001 1.1812E-001 9.7812E-001
5.6200E-001 1.1660E-001 9.7660E-001
5.6200E-001 1.1000E-001 9.7000E-001
2.0000E-002 1.1000E-001 9.7000E-001
2.5130E-002 1.2070E-001 9.8780E-001
5.1100E-002 1.2290E-001 9.9140E-001
8.2300E-002 1.2400E-001 9.9330E-001
1.0600E-001 1.2560E-001 9.9590E-001
1.3300E-001 1.2620E-001 9.9690E-001
1.6900E-001 1.2640E-001 9.9740E-001
2.0100E-001 1.2720E-001 9.9870E-001
2.3300E-001 1.2730E-001 9.9870E-001
2.6400E-001 1.2720E-001 9.9870E-001
3.0500E-001 1.2700E-001 9.9830E-001
3.4400E-001 1.2690E-001 9.9820E-001
3.8200E-001 1.2590E-001 9.9650E-001
4.1900E-001 1.2430E-001 9.9380E-001
4.4500E-001 1.2340E-001 9.9230E-001
4.7500E-001 1.2180E-001 9.8970E-001
4.9100E-001 1.4150E-001 1.0065E-000
5.1700E-001 1.4130E-001 1.0063E-000
5.3700E-001 1.4160E-001 1.0068E-000
5.3700E-001 1.1299E-001 9.8110E-001
5.6200E-001 1.1481E-001 9.7801E-001
5.6200E-001 1.1000E-001 9.7000E-001
2.0000E-002 1.1000E-001 9.7000E-001
2.5130E-002 1.2070E-001 9.8780E-001
5.1100E-002 1.2290E-001 9.9140E-001
8.2300E-002 1.2400E-001 9.9330E-001
1.0600E-001 1.2560E-001 9.9590E-001
1.3300E-001 1.2620E-001 9.9690E-001
1.6900E-001 1.2640E-001 9.9740E-001
2.0100E-001 1.2720E-001 9.9870E-001
2.3300E-001 1.2730E-001 9.9870E-001
2.6400E-001 1.2720E-001 9.9870E-001
3.0500E-001 1.2700E-001 9.9830E-001
3.4400E-001 1.2690E-001 9.9820E-001
3.8200E-001 1.2590E-001 9.9650E-001
4.1900E-001 1.2430E-001 9.9380E-001
4.4500E-001 1.2340E-001 9.9230E-001
4.7500E-001 1.2180E-001 9.8970E-001
4.9100E-001 1.1913E-001 9.8710E-001
5.1700E-001 1.1621E-001 9.8450E-001
5.3700E-001 1.1299E-001 9.8110E-001
5.3700E-001 1.1299E-001 9.8110E-001
5.6200E-001 1.1481E-001 9.7801E-001
5.6200E-001 1.1000E-001 9.7000E-001
2.0000E-002 1.1000E-001 9.7000E-001
2.5130E-002 1.1000E-001 9.9080E-001

5.1100E-002 1.1000E-001 9.9500E-001	2.0100E-001 8.1300E-002 9.8720E-001	3.8200E-001 9.4100E-002 9.9650E-001
8.2300E-002 1.1000E-001 9.9720E-001	2.3300E-001 8.1300E-002 9.8730E-001	4.1900E-001 9.5700E-002 9.9380E-001
1.0600E-001 1.1000E-001 1.0002E-000	2.6400E-001 8.1300E-002 9.8720E-001	4.4500E-001 9.6600E-002 9.9230E-001
1.3300E-001 1.1000E-001 1.0014E-000	3.0500E-001 8.1700E-002 9.8700E-001	4.7500E-001 9.8200E-002 9.8970E-001
1.6900E-001 1.1000E-001 1.0019E-000	3.4400E-001 8.1800E-002 9.8690E-001	4.9100E-001 7.8500E-002 1.0065E-000
2.0100E-001 1.1000E-001 1.0035E-000	3.8200E-001 8.3500E-002 9.8590E-001	5.1700E-001 7.8700E-002 1.0063E-000
2.3300E-001 1.1000E-001 1.0035E-000	4.1900E-001 8.6200E-002 9.8430E-001	5.3700E-001 7.8400E-002 1.0068E-000
2.6400E-001 1.1000E-001 1.0035E-000	4.4500E-001 8.7700E-002 9.8340E-001	5.3700E-001 1.0701E-001 9.8110E-001
3.0500E-001 1.1000E-001 1.0030E-000	4.7500E-001 9.0300E-002 9.8180E-001	5.6200E-001 1.0519E-001 9.7801E-001
3.4400E-001 1.1000E-001 1.0028E-000	4.9100E-001 8.4300E-002 9.8900E-001	5.6200E-001 1.1000E-001 9.7000E-001
3.8200E-001 1.1000E-001 1.0009E-000	5.1700E-001 8.4300E-002 9.8870E-001	2.0000E-002 1.1000E-001 9.7000E-001
4.1900E-001 1.1000E-001 9.9770E-001	5.3700E-001 8.5000E-002 9.8750E-001	2.5130E-002 9.9300E-002 9.8780E-001
4.4500E-001 1.1000E-001 9.9600E-001	5.3700E-001 9.8900E-002 9.7299E-001	5.1100E-002 9.7100E-002 9.9140E-001
4.7500E-001 1.1000E-001 9.9300E-001	5.6200E-001 1.0199E-001 9.7481E-001	8.2300E-002 9.6000E-002 9.9330E-001
4.9100E-001 1.1000E-001 9.8940E-001	5.6200E-001 1.1000E-001 9.7000E-001	1.0600E-001 9.4400E-002 9.9590E-001
5.1700E-001 1.1000E-001 9.8580E-001	2.0000E-002 1.1000E-001 9.7000E-001	1.3300E-001 9.3800E-002 9.9690E-001
5.3700E-001 1.1000E-001 9.8150E-001	2.5130E-002 9.2200E-002 9.8070E-001	1.6900E-001 9.3600E-002 9.9740E-001
5.3700E-001 1.1000E-001 9.8150E-001	5.1100E-002 8.8600E-002 9.8290E-001	2.0100E-001 9.2800E-002 9.9870E-001
5.6200E-001 1.1000E-001 9.7934E-001	8.2300E-002 8.6700E-002 9.8400E-001	2.3300E-001 9.2700E-002 9.9870E-001
5.6200E-001 1.1000E-001 9.7000E-001	1.0600E-001 8.4100E-002 9.8560E-001	2.6400E-001 9.2800E-002 9.9870E-001
2.0000E-002 1.1000E-001 9.7000E-001	1.3300E-001 8.3100E-002 9.8620E-001	3.0500E-001 9.3000E-002 9.9830E-001
2.5130E-002 8.9200E-002 9.7000E-001	1.6900E-001 8.2600E-002 9.8640E-001	3.4400E-001 9.3100E-002 9.9820E-001
5.1100E-002 8.5000E-002 9.7000E-001	2.0100E-001 8.1300E-002 9.8720E-001	3.8200E-001 9.4100E-002 9.9650E-001
8.2300E-002 8.2800E-002 9.7000E-001	2.3300E-001 8.1300E-002 9.8730E-001	4.1900E-001 9.5700E-002 9.9380E-001
1.0600E-001 7.9800E-002 9.7000E-001	2.6400E-001 8.1300E-002 9.8720E-001	4.4500E-001 9.6600E-002 9.9230E-001
1.3300E-001 7.8600E-002 9.7000E-001	3.0500E-001 8.1700E-002 9.8700E-001	4.7500E-001 9.8200E-002 9.8970E-001
1.6900E-001 7.8100E-002 9.7000E-001	3.4400E-001 8.1800E-002 9.8690E-001	4.9100E-001 9.1000E-002 9.9570E-001
2.0100E-001 7.6500E-002 9.7000E-001	3.8200E-001 8.3500E-002 9.8590E-001	5.1700E-001 9.1300E-002 9.9570E-001
2.3300E-001 7.6500E-002 9.7000E-001	4.1900E-001 8.6200E-002 9.8430E-001	5.3700E-001 9.2500E-002 9.9500E-001
2.6400E-001 7.6500E-002 9.7000E-001	4.4500E-001 8.7700E-002 9.8340E-001	5.3700E-001 1.0701E-001 9.8110E-001
3.0500E-001 7.7000E-002 9.7000E-001	4.7500E-001 9.0300E-002 9.8180E-001	5.6200E-001 1.0519E-001 9.7801E-001
3.4400E-001 7.7200E-002 9.7000E-001	4.9100E-001 7.3500E-002 1.0015E-000	5.6200E-001 1.1000E-001 9.7000E-001
3.8200E-001 7.9100E-002 9.7000E-001	5.1700E-001 7.3700E-002 1.0013E-000	2.0000E-002 1.1000E-001 9.7000E-001
4.1900E-001 8.2300E-002 9.7000E-001	5.3700E-001 7.3200E-002 1.0016E-000	2.5130E-002 9.9300E-002 9.8780E-001
4.4500E-001 8.4000E-002 9.7000E-001	5.3700E-001 9.8900E-002 9.7299E-001	5.1100E-002 9.7100E-002 9.9140E-001
4.7500E-001 8.7000E-002 9.7000E-001	5.6200E-001 1.0199E-001 9.7481E-001	8.2300E-002 9.6000E-002 9.9330E-001
4.9100E-001 9.0600E-002 9.7000E-001	5.6200E-001 1.1000E-001 9.7000E-001	1.0600E-001 9.4400E-002 9.9590E-001
5.1700E-001 9.4200E-002 9.7000E-001	2.0000E-002 1.1000E-001 9.7000E-001	1.3300E-001 9.3800E-002 9.9690E-001
5.3700E-001 9.8500E-002 9.7000E-001	2.5130E-002 9.5300E-002 9.8470E-001	1.6900E-001 9.3600E-002 9.9740E-001
5.3700E-001 9.8500E-002 9.7000E-001	5.1100E-002 9.2300E-002 9.8770E-001	2.0100E-001 9.2800E-002 9.9870E-001
5.6200E-001 1.0066E-001 9.7000E-001	8.2300E-002 9.0700E-002 9.8930E-001	2.3300E-001 9.2700E-002 9.9870E-001
5.6200E-001 1.1000E-001 9.7000E-001	1.0600E-001 8.8600E-002 9.9140E-001	2.6400E-001 9.2800E-002 9.9870E-001
2.0000E-002 1.1000E-001 9.7000E-001	1.3300E-001 8.7800E-002 9.9220E-001	3.0500E-001 9.3000E-002 9.9830E-001
2.5130E-002 9.2200E-002 9.8070E-001	1.6900E-001 8.7400E-002 9.9260E-001	3.4400E-001 9.3100E-002 9.9820E-001
5.1100E-002 8.8600E-002 9.8290E-001	2.0100E-001 8.6300E-002 9.9370E-001	3.8200E-001 9.4100E-002 9.9650E-001
8.2300E-002 8.6700E-002 9.8400E-001	2.3300E-001 8.6300E-002 9.9370E-001	4.1900E-001 9.5700E-002 9.9380E-001
1.0600E-001 8.4100E-002 9.8560E-001	2.6400E-001 8.6300E-002 9.9370E-001	4.4500E-001 9.6600E-002 9.9230E-001
1.3300E-001 8.3100E-002 9.8620E-001	3.0500E-001 8.6600E-002 9.9340E-001	4.7500E-001 9.8200E-002 9.8970E-001
1.6900E-001 8.2600E-002 9.8640E-001	3.4400E-001 8.6800E-002 9.9320E-001	4.9100E-001 1.0087E-001 9.8710E-001
2.0100E-001 8.1300E-002 9.8720E-001	3.8200E-001 8.8200E-002 9.9180E-001	5.1700E-001 1.0379E-001 9.8450E-001
2.3300E-001 8.1300E-002 9.8730E-001	4.1900E-001 9.0400E-002 9.8960E-001	5.3700E-001 1.0701E-001 9.8110E-001
2.6400E-001 8.1300E-002 9.8720E-001	4.4500E-001 9.1600E-002 9.8840E-001	5.3700E-001 1.0701E-001 9.8110E-001
3.0500E-001 8.1700E-002 9.8700E-001	4.7500E-001 9.3800E-002 9.8620E-001	5.6200E-001 1.0519E-001 9.7801E-001
3.4400E-001 8.1800E-002 9.8690E-001	4.9100E-001 7.6000E-002 1.0040E-000	5.6200E-001 1.1000E-001 9.7000E-001
3.8200E-001 8.3500E-002 9.8590E-001	5.1700E-001 7.6200E-002 1.0038E-000	2.0000E-002 1.1000E-001 9.7000E-001
4.1900E-001 8.6200E-002 9.8430E-001	5.3700E-001 7.5800E-002 1.0042E-000	2.5130E-002 1.1000E-001 9.9080E-001
4.4500E-001 8.7700E-002 9.8340E-001	5.3700E-001 1.0188E-001 9.7812E-001	5.1100E-002 1.1000E-001 9.9500E-001
4.7500E-001 9.0300E-002 9.8180E-001	5.6200E-001 1.0340E-001 9.7660E-001	8.2300E-002 1.1000E-001 9.9720E-001
4.9100E-001 9.2900E-002 9.7913E-001	5.6200E-001 1.1000E-001 9.7000E-001	1.0600E-001 1.1000E-001 1.0002E-000
5.1700E-001 9.5500E-002 9.7621E-001	2.0000E-002 1.1000E-001 9.7000E-001	1.3300E-001 1.1000E-001 1.0014E-000
5.3700E-001 9.8900E-002 9.7299E-001	2.5130E-002 9.9300E-002 9.8780E-001	1.6900E-001 1.1000E-001 1.0019E-000
5.3700E-001 9.8900E-002 9.7299E-001	5.1100E-002 9.7100E-002 9.9140E-001	2.0100E-001 1.1000E-001 1.0035E-000
5.6200E-001 1.0199E-001 9.7481E-001	8.2300E-002 9.6000E-002 9.9330E-001	2.3300E-001 1.1000E-001 1.0035E-000
5.6200E-001 1.1000E-001 9.7000E-001	1.0600E-001 9.4400E-002 9.9590E-001	2.6400E-001 1.1000E-001 1.0035E-000
2.0000E-002 1.1000E-001 9.7000E-001	1.3300E-001 9.3800E-002 9.9690E-001	3.0500E-001 1.1000E-001 1.0030E-000
2.5130E-002 9.2200E-002 9.8070E-001	1.6900E-001 9.3600E-002 9.9740E-001	3.4400E-001 1.1000E-001 1.0028E-000
5.1100E-002 8.8600E-002 9.8290E-001	2.0100E-001 9.2800E-002 9.9870E-001	3.8200E-001 1.1000E-001 1.0009E-000
8.2300E-002 8.6700E-002 9.8400E-001	2.3300E-001 9.2700E-002 9.9870E-001	4.1900E-001 1.1000E-001 9.9770E-001
1.0600E-001 8.4100E-002 9.8560E-001	2.6400E-001 9.2800E-002 9.9870E-001	4.4500E-001 1.1000E-001 9.9600E-001
1.3300E-001 8.3100E-002 9.8620E-001	3.0500E-001 9.3000E-002 9.9830E-001	4.7500E-001 1.1000E-001 9.9300E-001
1.6900E-001 8.2600E-002 9.8640E-001	3.4400E-001 9.3100E-002 9.9820E-001	4.9100E-001 1.1000E-001 9.8940E-001

5.1700E-001 1.1000E-001 9.8580E-001
5.3700E-001 1.1000E-001 9.8150E-001
5.3700E-001 1.1000E-001 9.8150E-001
5.6200E-001 1.1000E-001 9.7934E-001
5.6200E-001 1.1000E-001 9.7000E-001

E.3 Clean Wing Lines

TITLE = "CF-18"
VARIABLES = "Z"
"X"
"Y"
ZONE T="Line 1"
I=11, J=1, K=1,F=POINT
DT=(SINGLE SINGLE SINGLE)
1.0853E+000 2.7202E-001 8.5608E-001
1.0000E+000 2.6792E-001 8.5705E-001
9.1474E-001 2.6383E-001 8.5803E-001
8.2948E-001 2.5973E-001 8.5907E-001
7.4421E-001 2.5973E-001 8.5999E-001
6.5895E-001 2.5973E-001 8.6067E-001
5.7369E-001 2.6383E-001 8.6171E-001
4.8843E-001 2.6587E-001 8.6276E-001
4.0317E-001 2.6792E-001 8.6361E-001
3.1791E-001 2.7202E-001 8.6484E-001
2.3264E-001 2.7530E-001 8.6588E-001
ZONE T="Line 2"
I=10, J=1, K=1,F=POINT
DT=(SINGLE SINGLE SINGLE)
1.0853E+000 2.6781E-001 9.1137E-001
1.0000E+000 2.6581E-001 9.1641E-001
9.1474E-001 2.6180E-001 9.2145E-001
8.2948E-001 2.6220E-001 9.2648E-001
7.4421E-001 2.5779E-001 9.4825E-001
6.5895E-001 2.6180E-001 9.4916E-001
5.7369E-001 2.6421E-001 9.3947E-001
4.8843E-001 2.6581E-001 9.4317E-001
4.0317E-001 2.6781E-001 9.4712E-001
3.5201E-001 2.6781E-001 9.5681E-001
ZONE T="Line 3"
I=11, J=1, K=1,F=POINT
DT=(SINGLE SINGLE SINGLE)
1.0853E+000 2.7602E-001 3.7000E-001
1.0000E+000 2.7602E-001 3.7000E-001
9.1474E-001 2.7763E-001 3.7000E-001
8.2948E-001 2.8404E-001 3.7000E-001
7.4421E-001 2.9206E-001 3.7000E-001
6.5895E-001 2.9607E-001 3.7000E-001
5.7369E-001 3.0408E-001 3.7000E-001
4.8843E-001 3.0809E-001 3.7000E-001
4.0317E-001 3.1611E-001 3.7000E-001
3.1791E-001 3.2413E-001 3.7000E-001
2.3264E-001 3.3054E-001 3.7000E-001
ZONE T="Line 4"
I=11, J=1, K=1,F=POINT
DT=(SINGLE SINGLE SINGLE)
1.0853E+000 2.8478E-001 5.0459E-001
1.0000E+000 2.8478E-001 5.0644E-001
9.1474E-001 2.8077E-001 5.0829E-001
8.2948E-001 2.8077E-001 5.1014E-001
7.4421E-001 2.8478E-001 5.1200E-001
6.5895E-001 2.8879E-001 5.1340E-001
5.7369E-001 2.9120E-001 5.1492E-001
4.8843E-001 2.9280E-001 5.1631E-001
4.0317E-001 2.9922E-001 5.1853E-001
3.1791E-001 3.0483E-001 5.2121E-001
2.3264E-001 3.1285E-001 5.2389E-001
ZONE T="Line 5"
I=11, J=1, K=1,F=POINT
DT=(SINGLE SINGLE SINGLE)
1.0853E+000 2.9451E-001 6.6587E-001
1.0000E+000 2.9291E-001 6.6587E-001
9.1474E-001 2.9050E-001 6.6587E-001
8.2948E-001 2.8649E-001 6.6587E-001
7.4421E-001 2.8649E-001 6.6587E-001
6.5895E-001 2.8649E-001 6.6587E-001
5.7369E-001 2.8649E-001 6.4891E-001
4.8843E-001 2.9050E-001 6.5459E-001
4.0317E-001 2.9451E-001 6.6032E-001
3.1791E-001 2.9852E-001 6.7926E-001
2.3264E-001 3.0172E-001 6.7532E-001
ZONE T="Line 6"
I=11, J=1, K=1,F=POINT
DT=(SINGLE SINGLE SINGLE)
1.0853E+000 2.7884E-001 5.9784E-001
1.0000E+000 2.7564E-001 6.1082E-001
9.1474E-001 2.7323E-001 6.2380E-001
8.2948E-001 2.6922E-001 6.3678E-001
7.4421E-001 2.6922E-001 6.7583E-001
6.5895E-001 2.7323E-001 6.8212E-001
5.7369E-001 2.7564E-001 6.8706E-001
4.8843E-001 2.7724E-001 6.7459E-001
4.0317E-001 2.8125E-001 7.0527E-001
3.1791E-001 2.8526E-001 7.1263E-001
2.3264E-001 2.8927E-001 7.1966E-001
ZONE T="Line 7"
I=11, J=1, K=1,F=POINT
DT=(SINGLE SINGLE SINGLE)
1.0853E+000 2.6497E-001 6.9238E-001
1.0000E+000 2.6096E-001 7.0245E-001
9.1474E-001 2.5695E-001 7.1252E-001
8.2948E-001 2.5695E-001 7.2259E-001
7.4421E-001 2.5695E-001 7.3267E-001
6.5895E-001 2.6336E-001 6.8894E-001
5.7369E-001 2.6657E-001 7.7460E-001
4.8843E-001 2.7138E-001 7.7879E-001
4.0317E-001 2.7699E-001 7.8780E-001
3.1791E-001 2.8100E-001 7.9458E-001
2.3264E-001 2.8902E-001 8.1380E-001
ZONE T="Line 8"
I=10, J=1, K=1,F=POINT
DT=(SINGLE SINGLE SINGLE)
1.0853E+000 2.6068E-001 9.1018E-001
1.0000E+000 2.5426E-001 9.2653E-001
9.1474E-001 2.5266E-001 9.4288E-001
8.2948E-001 2.4865E-001 9.5923E-001
7.4421E-001 2.4865E-001 1.0156E+000
6.5895E-001 2.4865E-001 1.0200E+000
5.7369E-001 2.4865E-001 1.0030E+000
4.8843E-001 2.5266E-001 1.0167E+000
4.0317E-001 2.5426E-001 1.0303E+000
3.2643E-001 2.5907E-001 1.0702E+000
ZONE T="Line 9"
I=11, J=1, K=1,F=POINT
DT=(SINGLE SINGLE SINGLE)
1.0853E+000 2.3751E-001 1.2087E+000
1.0000E+000 2.2789E-001 1.2152E+000
9.1474E-001 2.1987E-001 1.2217E+000
8.2948E-001 2.1346E-001 1.2282E+000
7.4421E-001 2.1346E-001 1.2323E+000
6.5895E-001 2.1346E-001 1.2540E+000
5.7369E-001 2.1346E-001 1.2574E+000
4.8843E-001 2.1346E-001 1.2625E+000
4.0317E-001 2.1586E-001 1.2654E+000
3.1791E-001 2.1185E-001 1.2682E+000
2.9233E-001 2.1185E-001 1.2691E+000
ZONE T="Line 10"
I=13, J=1, K=1,F=POINT
DT=(SINGLE SINGLE SINGLE)
1.0853E+000 2.9909E-001 1.3972E+000
1.0000E+000 2.8305E-001 1.4134E+000
9.1474E-001 2.7103E-001 1.4333E+000
8.2948E-001 2.5499E-001 1.4488E+000
7.4421E-001 2.4297E-001 1.5059E+000
6.5895E-001 2.3094E-001 1.4979E+000
5.7369E-001 2.1891E-001 1.5067E+000
4.8843E-001 2.1089E-001 1.5187E+000
4.0317E-001 2.0288E-001 1.5316E+000
3.1791E-001 1.9646E-001 1.5319E+000
2.3264E-001 1.8844E-001 1.5398E+000
1.4738E-001 1.8844E-001 1.5477E+000
6.2119E-002 1.8844E-001 1.5556E+000
ZONE T="Line 11"
I=12, J=1, K=1,F=POINT
DT=(SINGLE SINGLE SINGLE)
1.0853E+000 1.7179E-001 3.7000E-001
1.0000E+000 1.7981E-001 3.7000E-001
9.1474E-001 1.8382E-001 3.7000E-001
8.2948E-001 1.9424E-001 3.7000E-001
7.4421E-001 1.9985E-001 3.7000E-001
6.5895E-001 2.1188E-001 3.7000E-001
5.7369E-001 2.1589E-001 3.7000E-001
4.8843E-001 2.2391E-001 3.7000E-001
4.0317E-001 2.2952E-001 3.7000E-001
3.1791E-001 2.3433E-001 3.7000E-001
2.3264E-001 2.3593E-001 3.7000E-001
1.8149E-001 2.3593E-001 3.7000E-001
ZONE T="Line 12"
I=12, J=1, K=1,F=POINT
DT=(SINGLE SINGLE SINGLE)
1.0853E+000 2.1325E-001 4.1902E-001
1.0000E+000 2.0924E-001 4.2968E-001
9.1474E-001 2.0683E-001 4.4034E-001
8.2948E-001 2.0683E-001 4.5100E-001
7.4421E-001 2.0683E-001 4.6166E-001
6.5895E-001 2.0683E-001 5.1300E-001
5.7369E-001 2.0683E-001 5.1300E-001
4.8843E-001 2.1325E-001 5.1300E-001
4.0317E-001 2.1325E-001 5.1300E-001
3.1791E-001 2.1325E-001 5.1300E-001
2.3264E-001 2.1325E-001 5.1300E-001
1.6443E-001 2.1325E-001 5.1300E-001
ZONE T="Line 13"
I=12, J=1, K=1,F=POINT
DT=(SINGLE SINGLE SINGLE)
1.0853E+000 1.9609E-001 6.5544E-001
1.0000E+000 1.9449E-001 6.6041E-001
9.1474E-001 1.9208E-001 6.6537E-001
8.2948E-001 1.8967E-001 6.7033E-001
7.4421E-001 1.8967E-001 6.5111E-001
6.5895E-001 1.8967E-001 6.6150E-001
5.7369E-001 1.8967E-001 6.8341E-001
4.8843E-001 1.8967E-001 6.9021E-001
4.0317E-001 1.8967E-001 7.0265E-001
3.1791E-001 1.8967E-001 7.0734E-001
2.3264E-001 1.8967E-001 7.1203E-001
2.1559E-001 1.8967E-001 7.1299E-001
ZONE T="Line 14"
I=12, J=1, K=1,F=POINT
DT=(SINGLE SINGLE SINGLE)
1.0853E+000 1.6860E-001 7.9408E-001
1.0000E+000 1.6860E-001 7.9408E-001
9.1474E-001 1.6860E-001 7.9408E-001
8.2948E-001 1.6860E-001 7.9408E-001
7.4421E-001 1.6860E-001 7.9408E-001
6.5895E-001 1.6860E-001 7.9408E-001
5.7369E-001 1.7020E-001 7.7463E-001
4.8843E-001 1.7261E-001 7.8031E-001
4.0317E-001 1.7501E-001 7.8455E-001

3.1791E-001 1.7661E-001 8.0394E-001
2.3264E-001 1.7661E-001 8.0394E-001
2.1559E-001 1.7661E-001 8.0394E-001
ZONE T="Line 15"
I=12, J=1, K=1,F=POINT
DT=(SINGLE SINGLE SINGLE)
1.0853E+000 1.7579E-001 6.5064E-001
1.0000E+000 1.6937E-001 6.6726E-001
9.1474E-001 1.7178E-001 6.8388E-001
8.2948E-001 1.7178E-001 7.0050E-001
7.4421E-001 1.6777E-001 7.2198E-001
6.5895E-001 1.6617E-001 7.3753E-001
5.7369E-001 1.6617E-001 7.4675E-001
4.8843E-001 1.6617E-001 7.6218E-001
4.0317E-001 1.6617E-001 7.8994E-001
3.1791E-001 1.6617E-001 8.0437E-001
2.3264E-001 1.6617E-001 8.1909E-001
2.1559E-001 1.6617E-001 8.2182E-001
ZONE T="Line 16"
I=10, J=1, K=1,F=POINT
DT=(SINGLE SINGLE SINGLE)
1.0853E+000 1.7158E-001 9.0881E-001
1.0000E+000 1.6597E-001 9.1232E-001
9.1474E-001 1.6036E-001 9.1583E-001
8.2948E-001 1.5394E-001 9.1935E-001
7.4421E-001 1.5234E-001 9.2222E-001
6.5895E-001 1.4993E-001 9.2588E-001
5.7369E-001 1.4753E-001 9.2741E-001
4.8843E-001 1.4592E-001 9.3189E-001
4.0317E-001 1.4432E-001 9.3609E-001
3.4348E-001 1.4432E-001 9.3904E-001
ZONE T="Line 17"
I=10, J=1, K=1,F=POINT
DT=(SINGLE SINGLE SINGLE)
1.0853E+000 1.5836E-001 9.4753E-001
1.0000E+000 1.5436E-001 9.5415E-001
9.1474E-001 1.4874E-001 9.6076E-001
8.2948E-001 1.4233E-001 9.6738E-001
7.4421E-001 1.4073E-001 9.7360E-001
6.5895E-001 1.3832E-001 9.8030E-001
5.7369E-001 1.3591E-001 9.9132E-001
4.8843E-001 1.3591E-001 9.9710E-001
4.0317E-001 1.3591E-001 1.0037E+000
3.2643E-001 1.3431E-001 1.0078E+000
ZONE T="Line 18"
I=11, J=1, K=1,F=POINT
DT=(SINGLE SINGLE SINGLE)
1.0853E+000 1.2748E-001 1.2042E+000
1.0000E+000 1.1946E-001 1.2106E+000
9.1474E-001 1.1144E-001 1.2170E+000
8.2948E-001 1.0743E-001 1.2234E+000
7.4421E-001 1.0102E-001 1.2259E+000
6.5895E-001 9.9416E-002 1.2487E+000
5.7369E-001 9.5407E-002 1.2526E+000
4.8843E-001 9.1398E-002 1.2441E+000
4.0317E-001 8.7389E-002 1.2529E+000
3.1791E-001 8.3380E-002 1.2554E+000
3.0085E-001 8.3380E-002 1.2570E+000
ZONE T="Line 19"
I=13, J=1, K=1,F=POINT
DT=(SINGLE SINGLE SINGLE)
1.0853E+000 4.2117E-001 1.2356E+000
1.0000E+000 4.1315E-001 1.2739E+000
9.1474E-001 4.0112E-001 1.3853E+000
8.2948E-001 3.8910E-001 1.4064E+000
7.4421E-001 3.7466E-001 1.4275E+000
6.5895E-001 3.6023E-001 1.4813E+000
5.7369E-001 3.4580E-001 1.4919E+000
4.8843E-001 3.3137E-001 1.5024E+000
4.0317E-001 3.1694E-001 1.5129E+000
3.1791E-001 3.0491E-001 1.5156E+000
2.3264E-001 2.9288E-001 1.5303E+000
1.4738E-001 2.8487E-001 1.5449E+000
5.3593E-002 2.8086E-001 1.5611E+000
ZONE T="Line 20"
I=11, J=1, K=1,F=POINT
DT=(SINGLE SINGLE SINGLE)
1.0853E+000 1.9200E-001 6.6587E-001
1.0000E+000 1.9040E-001 6.6587E-001
9.1474E-001 1.9040E-001 6.6587E-001
8.2948E-001 1.9040E-001 6.6587E-001
7.4421E-001 1.9040E-001 6.6587E-001
6.5895E-001 1.9200E-001 6.6587E-001
5.7369E-001 1.9441E-001 6.6587E-001
4.8843E-001 1.9681E-001 6.6587E-001
4.0317E-001 1.9441E-001 6.6587E-001
3.1791E-001 1.9842E-001 6.6587E-001
2.2412E-001 1.9842E-001 6.6587E-001
ZONE T="Line 21"
I=12, J=1, K=1,F=POINT
DT=(SINGLE SINGLE SINGLE)
1.0853E+000 1.2368E-001 3.7000E-001
1.0000E+000 1.2368E-001 3.7000E-001
9.1474E-001 1.2368E-001 3.7000E-001
8.2948E-001 1.2529E-001 3.7000E-001
7.4421E-001 1.2769E-001 3.7000E-001
6.5895E-001 1.3010E-001 3.7000E-001
5.7369E-001 1.3170E-001 3.7000E-001
4.8843E-001 1.3331E-001 3.7000E-001
4.0317E-001 1.3571E-001 3.7000E-001
3.1791E-001 1.3571E-001 3.7000E-001
2.3264E-001 1.3571E-001 3.7000E-001
1.9001E-001 1.3571E-001 3.7000E-001
ZONE T="Line 22"
I=12, J=1, K=1,F=POINT
DT=(SINGLE SINGLE SINGLE)
1.0853E+000 1.1058E-001 3.7897E-001
1.0000E+000 1.1058E-001 3.8698E-001
9.1474E-001 1.1058E-001 3.9498E-001
8.2948E-001 1.1058E-001 4.0299E-001
7.4421E-001 1.1058E-001 4.1099E-001
6.5895E-001 1.1058E-001 4.1900E-001
5.7369E-001 1.1459E-001 4.2700E-001
4.8843E-001 1.1459E-001 4.3501E-001
4.0317E-001 1.1459E-001 4.4301E-001
3.1791E-001 1.1459E-001 4.4370E-001
2.3264E-001 1.1219E-001 4.5502E-001
1.8149E-001 1.1219E-001 4.5586E-001
ZONE T="Line 23"
I=12, J=1, K=1,F=POINT
DT=(SINGLE SINGLE SINGLE)
1.0853E+000 1.0417E-001 5.7537E-001
1.0000E+000 1.0096E-001 5.8224E-001
9.1474E-001 9.8555E-002 5.8911E-001
8.2948E-001 9.6150E-002 5.9599E-001
7.4421E-001 9.4546E-002 6.0286E-001
6.5895E-001 9.4546E-002 6.0973E-001
5.7369E-001 9.2943E-002 6.1661E-001
4.8843E-001 9.0538E-002 6.2040E-001
4.0317E-001 9.0538E-002 6.2814E-001
3.1791E-001 8.8132E-002 6.3922E-001
2.3264E-001 8.6529E-002 6.4497E-001
1.4738E-001 8.6529E-002 6.6587E-001
ZONE T="Line 24"
I=12, J=1, K=1,F=POINT
DT=(SINGLE SINGLE SINGLE)
1.0853E+000 9.2424E-002 5.8617E-001
1.0000E+000 8.8415E-002 5.9665E-001
9.1474E-001 8.8415E-002 6.0713E-001
8.2948E-001 8.6811E-002 6.1760E-001
7.4421E-001 8.4406E-002 6.2808E-001
6.5895E-001 8.4406E-002 6.3856E-001
5.7369E-001 8.4406E-002 6.4903E-001
4.8843E-001 8.4406E-002 6.6076E-001
4.0317E-001 8.4406E-002 6.6124E-001
3.1791E-001 8.4406E-002 6.7422E-001
2.3264E-001 8.4406E-002 7.0051E-001
1.3033E-001 8.4406E-002 7.0868E-001
ZONE T="Line 25"
I=12, J=1, K=1,F=POINT
DT=(SINGLE SINGLE SINGLE)
1.0853E+000 8.8397E-002 7.7758E-001
1.0000E+000 8.0379E-002 7.8012E-001
9.1474E-001 7.6370E-002 7.8266E-001
8.2948E-001 7.2361E-002 7.8520E-001
7.4421E-001 7.0758E-002 7.8774E-001
6.5895E-001 6.8352E-002 7.9027E-001
5.7369E-001 6.4344E-002 7.9281E-001
4.8843E-001 6.2740E-002 7.9367E-001
4.0317E-001 6.0335E-002 7.9618E-001
3.1791E-001 5.7929E-002 7.9932E-001
2.3264E-001 5.6326E-002 8.0256E-001
2.0706E-001 5.6326E-002 8.0377E-001
ZONE T="Line 26"
I=12, J=1, K=1,F=POINT
DT=(SINGLE SINGLE SINGLE)
1.0853E+000 5.4147E-002 7.5216E-001
1.0000E+000 5.4147E-002 7.6012E-001
9.1474E-001 5.4147E-002 7.6808E-001
8.2948E-001 5.4147E-002 7.7604E-001
7.4421E-001 5.4147E-002 7.8400E-001
6.5895E-001 5.4147E-002 7.9196E-001
5.7369E-001 5.4147E-002 7.9992E-001
4.8843E-001 5.4147E-002 8.0799E-001
4.0317E-001 5.4147E-002 7.9487E-001
3.1791E-001 5.4147E-002 8.1594E-001
2.3264E-001 5.4147E-002 8.2728E-001
1.9854E-001 5.4147E-002 8.3181E-001
ZONE T="Line 27"
I=12, J=1, K=1,F=POINT
DT=(SINGLE SINGLE SINGLE)
1.0853E+000 7.3021E-002 8.0659E-001
1.0000E+000 6.9012E-002 8.1895E-001
9.1474E-001 6.5003E-002 8.3132E-001
8.2948E-001 6.0994E-002 8.4369E-001
7.4421E-001 5.6985E-002 8.5606E-001
6.5895E-001 5.5382E-002 8.6842E-001
5.7369E-001 5.0571E-002 8.8079E-001
4.8843E-001 5.6985E-002 8.8488E-001
4.0317E-001 4.7364E-002 9.2914E-001
3.1791E-001 4.4959E-002 9.3444E-001
2.3264E-001 4.4959E-002 9.4103E-001
1.8149E-001 4.4959E-002 9.6174E-001
ZONE T="Line 28"
I=12, J=1, K=1,F=POINT
DT=(SINGLE SINGLE SINGLE)
1.0853E+000 6.2309E-002 7.3247E-001
1.0000E+000 5.8300E-002 7.5646E-001
9.1474E-001 5.4291E-002 7.8045E-001
8.2948E-001 4.7877E-002 8.0444E-001
7.4421E-001 4.4670E-002 8.2843E-001
6.5895E-001 3.9859E-002 8.5241E-001
5.7369E-001 3.8255E-002 8.7640E-001
4.8843E-001 3.4247E-002 9.0928E-001
4.0317E-001 3.0238E-002 9.6387E-001
3.1791E-001 2.8634E-002 9.7795E-001
2.3264E-001 2.5804E-002 9.9036E-001
1.7296E-001 2.3823E-002 1.0099E+000
ZONE T="Line 29"
I=11, J=1, K=1,F=POINT
DT=(SINGLE SINGLE SINGLE)
1.0853E+000 -5.0329E-003 1.1273E+000
1.0000E+000 -9.0418E-003 1.1391E+000

```
 9.1474E-001 -1.3051E-002 1.1508E+000
 8.2948E-001 -1.9465E-002 1.1625E+000
 7.4421E-001 -2.2672E-002 1.1742E+000
 6.5895E-001 -2.5077E-002 1.1859E+000
 5.7369E-001 -2.9086E-002 1.1976E+000
 4.8843E-001 -3.0690E-002 1.1805E+000
 4.0317E-001 -3.0690E-002 1.2088E+000
 3.1791E-001 -3.0690E-002 1.2355E+000
 2.9233E-001 -3.0690E-002 1.2394E+000
ZONE T="Line 30"
 I=13, J=1, K=1,F=POINT
DT=(SINGLE SINGLE SINGLE )
 1.0853E+000 -5.3864E-002 1.3264E+000
 1.0000E+000 -6.1882E-002 1.3418E+000
 9.1474E-001 -6.5891E-002 1.3573E+000
 8.2948E-001 -6.9900E-002 1.3727E+000
 7.4421E-001 -7.3908E-002 1.3882E+000
 6.5895E-001 -7.7917E-002 1.4036E+000
 5.7369E-001 -8.1926E-002 1.4191E+000
 4.8843E-001 -8.4332E-002 1.3845E+000
 4.0317E-001 -8.5935E-002 1.4717E+000
 3.1791E-001 -8.9944E-002 1.4843E+000
 2.3264E-001 -9.3953E-002 1.4502E+000
 1.4738E-001 -9.5556E-002 1.5093E+000
 6.2119E-002 -9.7962E-002 1.5248E+000
ZONE T="Line 31"
 I=13, J=1, K=1,F=POINT
DT=(SINGLE SINGLE SINGLE )
 1.0853E+000 -5.3321E-002 1.3166E+000
 1.0000E+000 -6.1339E-002 1.3321E+000
 9.1474E-001 -6.5348E-002 1.3475E+000
 8.2948E-001 -6.9357E-002 1.3630E+000
 7.4421E-001 -7.3366E-002 1.3784E+000
 6.5895E-001 -7.7374E-002 1.4143E+000
 5.7369E-001 -8.1383E-002 1.4269E+000
 4.8843E-001 -8.3789E-002 1.4022E+000
 4.0317E-001 -8.5392E-002 1.4211E+000
 3.1791E-001 -8.9401E-002 1.4745E+000
 2.3264E-001 -9.3410E-002 1.4871E+000
 1.4738E-001 -9.5014E-002 1.5087E+000
 6.2119E-002 -9.7419E-002 1.5192E+000
```

E.4 Stores Lines

```
TITLE = "CF-18"
VARIABLES = "Z"
"X"
"Y"
ZONE T="Line 1"
 I=12, J=1, K=1,F=POINT
DT=(SINGLE SINGLE SINGLE )
 6.3526E-001 4.1758E-003 8.0700E-001
 5.6200E-001 1.2967E-002 8.0298E-001
 4.8874E-001 2.0293E-002 7.9904E-001
 4.1548E-001 4.0806E-002 7.9538E-001
 3.4222E-001 5.9121E-002 7.9293E-001
 2.6896E-001 8.1099E-002 7.9241E-001
 1.9570E-001 1.0674E-001 8.0315E-001
 1.2244E-001 1.2286E-001 8.1363E-001
 4.9179E-002 1.3604E-001 8.2136E-001
-2.4081E-002 1.4337E-001 8.2136E-001
-9.7341E-002 1.5070E-001 8.2136E-001
-1.7060E-001 1.5802E-001 8.2136E-001
ZONE T="Line 2"
 I=12, J=1, K=1,F=POINT
DT=(SINGLE SINGLE SINGLE )
 6.3526E-001 8.4762E-002 1.0305E+000
 5.6200E-001 9.2088E-002 1.0356E+000
 4.8874E-001 9.9414E-002 1.0398E+000
 4.1548E-001 1.0674E-001 1.0466E+000
 3.4222E-001 1.1407E-001 1.0400E+000
 2.6896E-001 1.2139E-001 1.0353E+000
 1.9570E-001 1.3238E-001 1.0247E+000
 1.2244E-001 1.4337E-001 1.0196E+000
 4.9179E-002 1.4703E-001 1.0155E+000
-2.4081E-002 1.5070E-001 1.0145E+000
-9.7341E-002 1.5070E-001 1.0136E+000
-1.7060E-001 1.5802E-001 1.0127E+000
ZONE T="Line 3"
 I=12, J=1, K=1,F=POINT
DT=(SINGLE SINGLE SINGLE )
 6.3526E-001 -5.2967E-002 9.4975E-001
 5.6200E-001 -4.5641E-002 9.5572E-001
 4.8874E-001 -3.8315E-002 9.6095E-001
 4.1548E-001 -2.6593E-002 9.6388E-001
 3.4222E-001 -1.9267E-002 9.6684E-001
 2.6896E-001 -1.0476E-002 9.6986E-001
 1.9570E-001 4.1758E-003 9.7136E-001
 1.2244E-001 1.8828E-002 9.7136E-001
 4.9179E-002 3.4945E-002 9.6545E-001
-2.4081E-002 5.9121E-002 9.6024E-001
-9.7341E-002 7.3773E-002 9.6024E-001
-1.7060E-001 8.4762E-002 9.6024E-001
ZONE T="Line 4"
 I=12, J=1, K=1,F=POINT
DT=(SINGLE SINGLE SINGLE )
 6.3526E-001 5.1282E-004 8.3802E-001
 5.6200E-001 4.1758E-003 8.3802E-001
 4.8874E-001 4.1758E-003 8.4218E-001
 4.1548E-001 4.1758E-003 8.4763E-001
 3.4222E-001 7.8388E-003 8.4913E-001
 2.6896E-001 1.1502E-002 8.4913E-001
 1.9570E-001 1.8828E-002 8.4913E-001
 1.2244E-001 2.9817E-002 8.4913E-001
 4.9179E-002 3.7143E-002 8.4913E-001
-2.4081E-002 6.2784E-002 8.4913E-001
-9.7341E-002 7.7436E-002 8.4913E-001
-1.7060E-001 8.4762E-002 8.4913E-001
ZONE T="Line 5"
 I=12, J=1, K=1,F=POINT
DT=(SINGLE SINGLE SINGLE )
 6.3526E-001 -6.8132E-003 9.0469E-001
 5.6200E-001 -6.8132E-003 9.0469E-001
 4.8874E-001 -3.1502E-003 9.0469E-001
 4.1548E-001 5.1282E-004 9.0469E-001
 3.4222E-001 1.7363E-002 9.0469E-001
 2.6896E-001 4.8132E-002 9.0629E-001
 1.9570E-001 8.8425E-002 9.1348E-001
 1.2244E-001 1.1040E-001 9.1580E-001
 4.9179E-002 1.2872E-001 9.1580E-001
-2.4081E-002 1.4337E-001 9.1580E-001
-9.7341E-002 1.5802E-001 9.1580E-001
-1.2664E-001 1.6168E-001 9.1580E-001
ZONE T="Line 6"
 I=12, J=1, K=1,F=POINT
DT=(SINGLE SINGLE SINGLE )
 6.3526E-001 -5.8095E-002 9.0490E-001
 5.6200E-001 -4.8571E-002 9.0469E-001
 4.8874E-001 -3.9780E-002 9.0469E-001
 4.1548E-001 -2.8791E-002 9.0469E-001
 3.4222E-001 -1.7800E-002 9.0469E-001
 2.6896E-001 -1.6850E-003 9.0469E-001
 1.9570E-001 1.7363E-002 9.0895E-001
 1.2244E-001 3.4945E-002 9.1594E-001
 4.9179E-002 5.5458E-002 9.1580E-001
-2.4081E-002 7.0110E-002 9.1580E-001
-9.7341E-002 8.4762E-002 9.1580E-001
-1.7060E-001 9.5751E-002 9.1580E-001
ZONE T="Line 7"
 I=12, J=1, K=1,F=POINT
DT=(SINGLE SINGLE SINGLE )
 6.3526E-001 -5.5897E-002 9.0505E-001
 5.6200E-001 -4.8571E-002 9.0469E-001
 4.8874E-001 -3.9780E-002 9.0469E-001
 4.1548E-001 -2.8791E-002 9.0469E-001
 3.4222E-001 -1.7802E-002 9.0469E-001
 2.6896E-001 -3.1502E-003 9.0469E-001
 1.9570E-001 1.1502E-002 9.0860E-001
 1.2244E-001 2.6154E-002 9.1522E-001
 4.9179E-002 4.8132E-002 9.1580E-001
-2.4081E-002 6.2784E-002 9.1580E-001
-9.7341E-002 7.3773E-002 9.1580E-001
-1.7060E-001 8.4762E-002 9.1580E-001
ZONE T="Line 8"
 I=12, J=1, K=1,F=POINT
DT=(SINGLE SINGLE SINGLE )
 6.3526E-001 -3.2454E-002 9.0469E-001
 5.6200E-001 -2.5128E-002 9.0469E-001
 4.8874E-001 -1.4139E-002 9.0469E-001
 4.1548E-001 4.1758E-003 9.0469E-001
 3.4222E-001 2.7619E-002 9.0469E-001
 2.6896E-001 6.2784E-002 9.0767E-001
 1.9570E-001 1.0674E-001 9.1508E-001
 1.2244E-001 1.2872E-001 9.1580E-001
 4.9179E-002 1.4703E-001 9.1580E-001
-2.4081E-002 1.5802E-001 9.1580E-001
-9.7341E-002 1.6535E-001 9.1580E-001
-1.7060E-001 1.7267E-001 9.1580E-001
ZONE T="Line 9"
 I=12, J=1, K=1,F=POINT
DT=(SINGLE SINGLE SINGLE )
 7.8178E-001 7.7436E-002 9.0330E-001
 7.4515E-001 8.1099E-002 9.0608E-001
 7.0852E-001 9.2088E-002 9.0469E-001
 6.7189E-001 9.2088E-002 9.0469E-001
 6.3526E-001 9.2088E-002 9.0469E-001
 6.0596E-001 8.8425E-002 9.0469E-001
 5.8031E-001 9.5751E-002 9.0469E-001
 5.9130E-001 1.1040E-001 9.0469E-001
 6.0596E-001 1.1407E-001 9.0469E-001
 6.3526E-001 1.1773E-001 9.0469E-001
 7.0852E-001 1.1040E-001 9.0469E-001
 7.8178E-001 1.1407E-001 9.0330E-001
ZONE T="Line 10"
 I=14, J=1, K=1,F=POINT
DT=(SINGLE SINGLE SINGLE )
 7.8178E-001 -2.1465E-002 7.9358E-001
 7.0852E-001 -1.7802E-002 7.9358E-001
 6.3526E-001 -1.0476E-002 7.9517E-001
 5.6200E-001 -3.1502E-003 7.9816E-001
 4.8874E-001 4.1758E-003 7.9913E-001
 4.1548E-001 1.2967E-002 7.9913E-001
 3.4222E-001 2.6154E-002 7.9913E-001
 2.6896E-001 3.7143E-002 7.9913E-001
 1.9570E-001 4.8132E-002 7.9913E-001
 1.2244E-001 6.4249E-002 8.0026E-001
 4.9179E-002 7.7436E-002 8.0321E-001
-2.4081E-002 9.2088E-002 8.0303E-001
-9.7341E-002 1.0674E-001 7.9973E-001
-1.7060E-001 1.2139E-001 7.9668E-001
ZONE T="Line 11"
 I=14, J=1, K=1,F=POINT
DT=(SINGLE SINGLE SINGLE )
 7.8178E-001 -4.7106E-002 6.7391E-001
 7.0852E-001 -3.9780E-002 6.8573E-001
 6.3526E-001 -3.3919E-002 6.9745E-001
 5.6200E-001 -2.5128E-002 7.0895E-001
 4.8874E-001 -1.6337E-002 7.1833E-001
 4.1548E-001 -3.1502E-003 7.2461E-001
 3.4222E-001 1.1502E-002 7.3110E-001
```

2.6896E-001 2.6154E-002 7.3771E-001
1.9570E-001 4.0806E-002 7.4131E-001
1.2244E-001 6.1319E-002 7.4358E-001
4.9179E-002 7.7436E-002 7.4358E-001
-2.4081E-002 9.2088E-002 7.4027E-001
-9.7341E-002 1.0674E-001 7.3365E-001
-1.7060E-001 1.2139E-001 7.2704E-001
ZONE T="Line 1"
I=12, J=1, K=1,F=POINT
DT=(SINGLE SINGLE SINGLE)
6.3526E-001 4.1758E-003 8.0700E-001
5.6200E-001 1.2967E-002 8.0298E-001
4.8874E-001 2.0293E-002 7.9904E-001
4.1548E-001 4.0806E-002 7.9538E-001
3.4222E-001 5.9121E-002 7.9293E-001
2.6896E-001 8.1099E-002 7.9241E-001
1.9570E-001 1.0674E-001 8.0315E-001
1.2244E-001 1.2286E-001 8.1363E-001
4.9179E-002 1.3604E-001 8.2136E-001
-2.4081E-002 1.4337E-001 8.2136E-001
-9.7341E-002 1.5070E-001 8.2136E-001
-1.7060E-001 1.5802E-001 8.2136E-001
ZONE T="Line 2"
I=12, J=1, K=1,F=POINT
DT=(SINGLE SINGLE SINGLE)
6.3526E-001 8.4762E-002 1.0305E+000
5.6200E-001 9.2088E-002 1.0356E+000
4.8874E-001 9.9414E-002 1.0398E+000
4.1548E-001 1.0674E-001 1.0466E+000
3.4222E-001 1.1407E-001 1.0400E+000
2.6896E-001 1.2139E-001 1.0353E+000
1.9570E-001 1.3238E-001 1.0247E+000
1.2244E-001 1.4337E-001 1.0196E+000
4.9179E-002 1.4703E-001 1.0155E+000
-2.4081E-002 1.5070E-001 1.0145E+000
-9.7341E-002 1.5070E-001 1.0136E+000
-1.7060E-001 1.5802E-001 1.0127E+000
ZONE T="Line 3"
I=12, J=1, K=1,F=POINT
DT=(SINGLE SINGLE SINGLE)
6.3526E-001 -5.2967E-002 9.4975E-001
5.6200E-001 -4.5641E-002 9.5572E-001
4.8874E-001 -3.8315E-002 9.6095E-001
4.1548E-001 -2.6593E-002 9.6388E-001
3.4222E-001 -1.9267E-002 9.6684E-001
2.6896E-001 -1.0476E-002 9.6986E-001
1.9570E-001 4.1758E-003 9.7136E-001
1.2244E-001 1.8828E-002 9.7136E-001
4.9179E-002 3.4945E-002 9.6545E-001
-2.4081E-002 5.9121E-002 9.6024E-001
-9.7341E-002 7.3773E-002 9.6024E-001
-1.7060E-001 8.4762E-002 9.6024E-001
ZONE T="Line 4"
I=12, J=1, K=1,F=POINT
DT=(SINGLE SINGLE SINGLE)
6.3526E-001 5.1282E-004 8.3802E-001
5.6200E-001 4.1758E-003 8.3802E-001
4.8874E-001 4.1758E-003 8.4218E-001
4.1548E-001 4.1758E-003 8.4763E-001
3.4222E-001 7.8388E-003 8.4913E-001
2.6896E-001 1.1502E-002 8.4913E-001
1.9570E-001 1.8828E-002 8.4913E-001
1.2244E-001 2.9817E-002 8.4913E-001
4.9179E-002 3.7143E-002 8.4913E-001
-2.4081E-002 6.2784E-002 8.4913E-001
-9.7341E-002 7.7436E-002 8.4913E-001
-1.7060E-001 8.4762E-002 8.4913E-001
ZONE T="Line 5"
I=12, J=1, K=1,F=POINT
DT=(SINGLE SINGLE SINGLE)
6.3526E-001 -6.8132E-003 9.0469E-001
5.6200E-001 -6.8132E-003 9.0469E-001
4.8874E-001 -3.1502E-003 9.0469E-001
4.1548E-001 5.1282E-004 9.0469E-001
3.4222E-001 1.7363E-002 9.0469E-001
2.6896E-001 4.8132E-002 9.0629E-001
1.9570E-001 8.8425E-002 9.1348E-001
1.2244E-001 1.1040E-001 9.1580E-001
4.9179E-002 1.2872E-001 9.1580E-001
-2.4081E-002 1.4337E-001 9.1580E-001
-9.7341E-002 1.5802E-001 9.1580E-001
-1.2664E-001 1.6168E-001 9.1580E-001
ZONE T="Line 6"
I=12, J=1, K=1,F=POINT
DT=(SINGLE SINGLE SINGLE)
6.3526E-001 -5.8095E-002 9.0490E-001
5.6200E-001 -4.8571E-002 9.0469E-001
4.8874E-001 -3.9780E-002 9.0469E-001
4.1548E-001 -2.8791E-002 9.0469E-001
3.4222E-001 -1.7800E-002 9.0469E-001
2.6896E-001 -1.6850E-003 9.0469E-001
1.9570E-001 1.7363E-002 9.0895E-001
1.2244E-001 3.4945E-002 9.1594E-001
4.9179E-002 5.5458E-002 9.1580E-001
-2.4081E-002 7.0110E-002 9.1580E-001
-9.7341E-002 8.4762E-002 9.1580E-001
-1.7060E-001 9.5751E-002 9.1580E-001
ZONE T="Line 7"
I=12, J=1, K=1,F=POINT
DT=(SINGLE SINGLE SINGLE)
6.3526E-001 -5.5897E-002 9.0505E-001
5.6200E-001 -4.8571E-002 9.0469E-001
4.8874E-001 -3.9780E-002 9.0469E-001
4.1548E-001 -2.8791E-002 9.0469E-001
3.4222E-001 -1.7802E-002 9.0469E-001
2.6896E-001 -3.1502E-003 9.0469E-001
1.9570E-001 1.1502E-002 9.0860E-001
1.2244E-001 2.6154E-002 9.1522E-001
4.9179E-002 4.8132E-002 9.1580E-001
-2.4081E-002 6.2784E-002 9.1580E-001
-9.7341E-002 7.3773E-002 9.1580E-001
-1.7060E-001 8.4762E-002 9.1580E-001
ZONE T="Line 8"
I=12, J=1, K=1,F=POINT
DT=(SINGLE SINGLE SINGLE)
6.3526E-001 -3.2454E-002 9.0469E-001
5.6200E-001 -2.5128E-002 9.0469E-001
4.8874E-001 -1.4139E-002 9.0469E-001
4.1548E-001 4.1758E-003 9.0469E-001
3.4222E-001 2.7619E-002 9.0469E-001
2.6896E-001 6.2784E-002 9.0767E-001
1.9570E-001 1.0674E-001 9.1508E-001
1.2244E-001 1.2872E-001 9.1580E-001
4.9179E-002 1.4703E-001 9.1580E-001
-2.4081E-002 1.5802E-001 9.1580E-001
-9.7341E-002 1.6535E-001 9.1580E-001
-1.7060E-001 1.7267E-001 9.1580E-001
ZONE T="Line 9"
I=12, J=1, K=1,F=POINT
DT=(SINGLE SINGLE SINGLE)
7.8178E-001 7.7436E-002 9.0330E-001
7.4515E-001 8.1099E-002 9.0608E-001
7.0852E-001 9.2088E-002 9.0469E-001
6.7189E-001 9.2088E-002 9.0469E-001
6.3526E-001 9.2088E-002 9.0469E-001
6.0596E-001 8.8425E-002 9.0469E-001
5.8031E-001 9.5751E-002 9.0469E-001
5.9130E-001 1.1040E-001 9.0469E-001
6.0596E-001 1.1407E-001 9.0469E-001
6.3526E-001 1.1773E-001 9.0469E-001
7.0852E-001 1.1040E-001 9.0469E-001
7.8178E-001 1.1407E-001 9.0330E-001
ZONE T="Line 10"
I=14, J=1, K=1,F=POINT
DT=(SINGLE SINGLE SINGLE)
7.8178E-001 -2.1465E-002 7.9358E-001
7.0852E-001 -1.7802E-002 7.9358E-001
6.3526E-001 -1.0476E-002 7.9517E-001
5.6200E-001 -3.1502E-003 7.9816E-001
4.8874E-001 4.1758E-003 7.9913E-001
4.1548E-001 1.2967E-002 7.9913E-001
3.4222E-001 2.6154E-002 7.9913E-001
2.6896E-001 3.7143E-002 7.9913E-001
1.9570E-001 4.8132E-002 7.9913E-001
1.2244E-001 6.4249E-002 8.0026E-001
4.9179E-002 7.7436E-002 8.0321E-001
-2.4081E-002 9.2088E-002 8.0303E-001
-9.7341E-002 1.0674E-001 7.9973E-001
-1.7060E-001 1.2139E-001 7.9668E-001
ZONE T="Line 11"
I=14, J=1, K=1,F=POINT
DT=(SINGLE SINGLE SINGLE)
7.8178E-001 -4.7106E-002 6.7391E-001
7.0852E-001 -3.9780E-002 6.8573E-001
6.3526E-001 -3.3919E-002 6.9745E-001
5.6200E-001 -2.5128E-002 7.0895E-001
4.8874E-001 -1.6337E-002 7.1833E-001
4.1548E-001 -3.1502E-003 7.2461E-001
3.4222E-001 1.1502E-002 7.3110E-001
2.6896E-001 2.6154E-002 7.3771E-001
1.9570E-001 4.0806E-002 7.4131E-001
1.2244E-001 6.1319E-002 7.4358E-001
4.9179E-002 7.7436E-002 7.4358E-001
-2.4081E-002 9.2088E-002 7.4027E-001
-9.7341E-002 1.0674E-001 7.3365E-001
-1.7060E-001 1.2139E-001 7.2704E-001

TEST TARGET (QA-3)

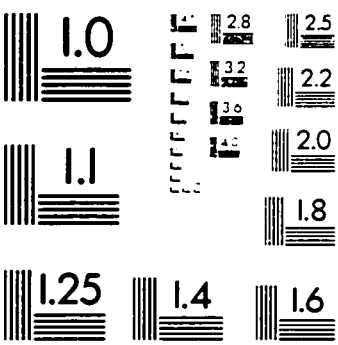

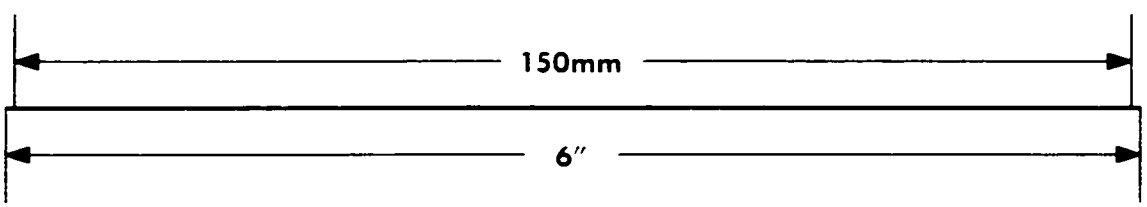

APPLIED IMAGE, Inc
1653 East Main Street
Rochester, NY 14609 USA
Phone: 716/482-0300
Fax: 716/288-5989